Electrochemical Carbon-Carbon and Carbon-Heteroatom Bond Formation to Access Bioactive Compounds

THESIS

Submitted in partial fulfillment of the requirements for the degree

of

DOCTOR OF PHILOSOPHY

by

Nagare Yadav Kacharu

ID. NO. 2019PHXF0433P

Under the supervision of

Prof. Indresh Kumar

and

Co-supervision of

Dr. Rahul Chaudhari

BITS Pilani

Pilani | Dubai | Goa | Hyderabad | Mumbai

BIRLA INSTITUTE OF TECHNOLOGY AND SCIENCE

PILANI (RAJASTHAN) INDIA

APRIL 2024

Dedicated

To

My Beloved Family

BIRLA INSTITUTE OF TECHNOLOGY AND SCIENCE
PILANI (RAJASTHAN)

CERTIFICATE

This is to certify that the thesis entitled **"Electrochemical Carbon-Carbon and Carbon-Heteroatom Bond Formation to Access Bioactive Compounds"** and submitted by **Mr. Nagare Yadav Kacharu** ID No **2019PHXF0433P** for the award of the Ph.D. degree of the Institute embodies his original work under my supervision.

Signature in full of the Supervisor:

Name: **PROF. INDRESH KUMAR**

Designation: **Professor**

Date:

Signature in full of the Co-supervisor:

Name: **DR. RAHUL CHAUDHARI**

Designation: **Manager**

Date:

ACKNOWLEDGEMENT

Initially, I express my heartfelt devotion to ***"God"*** for giving me strength, knowledge, and the capability to embark on and complete this research study. Now, it is the time of pleasure to recollect the countless cherished moments and the individuals who stood beside me throughout. Their unwavering support, guidance, motivation, and blessings at every stage have helped me to achieve this significant milestone in my life.

From the innermost core of my heart, I express my profound reverence and respect to my supervisor, Prof. Indresh Kumar, who introduced me to the fascinating realm of electrocatalysis and organocatalysis. I sincerely thank him for his encouragement, which carried me through difficult times, and his suggestions, which helped shape my research skills. His peaceful cooperation, industrious guidance, constant motivation, impeccable supervision, and timely criticism enabled me to understand better and remain optimistic throughout my Ph.D. tenure.

I express my gratitude to the past and current Vice-Chancellors, Directors, Deans, and Associate Deans of Birla Institute of Technology & Science, Pilani (BITS Pilani), for allowing me to pursue my doctoral studies by providing the necessary facilities. I extend my heartfelt appreciation to the office staff of AGSRD, whose secretarial assistance helped me in submitting the various evaluation documents on time. I would also like to acknowledge the former and current Head of the Department, DRC, Chemistry, BITS Pilani, Pilani Campus for their official support and encouragement. I sincerely thank Dr. Ranjan Sinha Thakur, the Librarian at BITS Pilani, and the entire library staff for their support and help while utilizing the library facilities. I am also thankful to BITS Pilani, Pilani campus, for its sophisticated analytical instrumentation facilities for analyzing research samples.

I am grateful to my Doctoral Advisory Committee members, Prof. Rajiv Sakhuja and Prof. Paritosh Shukla, for their excellent cooperation in refining my thesis. At the onset, their valuable suggestion for refining my proposal and seminar greatly impacted my research. I acknowledge them for their continuous suggestions and corrections to improve my thesis without any time limits. I am thankful to all the respectable faculty members of the chemistry department, BITS Pilani, for their generous help and fruitful discussions during the different stages of my doctoral study. I also thank all the chemistry department office staff for their support during my Ph.D. journey.

The friendly and encouraging atmosphere and the remarkable achievements made in Lab 3128 have left an indelible mark on my life. I am immensely proud and grateful to express my heartfelt thanks to my labmates Dr. Amol Pawar, Dr. Jyothi Yadav, Mrs. Mamta Katewa, Mr. Imtiyaz A. Shah, Mr. Atul J. Dolas, Mrs. Karishma Prabhu, Mr. Arun Patel,

ACKNOWLEDGEMENT

Ms. Reena Jangir, and Mr. Arpit Singh and Ms. Mainika for their love and support. I thank each of you individually for your cooperation, care, and company, which made my Ph.D. journey more comfortable at BITS Pilani.

I extend my warm thanks to research scholars and friends belonging from the chemistry department, BITS Pilani, Mr. Ram Prasad Bhatt, Ms. Shivani Thakkar, Mrs. Vishaka, Ms. Anuvasita, Ms. Pragya, Ms. Neha Meena, Dr. C. K. Mahesha, Dr. Bintu Kumar, Mr. Dhananjay Nipate, Mr. Prakash Taur, Mr. Prakash Swami, Mr. Amol Gadekar, Ms. Monika Malik, Ms. Prakriti, Mr. Narsimha, Mr. Bharat, Mr. Narendra, Mr. Somnath, Ms. Sushma, Mrs. Aishwarya, Ms. Prachi, Ms. Manisha, Ms. Disha, Ms. Annu, Mr. Sumit, Mr. Ajeet Sheoran, Mr. Ajeet Singh, Ms. Gurpreet Kaur, Ms. Bhawani, Dr. Vikki Shinde and Dr. Sonam for their continuous direct and indirect support in my research work.

I am deeply grateful to my parents, Mrs. Janabai Nagare and Mr. Kacharu Nagare, for their unwavering love, endless patience, and sacrifices to educate and prepare me to reach this milestone. Their presence has always been a source of comfort during stressful times. Words and this limited space cannot effectively express my gratitude to my parents.

I want to express my deep and sincere gratitude to my elder brother, Mr. Yogesh Nagare, who supported me morally and financially and made enormous contributions to help me reach this stage today.

I want to thank my wife, Mrs. Nikita Nagare, from the bottom of my heart for her constant support and encouragement during my doctoral studies.

I thank my loving sisters, Mrs. Vaishali Ghuge, Mrs. Babita Sonawane, and Mrs. Savita Ghuge, for their utmost moral support, love, and care in all aspects of my life.

I want to express my sincere gratitude to my teachers from school, college, and post-graduation who supported me directly or indirectly in reaching this level of achievement.

I sincerely thank SERB-FICCI and Praveen Laboratories Pvt. Ltd. (Surat) for their invaluable financial support through a prime minister research fellowship (PMRF). DST-FIST is also sincerely acknowledged for providing instrumentation facilities in the department. Lastly, I would like to thank my well-wishers, including teachers, relatives, and friends, whose faith, encouragement, and constant moral support contributed significantly to completing this work. I am deeply grateful to all of them.

Finally, I humbly bow my head to the Almighty, who gave me the strength to work hard and overcome challenging situations.

Nagare Yadav Kacharu

ABSTRACT

The work discussed in this thesis entitled **"Electrochemical Carbon-Carbon and Carbon-Heteroatom Bond Formation to Access Bioactive Compounds"** provides a brief description of the development of the new method for the synthesis of *α*-aminated esters, C2-heteroquaternary indolin-3-ones, 2,3-diarylquinoxalines, and dihydroindolo[1,2-*c*]quinazolin-12(6*H*)-one by using electrochemical oxidative process. The developed strategy utilizes commercially available inexpensive starting materials.

The First Chapter describes a brief historical overview, concepts, techniques, methodology, and the importance of electro-organic synthesis. This thesis work generally follows the electrochemical oxidative pathway; some of the selected electrochemical oxidative transformations are also discussed in this chapter.

The Second Chapter described an efficient electrochemical protocol for intermolecular oxidative coupling between *α*-aryl acetates (C(sp^3)-H bond) and secondary amines (N-H bond). The mild electrocatalytic condition furnishes *α*-amino-esters by stitching together two electronically mismatched units through C-N bond formation, with a high yield (up to 92%). The reactions can be scaled up without impacting the process efficiency, and the resulting *α*-amino-esters can be functionalized to other similar biorelevant compounds.

The Third chapter revealed a highly competent electrochemical method for directly synthesizing C2-quaternary-centered indolin-3-ones from 2-arylindoles. Including self-dimerization of 2-arylindoles, several nucleophiles, such as indole, 1,3-dicarbonyls, pyrrole, allylsilane, and TMSCN, were added to *in situ* generated indole-3-ones through oxidative dearomatization of 2-arylindoles with good yields. The developed method has been applied for the product's gram scale preparation, metagenediindole A synthesis and other late-stage synthetic transformations. This method has overcome limited nucleophiles addition to 2-arylindoles under electrochemical conditions.

The Fourth Chapter describes an efficient electrochemical protocol for directly synthesizing 2-aryl-3-(2-aminoaryl) quinoxalines from 2-aryl indoles. The reaction proceeds through in situ generations of 2-arylindole-3-ones under electrochemical oxidative dearomatization of 2-arylindoles, followed by a ring opening-cyclization sequence with 1,2-diamino arenes to construct substituted quinoxaline compounds with good yields. Apart from gram-scale synthesis, the prepared compounds were tested for late-stage functionalization.

ABSTRACT

Chapter Fifth describes a novel method for the electrochemical oxidative intermolecular [4 + 2] annulation of tertiary aryl amines and cyclic ketimines to access functionalized dihydroindolo[1,2-*c*]quinazolin-12(6*H*)-one moiety. This developed protocol can occur under air and metal-free conditions at room temperature, and a wide range of functional groups proved to be compatible under our optimized conditions. The reaction conditions were consistent with some drug structure derivatives.

The Sixth chapter is a compilation of the overall thesis work, and the future scope of the present research work has also been highlighted in this chapter.

TABLE OF CONTENTS

TABLE OF CONTENTS

TABLE OF CONTENTS

LIST OF TABLES

LIST OF FIGURES

LIST OF FIGURES

LIST OF ABBREVIATIONS / SYMBOLS

Abbreviation/Symbol	Description
α	Alpha
β	Beta
γ	Gamma
δ	Chemical Shift
Δ	Heat
Å	Angstrom
Ac	Acetyl
Aq	Aqueous
ACN	Acetonitrile
Ar	Aryl
Bu	Butyl
Calcd.	Calculated
J	Coupling constant
°C	Degree Centigrade
^{13}C-NMR	Carbon-13 Nuclear Magnetic Resonance
Cat.	Catalyst
CAN	Ceric Ammonium Nitrate
CCE	Constant Current Electrolysis
CPE	Constant Potential Electrolysis
Conc	Concentration
COSY	Correlation Spectroscopy (NMR)
$CDCl_3$	Deuterated Chloroform
d	Doublet
DBO	Dibenzoxazepine
DABCO	1,4-Diazabicyclo[2.2.2]octane
DBU	1,8-Diazabicyclo[5.4.0]undec-7-ene
dd	Doublet of doublet
DDQ	2,3-Dichloro-5,6-Dicyanobenzoquinone
DMSO	Dimethysulphoxide

LIST OF ABBREVIATIONS / SYMBOLS

DMSO-d_6	Deuterated Dimethysulphoxide
DCE	Dichloroethane
DCM	Dichloromethane
DMA	*N*,*N*-Dimethylacetamide
DMAD	Dimethyl Acetylene Dicarboxylate
DMF	*N*,*N*-Dimethylformamide
ESI	Electron Spray Ionization (MS)
EtOAc	Ethyl acetate
TEMPO	2,2,6,6-tetramethyl-1-piperidinyloxy
Equiv	Equivalent
E	Electrophile
g	Gram
HRMS	High Resolution Mass Spectra
HSQC	Heteronuclear Single Quantum Correlation
HOMO	Highest Occupied Molecular Orbital
IR	Infrared
Hz	Hertz
hr	Hour
Lit.	Literature
LUMO	Lowest Unoccupied Molecular Orbital
MS	Mass spectrometry
M.P	Melting point
m	Multiplet
mg	Milligram
MHz	Megahertz
mA	Milliampere
I	Current
min	Minutes
mL	Milliliter
mmol	Millimole

LIST OF ABBREVIATIONS / SYMBOLS

MW	Microwave
N_2	Nitrogen gas
Nu	Nucleophile
O_2	Oxygen gas
^{1}H-NMR	Proton Nuclear Magnetic Resonance
PEG	Polyethylene glycol
t-BuOK	Potassium *tert*-Butoxide
ppm	Parts per million
KI	Potassium Iodide
%	Percentage
p-TsOH	*p*-Toluenesulfonic acid
rt	Room temperature
s	Singlet
NBS	*N*-bromosuccinimide
NIS	*N*-iodosuccinimide
$NaHCO_3$	Sodium hydrogencarbonate
$Na_2S_2O_3$	Sodium thiosulfate
σ	Sigma
t	Triplet
TBAB	Tetrabutylammonium bromide
Ts	Tosyl
Tert-	Tertiary
TFA	Trifluoroacetic acid
THF	Tetrahydrofuran
TLC	Thin layer chromatography
TMS	Tetramethylsilane
TBHP	Tert-Butyl Hydroperoxide

CHAPTER 1

Introduction to Electro-Organic Synthesis

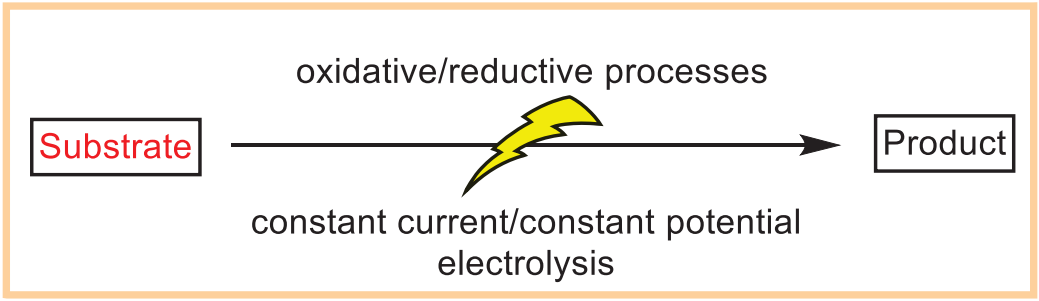

1.1 Introduction

The severe restrictions on fossil fuels and finite resources encourage scientists to reconsider chemical synthesis and develop sustainable solutions. Many scientists are researching green chemistry ideas to reduce the environmental effects of chemical processes. It includes implementing waste reduction methods, generating more energy-efficient processes, and employing renewable feedstocks. Sustainable chemical processes can encourage resource conservation and contribute to reducing carbon emissions.[1]

In an effort to cut waste production and carbon dioxide emissions, industries have shifted to renewable energy sources. Likewise, it would be ideal to see the development of new methods for organic synthesis that would improve the environmental friendliness of the processes used to create commercial products. In the big picture, this encourages creating a sustainable planet that permits an expanding economy. Using green chemistry techniques helps industrial businesses create distinct market sectors that enhance consumer satisfaction and talent retention. As such, a process's "greenness" increases its perceived value and gives it a competitive edge when dealing with "selection pressure" brought on by ever-improving synthetic procedures.[2-4]

Recent years have seen the acceptance of electro-organic synthesis as one of the critical techniques capable of achieving several desirable goals in the development of an environmentally friendly process by society. Electrochemistry is one of the most direct and closest approache to a chemist's interaction with molecules because the electrostatic interactions between electrons and nuclei are the most fundamental in chemistry. Electrochemistry is naturally redox chemistry because it directly uses an electrical potential to add or remove electrons from such interactions.[5a-m] Therefore, using electricity in organic synthesis eliminates hazardous, toxic, and sometimes expensive chemical oxidants, reductants, and their direct chemical waste. Hence, electro-organic synthesis is inherently green and efficient for achieving sustainable, eco-friendly organic synthesis.[6a-d]

This chapter aims to give readers a comprehensive grasp of electro-organic chemistry, including its history, development, and overview. Thus, this section will first provide a simplified timeline of historical milestones, followed by a detailed text description of some recent well-known and representative works of electro-organic synthesis **(Figure 1.1)** adapted from the work of the Baran group with general reaction schemes where necessary.[7-8]

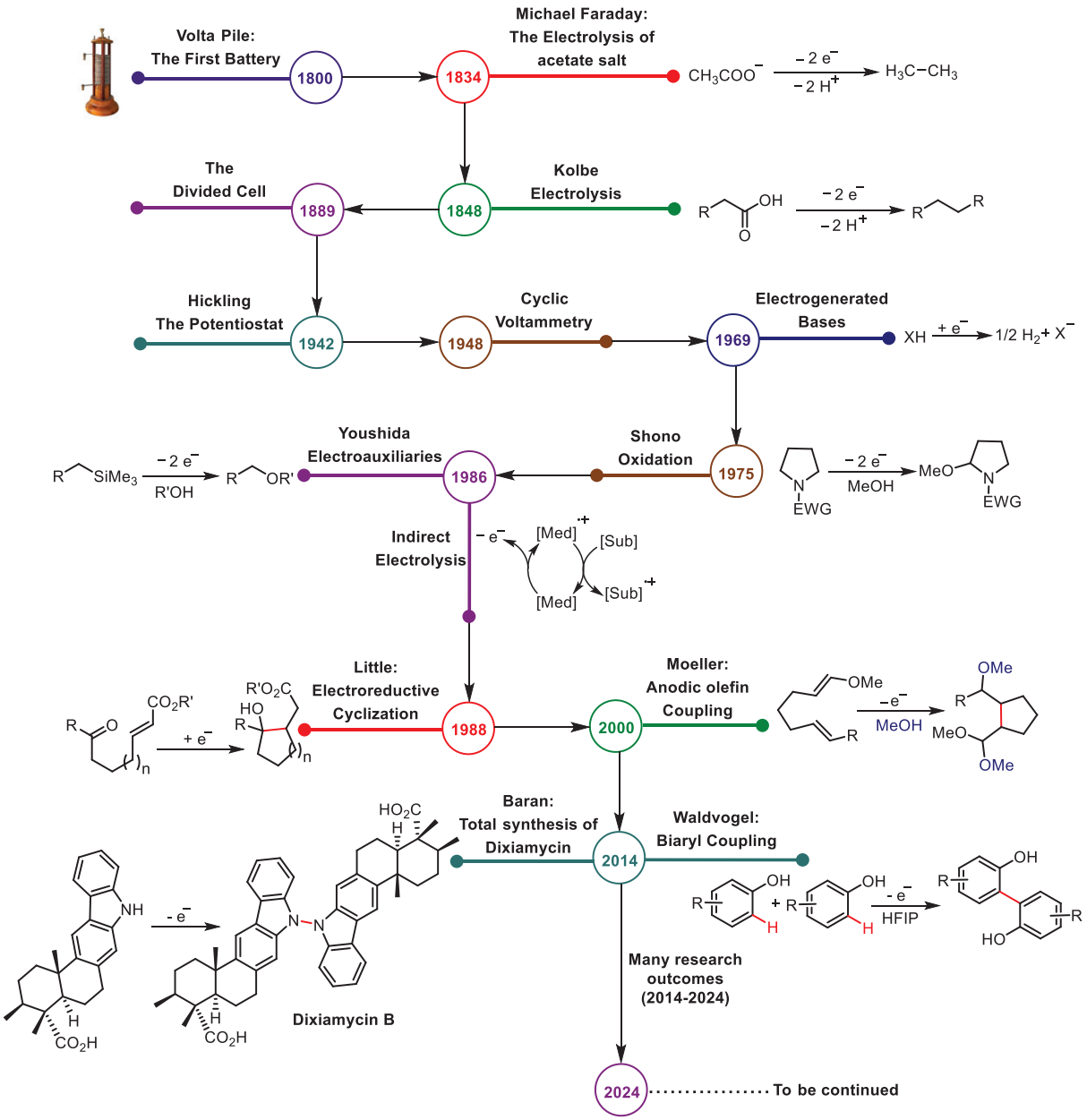

Figure 1.1 The history of electro-organic chemistry from 1800-2023

The history door of electro-organic synthesis was opened in 1800 with the invention of the Volta Pile. The Volta Pile, the first electric battery, enabled the continuous circulation of electrons over a circuit for the first time.[9] After three decades, the world has made significant progress in understanding the nature of electricity, thanks to Michael Faraday's essential discovery. The invention of electrochemical concepts like electrolysis, anode, and cathode, the discovery of ions

flowing through electrolyte solutions, and the establishment of Faraday's laws of electrolysis (**Eq. 1**)[10] can all be credited to Faraday's extensive studies.[11]

$$n_M = \frac{Q}{zeN_A}$$

n_M = Number of moles of metal species
Q = Charge passed
Z = Valency number of ions of a substrate
e = Elementary charge (1.602×10^{-19}C)
N = Avogadro's number (6.022×10^{23} mol^{-1})

(Eq.1)

Faraday discovered that acetate salts could be electrolyzed to yield ethane and carbon dioxide, and Kolbe produced alkyl radicals upon oxidation of fatty acids at a platinum anode, which subsequently dimerized to furnish alkanes later reaction became famous as Kolbe electrolysis **(Scheme 1.1)**.[10,12] But Faraday's has secured a position as a pioneer of electro-organic chemistry.

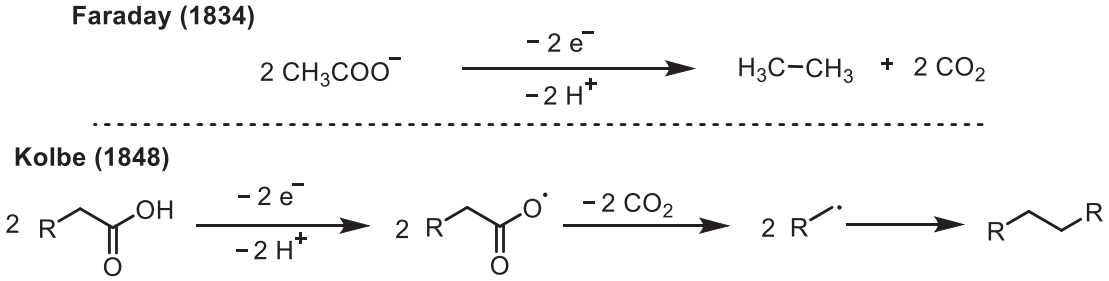

Scheme 1.1 First electro-organic synthesis reported by Faraday and Kolbe

1.2 Fundamental principles of electro-organic synthesis

In an electrochemical reaction at an anode, oxidation occurs, resulting in the removing one or more electrons from the highest occupied molecular orbital (*i.e.*, HOMO), forming a radical cation ($R^{+\bullet}$). At a cathode, reduction results in the addition of electrons into the lowest unoccupied molecular orbital (*i.e.*, LUMO), creating a radical anion ($R^{-\bullet}$) **(Figure 1.2)**.[13-14] The electrolytic interaction between the electrode and reactant can be direct or mediated by redox species, *i.e.*, indirect. These processes can be categorized as oxidation (at the anode) and reduction (at the cathode).

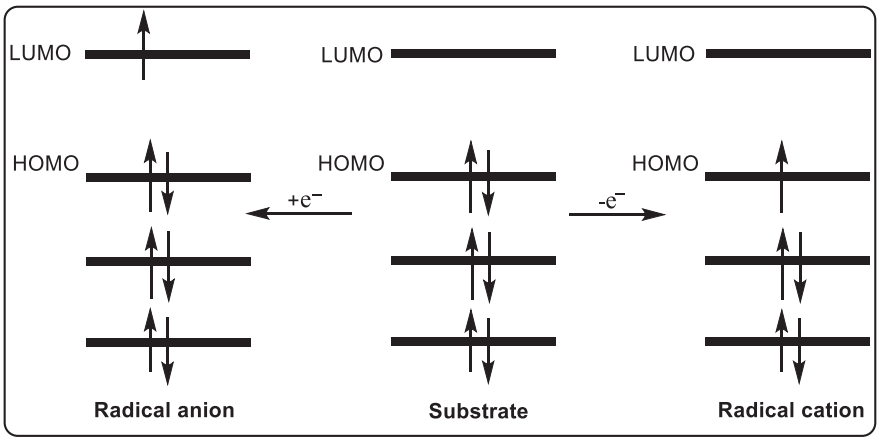

Figure 1.2 Mode of electrochemical reaction

The electrosynthesis of organic compounds can be achieved by either adding or removing electrons from an organic compound, forming a reactive intermediate; these reaction intermediates undergo disproportionation, oxidation, and reduction reactions to give respective cation, anion, free radicals, which undergo various reactions such as nucleophilic or electrophilic substitution, dimerization, and radical reaction, etc. All reactive intermediates and subsequent chemical reactions are shown in **(Figure 1.3)**.[15]

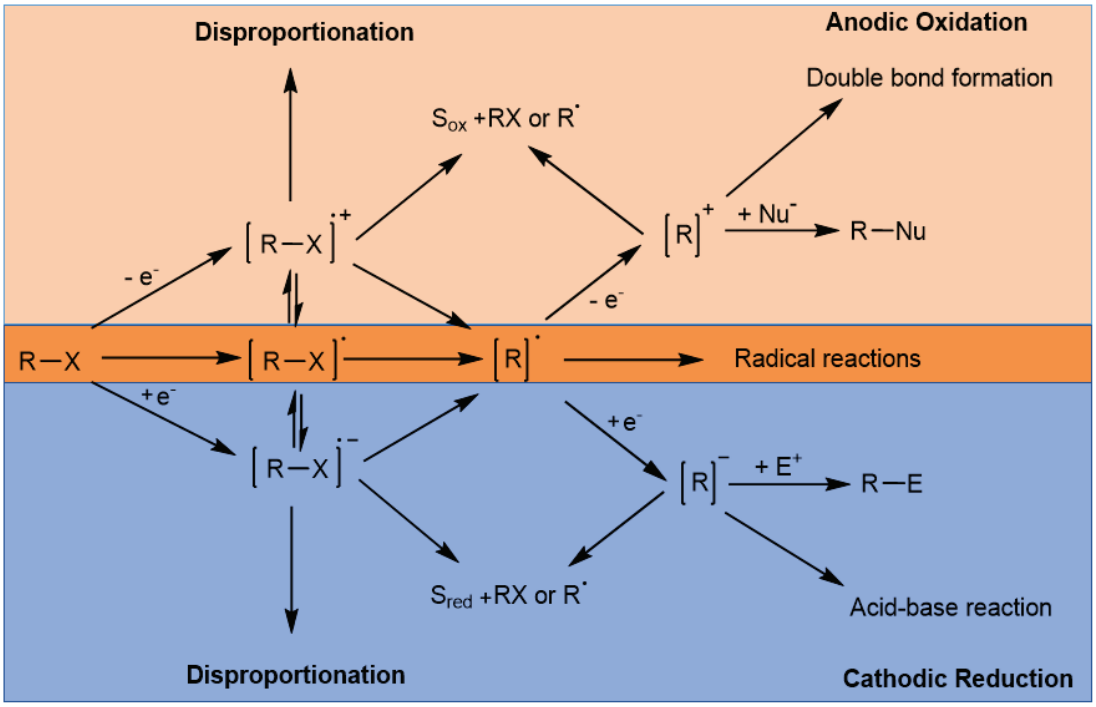

Figure 1.3 Possible pathways for reactivity after a single-electron transfer (X = leaving the group)

The transfer of electrons plays a crucial role in most of the chemical reactions to activate starting materials. Since the electron donor and acceptor are present in the same solution in the electrochemical technique, the activity of reactive intermediates is exceptionally high compared to conventional methods. Traditionally, substrate activation has been carried out by employing thermal or photo energy outside the reaction system. In contrast, in electrochemical reactions, active species are generated by the movement of electrons between the electrode and substrate. Reversal of the polarity of functional groups is a unique feature of electro-organic chemistry.[14] Electron-rich sites transform into electron-deficient centers by removing an electron. Similarly, the electron-deficient moiety is converted into an electron-rich center by adding an electron **(Figure 1.4)**.[16] This type of *in situ* conversion is challenging in conventional organic chemistry. Hence, this strategy becomes a powerful tool for constructing complex molecules.

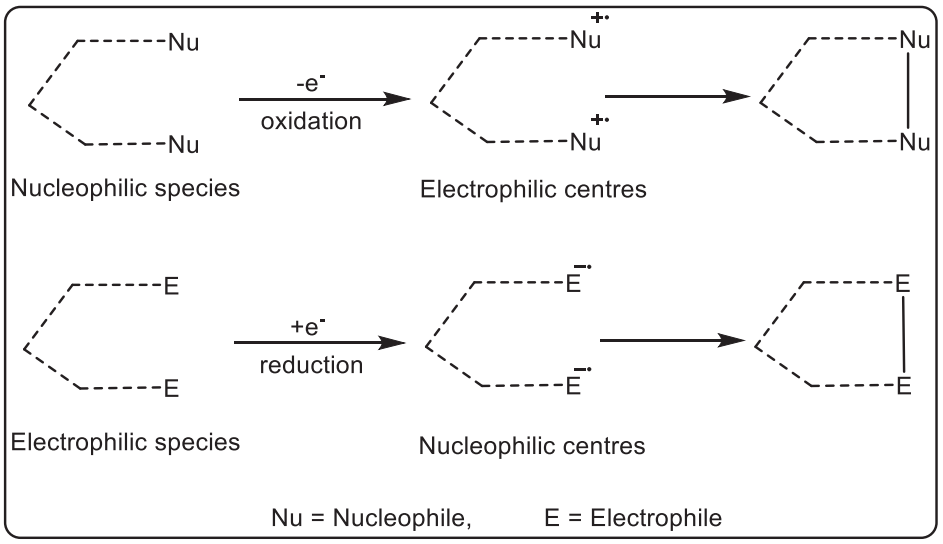

Figure 1.4 Electrochemical approach towards umpolung reactions

1.3 Basic requirements

Electrodes replace chemical oxidants and reductants in electrochemical processes, where electron transfer happens heterogeneously at the electrode surface, resulting in oxidation at the anode and reduction at the cathode. Usually, just one electrode (the working electrode) is designed to react. It produces the desired product, whereas the reaction at the opposite electrode (the counter electrode) is sacrificial. Even yet, it is feasible to profit from both half-cell processes simultaneously. As a result, an electrochemical reaction requires at least two electrodes: a positive electrode (the anode) where oxidation takes place and a negative electrode (the cathode)

where reduction occurs. The two electrodes need to be connected to the power source, and a supporting electrolyte is usually required to facilitate the passage of the electric charge through poorly conductive organic solvents. The laboratory setup for electrolysis varies from a very simple one (a beaker with two electrodes immersed in the solution) to sophisticated instruments. Still, regardless of being simple or complex, the various setups have standard basic requirements for successful electrolysis.[17-18]

1.3.1 The power supply

A power supply is an electrical source that maintains a continuous flow of electrons through the cell by applying enough voltage to overcome the cell's resistance. It has a vast and changeable range of capabilities and prices, ranging from relatively inexpensive tiny batteries to high-end, complex, programmable electronic devices that can accurately manage current and voltage across an extensive range of values and feed many cells simultaneously.

1.3.2 The electrolysis cells

The cell is a container that holds the electrolytic solution and at least two electrodes. It can be as simple as an open beaker, a flask with two electrodes linked to a power source, or a professionally built cell with different forms, materials, and degrees of sophistication depending on the demand and flow of electrochemical cells. **Section 1.4** gives detailed information about cell designs and kinds.

1.3.3 The electrodes

In concept, electrodes can comprise any conductive or semi-conductive substance. Like the cell and the power supply, it can range from inexpensive graphite (a pencil), aluminium foil, or metallic cutlery to immensely expensive or boron-doped diamond (BDD). Because electron transfer occurs at the electrode surface, electrodes are the most distinct feature of the cell and are critical to efficient electrochemical transformation. In addition to adequate electric conductivity, electrode materials should be corrosion-resistant and chemically inert. The principal electrode-related difficulty faced during electrolysis is electrode passivation, which occurs when an insulating layer forms on the electrode surface, reducing its activity owing to total or partial blocking of the electrode surface. The passive layer might be a metal oxide or polymeric film generated due to the oxidation of electron-rich organic molecules, particularly olefins and aromatic chemicals. Electrode passivation can be reduced by occasionally switching the

electrode polarity, using the same material for both the anode and the cathode, or adding an additive to boost the solubility of the polymeric material.[19]

1.3.4 Solvent and electrolyte

An electrolyte is a mixture subjected to electrolysis (the reaction mixture). It consists of the solvent or solvent mixture, supporting electrolytes, reactants, catalysts, additives, and products. The solvent system is critical for electrolysis success and achieving the desired outcome. The electrolysis in electro-organic synthesis is often done in organic solvents, which have weak electric conductivity and would need the addition of supporting electrolytes to reduce cell resistance and make the electrolysis practicable. The supporting electrolyte is a substance that is generally a salt (organic or inorganic) added to help electricity travel through the weakly conductive reaction medium. Sometimes, one or more reactants or additives required for the desired chemical reaction are ionizable and can serve as reactants while also increasing the conductivity of the combination, avoiding or reducing the need for additional supporting electrolytes. Inorganic salts like $LiClO_4$ or organic salts like pyridinium and quaternary ammonium salts can act as electrolytes. Organic salts like Bu_4NBF_4 and similar compounds have the benefit of being readily soluble in organic solvents, but their removal from the product might be challenging at times.[20]

1.4 Types of electrolysis cells

As previously said, electrolysis cells can range from elementary beaker-type cells to complicated custom-built cells. This section will discuss the fundamental types of electrolysis cells found in synthetic organic chemistry laboratories.

1.4.1. Undivided cells

The undivided cell is the most straightforward cell design **(Figure 1.5)**. The two electrodes in an undivided cell are immersed in the electrolytic solution stored in a vial, beaker, flask, or more elaborate, specifically built glassware or other materials; the distance between the two electrodes should be kept as small as possible to decrease cell resistance. A sequence of parallel plates can enhance the electrode surface area and, therefore, the cell production. Because there is no physical separation between the anode and the cathode in undivided cells, electrolyte components can reach both electrodes.[25] As a result, the reactive intermediates or intended product(s) generated at one electrode should not experience a reverse reaction at the other

electrode; otherwise, a "chemical short-cut" is developed, resulting in a non or less productive process. In the case of anodic oxidation, a scenario is generally avoided by selecting a simple sacrificial (non-productive) counter-reaction, such as hydrogen gas evolution from the reduction of protic solvents or acids at the cathode. Sometimes, the counter-reaction is productive (paired electrolysis), producing a reagent or a reactive species required to synthesize the desired product, or it can be exploited to make a second desirable product.

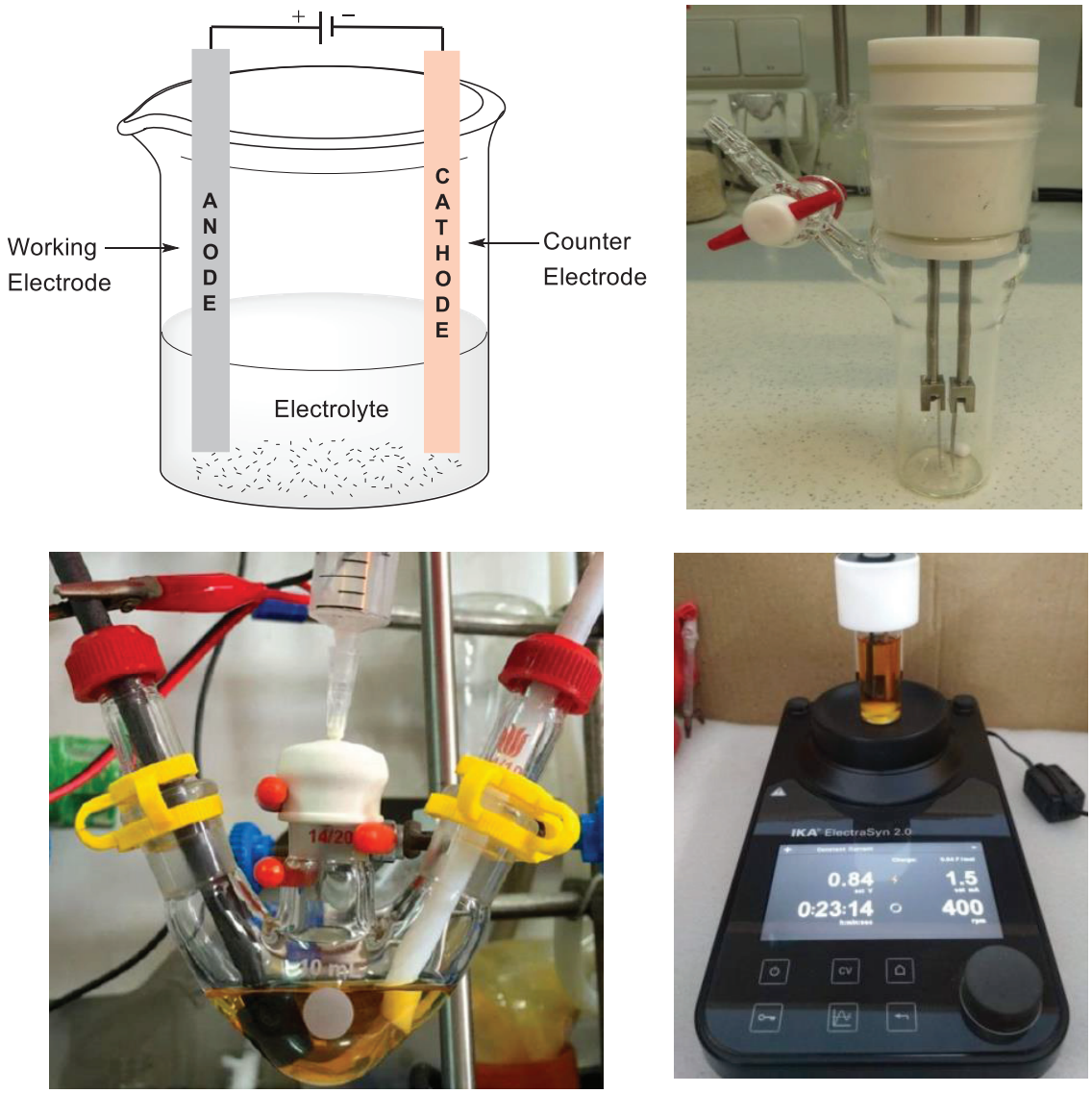

Figure 1.5 Undivided cell setup. Top left: Schematic representation; top right: Home-made; bottom left: Home-made; Commercially available electrasyn 2.0 from IKA

1.4.2 Divided cells

It is sometimes essential to physically separate the anode from the cathode to prevent a "chemical short-cut" or unwanted reaction at the counter electrode. The H-cell is a more elaborate split cell design (**Figure 1.6**). The divided cell is made up of two compartments that are physically separated by a porous material such as sintered glass or ceramics or an ion exchange membrane such as Nafion membranes; these separators allow ion exchange between the two separated compartments and thus allow conductivity, but they prevent chemicals (substrates, reagents, product) from mixing from one container with the other. One chamber contains the anode and is charged with an anodic electrolyte (anolyte), while the other includes the cathode and is filled with a cathodic electrolyte (catholyte). Although the divided cell is more sophisticated and complicated than a primary undivided cell, its usage is sometimes unavoidable; also, the physical separation of the anolyte and catholyte allows for easy paired electrolysis and simplifies product isolation.[18]

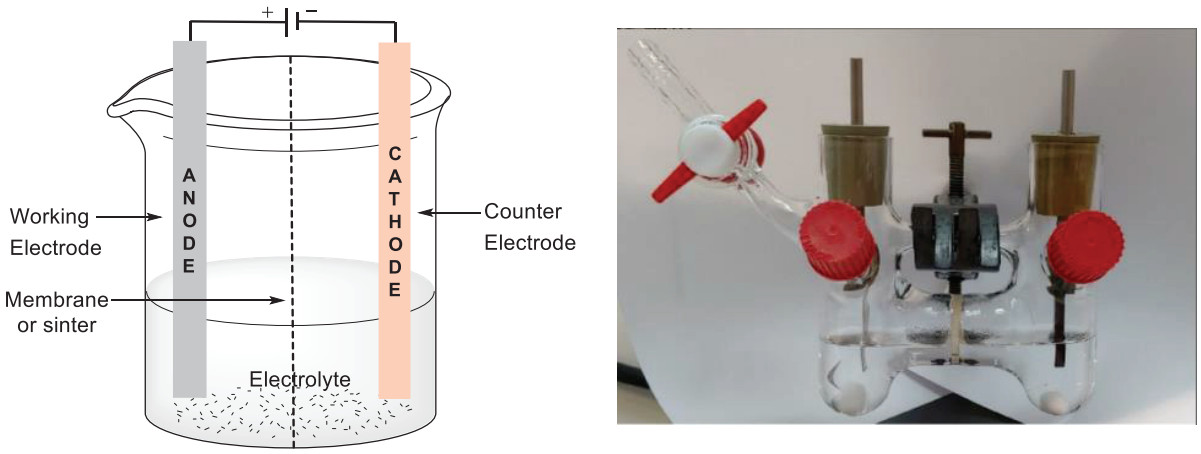

Figure 1.6 Divided cell setup

1.5 Control modes of electrolysis

Electrical factors can control electrochemical reactions. Ohm's law (V = IR), which applies to all types of electrolysis, may be used to deduce the fundamental notions of electrolysis.[17,18] As a result, electrolysis cells can operate in the following control modes:

1.5.1 Constant potential electrolysis (Potentiostatic operation)

Under the potentiostatic mode of operation, the electrolysis is performed at a constant potential applied over the whole electrolysis time, using a potentiostat as a power supply (**Figure 1.7**).

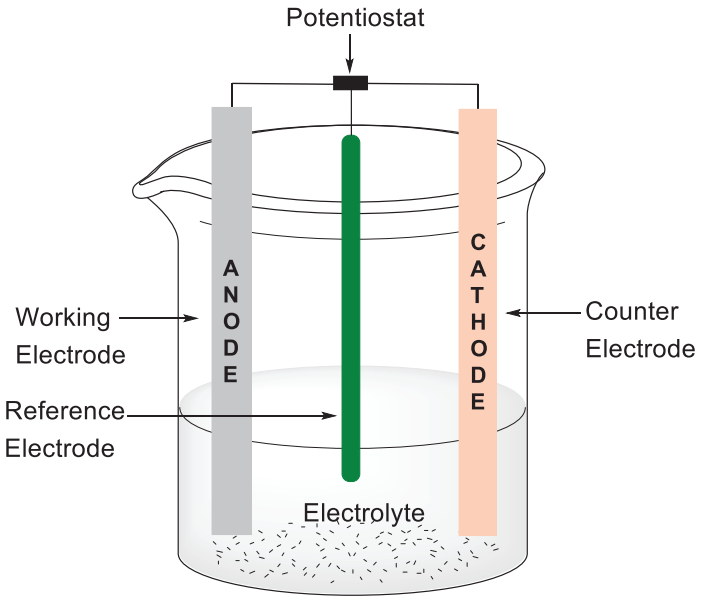

Figure 1.7 Schematic representation of electrolysis under potentiostatic mode of operation

The applied voltage is adjusted to a precise value corresponding to the redox potential of a particular substrate in the reaction mixture. As a result, the redox potential of the desired substrate must be determined in the same solvent system utilized for the reaction, which may be accomplished by doing a cyclic voltammetry experiment before the electrolysis.

The potentiostat frequently tunes the total voltage difference between the cathode and anode (E_{total}) to keep the working electrode potential ($E_{working}$) constant during electrolysis. The following equation can show E_{total}.

$$E_{total} = E_{working} + E_{counter} + iR$$

Where the $\mathbf{E_{working}}$ and $\mathbf{E_{counter}}$ abbreviations stand for the potentials of the working and counter electrodes, respectively, **i** is the applied current, and **R** is the resistance of the solution between the cathode and anode.

1.5.2 Constant current electrolysis (Galvanostatic operation)

Under the galvanostatic mode of operation, the electrolysis is performed at a constant current applied over the whole electrolysis time, using a galvanostat as a power supply. This operation mode is more straightforward than the potentiostatic mode, requiring only two electrodes, anode and cathode, and an inexpensive power supply **(Figure 1.8)**.

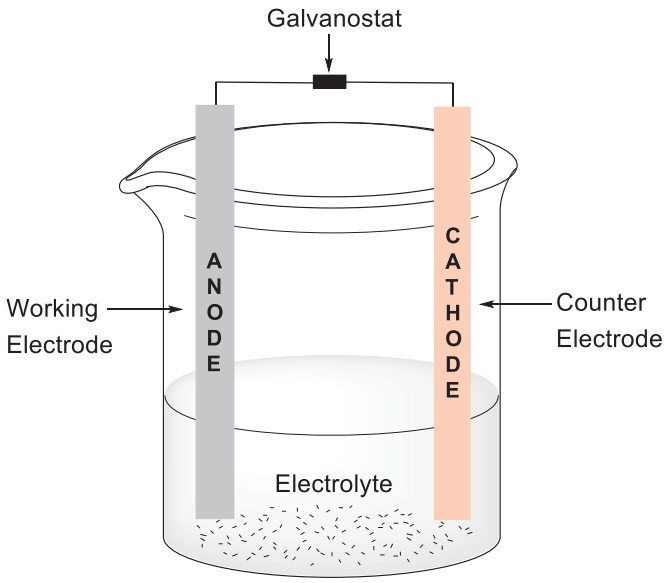

Figure 1.8. Schematic representation of electrolysis under a galvanostatic mode of operation

The current is kept constant throughout the reaction by varying the applied potential (roughly 0.80V to 2.30V) in the constant current electrolysis (CCE) method. The CCE method is more convenient than the complex constant potential electrolysis (CPE) method. It is utilized in reasonably large-scale and simple reactions (a simple mechanism). In this work, we mainly use the CCE method because of its simplicity and high productivity. The total amount of electricity passed (in Faradays/mole) is calculated by the following equation:

$$\text{Electricity passed (F/mole)} = \frac{I \times T}{96500 \times m}$$

where **I** is current in *mA* (milli amperes), **T** is the time in *seconds*, and **m** is the amount of substrate in moles.

1.6 Electrolysis techniques

In electro-organic chemistry, electron transfer processes at the electrode surface are heterogeneous. However, it realized that different electrolysis techniques can depend on the mode of electron transfer from/to the electrode surface, chemicals in the bulk solution and, the following chemical transformations. Generally, the electron transfer process could be direct or indirect.

1.6.1 Direct electrolysis

Direct electrolysis includes direct heterogeneous electron transfer at the electrode surface between the electrode and the chemical substrate. This heterogeneous electron transfer activates the initial material, producing reactive species that proceed through chemical transformations to make the end product **(Figure 1.9)**.[21-22]

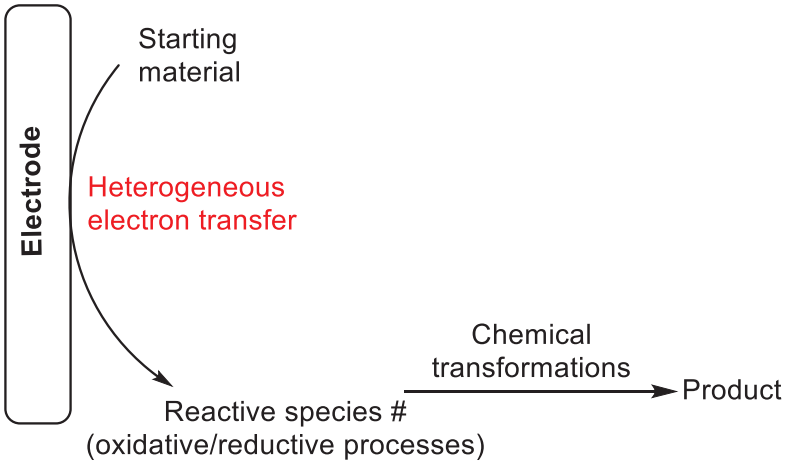

Figure 1.9 Schematic representation of direct electrolysis

1.6.2 Indirect electrolysis

Direct heterogeneous electron transfer between the electrode and the substrate can sometimes be slow and inefficient. In some situations, direct electrolysis may result in the development of polymeric films *e.g.,* oxidation of pyrrole and aniline, that coat the electrode surface, lowering conductivity and, in some cases, completely passivating the electrode. In such cases, where direct electrolysis is impractical, indirect electrolysis may be the answer. As an electron carrier in indirect electrolysis, a redox-active mediator is utilized. The mediator is activated at the electrode surface by heterogeneous electron transfer and subsequently conducts homogeneous electron transfer with the substrate in the bulk solution **(Figure 1.10)**. Compared to direct electrolysis, the use of redox mediators can increase the efficiency of the electron transfer and improve the selectivity of a reaction. Chiral electrocatalysts have also been investigated to conduct asymmetric electrocatalysis.[23-28]

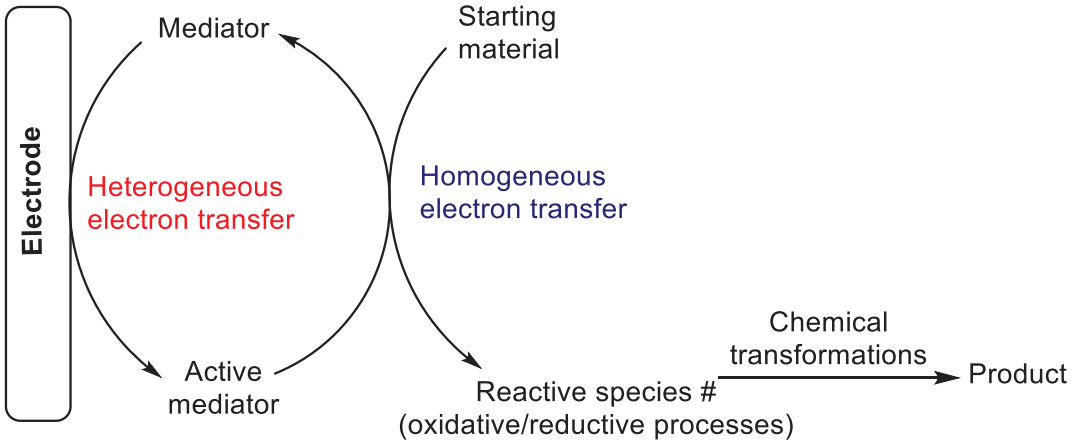

Figure 1.10 Schematic representation of indirect electrolysis

1.7 Cyclic voltammetry

Cyclic voltammetry (CV) is a powerful and popular electrochemical technique commonly employed to investigate the reduction and oxidation processes of molecular species. CV is also invaluable to study electron transfer-initiated chemical reactions, which include catalysis.[29-31] The traces in **Figure 1.11** are called voltammograms or cyclic voltammograms. The x-axis represents a parameter that is imposed on the system, here the applied potential (E), while the y-axis is the response, here the resulting current (i) passed. There are two kinds of CV conventions, as shown in **Figure 1.11.**

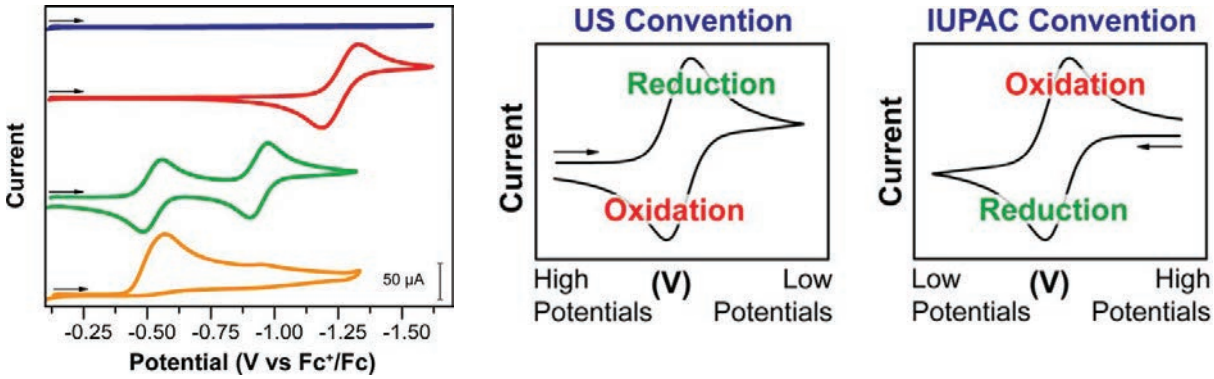

Figure 1.11 Cyclic voltammograms and their conventions

Electrochemical reversibility refers to the rate (rate constant) at which the electron transfer occurs between the working electrode (WE) and the redox species in the solution. If the rate is high then the transfer of electrons occurs rapidly without major thermodynamic hurdles, and it is known as an electrochemically reversible couple, whereas if the electron transfer occurs slowly (i.e. low rate constant) because of any barrier or complication, is referred to as an

electrochemically irreversible case. A rate of electron transfer between reversible and irreversible states comes under the quasi-reversible system. Nernst relationship is applicable every time if in the reversible system, both the oxidized and reduced structure are stable and the reaction can be run in both directions smoothly. Now we come to know that electrochemical reversibility is an operational thought that occurs during electrolysis. The electrochemical reaction may appear to be reversible in one kind of experiment and quasi-reversible or irreversible in other. According to the observation, the reversible nature of organic reactions is generally related to the formation of active species.

$$O_{(aq)} + n\,e^- \rightleftharpoons R^{n-}_{(aq)}$$

Where O and R are the oxidized and reduced form of a redox couple in an aqueous media. The electrochemical method involves the shifting of an electron across the interfacial area of an electrode and solution (aq) phase species.

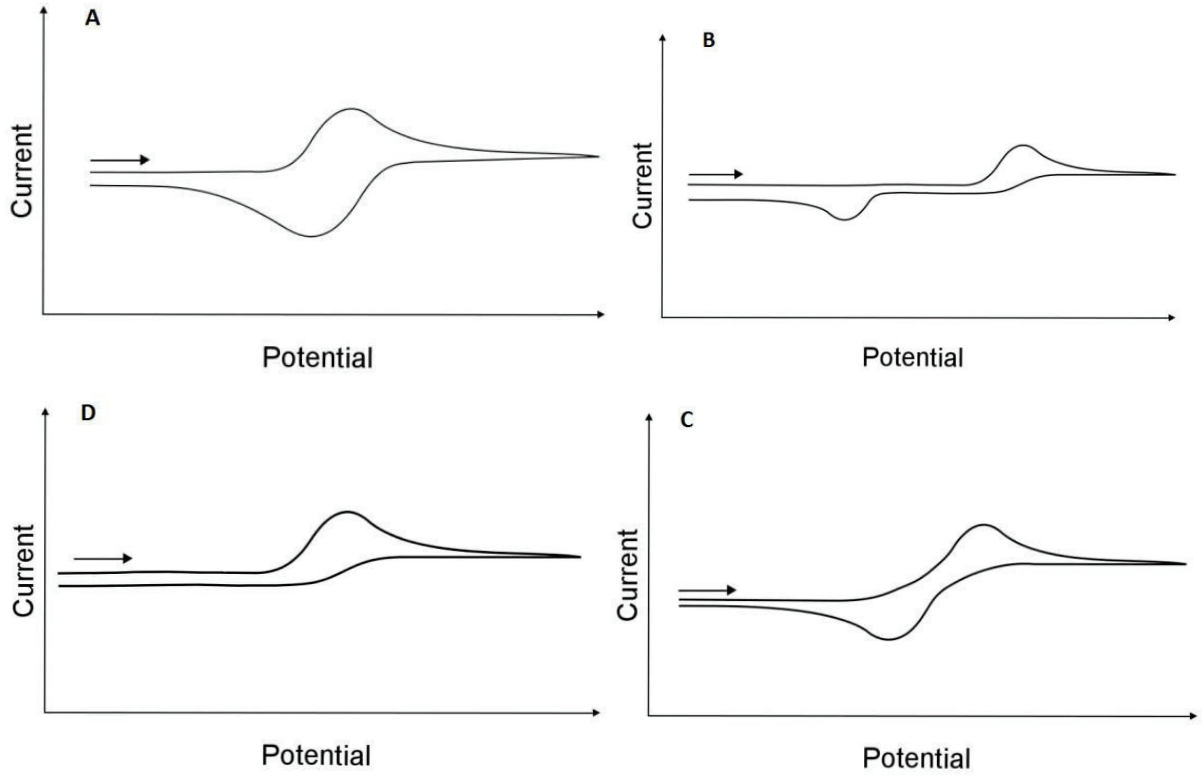

Figure 1.12 (A) Electrochemically reversible electron transfer; (B) Electrochemically irreversible electron transfer; (C) Electrochemically quasi-reversible electron transfers; (D) Chemically irreversible transfer of electron

Electrochemical reversibility is generally defined as the ratio of charge transfer to mass transfer, and mass transfer is dependent on the scan rate.

By using a cyclic voltameter we can find the reversible, irreversible, or quasi reversible nature of the reaction. Electrochemically reversible reactions yield the characteristic "duck curve" **(Figure 1.12A)** with peaks of similar magnitude on both the forward and reverse scans.

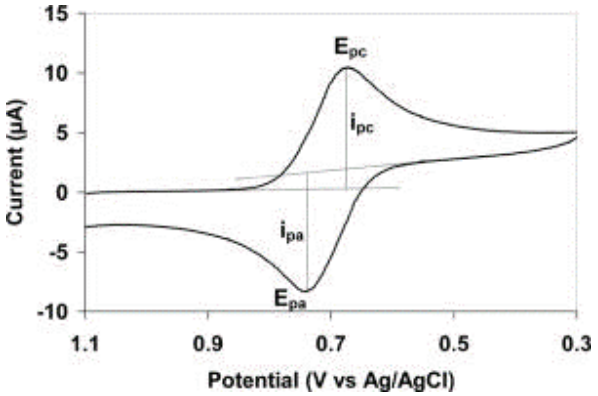

Figure 1.13 Typical cyclic voltammogram where i_{pc} and i_{pa} show the peak cathodic and anodic current respectively for a reversible reaction

Reversible reactions are characterized by the following points:

1. $\boldsymbol{i_{pa}/i_{pc} = 1}$ *i.e.* $\boldsymbol{i_{pa} = i_{pc}}$, (here anodic peak and cathodic peak current are represented by i_{pa} and i_{pc}).
2. In the reversible process current maximum occurs at the same voltage for all scan rates due to rapid electron transfer kinetics *i.e.* peak potential is independent of scan rate.
3. The separation of peak for the reversible reaction is **(0.059/n)V** (where n = number of electrons).
4. Standard potential $\boldsymbol{E^o = (E_{pa}+E_{pc})/2}$ **(**Where E_{pa} and E_{pc} are anodic and cathodic peak potential).

In irreversible or quasi-reversible reactions the value of *i*pa and *i*pc is never the same *i.e.* $\boldsymbol{i_{pa}/i_{pc} \neq 1}$. This deviation from unity is due to the consequent chemical reaction that is activated by the electron transfer. Such electrochemical reactions can be complex, involving association, dissociation, isomerization, etc. There is no proper rule that distinguishes quasi-reversible from irreversible reactions. During CV sometimes a reversible wave looks like a quasi-reversible wave, this is due to the dirty electrode (Fig. 1.12C). Maximum current occurs at different voltages since electron transfer processes are slow relative to voltage scan rate.

1.8 Electrochemical oxidative transformation

As mentioned in **section 1.2**, electrochemical reactions are divided into two categories: oxidative and reductive. Several groups have recently made significant efforts to develop electrochemical procedures since this thesis work generally follows the oxidative pathway; some of the selected electrochemical oxidative transformations are mentioned in **section 1.7**.

In this context, Baran and co-workers have developed some elegant electrochemical methods, including the direct decarboxylative *N*-alkylation of heterocycles. This method applies non-activated carboxylic acids as alkylating agents in the *N*-alkylation of heterocycles through an electrochemically driven anodic decarboxylative process. A broad substrate scope across various heterocycles and fewer synthetic steps are required to access such medicinally relevant structures **(Scheme 1.2)**.[32]

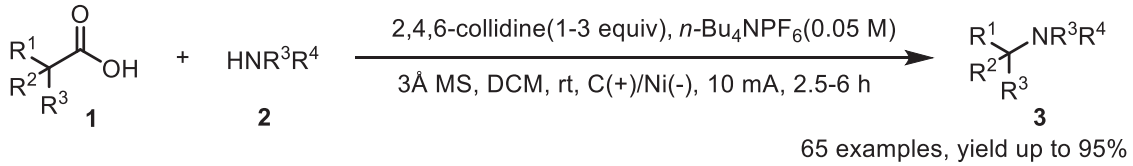

Scheme 1.2 Decarboxylative *N*-alkylation of heterocycles

Mei and co-workers reported an electrochemical oxidative asymmetric Mannich reaction of glycine esters **(4)** with cyclic ketones **(5)**. TEMPO was employed as a redox mediator in this reaction, effectively avoiding the excessive oxidation of the products. In addition, after a series of screenings, the authors used (*R*)-pyrrolidine-3-carboxylic acid as the chiral organocatalyst, platinum sheets as the anode and cathode with a constant current of 1.5 mA and DMSO as the Solvent. Under the optimal conditions, 41 Mannich-type amino acid derivatives **(6)** were reported with yields from 33% to 80% and good to excellent diastereoselectivity and enantioselectivity (up to 99% ee and up to 99:1 dr). Surprisingly, no electrolytes and sacrificial agents were used in this reaction system **(Scheme 1.3)**.[33]

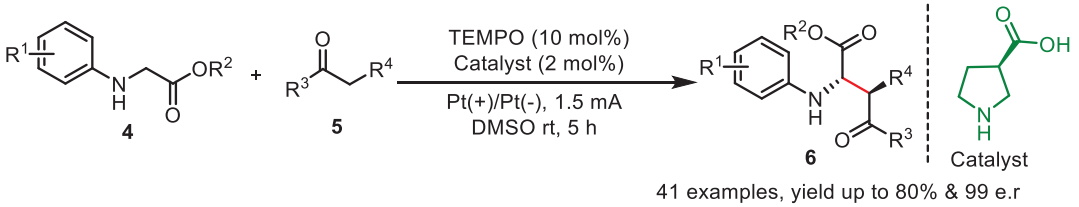

Scheme 1.3 Indirect electrochemical oxidative asymmetric Mannich reaction of glycine esters with cyclic ketones

In 2016, Zeng *et al*. reported an efficient electrochemical amino-oxygenation of styrenes **(7)** to synthesize 3-alkoxy-substituted indolines **(8) (Scheme 1.4)**. The reaction was performed in an undivided cell with graphite plates for both the anode and cathode. Different substituted *N*-(2-vinylphenyl) sulfonamides were compatible with the methodology. Mechanistic studies revealed that *in situ* generated molecular iodine was the active species. Intramolecular nucleophilic attack on the iodonium ion by the sulfonamide followed by nucleophilic substitution by methoxide gave the desired product.[34]

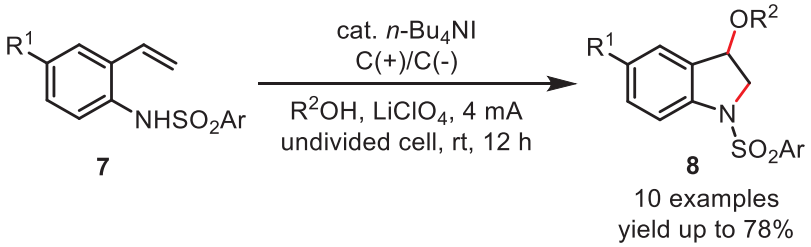

Scheme 1.4 Electrochemical synthesis of indolines mediated by *n*-Bu_4NI

In 2017, Lei and co-workers developed the intramolecular dehydrogenative $C(sp^2)$–$C(sp^2)$ bond formation of *N*-aryl enamines **(9)** for the synthesis of indoles **(10) (Scheme 1.5)**. Platinum plates, both the anode and cathode, were used in this electrosynthesis. Potassium iodide acted as both the supporting electrolyte and redox mediator for the oxidation of the substrates. The amidyl radical was proposed to be generated from the oxidation of the substrate by the *in situ* generated I^+. Further intramolecular radical cyclization gave the desired product. Moreover, this electrolytic system was also applicable to achieve the intramolecular dehydrogenative C–N bond formation of *N*-pyridyl enamines to synthesize imidazo[1,2-*a*]pyridines.[35]

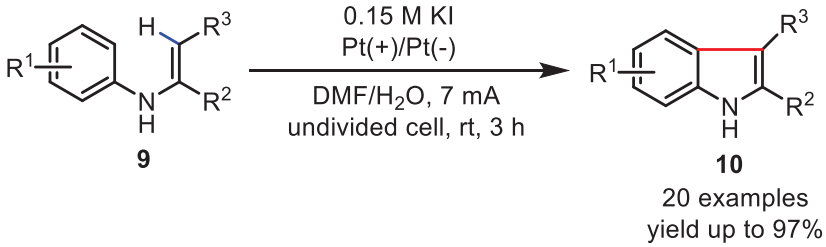

Scheme 1.5 Electrochemical intramolecular C–H/C–H cross-coupling for the synthesis of indoles

In 2018, Zeng and co-workers reported that CF_3SO_2Na, a stable and readily available reagent, can be used as a CF_3 source in the presence of a halogen mediator. Using a catalytic amount of

Bu_4NBr, electrolysis of acrylamides **(11)** afforded trifluoromethylated 2-indolinone **(12)** derivatives. The Br^- was initially oxidized to Br_2 on the anode. Br_2 then reacted with CF_3SO_2Na to produce CF_3SO_2Br, which was reduced on the cathode to afford an oxygen-centered radical intermediate. Subsequent elimination of SO_2 formed the CF_3 radical. The addition of the generated CF_3 radical to acrylamide allowed the radical cyclization reaction to proceed. Further oxidation on the anode and deprotonation afforded the desired products **(Scheme 1.6)**.[36]

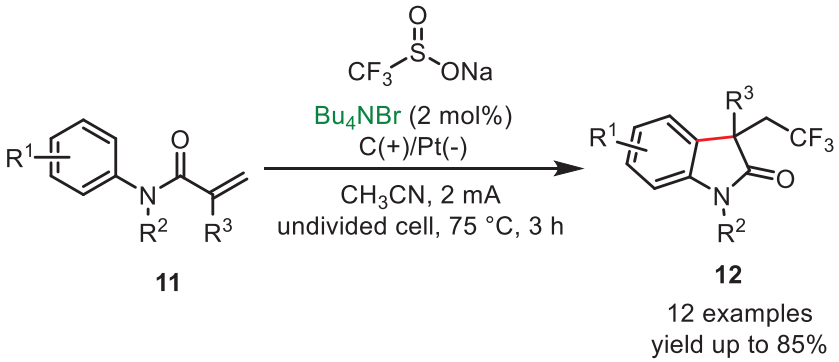

Scheme 1.6 Bromide-catalyzed tandem trifluoromethylation/cyclization of *N*-arylacrylamides

Zhou's team in 2021 developed a novel and efficient strategy for synthesizing 1,2-disubstituted benzimidazoles **(14)** *via* electrochemical oxidative dehydrogenation C–N bond formation. This electrosynthesis method could address the limitations of the C(sp^3)–H intramolecular amination. This electrochemical strategy provides a simple and practical approach to synthesizing benzimidazole derivatives with moderate to good yields under mild conditions. The reaction exhibited a wide range of substrates and avoided the use of metal catalysts and stoichiometric oxidants. In this reaction, tertiary amine was converted to a nitrogen-centered radical cation. After electron transfer and deprotonation, the imine cation is formed. The nucleophilic addition produces a cyclization product, and finally, anode oxidation aromatization gives the ultimate disubstituted benzimidazole product **(Scheme 1.7)**.[37]

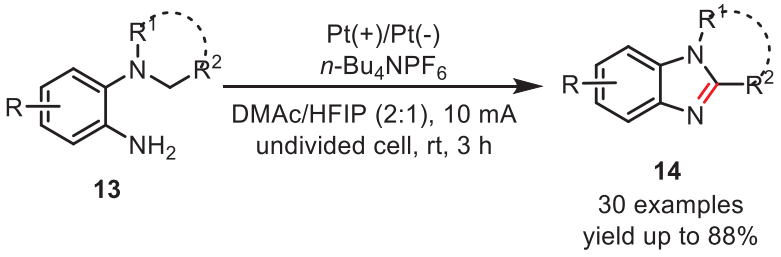

Scheme 1.7 Intramolecular amination with anilines

Ye and co-workers reported a significant method for utilization of α-methyl styrene derivatives (**15** and **16**) to accomplish [4+2] cycloaddition-rearrangement-aromatization in a metal-/oxidant-free electrochemical fashion by using tris(4-bromophenyl)amine (TBPA) as a mediator **(Scheme 1.8)**. This transformation was tolerant to various α-methyl styrene derivatives and could provide the corresponding products (**17**) in good yields. The typical features of this reaction are its scalability, absence of high valence substrates, oxidants, and metals, and significant synthetic value in constructing polycyclic aromatic compounds.[38]

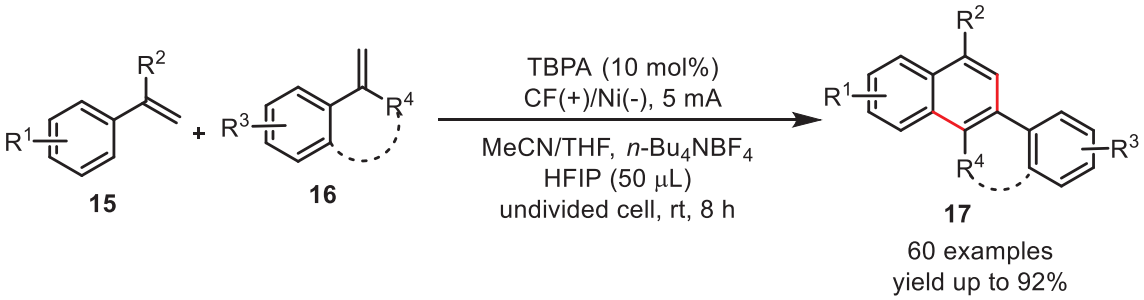

Scheme 1.8 Electron-catalyzed [4+2] cycloaddition of two-component α-methyl styrenes

Lei and co-workers reported a dearomative [4+2] cycloaddition between different indoles through an electrochemical fashion **(Scheme 1.9)**. Moreover, simple procedures could transform the product into useful synthetic intermediates and pharmaceutical compounds. In particular, this method applies to functionalize methionine, melatonin-involved cycloaddition, and cycloaddition involving loxoprofen, probenecid, and zaltoprofen. All of them exhibited non-negligible responsiveness. Additionally, the reaction shows reasonable practicability at gram-scale experiments and pyrimido[5,4-*b*]indoles synthesis in high yields that can be helpful synthetic intermediates. The possible mechanism of the reaction is as follows. Initially, the oxidation of indole (**18)** at the anode generates the indole radical cation. Simultaneously, (**19)** undergoes SET oxidation with the assistance of an equivalent base to generate the *N*-centred radical. The indole radical cation and the *N*-centred radical undergo a radical–radical cross-coupling reaction and subsequent intramolecular cycloaddition to give the product (**20)** with excellent regioselectivity. Hexafluoroisopropanol (HFIP) is produced simultaneously with cathodic reduction during the reaction, releasing hydrogen gas.[39]

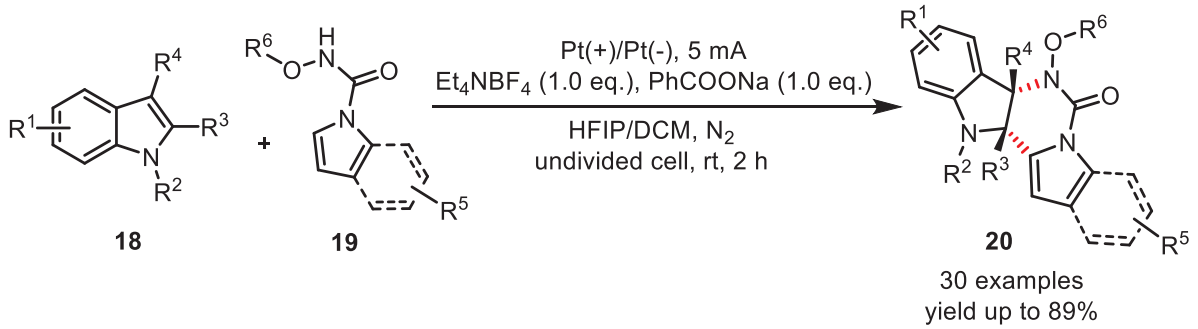

Scheme 1.9 Electrochemical catalyzed [4 + 2] cycloaddition between indoles and 1-alkyl indole derivatives

In 2022, Sun's group reported the electrochemical [3 + 2] cycloaddition of anilines **(21)** and 1,3-dicarbonyl **(22)** derivatives **(Scheme 1.10)**. The reaction is directly executed with 30 mol% TfOH in a solution of *n*-Bu_4NBF_4 in HFIP without the need for metal catalysts or external oxidants, providing a powerful method for the construction of a broad range of multi-substituted indoles **(23)**. The anodic oxidation of aniline and 1,3-dicarbonyl simultaneously forms nitrogen-centered radical and 1,3-dicarbonyl radical, in which nitrogen-centered radical resonates to give carbon-centered radical. Later, radical–radical cross-coupling and tautomerization followed intramolecular condensation to afford the final product. Meanwhile, the cathode reduces protons to H_2.[40]

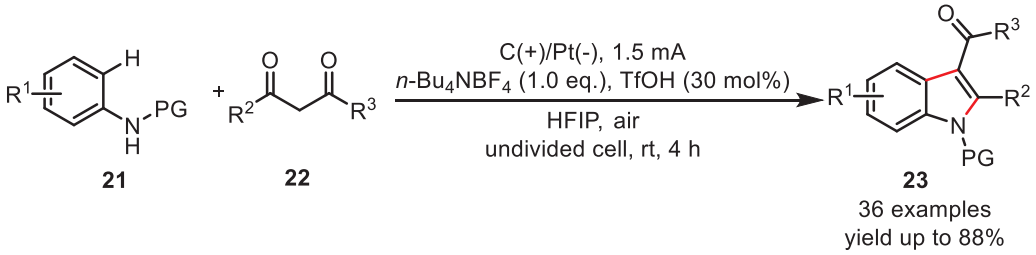

Scheme 1.10 Electrochemical [3 + 2] cycloaddition of anilines and 1,3-dicarbonyl derivatives

Lei and co-workers have recently reported an interesting electrochemical oxidative difunctionalization of diazo compounds (**25**) with two different nucleophiles (**24** and **26**) **(Scheme 1.11)**. The reaction can be carried out using inexpensive and commercially accessible radical sources (such as S and C) and nucleophiles (such as alcohol, amine, acid, and halogen anion). This straightforward approach eliminates the use of transition metals and external oxidants, as well as the pre-activation of substrates (such as electrophiles) and harsh conditions.

Excellent functional group compatibility, large-scale synthesis efficiency, and a wide range of synthetic applications demonstrate the transformation's capabilities.[41]

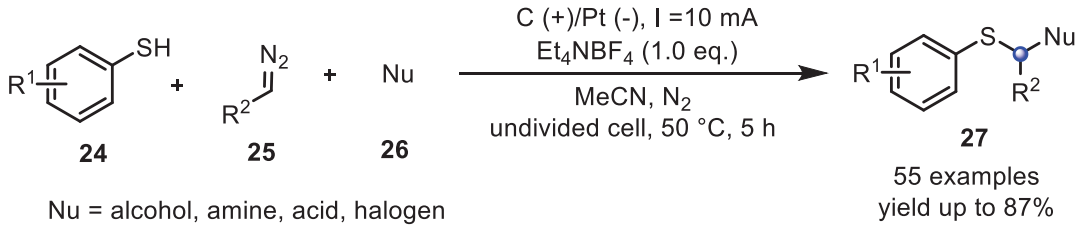

Scheme 1.11 Electrochemical oxidative difunctionalization of diazo compounds

1.9 Conclusion and outlook

The goal of this Ph.D. work is to broaden the scope of electro-organic synthesis to include the formation of carbon-carbon and carbon-nitrogen bonds using an electrochemical oxidative pathway. This chapter presents a brief historical overview, as well as concepts, techniques, methodology, and the importance of electro-organic synthesis. Recently, electro-organic synthesis has been recognized as one of the primary techniques capable of achieving several desirable goals to establish an environmentally friendly procedure. This methodology can be used to replace harmful redox reagents, decrease the energy requirement, and for the *in situ* generation of unstable reagents. The electrochemical technique is a simple and potent method in modern organic synthesis. The electrochemical process can accomplish various functional group conversions and carbon-carbon or carbon-heteroatom bond formations. Several electrochemical transformations and efficient processes were developed using batch or flow electrolysis cells. Electro-organic synthesis applications are not restricted to the small laboratory scale; specific large-scale production procedures have already been established and are involved in the creation of value-added compounds on an industrial scale. Electrolysis occurs on the electrode surface, allowing for selective redox chemical changes without external oxidizing or reducing reagents, eliminating the creation of chemical waste associated with previous approaches. As a result, electroorganic synthesis is innately greener than the traditional chemical approaches, lowering the environmental impact of chemical operations.

1.9 References

1. Pollok, D.; Waldvogel, S. R. *Chem. Sci.*, **2020**, *11*, 12386–2400.
2. Hammerich, O.; Speiser, B.; Editors, *Organic Electrochemistry: Revised and Expanded, Fifth Edition*, CRC Press, **2016**.

3. Fuchigami, T.; Atobe, M.; Inagi, S.; Editors, *Fundamentals and Applications of Organic Electrochemistry: Synthesis, Materials, Devices*, Wiley, **2014**.
4. Minteer, S. D.; Baran, P. *Acc. Chem. Res.* **2020**, *53*, 545–546.
5. (a) Zhu, C.; Ang, N. W. J.; Meyer, T. H.; Qiu, Y.; Ackermann, L. *ACS Cent. Sci.* **2021**, *7*, 415–431. (b) Novaes, L. F. T.; Liu, J.; Shen, Y.; Lu, L.; Meinhardt, J. M.; Lin, S. *Chem. Soc. Rev.* **2021**, *50*, 7941–8002. (c) Utley, J. *Chem. Soc. ReV.* **1997**, *26,* 157–167. (d) Moeller, K. D. *Tetrahedron* **2000**, *56,* 9527–9554. (e) Lund, H. J. *Electrochem. Soc.* **2002**, *149,* S21–S33. (f) Baijer, M. M.; Petrovich, J. J. *Physical Organic Chemistry*, Interscience, New York, Vol. VII, **1970**, 189–227. (g) Barclay, D. J. *J. Electroanal. Chem.* **1968**, *19*, 315–318. (h) Bard, A. J.; Faulkner, L. R. *Electrochemical Methods Fundamentals and Applications,* Wiley, New York, **1980**, 392. (i) Desbarres, J.; Plichet, P.; Benoit, R. L. *Electrochem. Acta* **1968**, *13*, 1899–1904. (j) Fry, A. J.; Chung, L. L.; Boekelheide, V. *Tetrahedron Lett.* **1974**, *15*, 445–450. (k) Mann, C. K. *In Electroanalytical chemistry* (A. J. Bard, ed.), Dekker, New York, **1969**, *3*, 57. (l) Puglisi, V. J.; Clapper, G. L.; Evans, D. H. *Anal. Chem.*, **1969**, *41*, 279–282. (m) Shono, T.; Kise, N.; Suzumoto, T.; Morimoto, T. *J. Am. Chem. Soc.* **1986**, *108*, 4676–4677.
6. (a) Elsherbini, M.; Wirth, T. *Acc. Chem. Res.* **2019**, *52*, 3287–3296. (b) Noël, T.; Cao, Y.; Laudadio, G. *Acc. Chem. Res.* **2019**, *52*, 2858–2869. (c) Pletcher, D.; Green, R. A.; Brown, R. C. D. *Chem. Rev.* **2018**, *118*, 4573–4591. (d) Atobe, M.; Tateno, H.; Matsumura, Y. *Chem. Rev.* **2018**, *118*, 4541–4572.
7. Yan, M.; Kawamata, Y.; Baran, P. S. *Chem. Rev.*, **2017**, *117*, 13230–3319.
8. Yan, M.; Kawamata, Y.; Baran, P. S. *Angew. Chem. Int. Ed.*, **2018**, *57*, 4149–4155.
9. Philos, V.; *Trans. R. Soc.,* **1800,** *90*, 403–431.
10. Faraday, M.; Philos. *Trans. R. Soc.,* **1834**, *124*, 77–122.
11. Lebreux, F. D. R.; Buzzo, F.; Marko, I. N. *Synlett.*, **2008**, *18*, 2815–2820.
12. Kolbe, H.; *J. Prakt. Chem.*, **1847**, *41*, 137–139.
13. Yoshida, J.; Kataoka, K.; Horcajada, Nagaki, R. *A. Chem. Rev.,* **2008**, *108,* 2265–2299.
14. Frontana-Uribe, B. A.; Little, R. D.; Ibanez, J. G.; Palma, A.; Vasquez-Medrano, R. G*reen Chem.,* **2010**, *12*, 2099–2119.

15. Leech, M. C.; Garcia, A. D.; Petti, A.; Dobbs, A. P.; Lam, K. *React. Chem. Eng*., **2020**, *5*, 977–990.
16. Little, R. D.; Moeller, K. D. *Interface*, **2002**, *11*, 36–42.
17. Schotten, C.; Nicholls, T. P.; Bourne, R. A.; Kapur, N.; Nguyen, B. N.; Willans, C. E. *Green Chem.* **2020**, *22*, 3358–3375.
18. Kingston, C.; Palkowitz, M. D.; Takahira, Y.; Vantourout, J. C.; Peters, B. K.; Kawamata, Y.; Baran, P. S. *Acc. Chem. Res.* **2020**, *53*, 72–83.
19. Heard, D. M.; Lennox, A. J. J. *Angew. Chem. Int. Ed.* **2020**, *59*, 18866–8884.
20. Elgrishi, N.; Rountree, K. J.; McCarthy, B. D.; Rountree, E. S.; Eisenhart, T. T.; Dempsey, J. L. *J. Chem. Educ.* **2018**, *95*, 197–206.
21. Chakraborty, P.; Mandal, R.; Garg, N.; Sundararaju, B. *Coord. Chem. Rev.* **2021**, *444*, 214065–214088.
22. Francke, R.; Little, R. D. *Chem. Soc. Rev.* **2014**, *43*, 2492–2521.
23. Arnaboldi, S.; Magni, M.; Mussini, P. R. *Curr. Opin. Electrochem.* **2018**, *8*, 60–72
24. Lin, Q.; Li, L.; Luo, S. *Chem. Eur. J.* **2019**, *25*, 10033–10044.
25. Ghosh, M.; Shinde, V. S.; Rueping, M. *Beilstein J. Org. Chem.* **2019**, *15*, 2710–2746.
26. Park, D. il; Jung, S.; Yoon, H. J.; Jin, K. *Electrochim. Acta.* **2021**, *139*, 271–276.
27. Deronzier, A.; Moutet, J.-C. *Platinum Metals Rev.* **1998**, *42*, 60–68.
28. Osa, T.; Kashiwagi, Y.; Mukai, K.; Ohsawa, A.; Bobbitt, J. M. *Chem. Lett.* **1990**, 75–78.
29. J. E. B. Randles, *Trans. Faraday Soc.*, **1948**, *44*, 327–338
30. N. Elgrishi, K. J. Rountree, B. D. McCarthy, E. S. Rountree, T. T. Eisenhart and J. L. Dempsey, *J. Chem. Educ.*, **2018**, *95*, 197–206.
31. E. Barrado, R. A. S. Couto, M. B. Quinaz, J. L. F. C. Lima and Y. Castrillejo, *J. Electroanal. Chem.*, **2014**, *720*, 139–146.
32. Sheng, T.; Zhang, H.-J.; Shang, M.; He, C.; Vantourout, J. C.; Baran, P. S. *Org. Lett.* **2020,** *22*, 7594–7598.
33. Wang, Z. H.; Gao, P. S.; Wang, X.; Gao, J. Q.; Xu, X. T.; He, Z.; Ma, C.; Mei, T. S. *J. Am. Chem. Soc.* **2021**, ***143***, 15599–15605.
34. Liang, S.; Zeng, C. C.; Luo, X. G.; Ren, F. Z.; Tian, H. Y.; Sun, B. G.; Little, R. D. *Green Chem.* **2016**, *18*, 2222–2230.

35. Tang, S.; Gao, X.; Lei, A. *Chem. Commun.* **2017**, *53*, 3354–3356.
36. Jiang, Y.-Y.; Dou, G.-Y.; Xu, K.; Zeng, C.-C. *Org. Chem. Front.* **2018**, *5*, 2573–2577.
37. Li, A.; Li, C.; Yang, T.; Yang, Z.; Liu, Y.; Li, L.; Tang, K.; Zhou, C. *J. Org. Chem.* **2023**, *88*, 1928–1935.
38. Ma, Y.; Lv, J.; Liu, C.; Yao, X.; Yan, G.; Yu, W.; Ye, J. *Angew. Chem., Int. Ed.* **2019**, *58*, 6756–6760.
39. Song, C.; Liu, K.; Jiang, X.; Dong, X.; Weng, Y.; Chiang, C.-W.; Lei, A. *Angew. Chem., Int. Ed.* **2020**, *59*, 7193–7197.
40. Chang, X.; Chen, X.; Lu, S.; Zhao, Y.; Ma, Y.; Zhang, D.; Yang, L.; Sun, P. *Adv. Synth. Catal.*, **2022**, *364*, 2865–2871.
41. Yang, D.; Guan, Z.; Peng, Y.; Zhu, S.; Wang, P.; Huang, Z.; Alhumade, H.; Gu, D.; Yi, H.; Lei, A. *Nat Commun* **2023**, *14*, 1476–1480.

CHAPTER 2

Electrochemical Oxidative Coupling between Benzylic C(sp^3)–H and N–H of Secondary Amines: Rapid Synthesis of *α*-Amino *α*-Aryl Esters

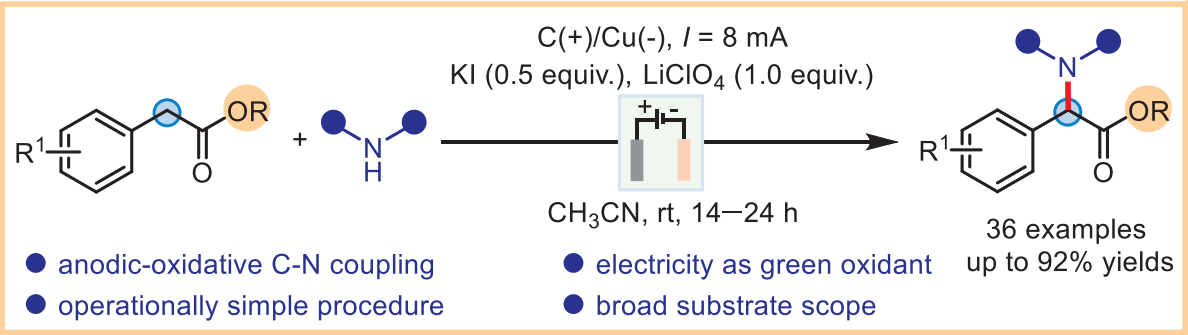

2.1 Introduction

The direct oxidative cross-dehydrogenative coupling (CDC) of C–H (carbon-hydrogen) and N–H (nitrogen-hydrogen) bonds to form a new C–N bond is indeed an essential and influential method in modern organic synthesis. This transformation allows for the efficient construction of C–N bonds, which are prevalent in a wide range of organic compounds, including pharmaceuticals, agrochemicals, and materials. This method offers several advantages including atom efficiency, less waste, and avoiding pre-functionalized starting materials. The CDC reaction involves directly coupling a C–H bond from one reactant and an N–H bond from another to form a new C–N bond. This process usually requires an oxidant or catalyst to promote the reaction.[1a] It represents a high-step and atom-economical process since prefunctionalization of the substrates is avoided, and hydrogen is the only formal byproduct.[1b] Along this line, significant advances have been made, especially in the oxidative C(sp^2)–H couplings to form various C–N bonds. The α-C(sp^3)–H functionalization and α-amination of carbonyl compounds remain a transformation of central importance in synthetic and medicinal chemistry as a straightforward route to versatile building units widely present in natural products and pharmaceuticals.[1c-g] A reaction between nucleophilic-synthons of carbonyl compounds, such as enolates or enamines with preformed electrophilic amine reagents, is a well-explored technique to access α-amino-carbonyls.[2] Besides, the reaction between pre-functionalized carbonyls and nucleophilic amine ($N^{-\delta}$) has also been explored along with other conventional methods.[3] The direct C(sp^3)−H functionalization will offer a straightforward approach to introduce functionality to organic skeletons.[4] The direct dehydrogenative C-N bond formation between the proximal position of carbonyls and the nucleophilic amine is the shortest route to access α-amino carbonyls. However, it requires a polarity reversal of two electronically mismatched units.[5] Despite remarkable recent advances for accessing α-amino-carbonyls, more strictly, these methods are mainly limited to the readily enolizable lower oxidation state substrates, such as aldehydes/ketones **(Scheme 2.1)**, and hardly applicable with esters. The direct decarboxylative coupling between highly activated acids with amine is an exciting way to access α-amino acid esters[6] and other methods.[7] Thus, developing a direct, simple, and environmental friendly process accessing α-amino carbonyls such as α-amino acid esters is highly desirable. Notably, α-amino acids and their derivatives have medicinal significance and importance in artificial sweeteners, food additives, cosmetic additives, and many more applications **(Figure 2.1)**.[8]

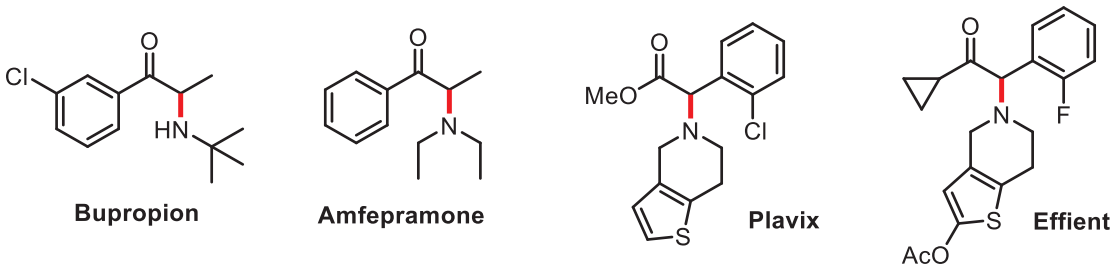

Figure 2.1 Representative examples of α-amino carbonyl compounds

In this context, MacMillan and coworkers developed direct α-amination of carbonyl compounds like ketones, esters, and aldehydes (**1**) with cyclic and acyclic secondary amines (**2**) under Cu-catalyzed aerobic conditions. In this reaction, copper(II) bromide (0.1 equiv.) acts as the brominating agent, and air is the oxidant to furnish α-aminated compounds (**3**) in up to 93% yield **(Scheme 2.1).**[5a]

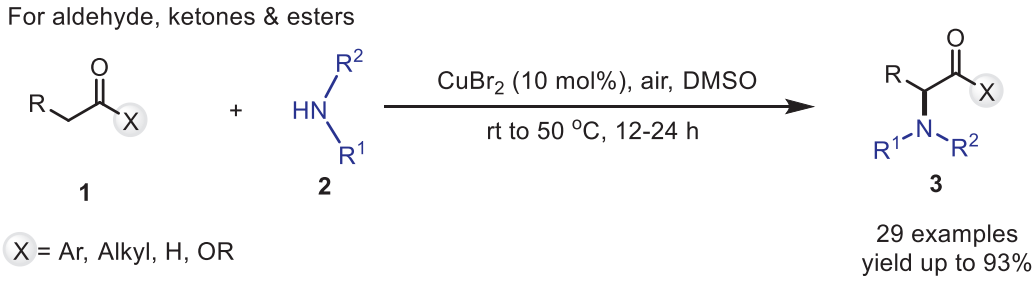

Scheme 2.1 Copper-catalyzed synthesis of α-aminated compounds

Initially, Prabhu and coworkers reported that aryl/heteroaryl-ketones (**4**) with aliphatic or aromatic substituents on the α-position were successfully aminated with cyclic secondary amines (**2**) when treated with *N*-iodosuccinimide (30 mol%) and tertbutyl hydroperoxide (3.0 equiv.) to afford desired products (**5**) in up to 80% yield **(Scheme 2.2)**. The use of the methodology was demonstrated by the synthesis of an ifenprodil derivative in 50% yield from commercially available starting materials.[5b]

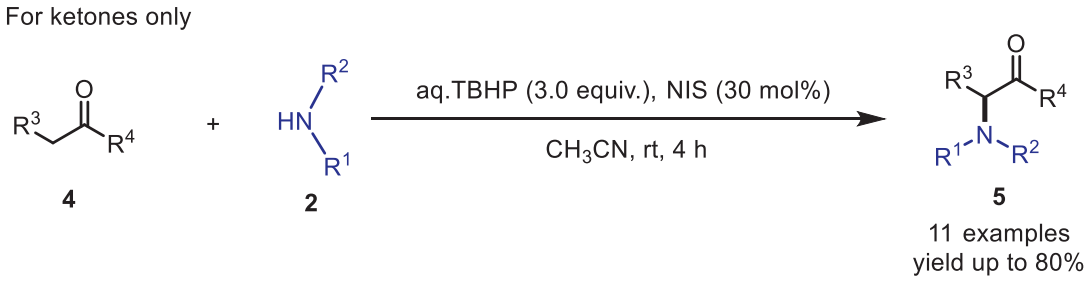

Scheme 2.2 NIS-catalyzed oxidative coupling of ketones and secondary amines

In 2015, the Sekar group developed an NBS-mediated open-flask synthesis of benzylic alcohols (**6**) and nitrogen nucleophiles (**2**) **(Scheme 2.3)**. This operationally simple transformation produced the desired products (**5**) in up to 94% yield, with secondary cyclic amines yielding the best results. Although the electronic properties of the aromatic substituent had no effects on yields, sterically hindered starting materials resulted in a significant decrease. From commercially available starting materials, 60% and 68% of the medicinally relevant amfepramone and pyrovalerone were obtained in a single step, respectively.[5c]

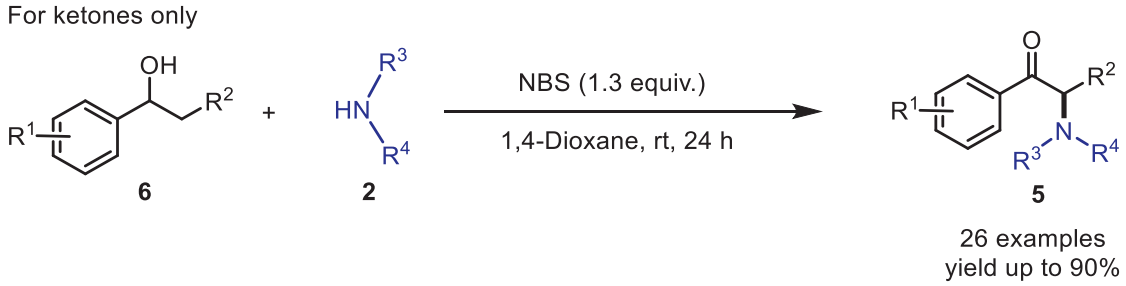

Scheme 2.3 NBS-mediated synthesis of *α*-amino ketones from benzylic alcohol

Guo and coworkers showed that the substrate scope could be extended to include primary and acyclic secondary amines (**2**) when employing ammonium iodide (15 mol%) and sodium percarbonate **(Scheme 2.4)**. Notably, amines containing reactive functional groups, such as allyl or aniline, were tolerated in this methodology. The synthesis of amfepramone in 72% yield demonstrated the procedure's utility.[5d]

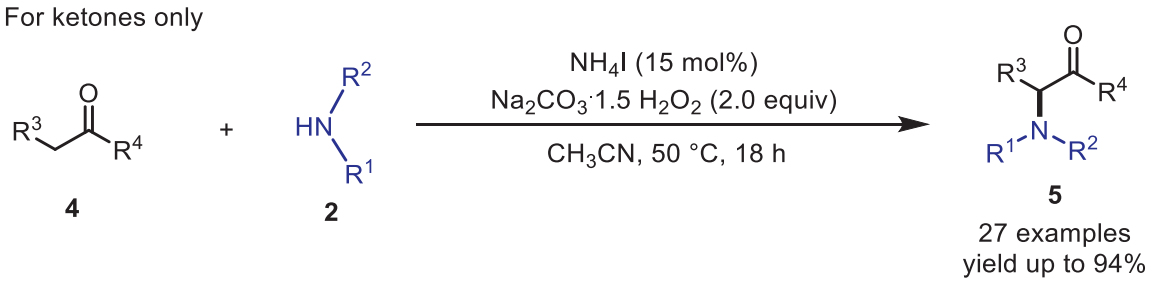

Scheme 2.4 NH_4I/peroxide-mediated *α*-amination of ketones

In 2016, electrochemical *α*-halogenation was applied to amino ketone synthesis to remove the stoichiometric oxidants or metals requirement. Liang *et al*. demonstrated that molecular iodine could be generated from ammonium iodide (0.5 equiv.) at the cell's graphite anode in an undivided cell, allowing for *α*-iodination of several mono disubstituted-ketones **(7)**. The transient *α*-iodocarbonyl was substituted *in situ* with a variety of secondary amines (**2**) to obtain the

desired α-amino ketones (**8**) in up to 75% yield, with cyclic amines performing on average better than acyclic substrates **(Scheme 2.5)**.[5e]

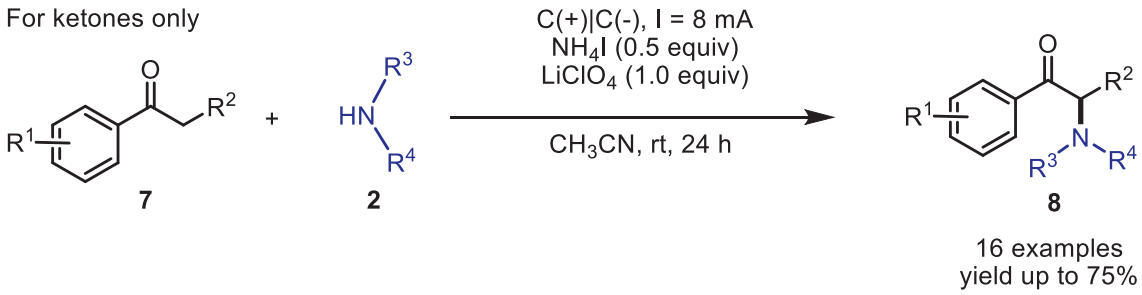

Scheme 2.5 Synthesis of α-amino ketones via the electrochemical oxidative cross-dehydrogenative coupling

On the other hand, electrochemical organic transformations have recently gained much attention as sustainable protocols under mild conditions.[9] The electrochemical oxidative C-H functionalization for C-C,[10] C-O[11] and C-N[12] bond formation has been achieved using metal-catalysis or metal-free conditions. Despite these efforts, the direct electrochemical amination of the C(sp^3)-H bond remains elusive.[13] In this chapter, we wish to disclose the synthesis of α-amino acid esters through electrochemical oxidative coupling between benzylic C(sp^3)-H bonds and secondary amines. The protocol offers mild and direct access to various α-amino acid esters under metal-free conditions while tolerating organic functionalities **(Scheme 2.6)**

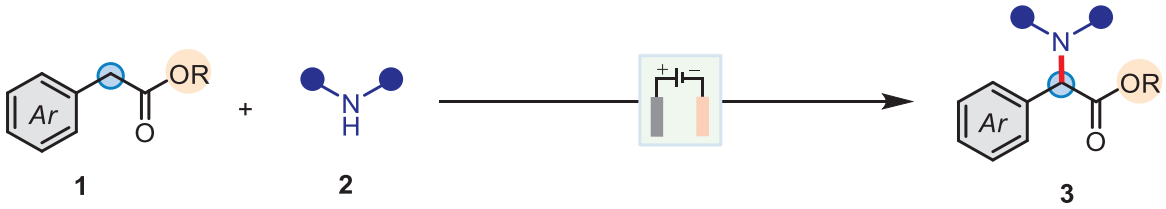

Scheme 2.6 Electrochemical amination of the α-aryl acetates

2.2 Results and discussion

To evaluate the feasibility of our proposed synthetic pathway, initially, we examined the model reaction; methyl 2-(3-chlorophenyl) acetate **1a,** and pyrrolidine **2a** were employed as model substrates (Table 2.1). Extensive experiments for finding suitable reaction parameters such as electrodes, electrolytes, catalysts, and solvents (Table 2.1) were performed and led to identifying the optimal reaction conditions. The desired α-amino ester **3aa** was obtained in 89% yield under optimized conditions (entry 1, Table 2.1). Next, increasing (entry 2, Table 2.1) or decreasing the applied current (entry 3, Table 2.1) from standard conditions to the vessel reduces the reaction

yields. A similar result with 45-65% yields was obtained by changing the electrode system under standardized conditions (entries 4-7, Table 2.1). When the iodide source changed as an NH_4I, the desired product yield decreased to 76% respectively (entry 8, Table 2.1). For instance, no desired product was found when NaBr were employed instead of KI (entry 9, Table 2.1). No desired product **3aa** was detected by without KI and electric current (entries 10–11, Table 2.1). Moreover, other electrolytes were also tested, such as *n*-Bu_4NBF_4 and *n*-Bu_4NClO_4, but all gave inferior results compared to $LiClO_4$ (entries 12–13, Table 2.1). The addition of bases (1.0 equiv.) under standard conditions (entries 14-15, Table 2.1) or varying solvent medium (entries 16-18, Table 2.1) did not improve the reaction yields. Thus, we prefer to perform the reaction under optimized conditions.

With the optimal conditions, the reaction's scope was investigated with various esters and amines (Table 2.1). Initially, pyrrolidine was tested with multiple meta-chlorophenyl acetic esters (-Me, -Et, -^{i}Pr, -^{t}Bu) and furnished corresponding α-amino-esters **3aa**-**3da** (up to 89%). Moreover, different ortho-chlorophenyl acetic esters (*i.e.*, -Me, -Et, -allyl, -cyclohexyl, -benzyl and -piperonyl) were initially employed with pyrrolidine to finish corresponding α-amino-esters **3ea**-**3ja** (up to 76%). Next, a series of methyl and ethyl α-aryl acetates having substitutions (halogens/electron-withdrawing group) at the different aromatic ring positions were tested with pyrrolidine, and corresponding final products **3ka-3ra** obtained up to 85%.

However, the reaction did not produce the desired outcome in the presence of electron-donating groups. The scope of various acyclic/cyclic secondary amines was tested with methyl 2-(3-chlorophenyl) acetate **1a** to yield corresponding products **3ab**-**3al** (up to 92%). A similar trend was observed in the formation of **3kc**-**3nc** and **3ef**-**3of**, where piperidine and morpholine were coupled with various esters. The protocol was extended with a secondary amine that exists in cetirizine, a drug molecule, and complementary product **3aj** was obtained with 68% yield under optimized conditions. The developed method is mainly limited to α-aryl acetates and secondary aliphatic amines. The reaction failed to give α-amino-α-aryl acetates with aniline(s)/primary/secondary aromatic amines or with sterically hindered aromatic esters/acids/amides and aliphatic ester under optimized conditions.

Table 2.1 Optimization of reaction conditions [a]

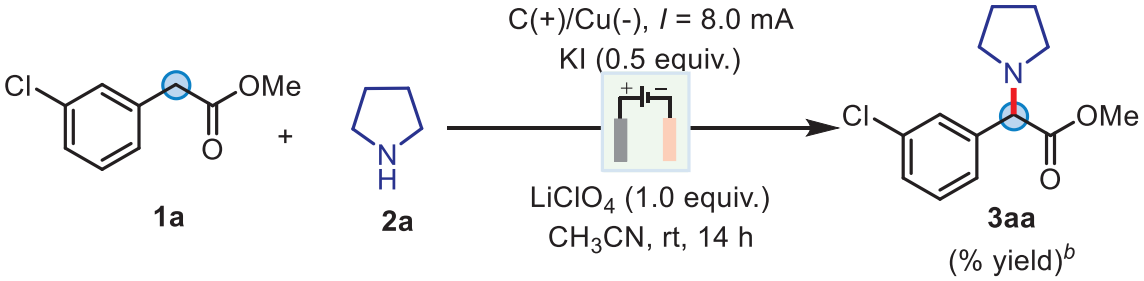

1a 2a 3aa (% yield)[b]

Entry	Variation from standard conditions	Yield (%)
1	none	89
2	I = 10.0 mA, instead of I = 8.0 mA	56
3	I = 6.0 mA, instead of I = 8.0 mA	71
4	C(+)/C(-) used instead of C(+)/Cu(-)	65
5	Cu(+)/C(-) used instead of C(+)/Cu(-)	-
6	C(+) | Pt(-) used instead of C(+)/Cu(-)	55
7	Pt(+) | Pt(-) used instead of C(+)/Cu(-)	45
8	TBAI (0.5 equiv.) used instead of KI (0.5 equiv.)	76
9	NaBr (0.5 equiv.) used instead of KI (0.5 equiv.)	0
10	without KI	-
11	without electricity	-
12	*n*-Bu_4NBF_4 (1.0 equiv.) used instead of $LiClO_4$ (1.0 equiv.)	81
13	*n*-Bu_4NClO_4 (1.0 equiv.) used instead of $LiClO_4$ (1.0 equiv.)	75
14	Lutidine (1.0 equiv.) used as an additive	74
15	K_2CO_3 (1.0 equiv.) used as an additive	68
16	MeOH as a solvent instead of CH_3CN	45
17	DMF as a solvent instead of CH_3CN	20
18	THF as a solvent instead of CH_3CN	38

[a]**Reaction conditions**: **1a** (1.0 mmol), **2a** (3.0 mmol), KI (0.5 mmol), $LiClO_4$ (1.0 mmol) in MeCN (10 mL), C-anode, Cu-cathode, undivided cell, constant current = 8 mA, at rt under N_2 atmosphere for 14 h. [b]All isolated yields were based on **1a**.

Table 2.2 Substrate scope of various esters 1[a]

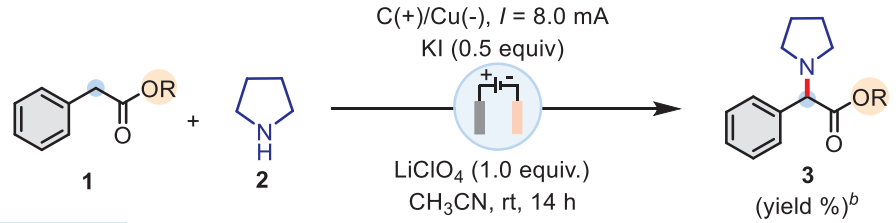

with various esters

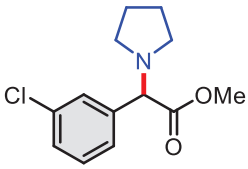
(3aa, 89%)

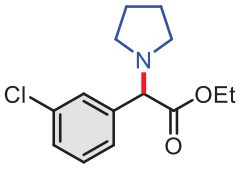
(3ba, 85%)

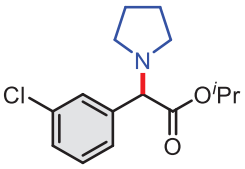
(3ca, 81%)

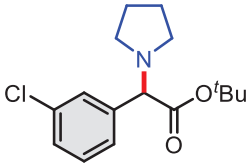
(3da, 72%)

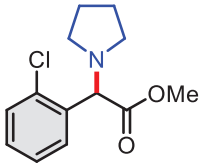
(3ea, 76%)

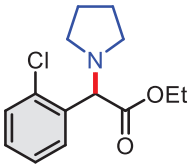
(3fa, 74%)

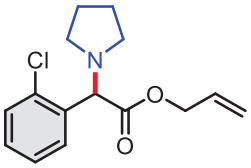
(3ga, 73%)

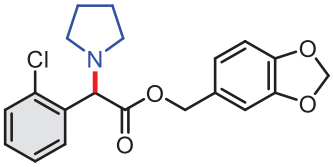
(3ha, 68%)

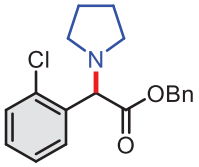
(3ia, 70%)

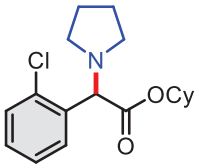
(3ja, 69%)

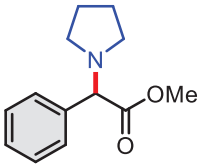
(3ka, 81%)

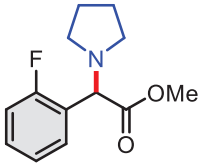
(3la, 71%)

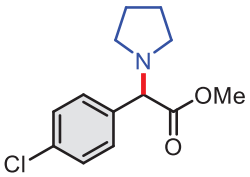
(3ma, 85%)

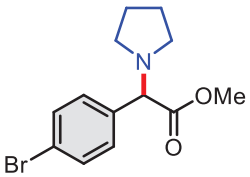
(3na, 83%)

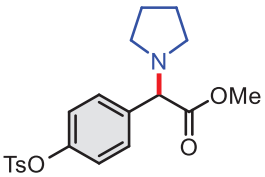
(3oa, 78%)

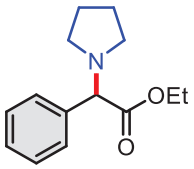
(3pa, 77%)

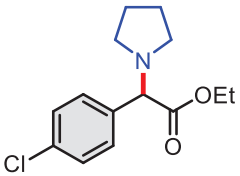
(3qa, 79%)

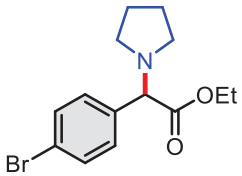
(3ra, 77%)

[a]**Reaction conditions**: **ester** (1.0 mmol), **amine** (3.0 mmol), KI (0.5 mmol), $LiClO_4$ (1.0 mmol) in CH_3CN (10 mL), C-anode, Cu-cathode, undivided cell, constant current = 8 mA, at rt under N_2 atmosphere for 12-20 h. [b]All isolated yields were based on **ester**.

Table 2.3 Substrate scope of various amines and esters[a]

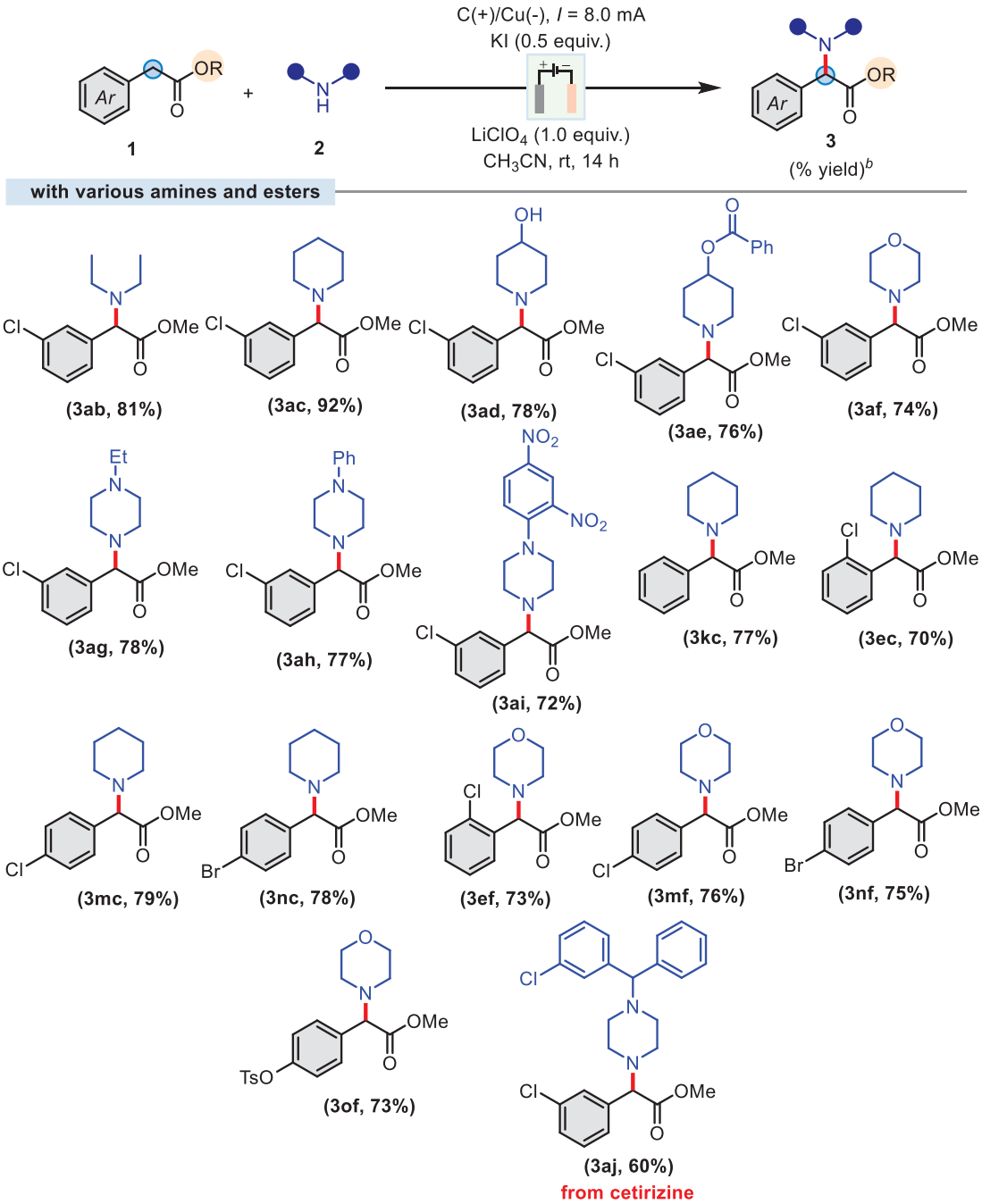

[a]**Reaction conditions**: **ester** (1.0 mmol), **amine** (3.0 mmol), KI (0.5 mmol), $LiClO_4$ (1.0 mmol) in CH_3CN (10 mL), C-anode, Cu-cathode, undivided cell, constant current = 8 mA, at rt under N_2 atmosphere for 12-20 h. [b]All isolated yields were based on **ester**.

2.3 Cyclic voltammetry experiment

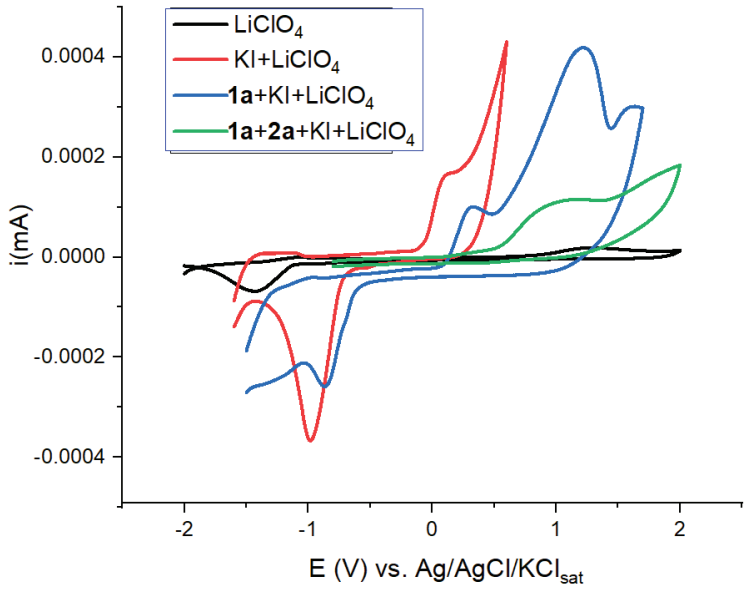

Figure 2.2 Cyclic voltammogram of $CH_3CN/LiClO_4$ (10 mL, 0.1 M) (**black**); **KI** (0.01 M) in $CH_3CN/LiClO_4$ (10 mL, 0.1 M) (**red**); **ester 1a** (0.01 M), **KI** (0.01 M) in $CH_3CN/LiClO_4$ (10 mL, 0.1 M) (**blue**); **ester 1a** (0.01 M), **pyrrolidine 2a** (0.01 M), **KI** (0.01 M) in $CH_3CN/LiClO_4$ (10 mL, 0.1 M) (**green**); Reference electrode: Ag/AgCl (3 M KCl), scan rate: 0.2 V/s.

For clarification of the reaction mechanism, electroanalytical measurements were performed. The cyclic voltammogram (CV) of KI with $LiClO_4$ as an electrolyte showed redox Potential (peak potentials: +0.211 and -0.911 V vs Ag/AgCl as reference electrode). The CV of the substrates **1a**, KI, and $LiClO_4$ showed oxidation potential: +1.30 V vs Ag/AgCl as the reference electrode. Finally, the CV of all the reacting species **1a**, **2a**, KI, and $LiClO_4$ showed oxidation potential: +1.05 V vs Ag/AgCl as a reference electrode (Figure 2.2). The formation of iodo-compound **9** through the combination of ester **1** with *in situ* generated I_2 could be the initial outcome before reacting with amine **2.**

2.4 Control experiments, Reaction mechanism, Synthetic applications

A set of control experiments were performed to gain more mechanistic insights into the electrochemical process. Initially, α-iodo- α-aryl methyl acetate 38 (45%) was isolated when a controlled experiment was conducted with amine **2a** (1.0 equiv.) under optimized conditions (**Scheme 2.7 (i)**). The resulting iodo-ester **9** was separately reacted with amine **2a** (2.5 equiv.) to furnish **3aa** (89% yield), which confirms that the reaction proceeds through α-iodination,

followed by displacement with the amine to provide the desired compound (**Scheme 2.7 (ii)**). On the other hand, the product **3aa** formation was not observed with BHT or TEMPO as a radical scavenger under the standard electrochemical conditions, confirming the radical pathway of the reaction at the intermediate steps (**Scheme 2.7 (iii)**).

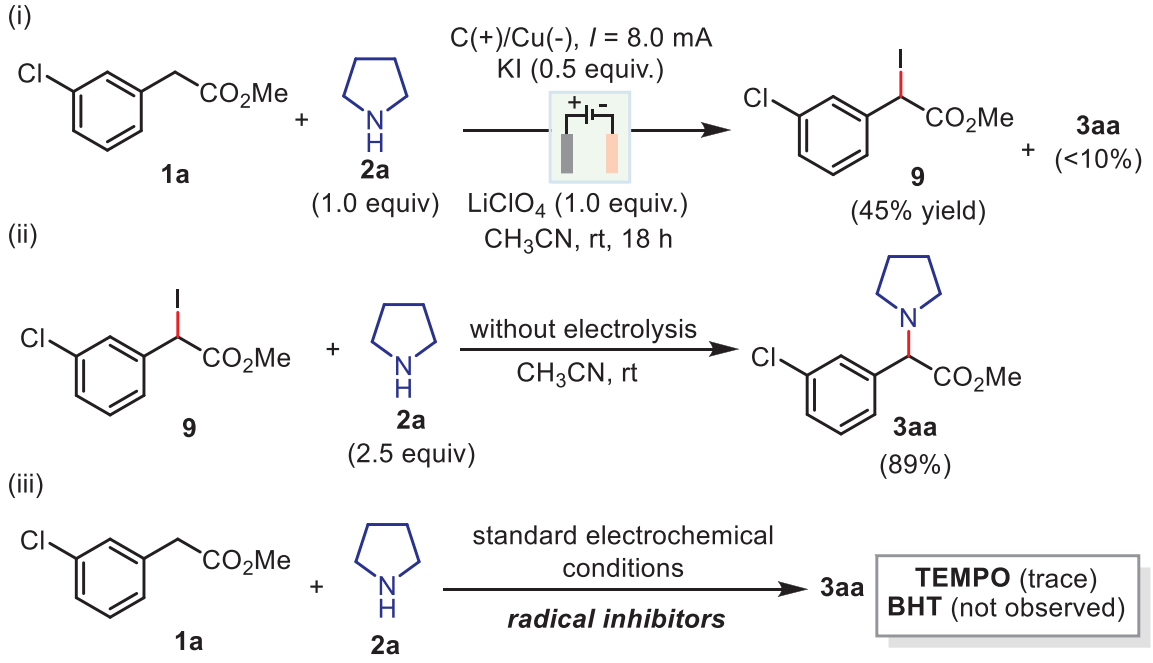

Scheme 2.7 Set of control experiments

We proposed a reaction mechanism based on the cyclic voltammogram (CV) and other controlled experimental observations (Scheme 2.8). Ester **9** could be generated through a radical pathway in which intermediate (**A**) developed through the sequential reaction with radical iodine (I^*). Once the critical intermediate **9** is formed, it soon undergoes a nucleophilic substitution reaction with an amine **2a**, leading to the final α-amination product **3aa**, accompanying the second molecular HI. Simultaneously, the *in situ* generated HI is reduced to evolve H_2 on the cathode surface and regenerate iodide-ion and the step of α-iodination of ester **1a**; thus, requiring a catalytic amount of KI. Alternatively, ester **1a** could react with molecular iodine, *in situ* generated through the anodic oxidation, to α-iodo-ester **9**, which will undergo a displacement reaction with an amine.

The practical utility of the developed electrochemical protocol was demonstrated for the gram-scale, and **3ac** (1.30 g, 90% yield) was obtained without much variation in the product yield under optimized conditions (eq. 1, Scheme 2.9). Besides, synthetic conversion of ester **3ac** was

performed to corresponding azido compound **10** (58% yield) with a three-step protocol (eq. 2, Scheme 2.9). Similarly, *α*-amino ester **3ec** was efficiently transformed to the corresponding amide **11** (76% yield) (eq. 3, Scheme 2.9).

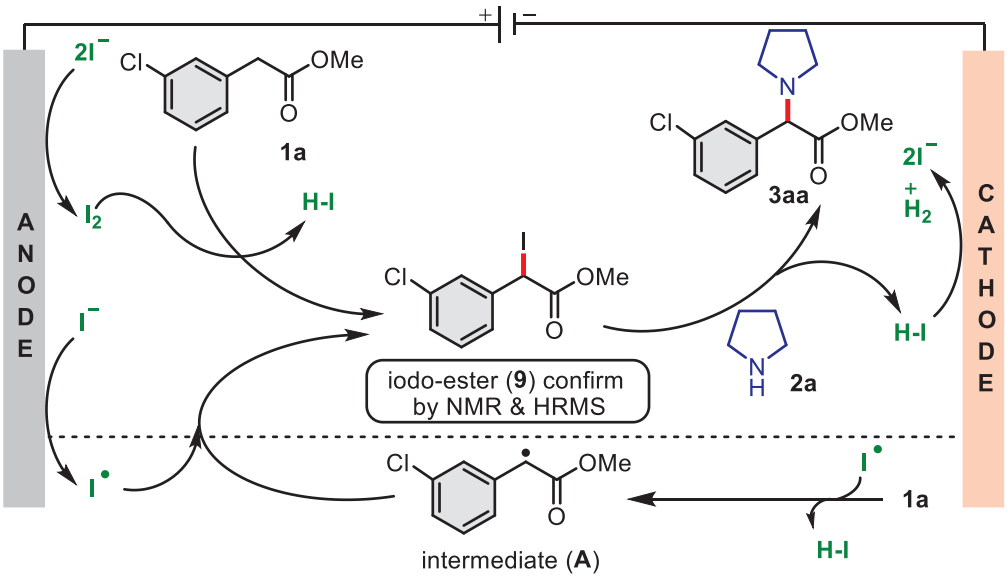

Scheme 2.8 Proposed reaction mechanism for the electrochemical amination of *α*-aryl acetates

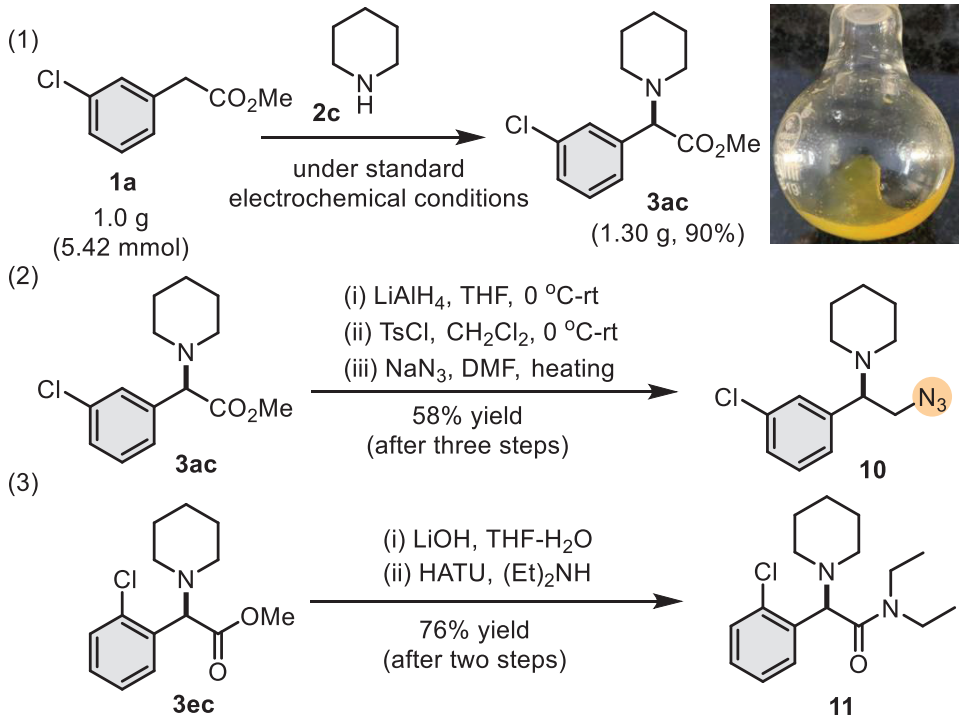

Scheme 2.9 Gram scale synthesis and synthetic applications to azido- and amide compounds

2.5 Conclusions

In summary, we have developed an efficient electrochemical protocol for intermolecular oxidative coupling between α-aryl acetates (C(sp^3)-H bond) and secondary amines (N-H bond). The mild electrocatalytic condition furnishes α-amino-esters by stitching together two electronically mismatched units through C-N bond formation, with a high yield (up to 92%). The reactions can be scaled up without impacting the process efficiency, and the resulting α-amino-esters can be functionalized to other similar biorelevant compounds.

2.6 General experimental methods

Unless otherwise stated, all commercially available compounds were used as received without further purification. Graphite and other electrodes were purchased from IKA, and all the electrochemical reactions were performed under N_2 at room temperature using IKA Electrasyn 2.0. Cyclic Voltammetric (CV) experiments were performed using CH Instruments electrochemical Analyzer (Model CHI1200B). CH_3CN and other solvents were obtained from Merck Life Science Private Limited and were distilled from appropriate drying agents before use in the reactions. All the α-aryl acetates were prepared using the reported procedure.[14] Reactions under the standard conditions were monitored by thin-layer chromatography (TLC) on Merck silica gel 60 F254 pre-coated plates (0.25 mm) under UV light at 254 nm. Column chromatographic purification was performed on silica gel (100–200 mesh) using an eluent of petroleum ether and ethyl acetate. Chemical yields refer to pure (>95% purity by ^{1}H NMR), isolated substances. Nuclear magnetic resonance (NMR) spectroscopy was recorded on a 400 MHz-NMR Spectrometer (Bruker). ^{1}H and ^{13}C NMR spectra were recorded in CDCl3 and calibrated to the solvent resonance as internal standard (^{1}H NMR, $CDCl_3$ at 7.26 ppm, ^{13}C NMR, $CDCl_3$ at 77.0 ppm). High-resolution mass spectra were recorded on Agilent 6545 Q-TOF LC/MS. Melting points were determined by EZ–Melt Automated Melting Point Apparatus.

2.6.1 General procedure for electrochemical *α*-amination of esters: A 10 mL dried undivided reaction cell equipped with a stirring bar was charged with appropriate α-aryl acetates **1** (1.0 mmol, 1.0 equiv), secondary amine **2** (3.0 mmol, 3.0 equiv), KI (83 mg, 0.5 mmol, 0.5 equiv), and $LiClO_4$ (106 mg, 1.0 mmol, 1.0 equiv) dissolved in CH_3CN (10.0 mL). The reaction mixture was electrolyzed using a Graphite plate anode and Copper plate cathode at a constant current condition (8 mA) under the N_2 atmosphere at room temperature. The Reaction progress was monitored by TLC. The reaction mixture was evaporated under reduced pressure, and the residue

mass was quenched by stirring between saturated aqueous $Na_2S_2O_3$ solution (5.0 mL) and ethyl acetate (10.0 mL). The organic layer was separated, dried over anhydrous Na_2SO_4, and evaporated under reduced pressure. Purification on silica gel column chromatography using a mixture of petroleum ether and ethyl acetate (9:1 to 1:1) as eluent afforded pure *α*-amino *α*-aryl esters **3** (up to 92% yield).

2.6.2 Characterization data of synthesized compounds

Methyl 2-(3-chlorophenyl)-2-(pyrrolidin-1-yl)acetate (±3aa): Purification with petroleum ether: EtOAc (9/1) as eluent); colorless Liquid (226 mg, 89% yield).^{1}H NMR (400 MHz, $CDCl_3$) δ 7.49 (d, *J* = 2.0 Hz, 1H), 7.37 – 7.33 (m, 1H), 7.29 – 7.23 (m, 2H), 3.90 (s, 1H), 3.68 (s, 3H), 2.54 (td, *J* = 7.0, 2.6 Hz, 2H), 2.44 (qt, *J* = 4.5, 1.8 Hz, 2H), 1.80 (ddd, *J* = 6.4, 4.7, 2.3 Hz, 4H). $^{13}C\{^1H\}$ NMR (100 MHz, $CDCl_3$) δ 171.5, 139.2, 134.4, 129.7, 128.4 (2C), 126.5, 73.2, 52.4 (2C), 52.1, 23.2. HRMS (ESI-TOF) *m/z*: [M + H^+] Calcd for $C_{13}H_{17}ClNO_2$ 254.0942, Found 254.0941.

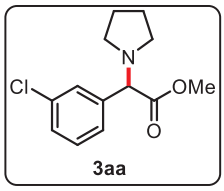

3aa

Ethyl 2-(3-chlorophenyl)-2-(pyrrolidin-1-yl) acetate (±3ba): Purification with petroleum ether: EtOAc (9/1) as eluent); colorless liquid (228 mg, 85% yield). ^{1}H NMR (400 MHz, $CDCl_3$) δ 7.51 (d, *J* = 2.1 Hz, 1H), 7.38 (dt, *J* = 6.3, 2.0 Hz, 1H), 7.30 – 7.26 (m, 2H), 4.27 – 4.08 (m, 2H), 3.89 (s, 1H), 2.57 (dd, *J* = 6.8, 2.2 Hz, 2H), 2.52 – 2.41 (m, 2H), 1.86 – 1.78 (m, 4H), 1.22 (t, *J* = 7.1 Hz, 3H). $^{13}C\{^1H\}$ NMR (100 MHz, $CDCl_3$) δ 171.1, 139.5, 134.4, 129.7, 128.5, 128.4, 126.5,73.4, 61.7, 52.4 (2C), 23.3 (2C), 14.0. HRMS (ESI-TOF) *m/z*: [M + H^+] Calcd for $C_{14}H_{19}ClNO_2$ 268.1099, Found 268.1098.

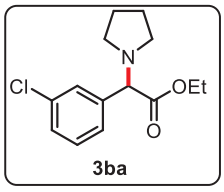

3ba

Isopropyl 2-(3-chlorophenyl)-2-(pyrrolidin-1-yl) acetate (±3ca): Purification with petroleum ether: EtOAc (9/1) as eluent); colorless liquid (228 mg, 81% yield). ^{1}H NMR (400 MHz, $CDCl_3$) δ 7.51 (d, *J* = 2.1 Hz, 1H), 7.40 – 7.36 (m, 1H), 7.32 – 7.25 (m, 2H), 5.04 (hept, *J* = 6.6 Hz, 1H), 3.85 (s, 1H), 2.63 – 2.52 (m, 2H), 2.46 (td, *J* = 8.2, 7.1, 5.1 Hz, 2H), 1.81 (ddd, *J* = 6.3, 4.9, 2.5 Hz, 4H), 1.24 (d, *J* = 6.2 Hz, 3H), 1.15 (d, *J* = 6.3 Hz, 3H). $^{13}C\{^1H\}$ NMR (100 MHz, $CDCl_3$) δ 170.7, 139.7, 134.3, 129.6, 128.5, 128.3, 126.5, 73.6, 68.5, 52.4 (2C), 23.4 (2C), 21.7, 21.4. HRMS (ESI-TOF) *m/z*: [M + H^+] Calcd for $C_{15}H_{21}ClNO_2$ 282.1255, Found 282.1263.

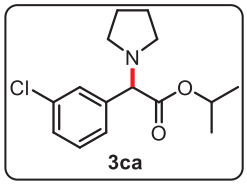

3ca

***tert*-Butyl 2-(3-chlorophenyl)-2-(pyrrolidin-1-yl)acetate (±3da):** Purification with petroleum ether: EtOAc (9/1) as eluent); colorless liquid (213 mg, 72% yield). ^{1}H NMR (400 MHz, $CDCl_3$) δ 7.51 (d, *J* = 2.0 Hz, 1H), 7.41 – 7.37 (m, 1H), 7.29 (dd, *J* = 4.8, 1.7 Hz, 2H), 3.82 (s, 1H), 2.64 – 2.56 (m, 2H), 2.54 – 2.45 (m, 2H), 1.84 – 1.80 (m, 4H), 1.42 (s, 9H). ^{13}C{^{1}H} NMR (100 MHz, $CDCl_3$) δ 170.2, 139.8, 134.2, 129.5, 128.4, 128.1, 126.5, 81.4, 73.8, 52.2 (2C), 27.8 (3C), 23.3 (2C). HRMS (ESI-TOF) *m*/*z*: [M + H$^+$] Calcd for $C_{16}H_{23}ClNO_2$ 296.1412, Found 295.1319.

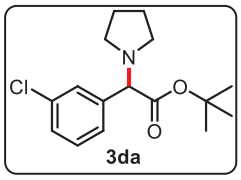

Methyl 2-(2-chlorophenyl)-2-(pyrrolidin-1-yl)acetate (±3ea): Purification with petroleum ether: EtOAc (9/1) as eluent); colorless Liquid (193 mg, 76% yield), ^{1}H NMR (400 MHz, $CDCl_3$) δ 7.68 (dd, *J* = 7.7, 1.9 Hz, 1H), 7.36 (dd, *J* = 7.8, 1.5 Hz, 1H), 7.29 – 7.24 (m, 1H), 7.21 (td, *J* = 7.6, 1.9 Hz, 1H), 4.67 (s, 1H), 3.68 (s, 3H), 2.63 (qd, *J* = 6.7, 3.0 Hz, 2H), 2.49 (td, *J* = 7.2, 2.5 Hz, 2H), 1.79 (dt, *J* = 6.1, 3.0 Hz, 4H). ^{13}C{^{1}H} NMR (100 MHz, $CDCl_3$) δ 171.6, 134.9, 133.9, 130.0, 129.6, 129.1, 127.1, 67.8, 52.1 (2C), 52.0 (2C), 23.3. HRMS (ESI-TOF) *m*/*z*: [M + H$^+$] Calcd for $C_{13}H_{17}ClNO_2$ 254.0942; Found 254.0938.

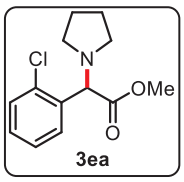

Ethyl 2-(2-chlorophenyl)-2-(pyrrolidin-1-yl) acetate (±3fa): Purification with petroleum ether: EtOAc (9/1) as eluent); colorless liquid (198 mg, 74% yield), ^{1}H NMR (400 MHz, CDCl3) δ 7.72 (dd, *J* = 7.7, 1.9 Hz, 1H), 7.39 (dd, *J* = 7.8, 1.5 Hz, 1H), 7.29 (td, *J* = 7.4, 1.6 Hz, 1H), 7.23 (td, *J* = 7.6, 1.9 Hz, 1H), 4.66 (s, 1H), 4.25 – 4.10 (m, 2H), 2.66 (td, *J* = 7.1, 2.4 Hz, 2H), 2.52 (td, *J* = 7.2, 2.5 Hz, 2H), 1.81 (dd, *J* = 6.3, 3.2 Hz, 4H), 1.22 (t, *J* = 7.1 Hz, 3H). ^{13}C{^{1}H} NMR (100 MHz, $CDCl_3$) δ 171.2, 135.0, 133.9, 130.0, 129.5, 129.0, 127.0, 68.0, 61.0, 52.0 (2C), 23.3 (2C), 14.1. HRMS (ESI-TOF) *m*/*z*: [M + H$^+$] Calcd for $C_{14}H_{19}ClNO_2$ 268.1099, Found 268.1095.

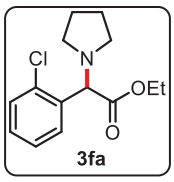

Allyl 2-(2-chlorophenyl)-2-(pyrrolidin-1-yl)acetate (±3ga): Purification with petroleum ether: EtOAc (9/1) as eluent); colorless Liquid (204 mg, 73% yield), ^{1}H NMR (400 MHz, $CDCl_3$) δ 7.74 (dd, *J* = 7.6, 1.7 Hz, 1H), 7.40 (dd, *J* = 7.8, 1.4 Hz, 1H), 7.32 – 7.22 (m, 2H), 5.86 (ddt, *J* = 16.1, 10.8, 5.5 Hz, 1H), 5.28 – 5.16 (m, 2H), 4.74 (s, 1H), 4.68 – 4.56 (m, 2H), 2.70 (dt, *J* = 10.5, 5.3 Hz, 2H), 2.59 – 2.50 (m, 2H), 1.90 – 1.76 (m, 4H). ^{13}C{^{1}H} NMR (100 MHz, $CDCl_3$) δ 170.7, 134.8, 133.9, 131.7, 130.1, 129.5, 129.1, 127.1, 118.1, 67.9, 65.4, 52.1 (2C), 23.3 (2C). HRMS (ESI-TOF) *m*/*z*: [M + H$^+$] Calcd for $C_{15}H_{19}ClNO_2$ 280.1099, Found 280.1106.

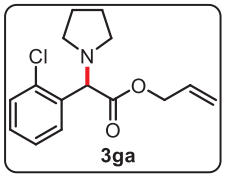

Benzo[*d*][1,3]dioxol-5-ylmethyl 2-(2-chlorophenyl)-2-(pyrrolidin-1-yl)acetate (±3ha):

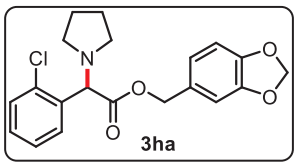

Purification with petroleum ether: EtOAc (8/2) as eluent); colorless liquid (254 mg, 68% yield). ^{1}H NMR (400 MHz, $CDCl_3$) δ 7.68 (dd, *J* = 7.5, 2.0 Hz, 1H), 7.36 (dd, *J* = 7.5, 1.8 Hz, 1H), 7.28 – 7.18 (m, 2H), 6.72 (s, 3H), 5.92 (s, 2H), 5.09 – 4.98 (m, 2H), 4.71 (s, 1H), 2.63 (td, *J* = 7.1, 2.3 Hz, 2H), 2.53 – 2.45 (m, 2H), 1.79 (dt, *J* = 6.0, 3.0 Hz, 4H). ^{13}C{^{1}H} NMR (100 MHz, $CDCl_3$) δ 170.9, 147.5, 147.3, 134.7, 133.8, 130.0, 129.4, 129.3, 129.0, 126.9, 121.8, 108.6, 107.9, 100.9, 67.8, 66.4, 51.9 (2C), 23.3 (2C). HRMS (ESI-TOF) *m*/*z*: [M + H$^+$] Calcd for $C_{20}H_{21}ClNO_4$ 374.1154, Found 374.1158.

Benzyl 2-(2-chlorophenyl)-2-(pyrrolidin-1-yl)acetate (±3ia): Purification with petroleum

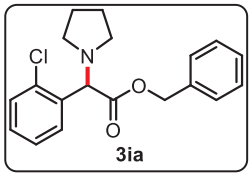

ether: EtOAc (8/2) as eluent); colorless liquid (231 mg, 70% yield). ^{1}H NMR (400 MHz, $CDCl_3$) δ 7.66 (dd, *J* = 7.4, 2.1 Hz, 1H), 7.35 (dd, *J* = 7.2, 2.1 Hz, 1H), 7.28 – 7.22 (m, 4H), 7.19 (td, *J* = 5.4, 2.5 Hz, 3H), 5.12 (q, *J* = 12.5 Hz, 2H), 4.71 (s, 1H), 2.61 (td, *J* = 7.1, 2.2 Hz, 2H), 2.52 – 2.44 (m, 2H), 1.77 (dt, *J* = 6.1, 3.1 Hz, 4H). ^{13}C{^{1}H} NMR (100 MHz, $CDCl_3$) δ 171.0, 135.7, 134.8, 133.9, 130.1, 129.5, 129.0, 128.4 (2C), 128.0, 127.8 (2C), 127.1, 67.9, 66.5, 52.0 (2C), 23.4 (2C). HRMS (ESI-TOF) *m*/*z*: [M + H$^+$] Calcd for $C_{19}H_{21}ClNO_2$ 330.1255, Found 330.1173.

Cyclohexyl 2-(2-chlorophenyl)-2-(pyrrolidin-1-yl)acetate (±3ja): Purification with petroleum

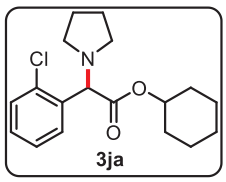

ether: EtOAc (9/1) as eluent); colorless liquid (222 mg, 69% yield), ^{1}H NMR (400 MHz, $CDCl_3$) δ 7.75 – 7.70 (m, 1H), 7.35 (dd, *J* = 7.8, 1.4 Hz, 1H), 7.29 – 7.17 (m, 2H), 4.80 (tt, *J* = 8.4, 3.7 Hz, 1H), 4.63 (s, 1H), 2.72 – 2.62 (m, 2H), 2.56 – 2.47 (m, 2H), 1.84 – 1.75 (m, 5H), 1.72 – 1.60 (m, 2H), 1.47 (m, 3H), 1.30 (m, 4H). ^{13}C{^{1}H} NMR (100 MHz, $CDCl_3$) δ 170.4, 135.2, 133.8, 130.0, 129.4, 128.9, 127.0, 73.0, 68.2, 52.1 (2C), 31.3, 31.0, 25.3, 23.4 (3C), 23.2. HRMS (ESI-TOF) *m*/*z*: [M + H$^+$] Calcd for $C_{18}H_{25}ClNO_2$ 322.1568, Found 322.1561.

Methyl 2-phenyl-2-(pyrrolidin-1-yl)acetate (±3ka): Purification with petroleum ether: EtOAc

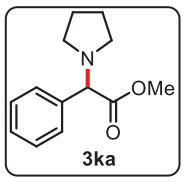

(9/1) as eluent); colorless liquid (178 mg, 81% yield). ^{1}H NMR (400 MHz, $CDCl_3$) δ 7.39 (dd, *J* = 7.8, 1.6 Hz, 2H), 7.27 – 7.20 (m, 3H), 3.86 (s, 1H), 3.59 (s, 3H), 2.52 – 2.45 (m, 2H), 2.36 (dd, *J* = 10.5, 3.2 Hz, 2H), 1.72 (td, *J* = 9.8, 8.3, 5.1 Hz, 4H). ^{13}C{^{1}H} NMR (100 MHz, $CDCl_3$) δ 172.0, 137.1, 128.4 (2C),

128.3 (2C), 128.2, 73.7, 52.4 (2C), 52.0, 23.2 (2C). HRMS (ESI-TOF) *m/z*: [M + H^+] Calcd for $C_{13}H_{18}NO_2$ 220.1332, Found 220.1328.

Methyl 2-(2-fluorophenyl)-2-(pyrrolidin-1-yl)acetate (±3la): Purification with petroleum ether: EtOAc (9/1) as eluent); colorless liquid (168 mg, 71% yield). ^{1}H NMR (400 MHz, $CDCl_3$) δ 7.60 (td, *J* = 7.5, 1.7 Hz, 1H), 7.33 – 7.26 (m, 1H), 7.19 – 7.13 (m, 1H), 7.10 – 7.03 (m, 1H), 4.50 (s, 1H), 3.71 (s, 3H), 2.63 (dt, *J* = 10.7, 5.3 Hz, 2H), 2.51 (dt, *J* = 7.9, 5.1 Hz, 2H), 1.85 – 1.77 (m, 4H). ^{13}C{^{1}H} NMR (100 MHz, $CDCl_3$) δ 171.6, 160.5 (d, *J* = 247.3 Hz), 130.0 (d, *J* = 3.4 Hz), 129.6 (d, *J* = 8.3 Hz), 124.3 (d, *J* = 3.5 Hz), 123.9 (d, *J* = 13.4 Hz), 115.5 (d, *J* = 22.5 Hz), 64.0, 52.1, 51.9 (2C), 23.3 (2C). HRMS (ESI-TOF) *m/z*: [M + H^+] Calcd for $C_{13}H_{17}FNO_2$ 238.1238, Found 238.1235.

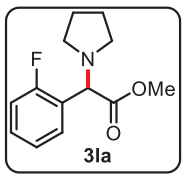

3la

Methyl 2-(4-chlorophenyl)-2-(pyrrolidin-1-yl)acetate (±3ma): Purification with petroleum ether: EtOAc (9/1) as eluent); colorless liquid (216 mg, 85% yield). ^{1}H NMR (400 MHz, $CDCl_3$) δ 7.42 (d, *J* = 8.5 Hz, 2H), 7.30 (d, *J* = 8.5 Hz, 2H), 3.90 (s, 1H), 3.68 (s, 3H), 2.58 – 2.50 (m, 2H), 2.46 – 2.38 (m, 2H), 1.80 (td, *J* = 5.7, 3.1 Hz, 4H). ^{13}C{^{1}H} NMR (100 MHz, $CDCl_3$) δ 171.2, 135.8, 134.10 129.6 (2C), 128.7 (2C), 73.0, 52.4 (C), 52.1, 23.2 (2C). HRMS (ESI-TOF) *m/z*: [M + H^+] Calcd for $C_{13}H_{17}ClNO_2$ 254.0942, Found 254.0937.

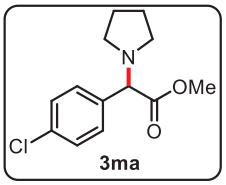

3ma

Methyl 2-(4-bromophenyl)-2-(pyrrolidin-1-yl)acetate (±3na): Purification with petroleum ether: EtOAc (9/1) as eluent); colorless liquid (246 mg, 83% yield). ^{1}H NMR (400 MHz, $CDCl_3$) δ 7.49 (d, *J* = 8.5 Hz, 2H), 7.38 (d, *J* = 8.5 Hz, 2H), 3.91 (s, 1H), 3.70 (s, 3H), 2.56 (dt, *J* = 6.0, 3.2 Hz, 2H), 2.48 – 2.41 (m, 2H), 1.82 (td, *J* = 5.7, 3.1 Hz, 4H). ^{13}C{^{1}H} NMR (100 MHz, $CDCl_3$) δ 171.8, 136.4, 131.7 (2C), 130.1 (2C), 122.3, 73.2, 52.5 (2C), 52.2, 23.3 (2C). HRMS (ESI-TOF) *m/z*: [M + H^+] Calcd for $C_{13}H_{17}BrNO_2$ 298.0437, Found 298.0424.

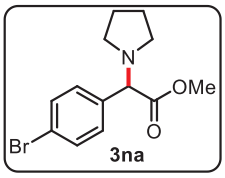

3na

Methyl 2-(pyrrolidin-1-yl)-2-(4-(tosyloxy)phenyl)acetate (±3oa): Purification with petroleum ether: EtOAc (8/2) as eluent); colorless liquid (304 mg, 78% yield). ^{1}H NMR (400 MHz, $CDCl_3$) δ 7.73 (d, *J* = 8.4 Hz, 2H), 7.42 (d, *J* = 8.6 Hz, 2H), 7.32 (d, *J* = 8.0 Hz, 2H), 6.98 (d, *J* = 8.7 Hz, 2H), 3.92 (s, 1H), 3.70 (s, 3H), 2.57 – 2.50 (m, 2H), 2.47 (s, 3H), 2.44 – 2.37 (m, 2H), 1.81 (td, *J* = 10.2, 8.5, 5.3 Hz, 4H). ^{13}C{^{1}H} NMR (100 MHz, $CDCl_3$) δ 171.7, 149.5, 145.4, 136.2, 132.5,

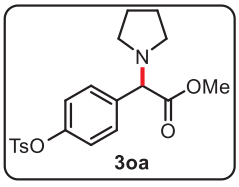

3oa

129.8 (2C), 129.7 (2C), 128.5 (2C), 122.5 (2C), 73.0, 52.5 (2C), 52.3, 23.3 (2C), 21.7. HRMS (ESI-TOF) *m/z*: [M + H^+] Calcd for $C_{20}H_{24}NO_5S$ 390.1370, Found 390.1377.

Ethyl 2-phenyl-2-(pyrrolidin-1-yl)acetate (±3pa): Purification with petroleum ether: EtOAc (9/1) as eluent); colorless liquid (180 mg, 77% yield). ^{1}H NMR (400 MHz, $CDCl_3$) δ 7.46 (dt, *J* = 8.4, 2.2 Hz, 2H), 7.34 – 7.27 (m, 3H), 4.22 – 4.06 (m, 2H), 3.89 (s, 1H), 2.55 (td, *J* = 7.1, 2.4 Hz, 2H), 2.47 – 2.38 (m, 2H), 1.83 – 1.73 (m, 4H), 1.18 (t, *J* = 7.1 Hz, 3H). ^{13}C{^{1}H} NMR (100 MHz, $CDCl_3$) δ 171.6, 137.4, 128.4 (2C), 128.3 (2C), 128.1, 73.9, 60.8, 52.4 (2C), 23.3 (2C), 14.0. HRMS (ESI-TOF) *m/z*: [M + H^+] Calcd for $C_{14}H_{20}NO_2$ 234.1489, Found 234.1486.

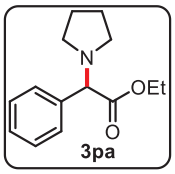

Ethyl 2-(4-chlorophenyl)-2-(pyrrolidin-1-yl)acetate (±3qa): Purification with petroleum ether: EtOAc (9/1) as eluent); colorless liquid (212 mg, 79% yield). ^{1}H NMR (400 MHz, $CDCl_3$) δ 7.44 (d, *J* = 8.4 Hz, 2H), 7.32 (d, *J* = 8.5 Hz, 2H), 4.21 – 4.09 (m, 2H), 3.89 (s, 1H), 2.56 (ddd, *J* = 8.7, 7.4, 4.2 Hz, 2H), 2.44 (ddd, *J* = 9.7, 7.7, 4.3 Hz, 2H), 1.81 (td, *J* = 5.8, 3.1 Hz, 4H), 1.21 (t, *J* = 7.1 Hz, 3H). ^{13}C{^{1}H} NMR (100 MHz, $CDCl_3$) δ 171.4, 136.1, 134.0, 129.7 (2C), 128.7 (2C), 73.3, 61.1, 52.4 (2C), 23.3 (2C), 14.1. HRMS (ESI-TOF) *m/z*: [M + H^+] Calcd for $C_{14}H_{19}ClNO_2$ 268.1099, Found 268.1096.

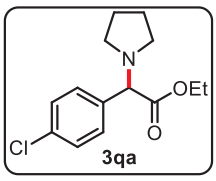

Ethyl 2-(4-bromophenyl)-2-(pyrrolidin-1-yl)acetate (±3ra): Purification with petroleum ether: EtOAc (9/1) as eluent); colorless liquid (240 mg, 77% yield). ^{1}H NMR (400 MHz, $CDCl_3$) δ 7.44 (d, *J* = 8.5 Hz, 2H), 7.34 (d, *J* = 8.5 Hz, 2H), 4.20 – 4.05 (m, 2H), 3.84 (s, 1H), 2.52 (td, *J* = 7.1, 2.4 Hz, 2H), 2.45 – 2.37 (m, 2H), 1.82 – 1.73 (m, 4H), 1.17 (t, *J* = 7.1 Hz, 3H). ^{13}C{^{1}H} NMR (100 MHz, $CDCl_3$) δ 171.2, 136.5, 131.6 (2C), 130.0 (2C), 122.1, 73.2, 61.0, 52.4 (2C), 23.3 (2C), 14.0. HRMS (ESI-TOF) *m/z*: [M + H^+] Calcd for $C_{14}H_{19}BrNO_2$ 312.0594, Found 312.0571.

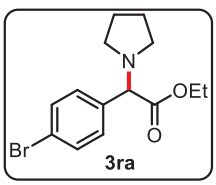

Methyl 2-(3-chlorophenyl)-2-(diethyl amino)acetate (±3ab): Purification with petroleum ether: EtOAc (9/1) as eluent); colorless liquid (208 mg, 81% yield). ^{1}H NMR (400 MHz, $CDCl_3$) δ 7.49 – 7.45 (m, 1H), 7.35 – 7.26 (m, 3H), 4.48 (s, 1H), 3.74 (s, 3H), 2.62 (q, *J* = 7.1 Hz, 4H), 1.02 (t, *J* = 7.2 Hz, 6H). ^{13}C{^{1}H} NMR (100 MHz, $CDCl_3$) δ 172.2, 139.3, 134.3, 129.6, 128.7, 128.1, 126.8, 68.7, 51.8, 43.7 (2C), 12.0 (2C). HRMS (ESI-TOF) *m/z*: [M + H^+] Calcd for $C_{13}H_{19}ClNO_2$ 256.1099, Found 256.1096.

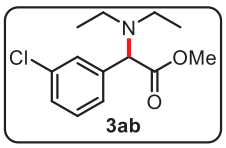

Methyl -2-(3-chlorophenyl)-2-(piperidin-1-yl)acetate (±3ac): Purification with petroleum ether: EtOAc (9/1) as eluent); Light Yellow Liquid (246 mg, 92% yield). ^{1}H NMR (400 MHz, $CDCl_3$) δ 7.46 (d, *J* = 2.0 Hz, 1H), 7.34 – 7.30 (m, 1H), 7.30 – 7.23 (m, 2H), 3.96 (s, 1H), 3.69 (s, 3H), 2.37 (m, 4H), 1.59 (quin, *J* = 5.5 Hz, 4H), 1.43 (m, *J* = 6.0 Hz, 2H). ^{13}C{^{1}H} NMR (100 MHz, $CDCl_3$) δ 171.6, 138.3, 134.3, 129.6, 128.7, 128.3, 126.8, 74.2, 52.2 (2C), 51.9, 25.7 (2C), 24.2. HRMS (ESI-TOF) *m/z*: [M + H$^+$] Calcd for $C_{14}H_{19}ClNO_2$ 268.1099, Found 268.1104.

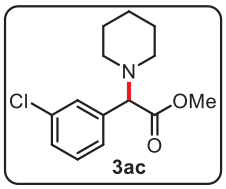

3ac

Methyl 2-(3-chlorophenyl)-2-(4-hydroxypiperidin-1-yl)acetate (±3ad): Purification with petroleum ether: EtOAc (7/3) as eluent); colorless liquid (222 mg, 78% yield). ^{1}H NMR (400 MHz, $CDCl_3$) δ 7.43 (s, 1H), 7.32 – 7.23 (m, 3H), 4.01 (s, 1H), 3.69 (s, 3H), 2.70 (ddt, *J* = 14.9, 9.1, 4.5 Hz, 2H), 2.30 – 2.20 (m, 1H), 2.19 – 2.10 (m, 1H), 2.06 (s, 1H), 1.93 – 1.82 (m, 2H), 1.62 (ddq, *J* = 18.7, 9.3, 5.8, 4.8 Hz, 2H). ^{13}C{^{1}H} NMR (100 MHz, $CDCl_3$) δ 171.5, 138.1, 134.4, 129.7, 128.6, 128.4, 126.8, 73.3, 67.5, 52.0, 48.7, 48.5, 34.1 (2C). HRMS (ESI-TOF) *m/z*: [M + H$^+$] Calcd for $C_{14}H_{19}ClNO_3$ 284.1048, Found 284.1044.

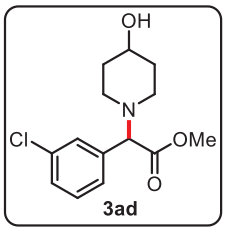

3ad

1-(1-(3-chlorophenyl)-2-methoxy-2-oxoethyl)piperidin-4-yl benzoate (±3ae): Purification with petroleum ether: EtOAc (8/2) as eluent); colorless semi-solid (295 mg, 76% yield). ^{1}H NMR (400 MHz, $CDCl_3$) δ 8.05 – 7.99 (m, 2H), 7.54 (tt, *J* = 6.9, 1.3 Hz, 1H), 7.48 (d, *J* = 1.7 Hz, 1H), 7.43 (t, *J* = 7.6 Hz, 2H), 7.36 – 7.27 (m, 3H), 5.07 (tt, *J* = 7.6, 3.8 Hz, 1H), 4.07 (s, 1H), 3.70 (s, 3H), 2.78 – 2.66 (m, 2H), 2.43 (q, *J* = 8.4 Hz, 2H), 2.08 – 1.99 (m, 2H), 1.94 – 1.83 (m, 2H). ^{13}C{^{1}H} NMR (100 MHz, $CDCl_3$) δ 171.3, 165.7, 138.0, 134.5, 132.8, 130.5, 129.8, 129.5 (2C), 128.7, 128.6, 128.3 (2C), 126.8, 73.3, 70.0, 52.1, 48.4, 48.2, 30.6 (2C). HRMS (ESI-TOF) *m/z*: [M + H$^+$] Calcd for $C_{21}H_{23}ClNO_4$ 388.1310, Found 388.1317.

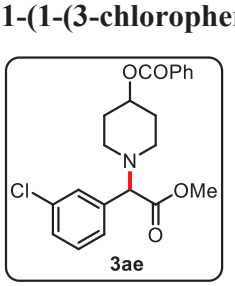

3ae

Methyl 2-(3-chlorophenyl)-2-morpholinoacetate (±3af): Purification with petroleum ether: EtOAc (9/1) as eluent); colorless semi-solid (200 mg, 74% yield). ^{1}H NMR (400 MHz, $CDCl_3$) δ 7.47 (d, *J* = 2.0 Hz, 1H), 7.36 – 7.24 (m, 3H), 3.96 (s, 1H), 3.75 – 3.71 (m, 4H), 3.70 (s, 3H), 2.45 (dd, *J* = 6.3, 3.2 Hz, 4H). ^{13}C{^{1}H} NMR (100 MHz, $CDCl_3$) δ 171.9, 137.4, 134.5, 129.8, 128.8, 128.7, 126.9, 73.7, 66.7 (2C), 52.1, 51.4 (2C). HRMS (ESI-TOF) *m/z*: [M + H$^+$] Calcd for $C_{13}H_{17}ClNO_3$ 270.0891, Found 270.0890.

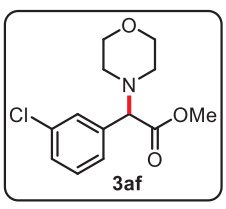

3af

Methyl 2-(3-chlorophenyl)-2-(4-ethylpiperazin-1-yl)acetate (±3ag): Purification with petroleum ether: EtOAc (8/2) as eluent); colorless semi-solid (230 mg, 78% yield). ^{1}H NMR (400 MHz, $CDCl_3$) δ 7.44 (d, *J* = 1.8 Hz, 1H), 7.30 (dq, *J* = 5.5, 1.8 Hz, 1H), 7.27 – 7.24 (m, 2H), 3.95 (s, 1H), 3.67 (s, 3H), 2.69 – 2.32 (m, 10H), 1.06 (t, *J* = 7.2 Hz, 3H). ^{13}C{^{1}H} NMR (100 MHz, $CDCl_3$) δ 171.3, 137.8, 134.5, 129.8, 128.7, 128.6, 127.0, 73.6, 52.4 (3C), 52.2, 52.1, 50.9, 11.8. HRMS (ESI-TOF) *m/z*: [M + H$^+$] Calcd for $C_{15}H_{22}ClN_2O_2$ 297.1364, Found 297.1352.

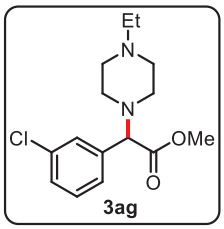

3ag

Methyl 2-(3-chlorophenyl)-2-(4-phenylpiperazin-1-yl)acetate (±3ah): Purification with petroleum ether: EtOAc (8/2) as eluent); colorless semi-solid (266 mg, 77% yield). ^{1}H NMR (400 MHz, $CDCl_3$) δ 7.50 (d, *J* = 1.9 Hz, 1H), 7.37 (dt, *J* = 6.7, 1.8 Hz, 1H), 7.32 (dt, *J* = 7.0, 1.6 Hz, 2H), 7.30 – 7.27 (m, 1H), 7.24 (dd, *J* = 7.0, 1.8 Hz, 1H), 6.91 (d, *J* = 1.0 Hz, 1H), 6.90 – 6.88 (m, 1H), 6.88 – 6.83 (m, 1H), 4.06 (s, 1H), 3.73 (s, 3H), 3.25 – 3.20 (m, 4H), 2.66 – 2.61 (m, 4H). ^{13}C{^{1}H} NMR (100 MHz, $CDCl_3$) δ 171.2, 151.1, 137.7, 134.6, 129.9, 129.1 (2C), 128.8, 128.7, 127.0, 119.8, 116.1 (2C), 73.5, 52.2, 51.0 (2C), 49.0 (2C). HRMS (ESI-TOF) *m/z*: [M + H$^+$] Calcd for $C_{19}H_{22}ClN_2O_2$ 345.1364, Found 345.1359.

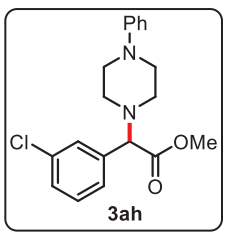

3ah

Methyl 2-(3-chlorophenyl)-2-(4-(2,4-dinitrophenyl)piperazin-1-yl)acetate (±3al): Purification with petroleum ether: EtOAc (1/1) as eluent); Yellow solid (mp = 185 °C), (314 mg, 72% yield). ^{1}H NMR (400 MHz, $CDCl_3$) δ 8.69 (d, *J* = 2.7 Hz, 1H), 8.27 (dd, *J* = 9.3, 2.7 Hz, 1H), 7.48 (s, 1H), 7.35 (q, *J* = 5.2, 3.7 Hz, 3H), 7.09 (d, *J* = 9.3 Hz, 1H), 4.13 (s, 1H), 3.74 (s, 3H), 3.36 – 3.30 (m, 4H), 2.71 – 2.65 (m, 4H). ^{13}C{^{1}H} NMR (100 MHz, $CDCl_3$) δ 170.7, 149.1, 138.7, 138.4, 136.8, 134.8, 130.0, 129.0, 128.8, 128.3, 127.0, 123.6, 119.3, 72.6, 52.4, 50.4 (2C), 50.1 (2C). HRMS (ESI-TOF) *m/z*: [M + H$^+$] Calcd for $C_{19}H_{20}ClN_4O_6$ 435.1066, Found 435.0993.

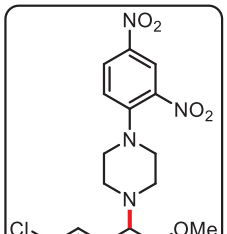

3al

Methyl-2-phenyl-2-(piperidin-1-yl)acetate (±3kc): Purification with petroleum ether: EtOAc (9/1) as eluent); colorless liquid (180 mg, 77% yield). ^{1}H NMR (400 MHz, $CDCl_3$) δ 7.42 (dt, *J* = 8.3, 2.3 Hz, 2H), 7.35 – 7.28 (m, 3H), 3.97 (s, 1H), 3.67 (s, 3H), 2.38 (m, 4H), 1.59 (quin, *J* = 5.5 Hz, 4H), 1.42 (m, 2H). ^{13}C{^{1}H} NMR

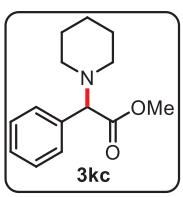

3kc

(100 MHz, $CDCl_3$) δ172.3, 136.2, 128.8, 128.4, 128.1, 75.0, 52.4 (2C), 51.8, 25.7 (2C),24.3. HRMS (ESI-TOF) *m/z*: [M + H^+] Calcd for $C_{14}H_{20}NO_2$ 234.1489, Found 234.1489.

Methyl 2-(2-chlorophenyl)-2-(piperidin-1-yl)acetate (±3ec): Purification with petroleum ether: EtOAc (9/1) as eluent); colorless liquid (188 mg, 70% yield). ^{1}H NMR (400 MHz, $CDCl_3$) δ 7.65 (dd, *J* = 7.7, 1.9 Hz, 1H), 7.34 (dd, *J* = 7.8, 1.5 Hz, 1H), 7.25 (td, *J* = 7.5, 1.5 Hz, 1H), 7.19 (td, *J* = 7.6, 1.9 Hz, 1H), 4.60 (s, 1H), 3.66 (s, 3H), 2.50 (dt, *J* = 10.6, 5.2 Hz, 2H), 2.39 (dt, *J* = 10.9, 5.4 Hz, 2H), 1.57 (quin, *J* = 5.2 Hz, 4H), 1.42 (quin, *J* = 5.9 Hz, 2H). ^{13}C{^{1}H} NMR (100 MHz, $CDCl_3$) δ171.4, 134.5, 134.1, 129.9, 129.5, 128.9, 126.8, 69.5, 52.1 (2C), 51.8, 25.9 (2C), 24.2. HRMS (ESI-TOF) *m/z*: [M + H^+] Calcd for $C_{14}H_{19}ClNO_2$ 268.1099, Found 268.1100.

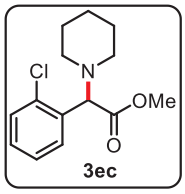

Methyl 2-(4-chlorophenyl)-2-(piperidin-1-yl)acetate (±3mc): Purification with petroleum ether: EtOAc (9/1) as eluent); colorless liquid (212 mg, 79% yield). ^{1}H NMR (400 MHz, $CDCl_3$) δ δ 7.37 (d, *J* = 8.5 Hz, 2H), 7.29 (d, *J* = 8.6 Hz, 2H), 3.94 (s, 1H), 3.67 (s, 3H), 2.35 (m, 4H), 1.57 (quin, *J* = 5.5 Hz, 4H), 1.43 (m, 2H). ^{13}C{^{1}H} NMR (100 MHz, $CDCl_3$) δ171.9, 134.8, 134.0, 130.1 (2C), 128.6 (2C), 74.1, 52.3 (2C), 51.9, 25.7 (2C), 24.2. HRMS (ESI-TOF) *m/z*: [M + H^+] Calcd for $C_{14}H_{19}ClNO_2$ 268.1099, Found 268.1097.

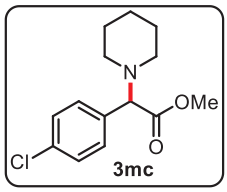

Methyl 2-(4-bromophenyl)-2-(piperidin-1-yl)acetate (±3nc): Purification with petroleum ether: EtOAc (9/1) as eluent); colorless liquid (244 mg, 78% yield). ^{1}H NMR (400 MHz, $CDCl_3$) δ 7.46 (d, *J* = 8.4 Hz, 2H), 7.33 (d, *J* = 8.1 Hz, 2H), 3.95 (s, 1H), 3.68 (d, *J* = 1.1 Hz, 3H), 2.37 (t, *J* = 5.4 Hz, 4H), 1.59 (quin, *J* = 5.3 Hz, 4H), 1.47 – 1.39 (m, 2H). ^{13}C{^{1}H} NMR (100 MHz, $CDCl_3$) δ 171.7, 135.4, 131.5 (2C), 130.4 (2C), 122.1, 74.1, 52.2 (2C), 51.9, 25.7 (2C), 24.2. HRMS (ESI-TOF) *m/z*: [M + H^+] Calcd for $C_{14}H_{19}BrNO_2$ 312.0594, Found 312.0571.

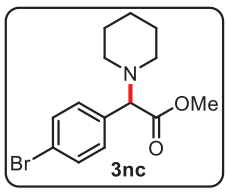

Methyl 2-(2-chlorophenyl)-2-morpholinoacetate (±3ef): Purification with petroleum ether: EtOAc (9/1) as eluent); colorless liquid (197 mg, 73% yield). ^{1}H NMR (400 MHz, $CDCl_3$) δ 7.65 (dd, *J* = 7.5, 2.0 Hz, 1H), 7.39 (dd, *J* = 7.7, 1.7 Hz, 1H), 7.29 (dd, *J* = 7.4, 5.6 Hz, 1H), 7.25 (dd, *J* = 7.5, 5.4 Hz, 1H), 4.68 (s, 1H), 3.72 (t, *J* = 4.7 Hz, 4H), 3.70 (s, 3H), 2.58 (dd, *J* = 10.6, 5.6 Hz, 2H), 2.52 – 2.46 (m, 2H). ^{13}C{^{1}H} NMR (100 MHz, $CDCl_3$) δ 171.0, 134.8, 133.1, 129.9, 129.7, 129.3, 127.0, 68.8,

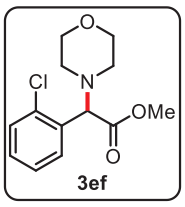

66.8 (2C), 52.0, 51.2 (2C). HRMS (ESI-TOF) *m/z*: [M + H^+] Calcd for $C_{13}H_{17}ClNO_3$ 270.0891, Found 270.0896.

Methyl 2-(4-chlorophenyl)-2-morpholinoacetate (±3mf): Purification with petroleum ether: EtOAc (9/1) as eluent); colorless liquid (205 mg, 76% yield). ^{1}H NMR (400 MHz, $CDCl_3$) δ 7.40 (d, *J* = 8.5 Hz, 2H), 7.33 (d, *J* = 8.6 Hz, 2H), 3.96 (s, 1H), 3.75 – 3.70 (m, 4H), 3.69 (s, 3H), 2.47 – 2.42 (m, 4H). ^{13}C{^{1}H} NMR (100 MHz, $CDCl_3$) δ 171.1, 134.3,133.9, 130.1 (2C), 128.8 (2C),73.5, 66.7 (2C), 52.0, 51.4 (2C). HRMS (ESI-TOF) *m/z*: [M + H^+] Calcd for $C_{13}H_{17}ClNO_3$ 270.0891, Found 270.0893.

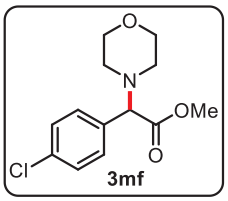

Methyl 2-(4-bromophenyl)-2-morpholinoacetate (±3nf): Purification with petroleum ether: EtOAc (9/1) as eluent); colorless liquid (236 mg, 75% yield). ^{1}H NMR (400 MHz, $CDCl_3$) δ 7.49 (d, *J* = 8.5 Hz, 2H), 7.34 (d, *J* = 8.5 Hz, 2H), 3.95 (s, 1H), 3.75 – 3.71 (m, 4H), 3.69 (s, 3H), 2.49 – 2.41 (m, 4H). ^{13}C{^{1}H} NMR (100 MHz, $CDCl_3$) δ 171.1, 134.4, 131.8 (2C), 130.4 (2C), 122.6, 73.6, 66.7 (2C), 52.1, 51.5 (2C). HRMS (ESI-TOF) *m/z*: [M + H^+] Calcd for $C_{13}H_{17}BrNO_3$ 314.0386, Found 314.0376.

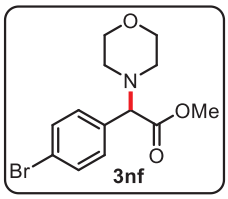

Methyl 2-morpholino-2-(4-(tosyloxy)phenyl)acetate (±3of): Purification with petroleum ether: EtOAc (7/3) as eluent); colorless semi-solid (296 mg, 73% yield). ^{1}H NMR (400 MHz, $CDCl_3$) δ 7.70 (d, *J* = 8.3 Hz, 2H), 7.37 (d, *J* = 8.6 Hz, 2H), 7.30 (d, *J* = 8.0 Hz, 2H), 6.97 (d, *J* = 8.7 Hz, 2H), 3.96 (s, 1H), 3.71 – 3.68 (m, 4H), 3.67 (s, 3H), 2.44 (s, 3H), 2.43 – 2.34 (m, 4H). ^{13}C{^{1}H} NMR (100 MHz, $CDCl_3$) δ 171.1, 149.6, 145.5, 134.1, 132.4, 130.1 (2C), 129.7 (2C), 128.4 (2C), 122.5 (2C), 73.4, 66.6 (2C), 52.1, 51.4 (2C), 21.7. HRMS (ESI-TOF) *m/z*: [M + H^+] Calcd for $C_{20}H_{24}NO_6S$ 406.1319, Found 406.1326.

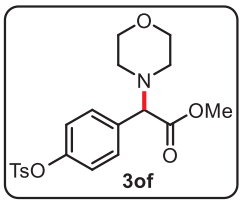

Methyl 2-(3-chlorophenyl)-2-(4-((4-chlorophenyl)(phenyl)methyl)piperazin-1-yl)acetate (±3aj): Purification with petroleum ether: EtOAc (8/2) as eluent); colorless semi-solid (282 mg, 60% yield). ^{1}H NMR (400 MHz, $CDCl_3$) δ 7.45 (s, 1H), 7.38 – 7.31 (m, 4H), 7.31 – 7.23 (m, 5H), 7.23 – 7.14 (m, 3H), 4.23 (s, 1H), 4.00 (s, 1H), 3.68 (s, 3H), 2.46 (m, 8H). ^{13}C{^{1}H} NMR (100 MHz, $CDCl_3$) δ 171.2, 137.7, 134.5, 132.5, 129.7, 129.2 (3C), 128.8, 128.6 (3C), 128.5,

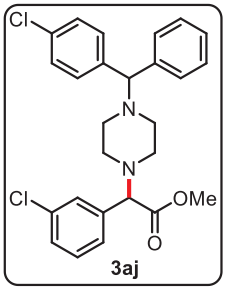

127.8 (3C), 127.2, 126.9, 75.2, 73.4, 52.1, 51.5 (2C), 51.1 (2C). HRMS (ESI-TOF) *m*/*z*: [M + H^+] Calcd for $C_{26}H_{27}Cl_2N_2O_2$ 469.1444 Found 469.1453.

Controlled Experiments: Electrolysis with constant current condition (8 mA) was carried out using Graphite plate anode and a Copper plate cathode for 12 h through an undivided reaction cell equipped with a stirring bar and methyl 2-(3-chlorophenyl)acetate **1a** (184 mg, 1.0 mmol, 1.0 equiv), pyrrolidine **2a** (71 mg, 1.0 mmol, 1.0 equiv), KI (83 mg, 0.5 mmol, 0.5 equiv), and $LiClO_4$ (106 mg, 1.0 mmol, 1.0 equiv) dissolved in 10.0 mL of CH_3CN. The Reaction progress was monitored by TLC. Using a reduced amount of amine **2a** (1.0 equiv.) under standard conditions, we observed the formation of *α*-iodo-ester **9** (139 mg, 45% yield) and expected product **3aa** (<10% yield), after purification.

Methyl 2-iodo-2-phenylacetate (±9): Purification with petroleum ether: EtOAc (9/1) as eluent);

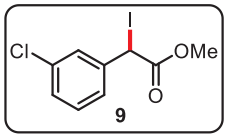

9

colorless liquid (139 mg, 45% yield). ^{1}H NMR (400 MHz, $CDCl_3$) δ 7.49 – 7.46 (m, 1H), 7.38 – 7.34 (m, 1H), 7.31 – 7.26 (m, 2H), 4.32 (s, 1H), 3.46 (s, 3H). $^{13}C\{^1H\}$ NMR (100 MHz, $CDCl_3$) δ 171.1, 137.9, 134.6, 130.0, 128.5, 128.4, 126.6, 54.4, 52.3. HRMS (ESI-TOF) *m*/*z*: [M + Na^+] Calcd for $C_9H_8IClO_2Na$ 332.9150, Found 332.9128.

To a stirred solution of **9** (130 mg, 0.4 mmol, 1.0 equiv) and **2a** (71 mg, 1.0 mmol, 2.5 equiv) in CH_3CN (4.0 mL) was added Et_3N (61 mg, 0.6 mmol, 1.5 equiv) and left for 3 h at room temperature. Once **9** disappeared from TLC, the reaction mixture was diluted with brine (4.0 mL) and extracted with ethyl acetate (10.0 mL). The combined organic layer was dried over anhydrous Na_2SO_4, concentrated, and purified to afford **3aa** (90 mg, 89%) as a pale yellow liquid.

Reaction in the presence of radical inhibitors (TEMPO/BHT). To a 10 mL dried undivided reaction cell equipped with a stirring bar were added methyl 2-(3-chlorophenyl) acetate **1a** (100 mg, 0.54 mmol, 1.0 equiv), pyrrolidine **2a** (114 mg, 1.6 mmol, 3.0 equiv), KI (45 mg, 0.27 mmol, 0.5 equiv), TEMPO (211 mg, 1.35 mmol, 2.5 equiv) **OR** BHT (297 mg, 1.35 mmol, 2.5 equiv), and $LiClO_4$ (57 mg, 1.0 mmol, 1.0 equiv) dissolved in 10.0 mL of CH_3CN. The combined reaction mixture was electrolyzed under standard conditions. The trace of product **3aa** was observed (TEMPO) or not observed (BHT) on TLC.

Gram-scale synthesis of 3ac: A 100 mL three-neck round bottom flask (as an undivided cell) was equipped with a graphite plate anode and a Copper plate cathode which was connected to a DC-regulated power supply. To the cell were added methyl 2-(3-chlorophenyl) acetate **1a** (1.0 g, 5.43 mmol, 1.0 equiv), piperidine **2c** (1.38 g, 16.25 mmol, 3.0 equiv), KI (0.45 g, 2.71 mmol, 0.5 equiv), and $LiClO_4$ (0.58 g, 5.43 mmol, 1.0 equiv) dissolved in 40.0 mL of CH_3CN. While stirring, the mixture was electrolyzed under constant current conditions (8 mA) under N_2 atmosphere at room temperature. The Reaction progress was monitored by TLC. Electrodes were washed with ethyl acetate (10 mL); when the reaction was finished, the solvent was removed under reduced pressure. The residue was poured into a saturated aqueous $Na_2S_2O_3$ (20.0 mL) and extracted with ethyl acetate (2 × 20.0 mL). The combined organic layer was separated, washed with brine, dried over anhydrous Na_2SO_4, and concentrated under reduced pressure. The crude cycloadduct was purified by column chromatography on silica gel using petroleum ether: EtOAc (9/1) afforded pure **3ac** (1.30 g, 90%).

1-(2-azido-1-(3-chlorophenyl)]ethyl)piperidine (±10): To a stirred solution of **3ac** (200 mg, 0.74 mmol, 1.0 equiv) in dry THF (10.0 mL) at 0°C was added $LiAlH_4$ (93 mg, 2.24 mmol, 3.0 equiv) portion-wise over 10 min. The combined mixture was stirred at room temperature for 4 hours before cooling to 0°C and quenched slowly with aqueous NH_4Cl solution (10.0 mL). The reaction mixture was further stirred with EtOAc (30.0 mL). The solid mass was removed by filtration, and the aqueous layer was again extracted with EtOAc (10.0 mL). The combined organic mixture was concentrated under reduced pressure, and crude alcohol was used further without purification.

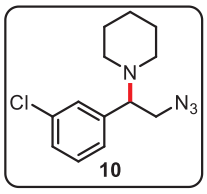

10

An oven-dried 25 mL round-bottom flask was charged with crude alcohol (200 mg, crude weight), Et_3N (146 µl, 1.05 mmol, 1.5 equiv), and DMAP (9.0 mg, 0.07 mmol, 0.1 equiv) in CH_2Cl_2 (5.0 mL) added a solution of TsCl (147 mg, 0.77 mmol, 1.1 equiv) in CH_2Cl_2 (3.0 mL) at 0 °C under N_2 atmosphere. The resulting mixture was further stirred at rt for 10 h before quenched with saturated aqueous $NaHCO_3$ (8.0 mL) and stirred with additional CH_2Cl_2 (10.0 mL). The combined organic layer was separated, dried over anhydrous Na_2SO_4, and concentrated under reduced pressure, and crude tosyl-product was used further without purification.

To a solution, crude tosylate (315 mg, crude weight) in DMF (4.0 ml) was added NaN_3 (98 mg, 1.5 mmol, 2.0 equiv) and heated at 65°C for 8 h. The mixture was cooled to room temperature

and stirred between H_2O (4.0 mL) and EtOAc (10.0 mL). The organic layer was separated and washed with brine, dried over anhydrous Na_2SO_4, and concentrated under reduced pressure. Purification by column chromatography using petroleum ether: EtOAc (8:2) as eluent) afforded **10** as a transparent oil (114 mg, 58% after three steps). ^{1}H NMR (400 MHz, $CDCl_3$) δ 7.33 – 7.29 (m, 3H), 7.20 (d, *J* = 10.1 Hz, 1H), 4.64 (dd, *J* = 9.8, 3.9 Hz, 1H), 2.70 (dd, *J* = 13.4, 9.8 Hz, 1H), 2.58 (dd, *J* = 9.9, 5.8 Hz, 2H), 2.52 (dd, *J* = 13.4, 3.9 Hz, 1H), 2.49 – 2.42 (m, 2H), 1.62 (m, 4H), 1.46 (quin, *J* = 5.7 Hz, 2H). ^{13}C{^{1}H} NMR (100 MHz, $CDCl_3$) δ 140.9, 134.4, 129.8, 128.1, 126.9, 124.9, 65.5, 62.5, 54.8 (2C), 25.8 (2C), 24.2. HRMS (ESI-TOF) *m*/*z*: [M + H^+] Calcd for $C_{13}H_{18}ClN_4$ 265.1215, Found 265.1219.

Benzo[*d*][1,3]dioxol-5-ylmethyl 2-(2-chlorophenyl)-2-(pyrrolidin-1-yl)acetate (±11): To a stirred solution of the ester **3ec** (100 mg, 0.37 mmol, 1. 0 equiv) in THF: H_2O (2:1, 6.0 mL) was added LiOH.H_2O (47 mg, 1.1 mmol, 3.0 equiv) at rt and further stirred for 8-10 h. The reaction mixture was evaporated to dryness and the resulting solid crude material was taken forward without purification. This crude solid mass was taken in DMF (4.0 mL), added DIPEA (70 µL, 0.4 mmol, 1.1 equiv), subsequently, EDC.HCl (1-ethyl-3(3-dimethylaminopropyl)-carbodiimidehydrochloride) (77 mg, 0.4 mmol, 1.1 equiv), HOBt (1-Hydroxybenzotriazole) (54 mg, 0.4 mmol, 1.1 equiv) and the diethyl amine (35 mg, 0.48 mmol, 1.3 equiv) was added at and cooled to 0°C. The reaction mixture was further stirred at rt for 12 h, before quenching with H_2O (5.0 mL) and stirred with EtOAc (10 mL). The organic layer was separated, dried over anhydrous Na_2SO_4, and concentrated under reduced pressure. Purification by column chromatography using petroleum ether: EtOAc (7/3) afforded **11** (87 mg, 76% after two steps) as a colorless liquid. ^{1}H NMR (400 MHz, $CDCl_3$) δ 7.68 (dd, *J* = 7.6, 2.0 Hz, 1H), 7.30 (dd, *J* = 7.7, 1.6 Hz, 1H), 7.22 – 7.12 (m, 2H), 4.72 (s, 1H), 3.33 (m, 2H), 3.18 (m, 2H), 2.56 – 2.45 (m, 2H), 2.41 (m, 2H), 1.56 – 1.43 (m, 4H), 1.34 (quin, *J* = 5.8 Hz, 2H), 0.99 (q, *J* = 7.1 Hz, 6H). ^{13}C{^{1}H} NMR (100 MHz, $CDCl_3$) δ 169.7, 134.4, 133.9, 131.2, 129.1, 128.8, 126.8, 65.6, 51.9 (2C), 41.2, 40.4, 25.9 (2C), 24.3, 14.1, 12.5. HRMS (ESI-TOF) *m*/*z*: [M + H^+] Calcd for $C_{17}H_{26}ClN_2O$ 309.1728, Found 309.1728.

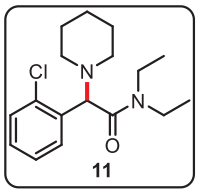

11

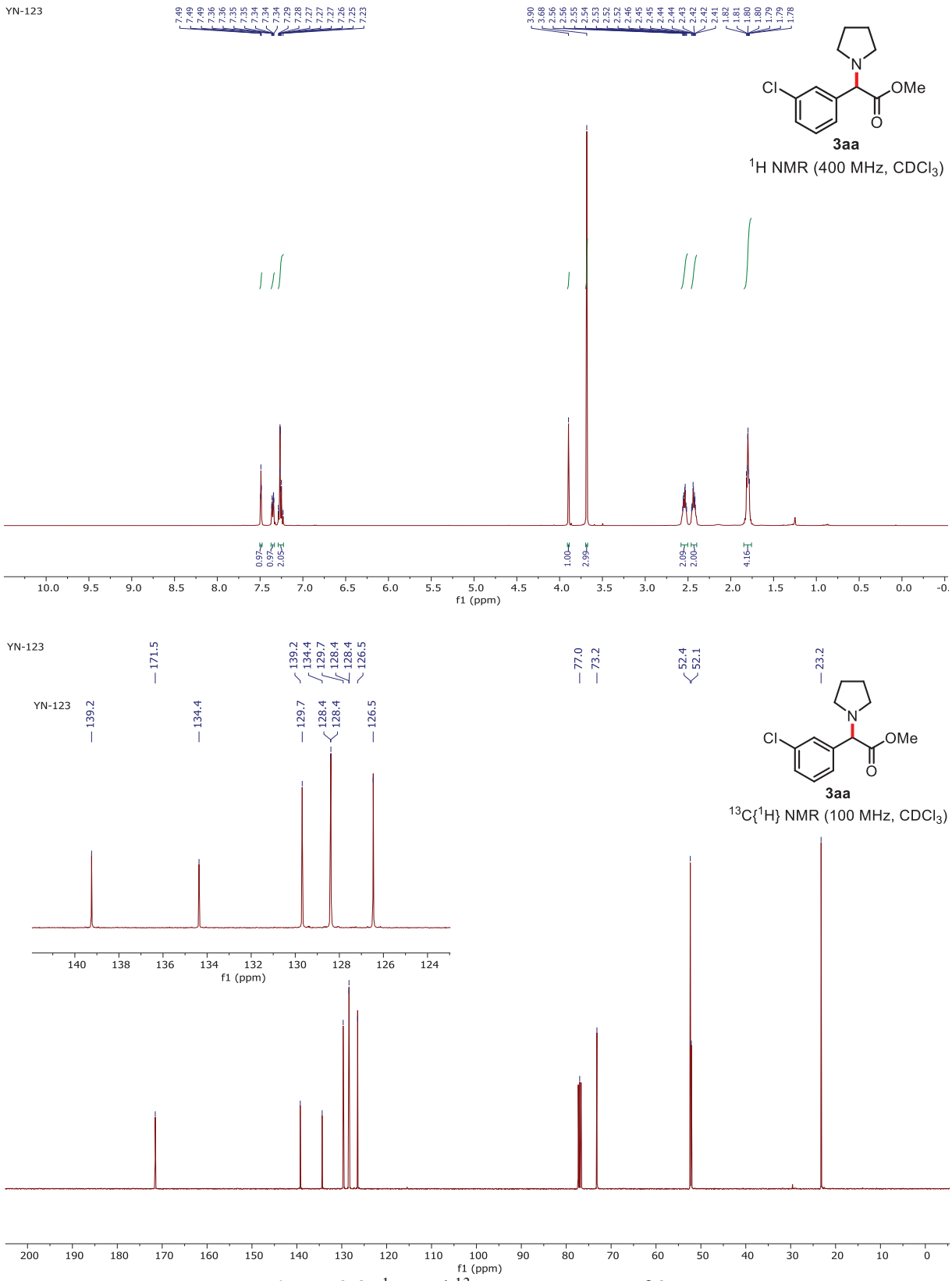

Figure 2.3: ^{1}H and ^{13}C NMR spectra of **3aa**

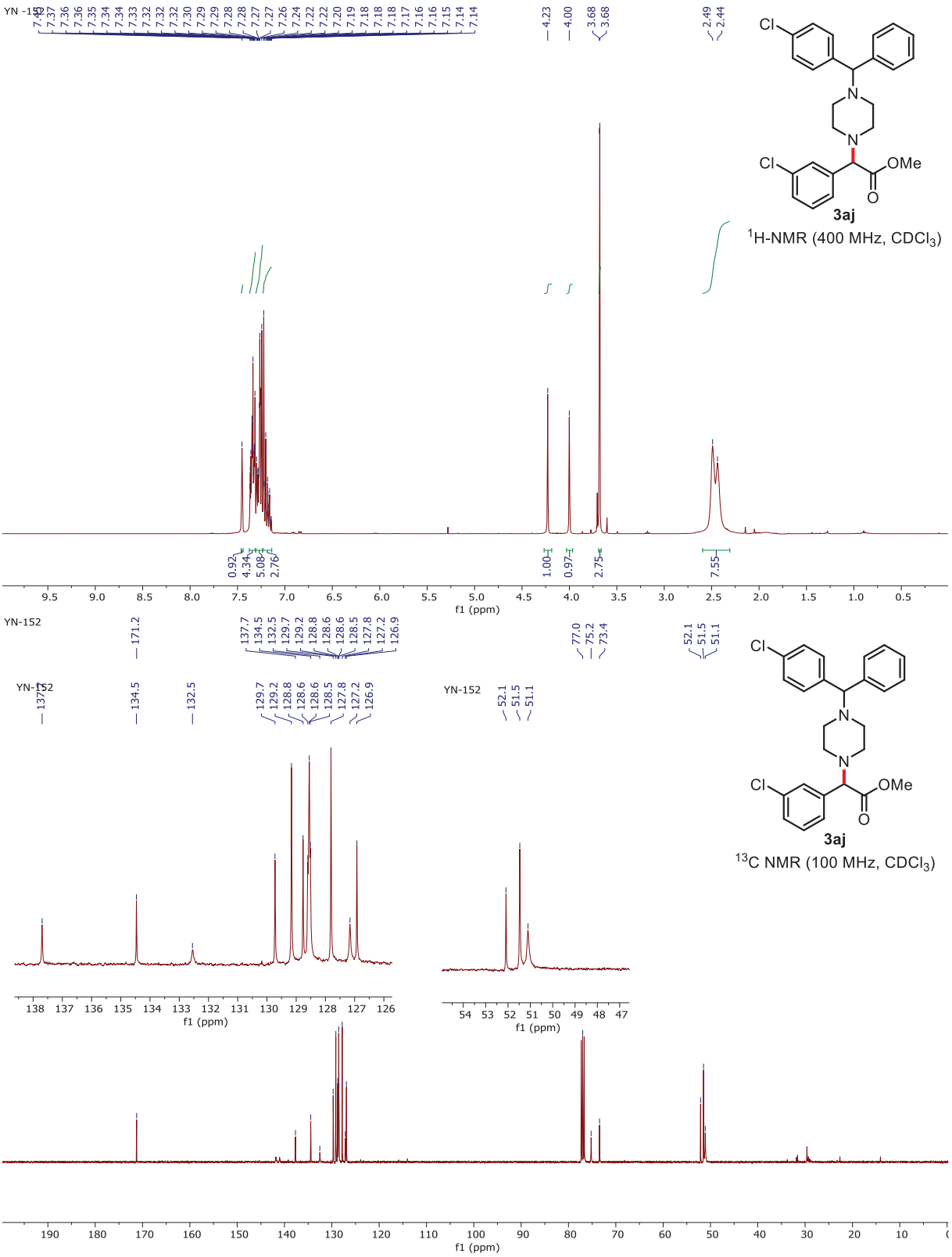

Figure 2.4: ^{1}H and ^{13}C NMR spectra of **3aj**

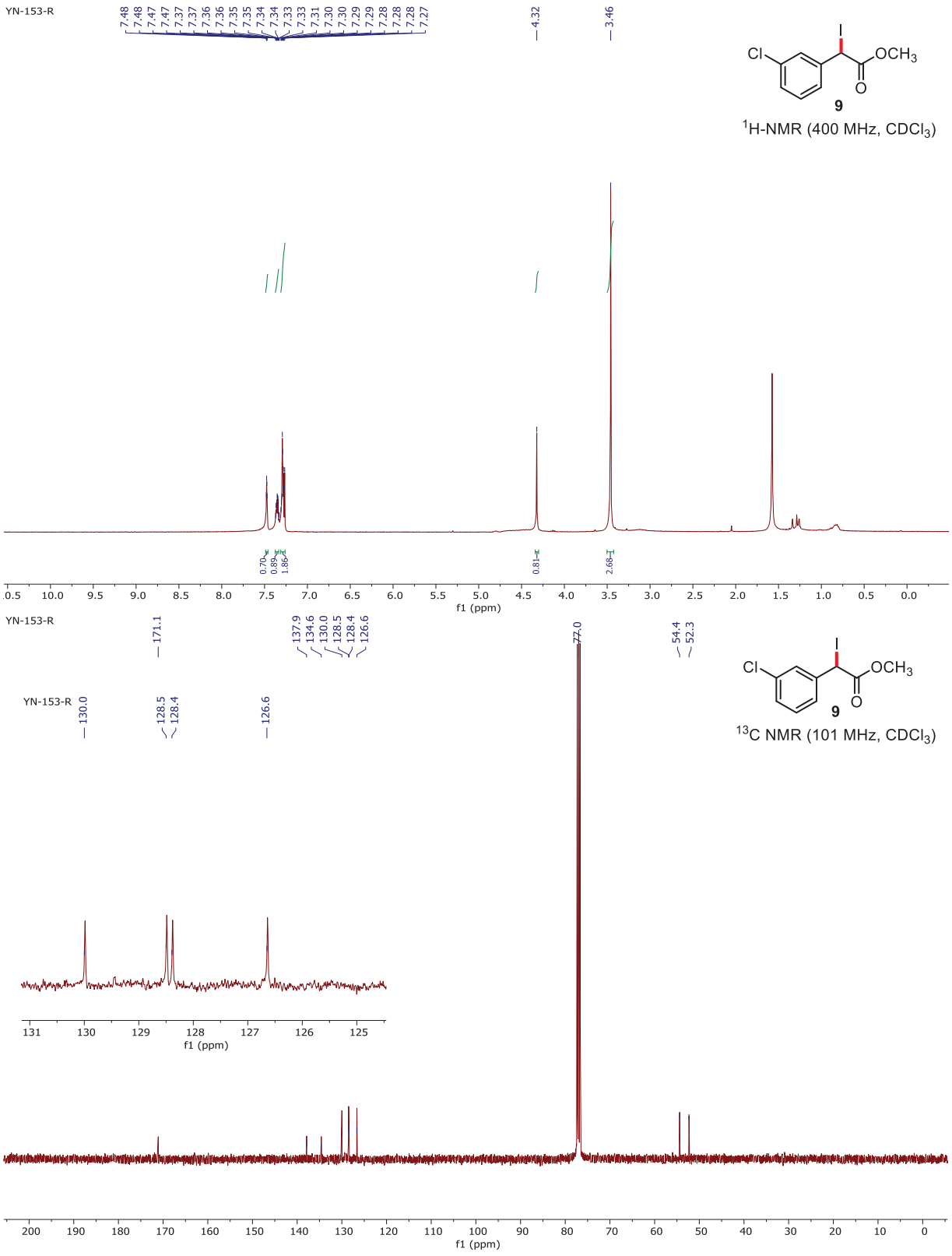

Figure 2.5: ^{1}H and ^{13}C NMR spectra of **9**

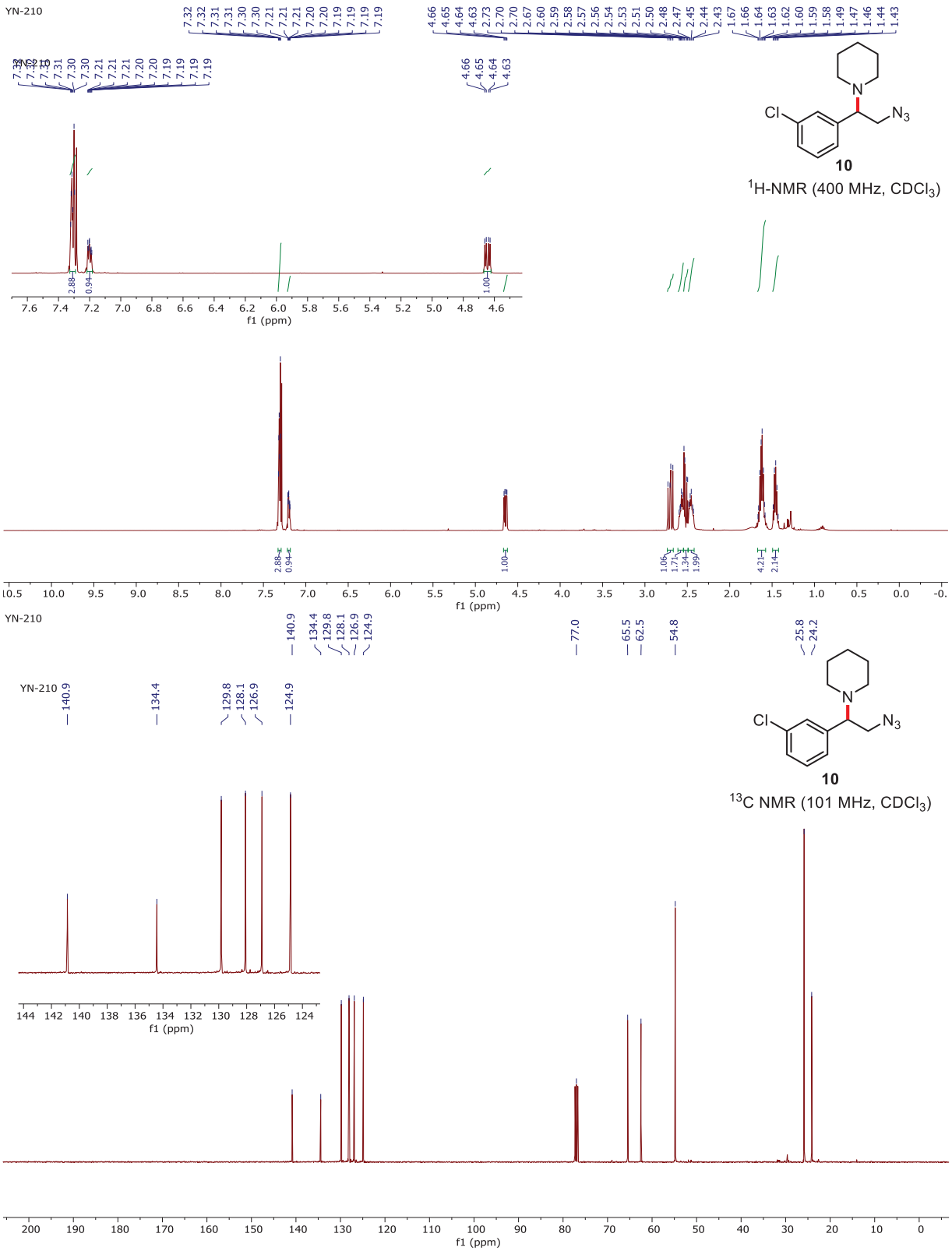

Figure 2.6: ^{1}H and ^{13}C NMR spectra of **10**

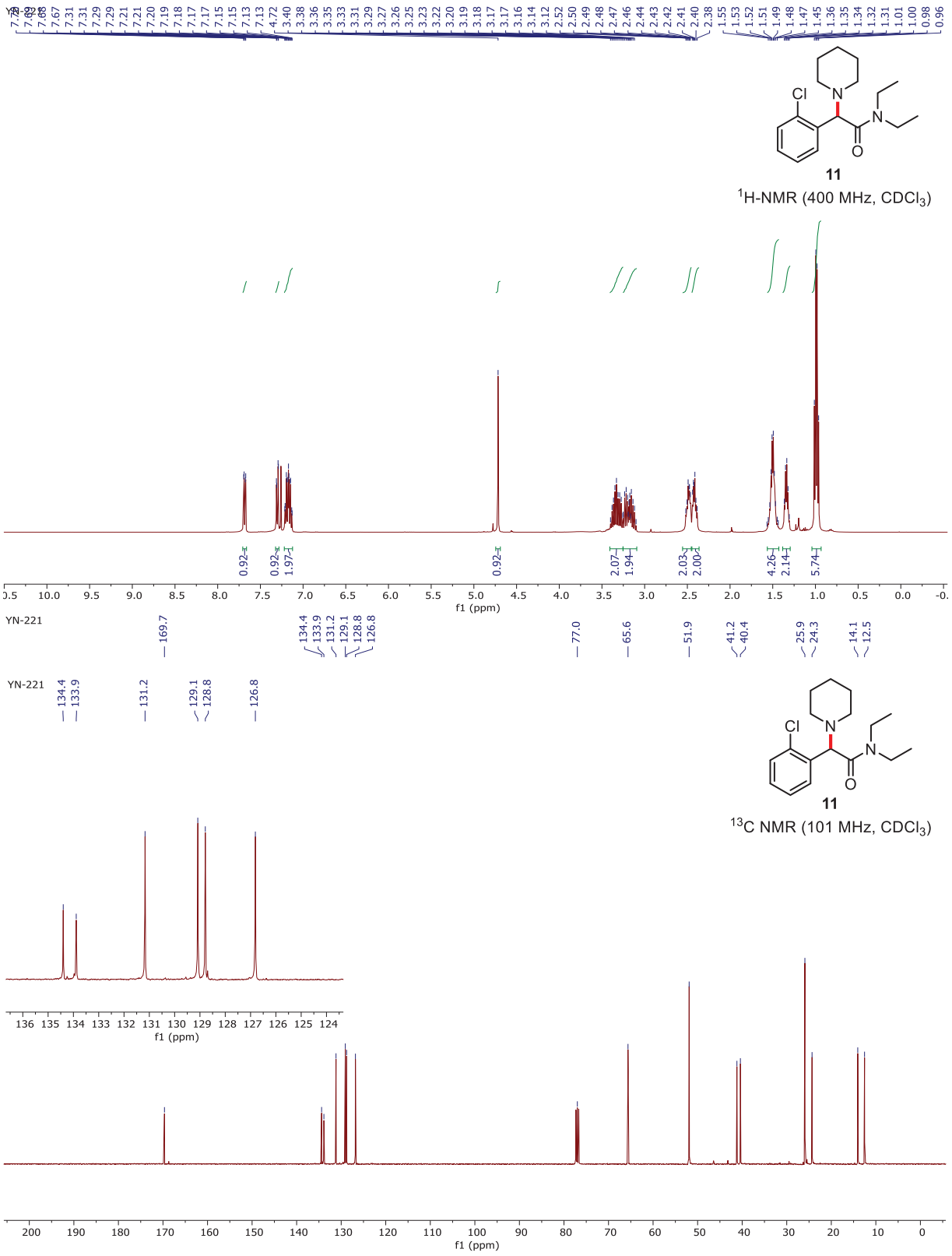

Figure 2.7: ^{1}H and ^{13}C NMR spectra of **11**

2.7 References

1. (a) Tian, T.; Li, Z.; Li, C.-J. *Green Chem*. **2021**, *23*, 6789–6862. (b) Godula, K.; Sames, D. *Science* **2006**, *312*, 67−72. For bioactive *α*-amino-ketones, see (c) Blough, B. E.; Landavazo, A.; Partilla, J. S.; Baumann, M. H.; Decker, A. M.; Page, K. M.; Rothman, R. B. *ACS Med. Chem. Lett*. **2014**, *5*, 623−627. (d) Meyers, M. C.; Wang, J.-L.; Iera, J. A.; Bang, J.-K.; Hara, T.; Saito, S.; Zambetti, G. P.; Appella, D. H. *J. Am. Chem. Soc*. **2005**, *127*, 6152−6153. (e) da Silva, G. R.; Corey, E. J. *J. Am. Chem. Soc*. **2019**, *141*, 20058−20061. (f) Yang, X.; Toste, F. D. *J. Am. Chem. Soc*. **2015**, *137*, 3205−3208. (g) Kiefl, G. M.; Gulder, T. *J. Am. Chem. Soc*. **2020**, *142*, 20577–20582.
2. (a) Tokumasu, K.; Yazaki, R.; Ohshima, T.; *J. Am. Chem. Soc*. **2016**, *138*, 2664−2669. (b) Erdik, E. *Tetrahedron.* **2004**, *60*, 8747–8782. (c) Selig, P. *Angew. Chem., Int. Ed*. **2013**, *52*, 7080–7082. (d) Smith, A. M. R.; Hii, K. K. *Chem. Rev*. **2011**, *111*, 1637–1656. (e) Ohmatsu, K.; Ando, Y.; Nakashima, T.; Ooi, T. *Chem*. **2016**, *1*, 802–810. (f) Trost, B. M.; Tracy, J. S.; Saget, T. *Chem. Sci*. **2018**, *9*, 2975–2980.
3. (a) Strehl, J.; Hilt, G. *Org. Lett*. **2020**, *22*, 5968–5972. (b) Miles, D. H.; Guasch, J.; Toste, F. D. *J. Am. Chem. Soc*. **2015**, *137*, 7632–7635. (c) Fisher, L. E.; Muchowski, J. M. A review. *Org. Prep. Proced. Int*. **1990**, *22*, 399–484.
4. (a) Newhouse, T.; Baran, P. S. *Angew. Chem., Int. Ed*. **2011**, *50*, 3362–3374. (b) Ramirez, T. A.; Zhao, B. G.; Shi, Y. *Chem. Soc. Rev*. **2012**, *41*, 931–942. (c) He, J.; Wasa, M.; Chan, K. S. L.; Shao, Q.; Yu, J.-Q. *Chem. Rev*. **2017**, *117*, 8754–8786. (d) Yi, H.; Zhang, G. T.; Lei, A. *Chem. Rev*. **2017**, *117*, 9016–9085. (e) Sauermann, N.; Meyer, T. H.; Ackermann, L. *ACS Catal*. **2018**, *8*, 7086–7103. (f) Wang, H.; Gao, X.; Lv, Z.; Abdelilah, T.; Lei, A. *Chem. Rev*. **2019**, *119*, 6769–6787. (g) Kawasaki, T.; Ishida, N.; Murakami, M. *J. Am. Chem. Soc*. **2020**, *142*, 3366–3370.
5. (a) Evans, R. E.; Zbieg, J. R.; Zhu, S.; Li, W.; Macmillan, D. W. C. *J. Am. Chem. Soc*. **2013**, *135*, 16074–16077. For direct *α*-amination of *in situ* generated ketones, see (b) Lamani, M.; Prabhu, K. R. *Chem. Eur. J*. **2012**, *18*, 14638–14642. (c) Guha, S.; Rajeshkumar, V.; Kotha, S. S.; Sekar, G. A. *Org. Lett*. **2015**, *17*, 406–409. (d) Jiang, Q.; Xu, B.; Zhao, A.; Jia, J.; Liu, T.; Guo, C. *J. Org. Chem*. **2014**, *79*, 8750–8756. (e) Liang, S.; Zeng, C.-C.; Tian, H.-Y.; Sun, B.-G.; Luo, X.-G.; Ren, F.-z. *J. Org. Chem*. **2016**, *81*, 11565–11573.

6. (a) Zhang, J.; Jiang, J.; Li, Y.; Zhao, Y.; Wan, X. *Org. Lett*. **2013**, *15*, 3222–3225. (b) Zhang, J.; Shao, Y.; Wang, Y.; Li, H.; Xu, D.; Wan, X. *Org. Biomol. Chem.* **2015**, *13*, 3982–3987.
7. (a) Ouyang, L.; Li, J.; Zheng, J.; Huang, J.; Qi, C.; Wu, W.; Jiang, H. *Angew. Chem. Int. Ed*. **2017**, *56*, 15926–15930. (b) Miura, T.; Morimoto, M.; Murakami, M. *Org. Lett*. **2012**, *14*, 5214–5217. (c) Haurena, C.; Gall, E. L.; Sengmany, S.; Martens, T.; Troupel, M. A *J. Org. Chem*. **2010**, *75*, 2645–2650. (d) Jia, W.-G.; Li, D.-D.; Dai, Y.-C.; Zhang, H.; Yan, L.-Q.; Sheng, E.-H.; Wei, Y.; Mu, X.-L.; Huang, K.-W. *Org. Biomol. Chem*., **2014**, *12*, 5509–5516. (e) Tran, T. V.; Le, H. T. N.; Ha, H. Q.; Duong, X. N. T.; Nguyen, L. H.-T.; Doan, T. L. H.; Nguyen, H. L.; Truong, T. *Catal. Sci. Technol*., **2017**, *7*, 3453–3458.
8. (a) Berg, J. M.; Tymoczko, J. L.; Stryer, L. Biochemistry, W. H. Freeman, New York **2002**. (b) Chemistry and Biochemistry of the Amino Acids (Ed.: G. C. Barrett), Chapman and Hall, London **1985**. (c) Wenger, R. M. *Angew. Chem. Int. Ed*. **1985**, *24*, 77–85. (d) Chatterjee, J.; Rechenmacher, F.; Kessler, H. *Angew. Chem. Int. Ed*., **2013**, *52*, 254–269.
9. (a) Francke, R.; Little, R. D. *Chem. Soc. Rev*. **2014**, *43*, 2492–2521. (b) Waldvogel, S. R.; Lips, S.; Selt, M.; Riehl, B.; Kampf, C. J. *Chem. Rev*. **2018**, *118*, 6706–6765. (c) Yan, M.; Kawamata, Y.; Baran, P. S. *Chem. Rev*. **2017**, *117*, 13230–13319. (d) Morofuji, T.; Shimizu, A.; Yoshida, J. I. *J. Am. Chem. Soc*. **2014**, *136*, 4496–4499.
10. (a) Liu, K.; Song, C.; Lei, A. **2018**, *16*, 2375–2387. (b) Jiao, K.-J.; Xing, Y.-K.; Yang, Q.-L.; Qiu, H.; Mei, T.-S. *Acc. Chem. Res*. **2020**, 53, 300–310. (c) Ma, C.; Fang, P.; Mei, T.-S. *ACS Catal*. **2018**, *8*, 7179–7189.
11. (a) Shrestha, A.; Lee, M.; Dunn, A. L.; Sanford, M. S. *Org. Lett*. **2018**, *20*, 204–207. (b) Das, A.; Nutting, J. E.; Stahl, S. S. *Chem. Sci*. **2019**, *10*, 7542–7548. (c) Vannucci, A. K.; Chen, Z.; Concepcion, J. J.; Meyer, T. J. *ACS Catal*. **2012**, *2*, 716–719.
12. (a) Dagar, N.; Sen, P. P.; Roy, S. R. *ChemSusChem*. **2021**, *14*, 1229–1257. (b) Sen, P. P.; Dagar, N.; Singh, S.; Roy, V. J.; Pathania, V.; Roy S. R. *Org. Biomol. Chem*., **2020**, *18*, 8994–9017.
13. (a) Herold, S.; Bafaluy, D.; Muñiz, K. *Green Chem*. **2018**, *20*, 3191–3196. (b) Wang, F.; Stahl, S. S. *Angew. Chem. Int. Ed*. **2019**, *58*, 6385–6390. (c) Hou, Z.-W.; Liu, D.-J.; Xiong, P.; Lai, X.-L.; Song, I.; Xu, H.-C. *Angew. Chem. Int. Ed*. **2021**, *60*, 2943–2947.
14. Thurow, S.; Fernandes, A. A. G.; Acosta, Y. Q.; Oliveira, M. F. D.; Oliveira, M. G. D.; Jurberg, I. D. *Org. Lett*. **2019**, *21*, 6909–6913.

CHAPTER 3

Electrochemical Oxidative Addition of Nucleophiles on 2-Arylindoles: Synthesis of C2-Heteroquaternary Indolin-3-ones

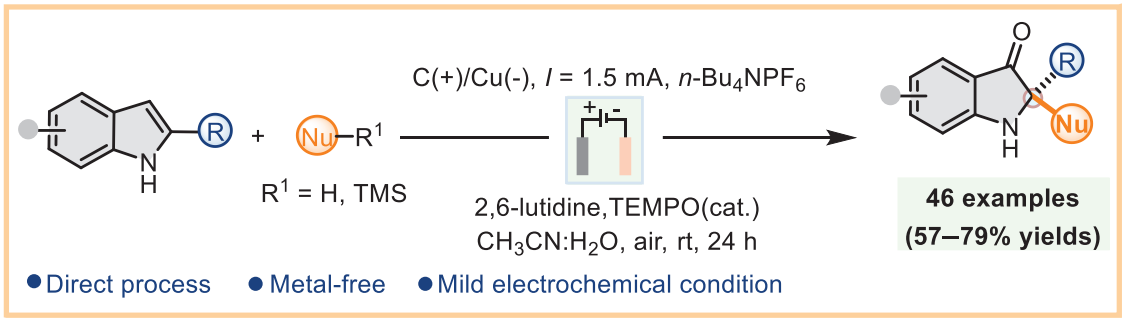

3.1 Introduction

2,2-Disubstituted 1,2-dihydro-3*H*-indol-3-one with a heteroquaternary stereocenter at the C2 position represents an elite unit as an integral part of many essential compounds **(Figure 3.1)**.[1-5] This unit has also been applied as a starting material to access complex polycyclic heterocycles.[6-8] The related compounds have also displayed exciting applications in optoelectronic and material science in recent years.[9-11]

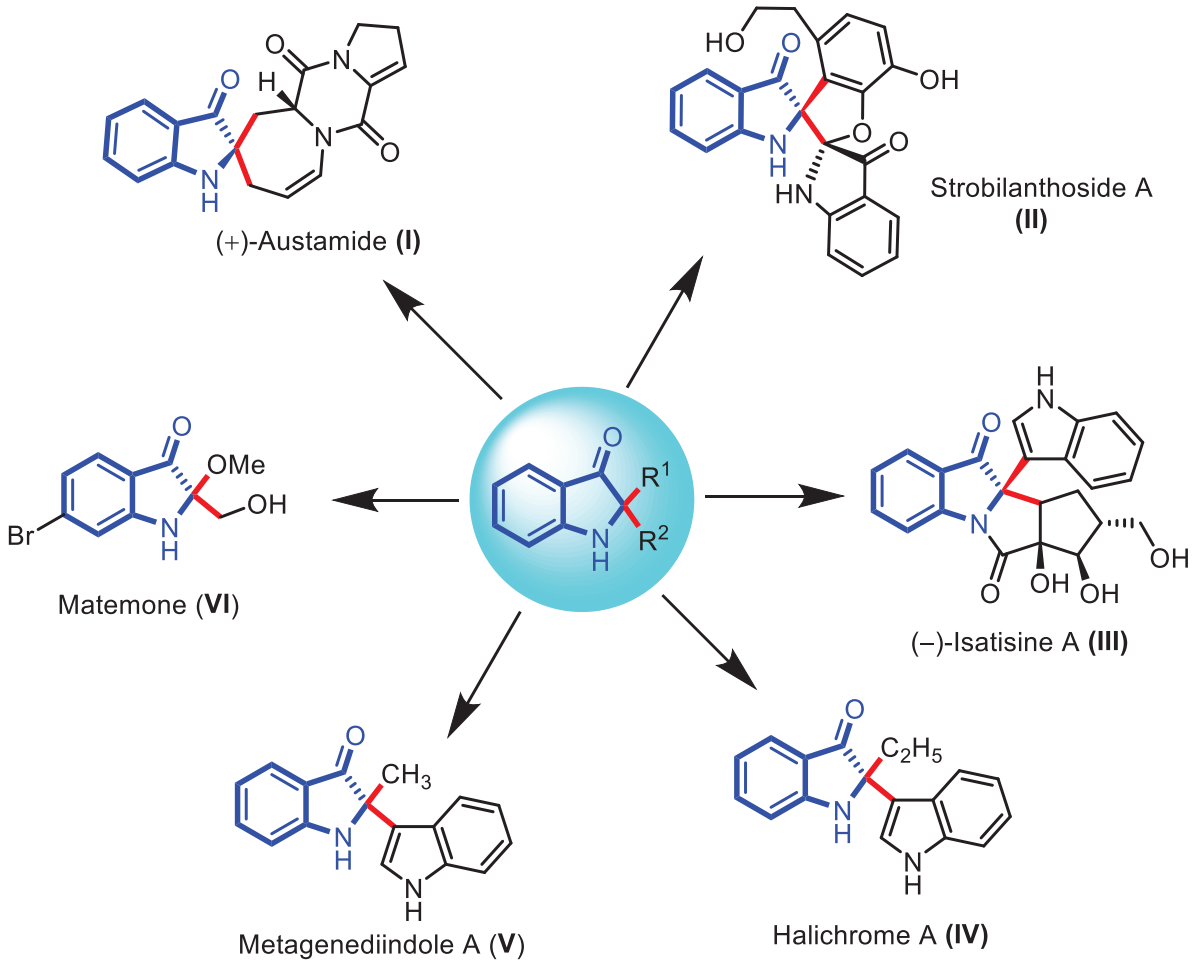

Figure 3.1 Selected natural products and bioactive compounds with the 2,2-disubstituted indolin-3-one

Due to the high synthetic and biological importance of C2-quaternary indoline-3-ones, several methods have been developed.[12] More firmly, these methods can be broadly divided into two main categories: *(i) chemoselective nucleophilic addition to preformed 2-arylindole-3-one, an activated cyclic C-acylimine* ***(Path 1, Figure 3.2)***,[13-24] *(ii) direct oxidative dearomative transformations on 2-arylindoles with various nucleophiles* ***(Path 2, Figure 3.2)***.[25-41] Additional

methods[42-47] that mainly involve transition-metals catalyzed transformations,[48-57] photooxidative rearrangements,[58-60] have also been developed to access this unit. Despite these existing methods, creating a more general strategy for accessing 2,2-disubstituted indolin-3-ones from 2-substituted indoles under mild conditions is highly attractive.

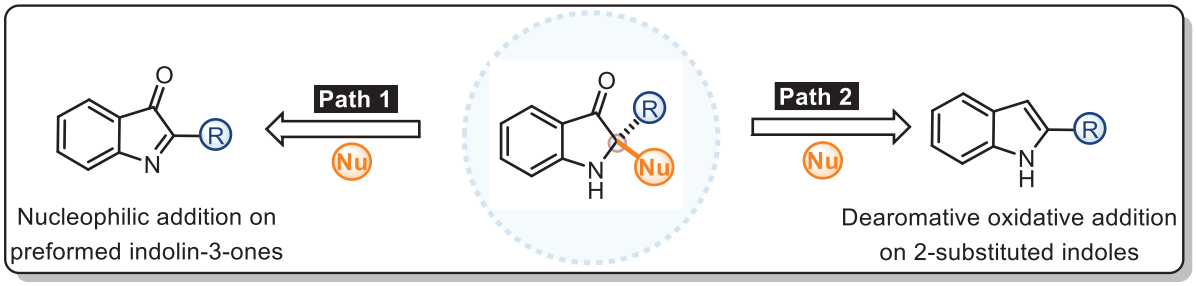

Figure 3.2 General routes to access 2,2-disubstituted indolin-3-ones

3.2 Direct oxidative dearomative transformations on 2-arylindoles (path 2)

3.2.1 Conventional methods

In this context, in 2012, Zhang and co-workers developed a copper-catalyzed method for the dimerization of 2-arylindoles **(1),** followed by cyclization to obtain the desired product **(2) (Scheme 3.1)**. This transformation provides a novel route for accessing fused nitrogen-containing heterocycles. An inexpensive copper catalyst and O_2 or air as the oxidant is a practical advantage. Incorporating an oxygen atom into the organic frameworks from atmospheric molecular oxygen (O_2) offers the ideal oxidation process.[25]

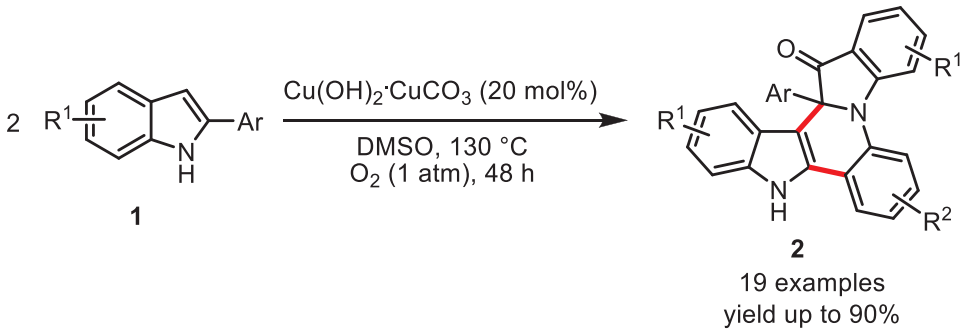

Scheme 3.1 Copper-catalyzed oxidative cyclization of various 2-arylindoles

Kong *et al.* have explored cu-catalyzed trimerization of indoles **(3)** to access indolin-3-one **(4)** decorated with quaternary carbon centers at the C-2 position using TEMPO as oxidant catalyst and benzoic acid as an additive in acetonitrile **(Scheme 3.2)**.[26]

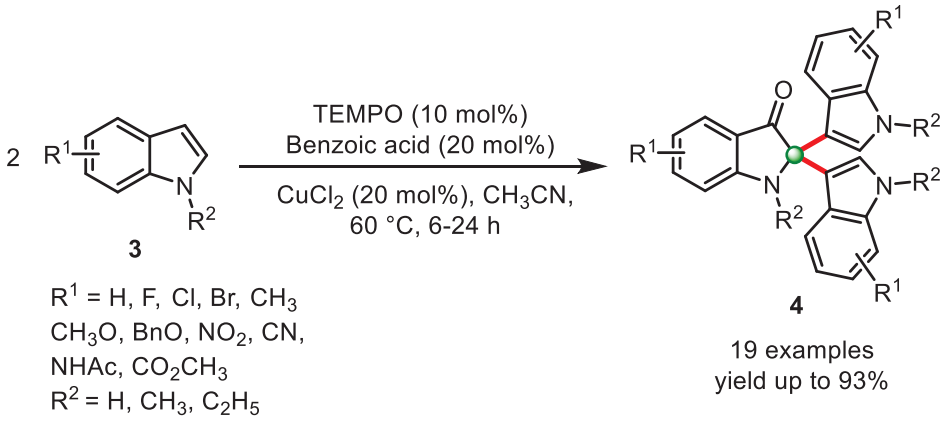

Scheme 3.2 TEMPO & Copper-catalyzed oxidative trimerization substituted indoles

Lin *et al*. demonstrated the silver-catalyzed oxidative self-dimerization of 2-substituted indole derivatives (**1**) using TEMPO as an oxidant and benzoic acid as an additive. Thus, 2,2-disubstituted indolin-3-one **(5)** was obtained with high regioselectivity and moderate to excellent yields (**Scheme 3.3**).[27] The whole procedure was carried out in pyridine as a solvent at 65 °C for 48 h using expensive chemicals like TEMPO, which makes this protocol less practical.

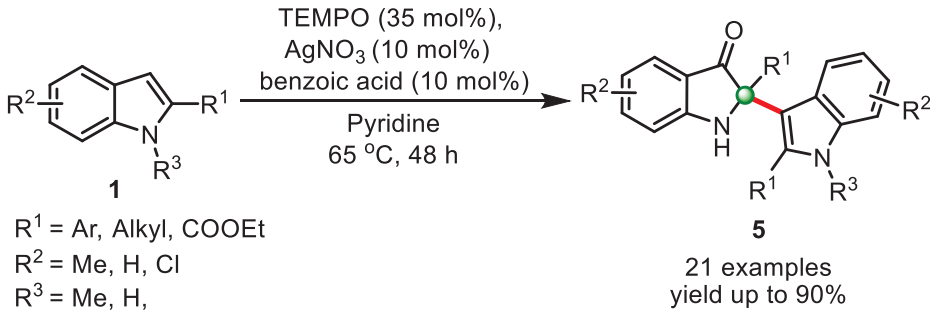

Scheme 3.3 Silver-catalyzed TEMPO oxidative homo dimerization of 2-aryl indole

On the other hand, cross-addition of indole to 2-substituted indole could be another way to achieve C2-quaternary indolin-3-ones; however, it is a difficult task to accomplish in terms of selectivity. In this context, Kashyap and co-workers developed an exciting and very first protocol for the Pd-catalyzed cross-addition of indoles **(3)** to 2-substituted indoles **(1)** to access 2,2-disubstituted indolin-3-ones **(6)** in a chemoselective fashion involving oxidative dearomatization of 2-aryl or 2- alky indoles from TBHP (t-butyl hydrogen peroxide), Manganese dioxide, and Kornblum−DeLaMare type reactions in acetonitrile at 65 °C (**Scheme 3.4**).[28]

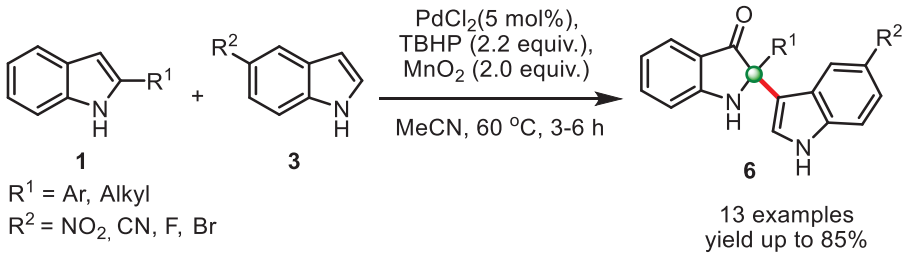

Scheme 3.4 Pd-catalyzed oxidative dearomatization of 2-aryl or 2-alkyl-indoles

In 2016, Li and co-workers developed copper-catalyzed oxidative dearomatization/spirocyclization of indole-2-carboxamides **(7)** using tert-butyl hydroperoxide (TBHP) as the oxidant that provides rapid and efficient access to C2-spiro-pseudoindoxyls **(8)**. Two of the sp^2 C–H bonds are functionalized during the reaction process, and the reaction likely proceeds via the formation of a highly reactive 3*H*-indol-3-one intermediate followed by aromatic electrophilic substitution with the *N*-aryl ring of the amide moiety (**Scheme 3.5**).[29]

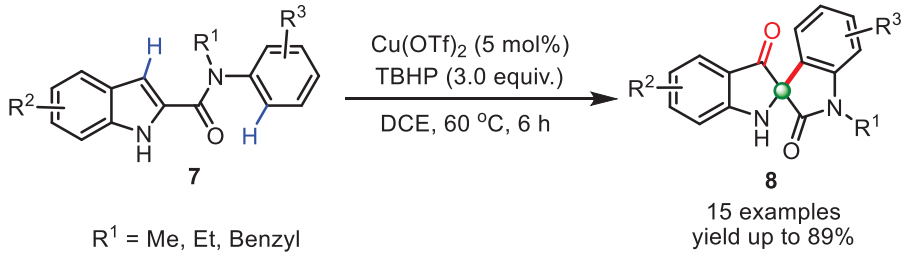

Scheme 3.5 Cu-catalyzed oxidative dearomatization/spirocyclization of indole-2-carboxamides

Zhou *et al*. have explored the Ru-catalyzed oxidative dearomatization of 2-alkyl or 2-aryl-substituted indoles **(1)** coupled with a cascade transformation; it provides a new system for the construction of indolin-3-ones **(5)** bearing a C2-quaternary functionality. This reaction occurs readily with $RuCl_3 \cdot 3H_2O$ as a catalyst, and $NaICO_4$ is used as an oxidant in acetonitrile. 2-(3-Indolyl)- substituted indolin-3-ones were obtained in medium to high yields (**Scheme 3.6**).[30]

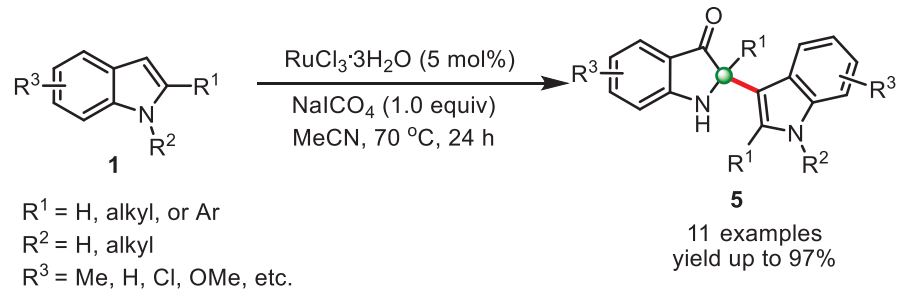

Scheme 3.6 Ru-catalyzed oxidative dearomatization of 2-substituted indole

In 2018, Li and co-workers developed the asymmetric oxidative Mannich reaction for the first time, combining photocatalysis with the non-natural catalytic activity of a hydrolase **(Scheme 3.7)**. In this approach, 2,2-disubstituted indole-3-ketones **(10)** were synthesized asymmetrically from 2-aryl indoles **(1)** by a one-pot method combining visible-light catalysis and enzymatic catalysis. Under the optimized conditions, which consist of $Ru(bpy)_3Cl_2$ as the photocatalyst, 0.16 mol% wheat germ lipase (WGL) as the biocatalyst, *N*, *N*-dimethylformamide (DMF) as the solvent, a 32 W compact fluorescent lamp (CFL) as the light source, and an oxygen atmosphere, the desired products were obtained with 10–70% yields, 32–86% ee and 3:1–5:1 dr. Different 2-arylindoles and aliphatic ketones were investigated, and all were well tolerated.[31]

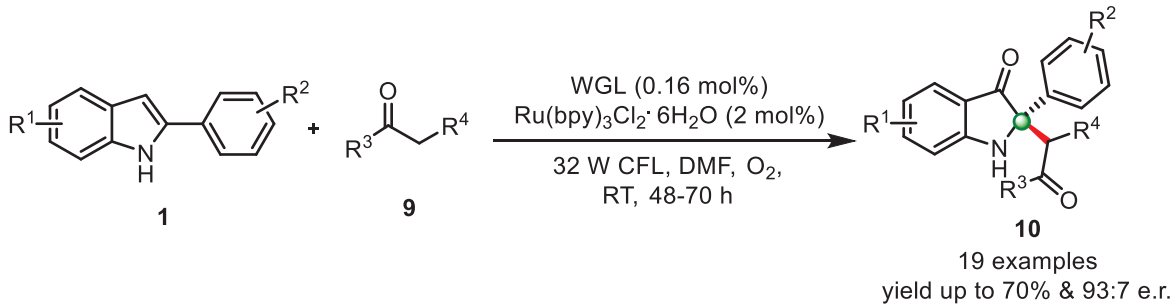

Scheme 3.7 Asymmetric oxidative Mannich reaction combining photocatalysis and enzymatic catalysis

Yu and co-workers developed a straightforward metal-free method for the synthesis of indolin-3-one for the cross-addition of indoles **(3)** with 2-substituted indoles **(1)** to access a series of 2,2-disubstituted indolin-3-ones **(6)**. The following transformation was carried out on a small-scale microwave at a high temperature **(Scheme 3.8)**.[32]

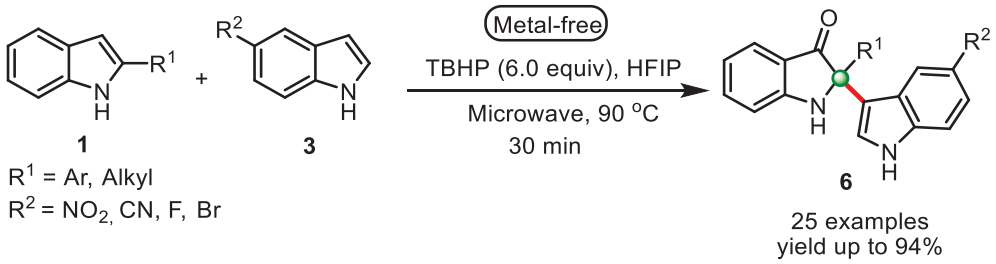

Scheme 3.8 Microwave-assisted synthesis of 2,2-disubstituted indolin-3-ones.

In 2019, Zhang's group reported an enantioselective oxidative Mannich reaction between aldehydes or ketones **(9)** and indolones, which were generated *in situ* through an oxygen atom transfer from an *N*-oxoammonium salt to a 2-substituted indole **(1)**. After an optimization

process, they selected $TEMPO^{+}OTf^{-}$ as the best *N*-oxoammonium salt to accomplish the *in situ* oxidation of C-2-substituted indole in 12 h. Then, the corresponding carbonyl compound and L-proline are added to obtain the desired product **(10)** in excellent stereocontrol through an asymmetric Mannich alkylation. With these conditions, they explored the scope of this transformation using differently substituted indoles, aldehydes, and ketones. These researchers could obtain the desired products in high to excellent yields, diastereomeric ratios, and enantiomeric excesses **(Scheme 3.9)**.[33]

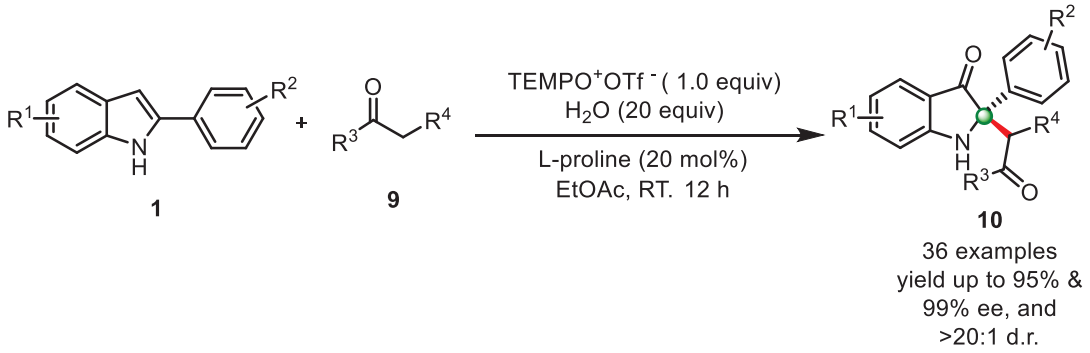

Scheme 3.9 Enantioselective dearomative oxyalkylation of 2 arylindoles with aldehydes and ketones

The same group described the TEMPO oxoammonium salt-mediated oxidative dearomatization of 2-arylindoles **(1)** at room temperature. Aryl, alkynyl, alkenyl potassium trifluoroborate, and allyl or cyanotrimethylsilane **(11)** were all compiled for these transformations. Under very mild conditions, dearomative oxyalkynylation and oxyalkenylation of indoles to structurally diverse 2,2-disubstituted indolin-3-ones **(12)** were developed for the first time with high atom economy. In addition, dearomative oxyarylation, oxyallylation, and oxycyanation of indoles were also demonstrated. Mechanism studies indicated that TEMPO oxoammonium salt was the sole oxidant source through an electron donor-acceptor (EDA) intermediate **(Scheme 3.10)**.[34]

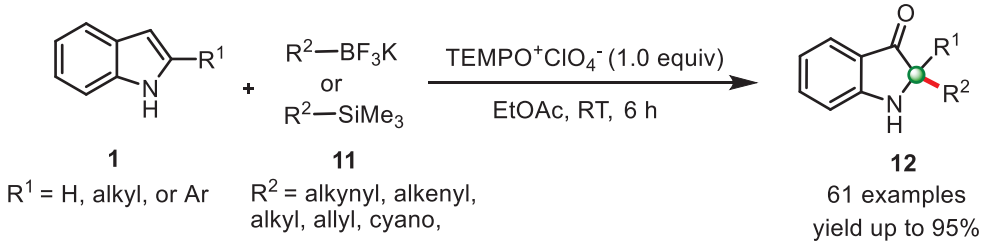

Scheme 3.10 $TEMPO^{+}ClO_4^{-}$ -mediated oxidative dearomatization of 2-substituted indoles

In continuation, Our group also developed an efficient protocol for synthesizing 2,2-disubstituted indolin-3-ones under mild conditions in the same year. This reaction involves the copper-catalyzed *in situ* oxidative dearomatization of 2-arylindoles **(1)** to indol-3-one, followed by self-dimerization **(5)** and cross-addition **(6)** with indoles **(3)** under favorable conditions. The result generates various C2-tetrasubstituted indolin-3-ones with good to high yields (62–82%) **(Scheme 3.11)**.[35]

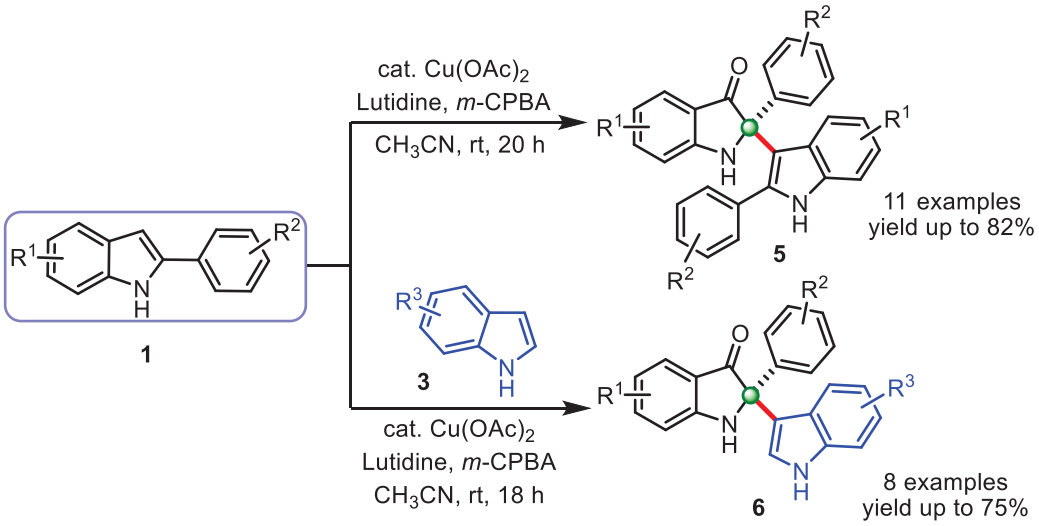

Scheme 3.11 Cu-catalyzed oxidative dimerization of 2-aryl indoles and cross-addition with indoles

Zhou *et al*. have explored the Ru-catalyzed oxidative dearomatization of 2-alkyl or 2-aryl-substituted indoles **(1)** coupled with a cascade transformation; it provides a new system for the construction of indolin-3-ones **(5)** bearing a C2-quaternary functionality. This reaction occurs readily with $RuCl_3 \cdot 3H_2O$ as a catalyst, and TBHP is used as an oxidant in ethyl acetate. 2-(3-Indolyl)- substituted indolin-3-ones were obtained in medium to high yields (**Scheme 3.12**).[36]

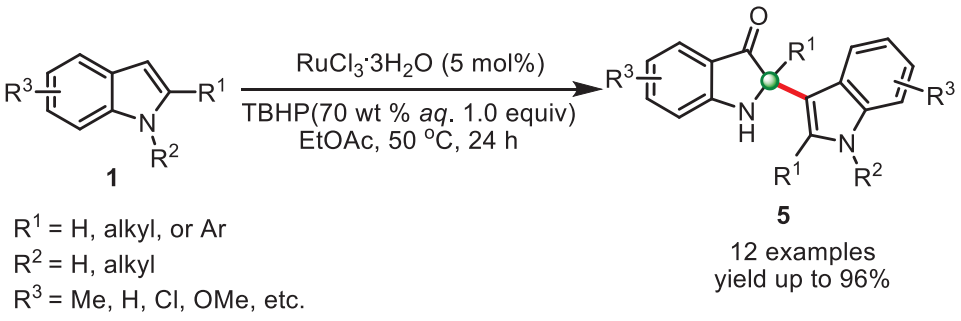

Scheme 3.12 Ru-catalyzed oxidative functionalization of 2-arylindoles

In 2020, Li and co-workers achieved an excellent result by combining photocatalysis and organocatalysis for asymmetric oxidative alkylation of 2-arylindoles **(1)** to access 2,2-disubstituted indolin-3-ones **(10)**. Under these conditions, which consisted of $Ru(bpy)_3Cl_2$ as a photocatalyst, l-proline or d-proline as an organocatalyst, 2,6-lutidine as an additive, ethanol as a solvent, and blue LEDs as the light source, under an oxygen atmosphere, the desired products were obtained with 20–92% yields, 90–99% ee and 5:1 to 20:1 d.r. 26 examples were reported. Various substituents on indole and both chain and cyclic aliphatic ketones **(9)** were well tolerated (**Scheme 3.13**).[37]

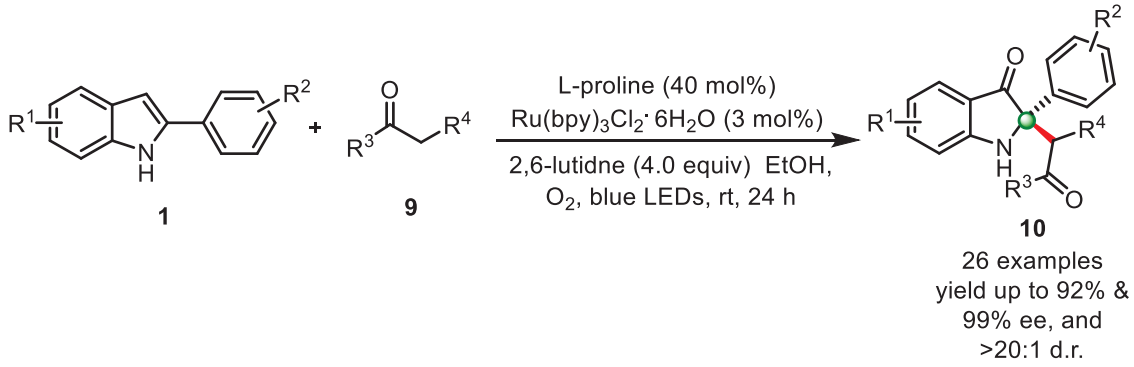

Scheme 3.13 Combination of photocatalysis and organocatalysis for asymmetric oxidative alkylation of 2-arylindoles

In 2020, Zhang and his team reported the oxidative dearomative cross-dehydrogenative coupling of 2-arylindoles **(1)** with various C-H nucleophiles **(13)**. This process features a broad substrate scope concerning indoles and nucleophiles, affording structurally diverse 2,2-disubstituted indolin-3-ones **(14)** in high yields (up to 99%). Moreover, various C-H nucleophiles such as pyrrole, thiophene, acetaldehyde, and acetone were also suitable substrates, and all the 2,2-disubstituted indolin-3-ones were obtained as racemic molecules. The oxidative dimerization and trimerization of indoles have also been demonstrated under the same conditions(**Scheme 3.14**).[38]

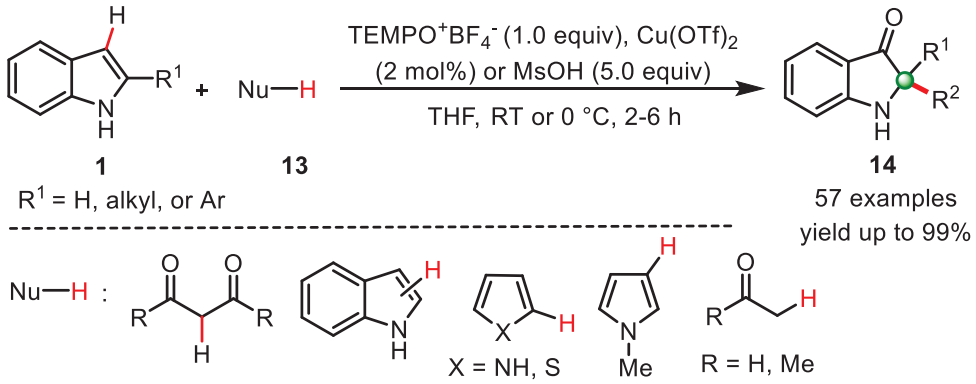

Scheme 3.14 Oxidative dearomative cross-dehydrogenative coupling of indoles with various C-H nucleophiles

Smith & co-workers developed an operationally simple method for converting 2-substituted indoles **(1)** to 2,2-disubstituted indoxyls **(16)** with a broad substrate scope for indole and nucleophiles **(15)**. This method provides convenient and relatively unique access to such heterocycles with 2,2-dialkyl substitution and free N–H groups, making it appealing for medicinal chemistry applications. They showcased its utility in concise total syntheses of trigonoliimine C (6 steps) and brevianamide A (7 steps), among the shortest approaches to these targets reported (**Scheme 3.15**).[39]

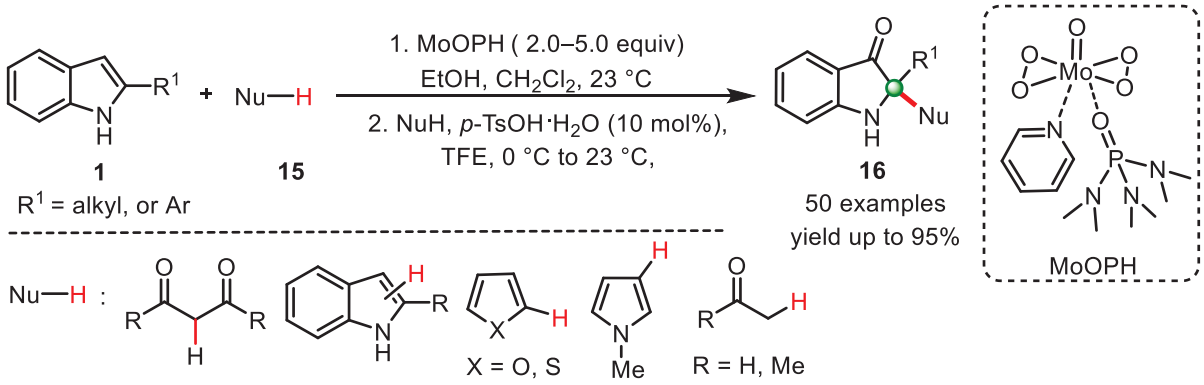

Scheme 3.15 Mo-catalyzed oxidative dearomatization of 2-substituted indoles with various C-H nucleophiles

Zhao *et al*. developed a protocol of one-pot asymmetric oxidative dearomatization of 2-substituted indoles **(1)** to realize the synthesis of C2-tetrasubstituted indolin-3-ones. This strategy combines transition-metal catalysis and organocatalysis and undergoes two processes, including CuI-catalyzed oxidative dearomatization of 2-substituted indoles using O_2 as green oxidant and

L-proline-promoted asymmetric Mannich reaction with ketones or aldehydes **(9)**. A series of chiral C2-tetrasubstituted indolin-3-ones **(10)** were synthesized via this strategy (**Scheme 3.16**).[40]

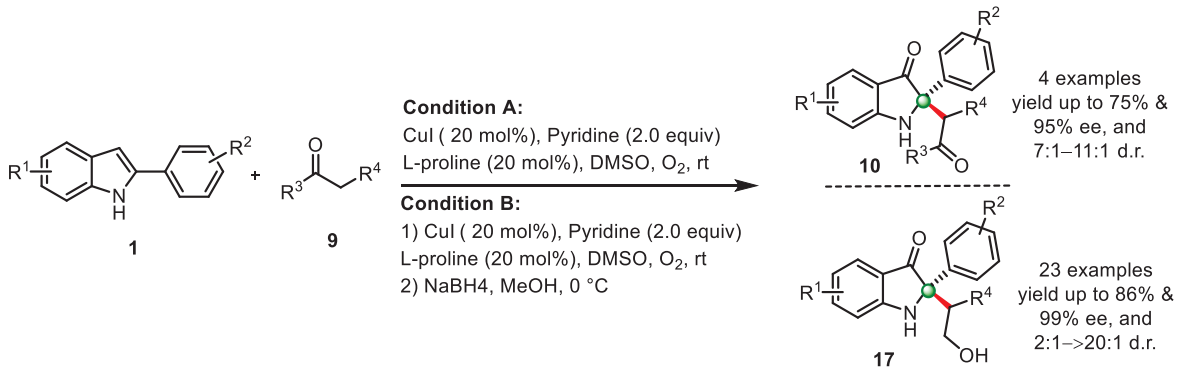

Scheme 3.16 Asymmetric oxidative dearomatization of 2-substituted indoles to construct the C2 tetrasubstituted indolin-3-ones

Patureau & co-workers reported the unprecedented Te-catalyzed dehydrogenative homo dimerization **(5)** of 2-substituted indoles **(1)**. This represents a rare redox-active phenotellurazine catalyst-enabled method and the first that does not involve a phenothiazine substrate. The most important features of this reaction are its O_2-mediated character and the absence of a background reaction when the Te(II) catalyst is omitted. Furthermore, this reaction is operational with only 10 mol % of Te catalyst loading **(Scheme 3.17)**.[41]

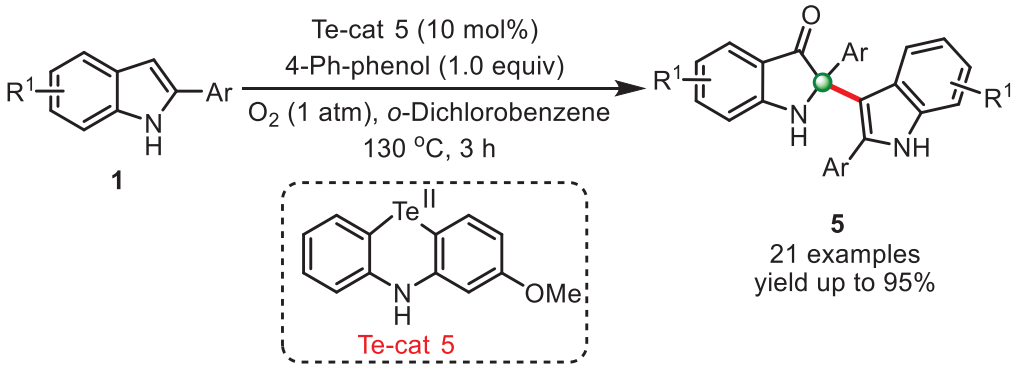

Scheme 3.17 Te-catalyzed dehydrogenative homo dimerization of 2-arylindoles.

3.2.2 Electrochemical methods

On the other hand, electrochemical synthesis has recently gained enormous interest due to using electrons as reagents for oxidative/reductive conversion and an excellent functional group tolerance under mild conditions.[61-66] The electrochemical strategies have recently been applied to a series of carbon-carbon/carbon-heteroatom bond-forming reactions along with cascade transformations. Under electrochemical conditions, oxidative dearomatization of 2-arylindoles and subsequent direct Mannich reaction of ketones using amine-catalysis have recently been developed to access 2,2-disubstituted indolin-3-ones.[67-70]

In this context, He and co-workers have created a direct enantioselective synthesis of C2-quaternary indolin-3-ones **(10)** by combining electrocatalysis with organocatalysts. This protocol utilized (2,2,6,6-tetramethylpiperidin-1-yl)oxyl (TEMPO) as a redox mediator. The experiment revealed that adding TEMPO could improve the yield, but the enantioselectivity and diastereoselectivity were unaffected. After extensive optimization of reaction conditions, the optimal reaction conditions were determined as follows: using platinum sheets as the anode and cathode, tetrabutylammonium perchlorate (TBAP) as the electrolyte, 10 mol% TEMPO as a redox mediator, *N*, *N*-dimethylformamide/2,2,2-trifluoroethanol (3:1) as a mixed solvent, benzoic acid as an additive at a constant current of 0.8 mA under an air atmosphere. The reaction shows good functional group tolerance **(Scheme 3.18)**.[71]

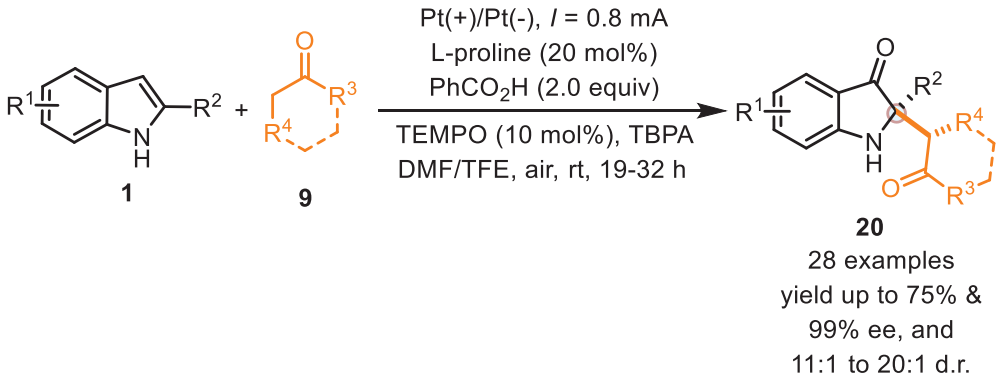

Scheme 3.18 Electrochemical oxidation of 2-arylindoles and subsequent Mannich reaction with proline

Long et al. recently developed an exciting method for the direct asymmetric synthesis of 2,2-disubstituted 3-carbonyl indoles by combining electrochemistry with Lipase catalysis. Various 2,2-disubstituted 3-carbonyl indoles **(10)** with stereogenic quaternary carbon centers can be directly synthesized from 2-substituted indoles **(1)** and ketones **(9)** in satisfactory yields with

good enantio- and diastereoselectivities under mild reaction conditions. Crucially, this unprecedented protocol demonstrated that hydrolase catalysis is compatible with organic electrosynthesis. This protocol expands the types of enzymes in enzymatic electrosynthesis, enabling the synthesis of complex chiral molecules without the need for any transition metals, ligands, or stoichiometric oxidants (**Scheme 3.19**).[72]

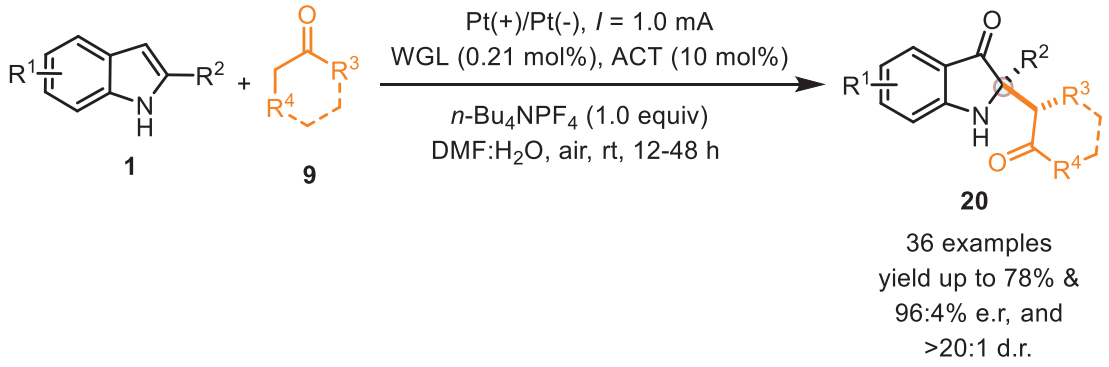

Scheme 3.19 Combination of electrocatalysis and enzymatic catalysis for asymmetric oxidative alkylation of 2-arylindoles

Despite the presence of these graceful electrochemical methods in combination with another catalysis, developing a more general approach that could overcome the nucleophile's limitation is still required. In this chapter, we disclose a simple study to access C2-tertiary carbon indolin-3-one **(16)** via oxidative-dearomatization followed by *in situ* addition of several nucleophiles under mild electrochemical conditions **(Scheme 3.20)**.

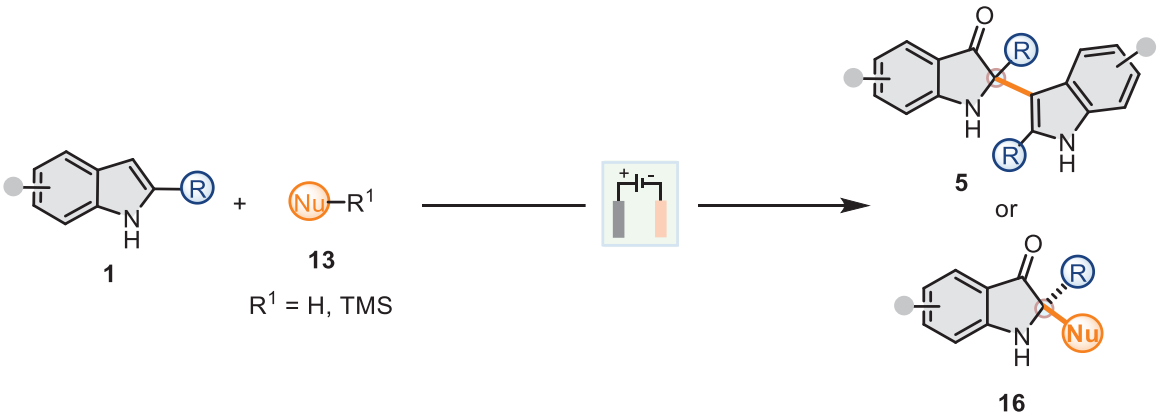

Scheme 3.20 Electrochemical oxidative synthesis of C2-quaternary indolin-3-ones with the various nucleophiles

3.3 Results and discussion

Considering this idea, we initiated our study with 2-phenyl indole **1a** as a suitable substrate for oxidative dimerization under electrochemical conditions (Table 3.1). Detailed studies concerning electrodes, electrolytes, catalysts, and solvents were carried out (Table 3.1) and led to the optimal reaction conditions. To our delight, 2-phenyl-2-(2-phenyl-1*H*-indol-3-yl)indolin-3-one **5a** was obtained in 76% yield under optimized conditions (entry 1, Table 3.1). The reaction furnishes a trace amount of the product in the absence of TEMPO (entry 2, Table 3.1) and *n*-Bu_4NPF_6 (entry 3, Table 3.1), whereas no **5a** was observed without current (entry 4, Table 3.1). Next, fewer results were obtained without lutidine (entry 5, Table 3.1). The addition of bases (2.0 equiv.) under standard conditions (entries 6-7, Table 3.1) and changing the electrode system under standardized conditions (entries 8-9, Table 3.1) didn't improve reaction yields. The reaction outcome did not improve either by decreasing (entry 10, Table 3.1) or increasing (entry 11, Table 3.1) the applied current. Product **5a** was obtained with 61% and 65% yields when TEMPO (10 mol%) (entry 12, Table 3.1) and 2,6-lutidine (1.0 equiv.) (entry 13, Table 3.1) were applied under standard conditions. A reduction in the yield (35%) was observed with N_2 purging instead of air (entry 14, Table 3.1). By varying solvent mediums like CH_3CN/TFE (9:1) and CH_3CN/HFIP (9:1) instead of CH_3CN/H_2O (9:1) (entries 15-16, Table 3.1) and other electrolytes were also tested, such as *n*-Bu_4NBF_4 and *n*-Bu_4NClO_4, but all gave inferior results compared to *n*-Bu_4NPF_6 (entries 17–18, Table 3.1). Moreover, other mediators, such as ferrocene and ammonium iodide, were also tested, with no improved result concerning standard reaction conditions. Therefore, we conducted our experiment under optimum conditions (entry 1, Table 3.1).

With the optimized conditions for the oxidative-dimerization of 2-arylindoles, we examine the method's scope with a variety of 2-arylindoles (Table 3.). 2-Arylindole **1** substituting with electron-donating/withdrawing groups at the C2-aryl ring produced corresponding dimerized products **5b**-**5i** with good yields (58-79%) under optimized conditions. While substitutions at the indole ring also furnished the complementary products **5j**-**5l** with promising results (64-68%) **(Table 3.2)**.

Table 3.1 Optimization of the reaction conditions[a]

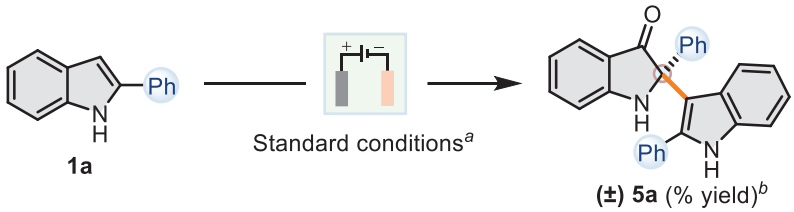

Entry	Variation from standard conditions	Yield (%)
1	none	76
2	without TEMPO	<10
3	without *n*-Bu_4NPF_6	<10
4	without current	-
5	without 2,6-lutidine	35
6	pyridine (2.0 equiv) used as an additive	60
7	K_2CO_3 (2.0 equiv) used as an additive	45
8	C(+)/C(-) used instead of C(+)/Cu(-)	56
9	C(+) | Pt(-) used instead of C(+)/Cu(-)	<10%
10	I = 1.0 mA, instead of I = 1.5 mA	45
11	I = 2.0 mA, instead of I = 1.5 mA	58
12	TEMPO (10 mol%) instead of (20 mol%)	61
13	2,6-lutidine (1.0 equiv) used instead of (2.0 equiv)	65
14	N_2 instead of air	35
15	CH_3CN/TFE (9:1) used instead of CH_3CN/H_2O (9:1)	64
16	CH_3CN/HFIP (9:1) used instead of CH_3CN/H_2O (9:1)	62
17	*n*-Bu_4NBF_4 (1.0 equiv.) used instead of $LiClO_4$ (1.0 equiv.)	45
18	*n*-Bu_4NClO_4 (1.0 equiv.) used instead of $LiClO_4$ (1.0 equiv.)	60
19	Cp_2Fe (20 mol%) used as a mediator	26
20	NH_4I (20 mol%) used as a mediator	<10

[a]**Reaction conditions**: **1a** (1.0 mmol, 2.0 equiv), *n*-Bu_4NPF_6 (0.5 mmol, 1.0 equiv), TEMPO (0.1 mmol, 20 mol%), 2,6-lutidine (1.0 mmol, 2.0 equiv) CH_3CN/H_2O (9:1), C(+) | Cu(–), undivided cell, constant current = 1.5 mA, air, rt, 24 h. [b]All isolated yields of **5a** after column chromatography were based on **1a**.

Table 3.2 Substrate scope for the self-dimerization of 2-arylindoles.

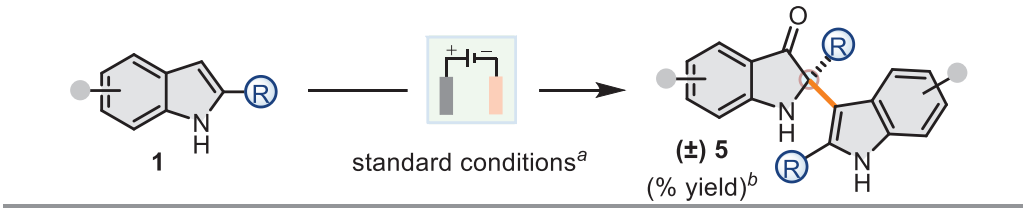

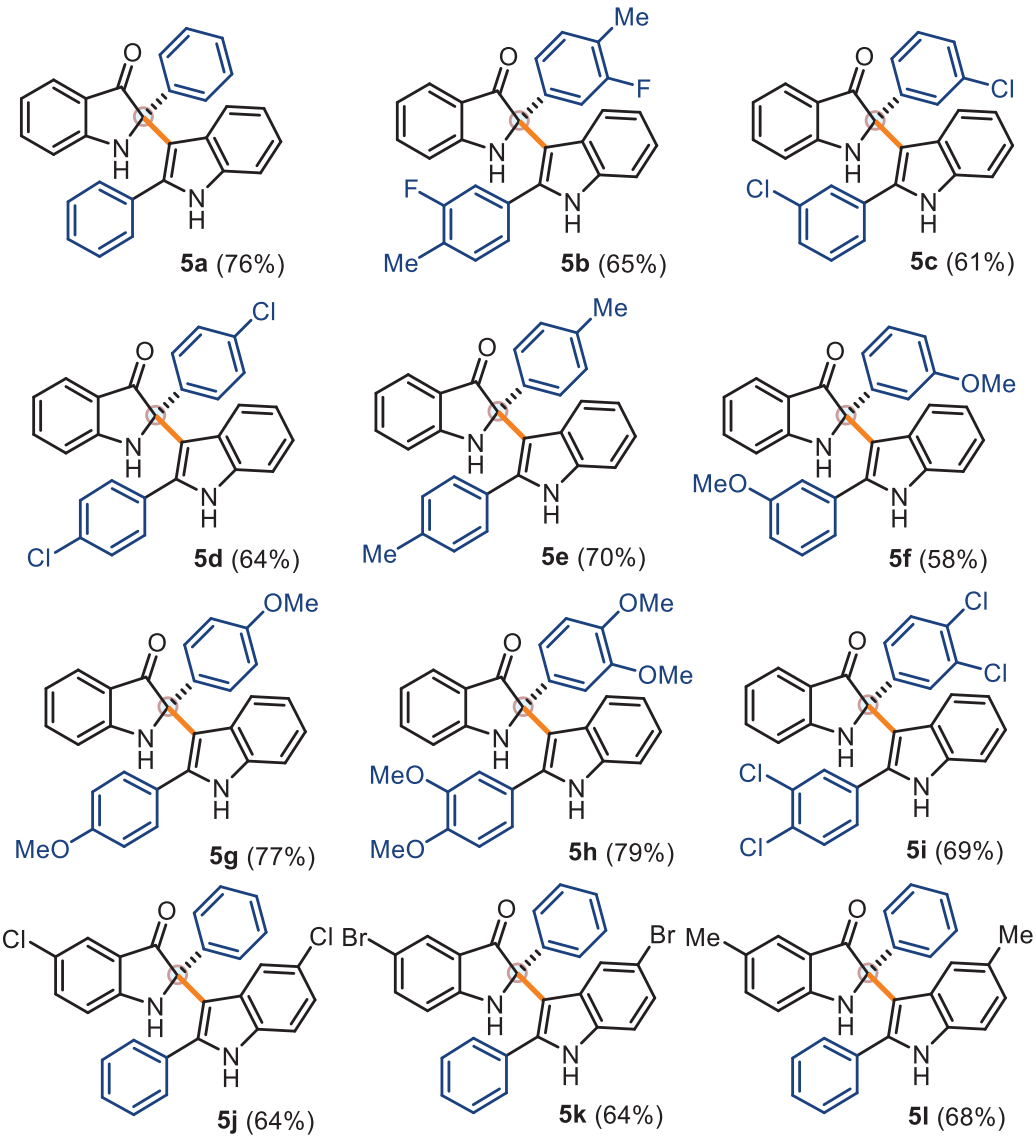

[a]**Reaction conditions**: **1** (1.0 mmol, 2.0 equiv), *n*-Bu_4NPF_6 (0.5 mmol, 1.0 equiv), TEMPO (0.1 mmol, 20 mol%), 2,6-lutidine (1.0 mmol, 2.0 equiv) CH_3CN/H_2O (9:1), C(+) | Cu(–), undivided cell, constant current = 1.5 mA, air, rt, 24 h. [b]All isolated yields of **5** after column chromatography were based on **1**.

Table 3.3 Optimization of the reaction conditions with **13h** as a nucleophile[a]

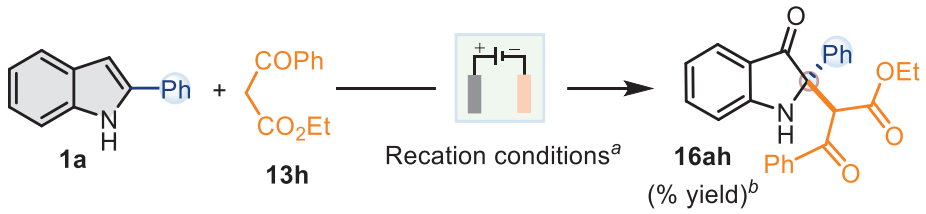

Entry	Variation from standard conditions	Yield (%)
1	none	73%
2	**13h** (1.0 equiv.) was used	51%
3	**13h** (2.0 equiv.) was used	60%
4	**13h** (4.0 equiv.) was used	73%

[a]**Reaction conditions**: **1a** (0.5 mmol, 1.0 equiv), **13h** (1.5 mmol, 3.0 equiv), *n*-Bu_4NPF_6 (0.5 mmol, 1.0 equiv), TEMPO (0.1 mmol, 20 mol%), 2,6-lutidine (1.0 mmol, 2.0 equiv) CH_3CN/H_2O (9:1), C(+) | Cu(–), undivided cell, constant current = 1.5 mA, rt, 24 h. [b]All isolated yield of **16ah** was based on **1a**.

Next, we explored the developed conditions with a slight variation for several other nucleophiles **13** with 2-arylindoles **1a (Table 3.4)**, and the results are shown in **Table 3.4**. Initially, indole **3a** and substituted indoles **3b-3c** were utilized as nucleophiles, resulting in **16aa** (70%) and **16ab-16ac** (62% and 73%).

Next, a series of 1,3-dicarbonyls such as 1,3-diesters **13d-13f**, 1,3-keto-esters **13g-13h**, and 1,3-diketocarbonyl **13i** as nucleophiles also furnished the corresponding products **16ad-16ai** (60-78%). A single crystal X-ray analysis confirmed the structure of product **16ah** (CCDC 2167742).[73] Other neutral nucleophiles such as methyl 2-cyanoacetate **13j**, allylsilane **13k**, pyrrole **13l**, and TMSCN **13m** also furnished corresponding products **16aj-16am** with good yields (60-67%) under standard conditions. Next, a series of 2-arylindoles with substitutions like-Me, F, Cl, and Br were examined on both the aryl rings. A series of related products **16bh-16jh** (59-74% yields) were obtained with ethyl 3-oxo-3-phenylpropanoate **13h** as a nucleophile. Later, the direct oxidative transformation was extensively expanded to the cross-combination of 2-arylindoles with several nucleophiles, and related products **16da-16le** were obtained with moderate to good yields (57–72%) under optimized conditions **(Table 3.4).**

Table 3.4 Substrate scope of 2-substituted indole **1** with various nucleophiles **13**.[a]

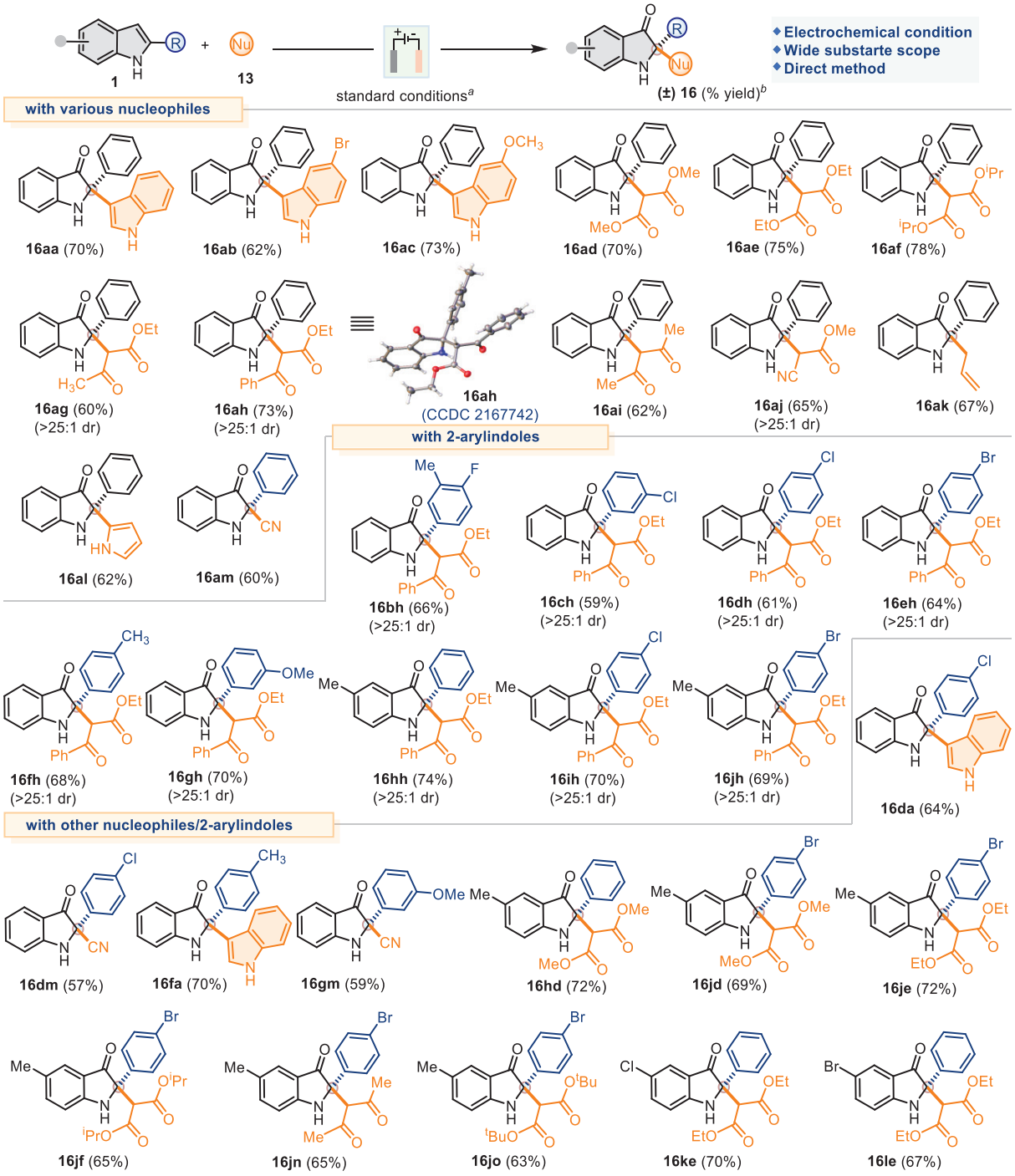

[a]**Reaction conditions**: **1a** (0.5 mmol, 1.0 equiv), **13h** (1.5 mmol, 3.0 equiv), *n*-Bu_4NPF_6 (0.5 mmol, 1.0 equiv), TEMPO (0.1 mmol, 20 mol%), 2,6-lutidine (1.0 mmol, 2.0 equiv) CH_3CN/H_2O (9:1), C(+) | Cu(–), undivided cell, constant current = 1.5 mA, air, rt, 24 h. [b]All isolated yields of **16** were based on **1**.

3.4 Cyclic voltammetry experiment

Cyclic voltammetry (CV) was performed using a three-electrodes cell (glassy carbon as the working electrode, Pt wire as the auxiliary electrode, and Ag/AgCl as reference electrode) in CH_3CN: H_2O (9:1) and *n*-Bu_4NPF_6 (0.02 M solution) as the supporting electrolyte at room temperature. The scan rate was 0.2 V/s, ranging from −1.0 V to +2.0 V; Ag/AgCl as the reference electrode. The CV was plotted using the IUPAC convention **(Figure 3.3)**. Oxidation potential was measured for **1a** (E_{ox} = +1.30 V vs. Ag/AgCl as reference electrode) and TEMPO (E_{ox} = +0.89 V vs Ag/AgCl as reference electrode), respectively. In comparison, **1a**+**13h**+TEMPO showed oxidation potential [E_{ox} = +1.40 V vs. Ag/AgCl as reference electrode).

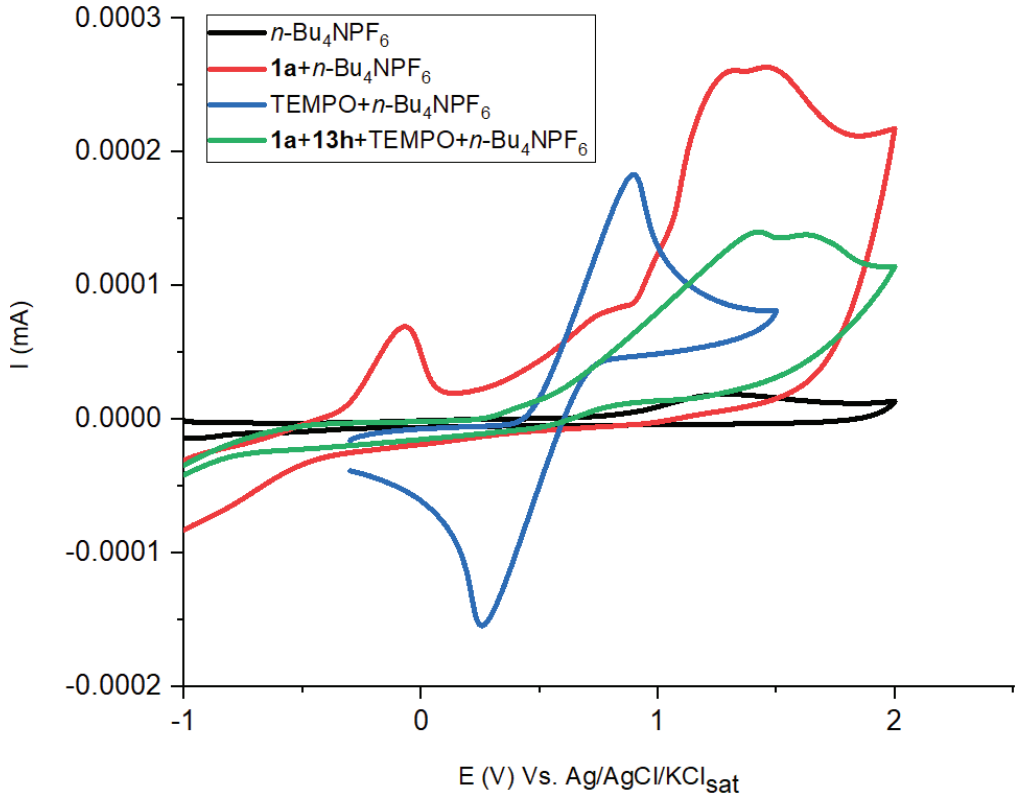

Figure 3.3 Cyclic voltammogram of CH_3CN/H_2O/*n*-Bu_4NPF_6 (12 mL, 0.02M) (**Black**); **1a** (2.0 mM) in CH_3CN/H_2O/*n*-Bu_4NPF_6 (12 mL, 0.02M) (**Red**); TEMPO (2.0 mM) in CH_3CN/H_2O/*n*-Bu_4NPF_6 (12 mL, 0.02M) (**Blue**); **1a** (2.0 mM), **13h** (2.0 mM), TEMPO (2.0 mM) in CH_3CN/H_2O/*n*-Bu_4NPF_6 (12 mL, 0.02M) (**Green**); Reference electrode: Ag/AgCl (3M KCl), scan rate: 0.2 V/s. all experiments done at room temperature.

3.5 Control experiments, Reaction mechanism, Synthetic applications

The product **16ah** formation was not observed with BHT or TEMPO as a radical scavenger under the standard electrochemical conditions, confirming the radical nature of the reaction at the intermediate step (**Scheme 3.21**).

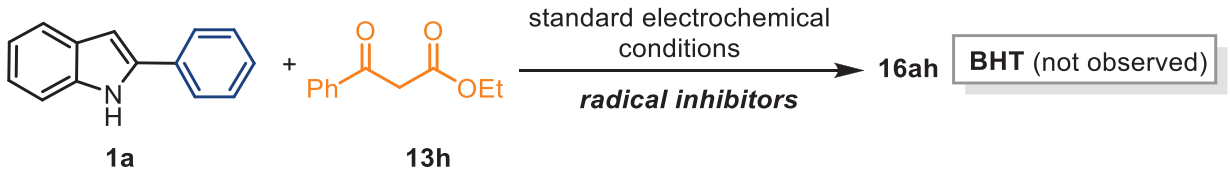

Scheme 3.21: Control experiment

A probable mechanism has been proposed based on the literature available in this direction.[71-72] As shown in Scheme 3.21, TEMPO underwent oxidation at the anode to generate $TEMPO^+$, which could oxidize 2-arylindole **1** to radical cation **A**. After deprotonation, radical B and the subsequently resonating radical **C** are generated from **A**. The radical **C** reacts with O_2 to create radical **D**, which converts to radical **E** before generating indole-3-one F by discharging a hydroxyl radical. Finally, various nucleophiles react with **F** and furnished product **16**. *In situ,* HRMS data confirmed the formation of intermediate 2-phenylindole-3-one F (Ar = Ph).

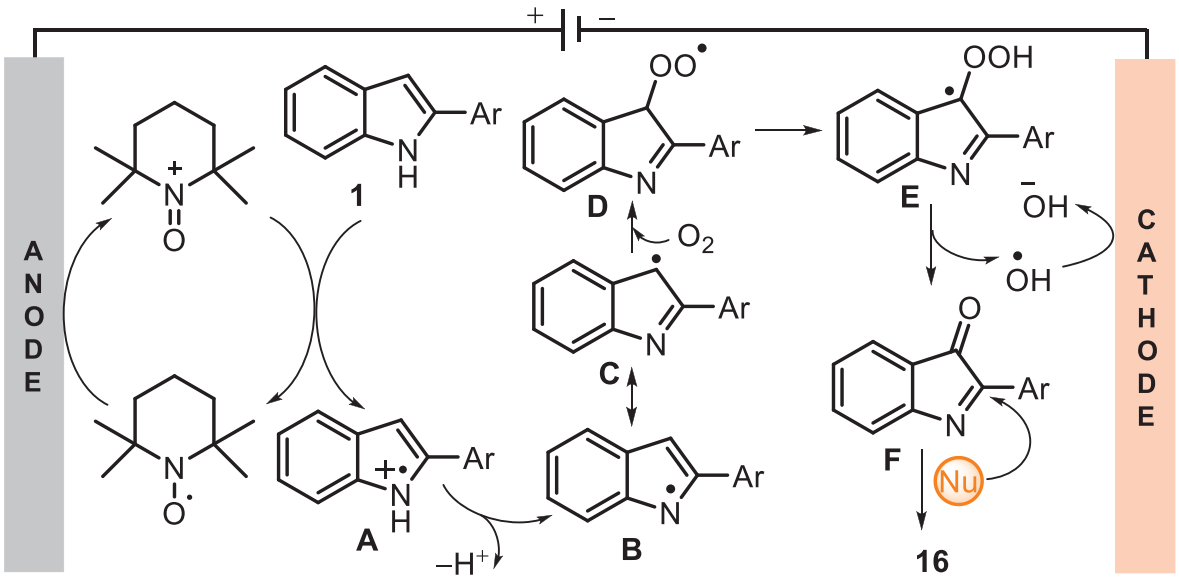

Scheme 3.22: A tentative mechanism for the electrochemical synthesis of C2-quaternary indoline-3-ones (**16**)

The practicality of the developed method was shown at the gram-scale preparation of compound **16ah** (1.02 g, 65% yield) under optimized conditions (Scheme 3.23a). Next, the developed method was applied successfully for the synthesis of metagenediindole A (65% yield) (Scheme 3.23b(i)). Additional synthetic transformations were performed to access 1*H*-pyrazole-fused indolin-3-one **18** (82%, Scheme 3.23b(ii)) and 1,2-dihydro-3*H*-pyrazol-3-one based indolin-3-one **19** (78%, Scheme 3.23b(iii)), respectively, when compound **16ai** and **16dh** were treated with hydrazine-hydrate in EtOH under reflux conditions.

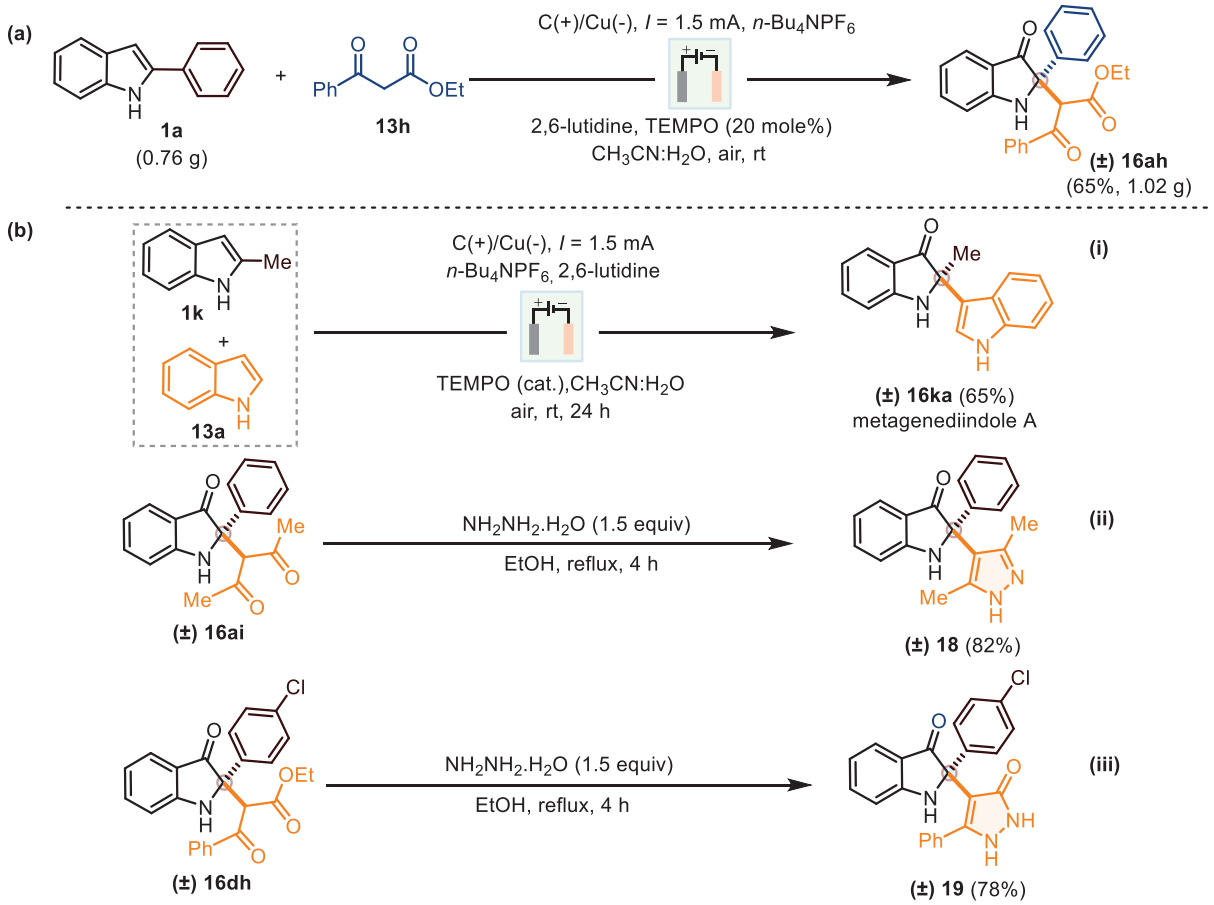

Scheme 3.23 Synthetic applications **(a)** gram-scale synthesis of **16ah**; **(b)** (i) synthesis of metagenediindole A, access to (ii) 1*H*-pyrazole-fused indolin-3-one **18**, (iii) 1,2-dihydro-3H-pyrazol-3-one based indolin-3-one **19**

3.6 Conclusion

In conclusion, we have established a highly competent electrochemical method for directly synthesizing C2-quaternary-centered indolin-3-ones from 2-arylindoles. Including self-dimerization of 2-arylindoles, several nucleophiles, such as indole, 1,3-dicarbonyls, pyrrole,

allylsilane, and TMSCN, were added to *in situ* generated indole-3-ones through oxidative dearomatization of 2-arylindoles with good yields. The developed method has been applied for the product's gram scale preparation, metagenediindole A synthesis, and other late-stage synthetic transformations. This method has overcome limited nucleophiles addition to 2-arylindoles under electrochemical conditions.

3.7 General experimental methods

All reactions were observed using Thin-layer chromatography (on SiO_2 gel F254 plates) and performed on IKA ElectroSyn 2.0 Pro under standard conditions. The desired compounds were purified through Flash column chromatography packed with silica gel (100-200 mesh size) as the stationary phase and a mixture of petroleum ether-acetone as an eluent. Melting points were determined in open capillary tubes on an EZ-Melt Automated melting point apparatus. NMR spectra were recorded on a Bruker AV 400 spectrometer. The chemical shifts were reported in parts per million (ppm) using deuterated solvent as the internal standard. High-resolution mass spectra (HRMS-ESI) were recorded using a quadrupole time-of-flight (Q-TOF) mass spectrometer (Applied Biosystems). The cyclic voltammetry was performed using CH Instruments Electrochemical Analyzer (Model CHI1200B) with a three-electrodes cell (glassy carbon as the working electrode (3-mm diameter, circular), Pt wire as the auxiliary electrode, and Ag/AgCl as the reference electrode). Before experimenting, the electrode was polished with Micro Polish Alumina Powder 0.05 μm as per the following method: The alumina (0.05 μm) was mixed with water on the polishing pad to make a paste. The working electrode was then rubbed on the polishing pad with some alumina paste while ensuring that the face of the working electrode remained flat, and polishing was performed in figure-8 so that grooves did not develop on the electrode surface. After polishing for about 30 seconds, the electrode was sonicated in deionized water for no more than 1-minute. Finally, the electrode was washed with deionized water, and the electrode surface was dried before use. All cyclic voltammetry experiments were performed after nitrogen purging for deoxygenation purposes. The cyclic voltammetry was performed using CH Instruments electrochemical Analyzer (Model CHI1200B). All the chemicals were obtained from the commercial supplier and were used without purification. All starting 2-arylindoles were prepared using the reported procedure,[74] whereas a few cross-indole products were matched with the reported ones.[35, 38] Oil baths were used for heating conditions.

3.7.1 General procedure for the synthesis of compound 5

A 10 mL dried undivided reaction cell with a stirring bar was charged with **1** (1.0 mmol, 2.0 equiv), *n*-Bu_4NPF_6 (193 mg, 0.5 mmol, 1.0 equiv), and TEMPO (15 mg, 0.1 mmol, 20 mol %), 2,6-lutidine (1.0 mmol, 2.0 equiv) in CH_3CN: H_2O (10 mL, 9:1). The Graphite-plate anode and Copper-plate cathode were dipped into the reaction mixture and electrolyzed at a constant current condition (1.5 mA) under an air atmosphere at room temperature, and TLC monitored the reaction. Upon completion, the reaction mixture was evaporated under reduced pressure, and crude mass was stirred between ethyl acetate (10 mL) and NH_4Cl (10 mL, 10% solution) for five minutes. The organic phase was separated, dried over anhydrous Na_2SO_4 and evaporated under reduced pressure. Purification of crude mass on silica gel column chromatography using a mixture of petroleum ether and acetone as eluent-furnished product **5** (61-79% yields).

3.7.2 General procedure for the synthesis of compound 16

A 10 mL dried undivided reaction cell with a stirring bar was charged with **1** (0.5 mmol, 1.0 equiv), nucleophiles **13** (1.5 mmol, 3.0 equiv), *n*-Bu_4NPF_6 (193 mg, 0.5 mmol, 1.0 equiv), and TEMPO (15 mg, 0.1 mmol, 20 mol%), 2,6-lutidine (1.0 mmol, 2.0 equiv) in CH_3CN: H_2O (10 mL, 9:1). Graphite-plate anode and Copper-plate cathode were dipped into the reaction mixture and electrolyzed at a constant current condition (1.5 mA) under an air atmosphere at room temperature, and TLC monitored the reaction. Upon completion, the reaction mixture was evaporated under reduced pressure, and crude mass was stirred between ethyl acetate (10 mL) and NH_4Cl (10 mL, 10% solution) for five minutes. The organic phase was separated, dried over anhydrous Na_2SO_4, and evaporated under reduced pressure. Purification of crude mass on silica gel column chromatography using a mixture of petroleum ether and acetone as eluent furnished product **16** (57-78% yields).

3.7.3 Characterization data of synthesized compounds

2-Phenyl-2-(2-phenyl-1*H*-indol-3-yl)indolin-3-one (±5a): Purification with petroleum ether: acetone (9/1) as eluent); yellow solid (152 mg, 76% yield, mp = 207-212 °C). ^1H NMR (400 MHz, $CDCl_3$) δ 8.11 (s, 1H), 7.53 – 7.47 (m, 2H), 7.47 – 7.42 (m, 1H), 7.40 (d, *J* = 7.7 Hz, 1H), 7.32 (d, *J* = 8.1 Hz, 1H), 7.28 – 7.22 (m, 1H), 7.21 – 7.10 (m, 8H), 7.00 (d, *J* = 8.0 Hz, 1H), 6.93 (m, 1H), 6.80 (t, *J* = 7.7 Hz, 1H), 6.71 (d, *J* = 8.2 Hz, 1H), 5.17 (s, 1H). $^{13}C\{^1H\}$ NMR (100 MHz, $CDCl_3$) δ 200.3, 159.4 140.4, 137.1, 137.1, 135.5, 133.3, 129.7 (2C), 128.3 (2C), 127.7

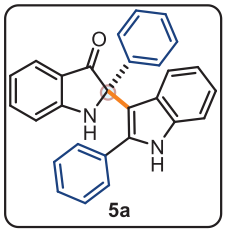

5a

(2C), 127.5, 127.4, 127.2 (2C), 125.4 (2C), 122.4, 121.6, 120.4, 120.0, 119.2, 112.3, 112.1, 110.7, 72.1. HRMS (ESI-TOF) *m/z*: [M + H^+] Calcd for $C_{28}H_{21}N_2O$ 401.1648, Found 401.1642.

2-(4-Fluoro-3-methylphenyl)-2-(2-(4-fluoro-3-methylphenyl)-1*H*-indol-3-yl)indolin-3-one

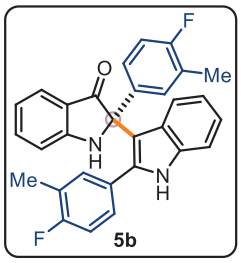

(±5b): Purification with petroleum ether: acetone (9/1) as eluent; yellow solid (151 mg, 65% yield, mp = 222-225 °C). ^{1}H NMR (400 MHz, $CDCl_3$ with few drops of DMSO-d_6) δ 8.15 (s, 1H), 7.49 (t, *J* = 7.6 Hz, 1H), 7.39 (d, *J* = 7.8 Hz, 1H), 7.29 (t, *J* = 8.0 Hz, 3H), 7.15 (t, *J* = 6.8 Hz, 1H), 6.95 (dd, *J* = 9.4, 6.5 Hz, 2H), 6.90 (t, *J* = 5.6 Hz, 1H), 6.85 – 6.76 (m, 5H), 5.22 (s, 1H), 2.12 (s, 3H), 2.01 (s, 3H). ^{13}C{^{1}H} NMR (100 MHz, $CDCl_3$, few drops of DMSO-d_6) δ 200.8, 160.3 (d, *J* = 246.9 Hz), 160.2 (d, *J* = 244.3 Hz), 159.3, 136.8, 136.5, 135.4, 135.0 (d, *J* = 2.6 Hz), 132.9 (d, *J* = 5.2 Hz), 130.2 (d, *J* = 5.2 Hz), 128.8 (d, *J* = 2.9 Hz), 128.1 (d, *J* = 7.8 Hz), 126.9, 125.7 (d, *J* = 7.7 Hz), 124.5, 123.4 (d, *J* = 17.5 Hz), 123.2 (d, *J* = 17.7 Hz), 121.2, 120.2, 119.4, 118.9, 118.1, 113.5, 113.4 (d, *J* = 43.6 Hz), 111.9, 111.2, 110.8, 70.8, 14.0 (d, *J* = 3.0 Hz), 13.7 (d, *J* = 3.4 Hz). ^{19}F NMR (376 MHz, $CDCl_3$) δ -118.4, -120.3. HRMS (ESI-TOF) *m/z*: [M + H^+] Calcd for $C_{30}H_{23}F_2N_2O$ 465.1773, Found 465.1779.

2-(3-Chlorophenyl)-2-(2-(3-chlorophenyl)-1*H*-indol-3-yl)indolin-3-one (±5c): Purification

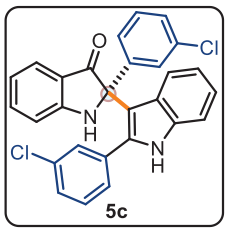

with petroleum ether: acetone (9/1) as eluent; yellow solid (143 mg, 61% yield, mp = 161-165 °C). ^{1}H NMR (400 MHz, $CDCl_3$) δ 8.20 (s, 1H), 7.55 – 7.50 (m, 2H), 7.46 (d, *J* = 7.3 Hz, 1H), 7.38 (dt, *J* = 7.5, 1.5 Hz, 1H), 7.33 (d, *J* = 8.1 Hz, 1H), 7.22 – 7.16 (m, 2H), 7.13 – 7.01 (m, 5H), 6.94 (d, *J* = 4.0 Hz, 2H), 6.88 (dt, *J* = 7.1, 3.1 Hz, 2H), 5.21 (s, 1H). ^{13}C{^{1}H} NMR (100 MHz, $CDCl_3$) δ 199.9, 159.3, 141.9, 137.7, 135.9, 135.6, 134.5, 134.1, 133.6, 130.0, 129.5, 128.9, 128.4, 127.8, 127.7, 127.1, 127.0, 125.8, 125.5, 122.9, 121.0, 120.4, 120.4, 120.1, 112.7, 112.4, 111.0, 71.4. HRMS (ESI-TOF) *m/z*: [M + H^+] Calcd for $C_{28}H_{19}Cl_2N_2O$ 469.0869, Found 469.0865.

2-(4-Chlorophenyl)-2-(2-(4-chlorophenyl)-1*H*-indol-3-yl)indolin-3-one (±5d): Purification

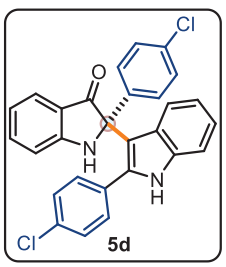

with petroleum ether: acetone (9/2) as eluent; yellow solid (150 mg, 64% yield, mp = 196-200 °C). ^{1}H NMR (400 MHz, $CDCl_3$) δ 8.14 (s, 1H), 7.53 (dd, *J* = 7.2, 1.2 Hz, 1H), 7.47 (d, *J* = 8.7 Hz, 2H), 7.38 (dd, *J* = 13.9, 7.9 Hz, 2H), 7.23 – 7.16 (m, 3H), 7.13 (d, *J* = 8.5 Hz, 2H), 7.04 (d, *J* = 8.5 Hz, 2H),

6.95 (dt, *J* = 16.1, 8.0 Hz, 2H), 6.91 – 6.84 (m, 2H), 5.20 (s, 1H). $^{13}C\{^{1}H\}$ NMR (100 MHz, $CDCl_3$) δ 199.7, 159.2, 138.7, 137.5, 135.8, 135.5, 134.6, 133.7, 131.2, 132.0, 131.1 (2C), 128.7 (2C), 128.4 (2C), 127.8 (2C), 127.1, 125.5, 122.8, 121.1, 120.5, 120.4, 119.8, 112.5, 110.9, 71.4. HRMS (ESI-TOF) *m/z*: [M + H^+] Calcd for $C_{28}H_{19}Cl_2N_2O$ 469.0869, Found 469.0871.

2-(*p*-Tolyl)-2-(2-(*p*-tolyl)-1*H*-indol-3-yl)indolin-3-one (±5e): Purification with petroleum ether: acetone (9/1) as eluent; yellow solid (150 mg, 70% yield, mp = 159-162 °C). ^{1}H NMR (400 MHz, $CDCl_3$) δ 8.10 (s, 1H), 7.46 – 7.40 (m, 1H), 7.40 – 7.34 (m, 3H), 7.28 (d, *J* = 8.1 Hz, 1H), 7.13 (t, *J* = 8.0 Hz, 1H), 7.04 – 6.90 (m, 8H), 6.78 (t, *J* = 7.4 Hz, 1H), 6.68 (d, *J* = 8.2 Hz, 1H), 5.17 (s, 1H), 2.33 (s, 3H), 2.27 (s, 3H). $^{13}C\{^{1}H\}$ NMR (100 MHz, $CDCl_3$) δ 200.5, 159.1, 138.0, 137.5, 137.1, 137.0, 136.9, 135.5, 130.3, 129.5, 128.9 (2C), 128.3 (2C), 127.5, 127.1 (2C), 125.3, 122.1, 121.6 (2C), 120.4, 119.8, 118.9, 112.1, 111.8, 110.6, 71.9, 21.2, 21.0. HRMS (ESI-TOF) *m/z*: [M + H^+] Calcd for $C_{30}H_{25}N_2O$ 429.1961, Found 429.1959.

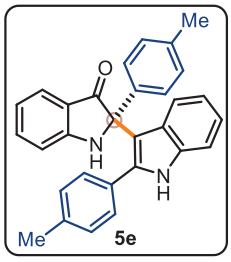

2-(3-Methoxyphenyl)-2-(2-(3-methoxyphenyl)-1*H*-indol-3-yl)indolin-3-one (±5f): Purification with petroleum ether: acetone (9/1) as eluent; yellow solid (134 mg, 58% yield, mp = 204-208 °C). ^{1}H NMR (400 MHz, $CDCl_3$) δ 8.10 (s, 1H), 7.49 – 7.41 (m, 2H), 7.32 (d, *J* = 8.2 Hz, 1H), 7.17 – 7.04 (m, 6H), 6.94 (t, *J* = 7.3 Hz, 1H), 6.80 (m, 3H), 6.71 (m, 2H), 6.64 (m, 1H), 5.20 (s, 1H), 3.67 (s, 3H), 3.56 (s, 3H). $^{13}C\{^{1}H\}$ NMR (100 MHz, $CDCl_3$) δ 200.1, 159.4, 159.2, 158.7, 141.9, 137.1, 137.0, 135.4, 134.6, 129.2, 128.8, 127.3, 125.4, 122.4, 121.8, 121.5, 120.4, 120.1, 119.7, 119.2, 114.8, 114.7 (2C), 113.2, 112.9, 112.2, 110.7, 72.0, 55.2, 54.9. HRMS (ESI-TOF) *m/z*: [M + H^+] Calcd for $C_{30}H_{25}N_2O_3$ 461.1860, Found 461.1866.

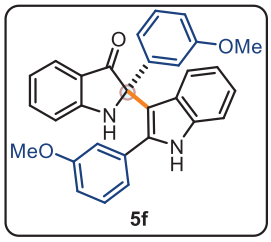

2-(4-Methoxyphenyl)-2-(2-(4-methoxyphenyl)-1*H*-indol-3-yl)indolin-3-one (±5g): Purification with petroleum ether: acetone (9/1) as eluent; yellow solid (177 mg, 77% yield, mp = 182-185 °C). ^{1}H NMR (400 MHz, $CDCl_3$) δ 8.07 (s, 1H), 7.46 – 7.37 (m, 4H), 7.30 (d, *J* = 8.1 Hz, 1H), 7.15–7.11 (m, 1H), 7.02 (d, *J* = 8.7 Hz, 2H), 6.99–6.90 m, 2H), 6.78 (t, *J* = 7.2 Hz, 1H), 6.75 – 6.70 (m, 3H), 6.65 (d, *J* = 8.7 Hz, 2H), 5.18 (s, 1H), 3.77 (s, 3H), 3.73 (s, 3H). $^{13}C\{^{1}H\}$ NMR (100 MHz, $CDCl_3$) δ 200.6, 159.5, 159.2, 159.1, 137.0, 136.8, 135.4, 132.5, 131.0 (2C), 128.4 (2C), 127.5, 125.5, 125.4, 122.2, 121.5, 120.5, 119.9, 119.0, 113.7 (2C), 113.1 (2C),

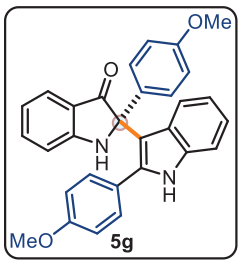

112.2, 112.2, 110.6, 71.6, 55.3, 55.2. HRMS (ESI-TOF) *m/z*: [M + H^+] Calcd for $C_{30}H_{25}N_2O_3$ 461.1860, Found 461.1866.

2-(3,4-Dimethoxyphenyl)-2-(2-(3,4-dimethoxyphenyl)-1*H*-indol-3-yl)indolin-3-one (±5h):

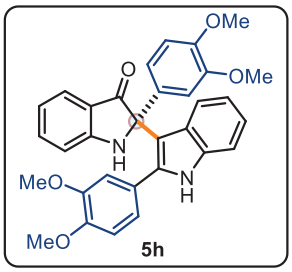

Purification with petroleum ether: acetone (8/2) as eluent; yellow solid (206 mg, 79% yield, mp = 207-210 ºC). ^{1}H NMR (400 MHz, $CDCl_3$) δ 8.12 (s, 1H), 7.48 – 7.40 (m, 2H), 7.31 (d, *J* = 8.1 Hz, 1H), 7.18 – 7.09 (m, 1H), 7.08 – 7.03 (m, 1H), 7.03 – 6.95 (m, 2H), 6.95 – 6.88 (m, 1H), 6.84 – 6.78 (m, 2H), 6.79 – 6.74 (m, 1H), 6.72 – 6.66 (m, 2H), 6.61 (d, *J* = 1.9 Hz, 1H), 5.22 (s, 1H), 3.86 (s, 3H), 3.81 (s, 3H), 3.69 (s, 3H), 3.52 (s, 3H). ^{13}C{^{1}H} NMR (100 MHz, $CDCl_3$) δ 200.4, 159.2, 149.1, 148.8, 148.7, 148.0 137.0 (2C), 135.3, 132.9, 127.5, 125.9, 125.5, 122.2, 121.9, 121.5, 120.6, 120.0, 119.2 (2C), 113.3, 112.1, 111.9, 111.3, 110.7, 110.6, 110.5, 71.8, 55.9, 55.9 (2C), 55.4. HRMS (ESI-TOF) *m/z*: [M + H^+] Calcd for $C_{32}H_{29}N_2O_5$ 521.2071, Found 521.2067.

2-(3,4-Dichlorophenyl)-2-(2-(3,4-dichlorophenyl)-1*H*-indol-3-yl)indolin-3-one (±5i):

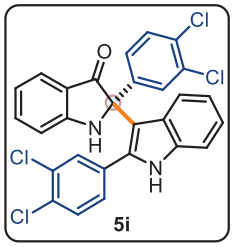

Purification with petroleum ether: acetone (9/1) as eluent; yellow solid (186 mg, 69% yield, mp = 182-184 ºC). ^{1}H NMR (400 MHz, $CDCl_3$) δ 8.34 (s, 1H), 7.63 (d, *J* = 2.0 Hz, 1H), 7.58 – 7.51 (m, 1H), 7.37 (d, *J* = 7.6 Hz, 1H), 7.31 (dd, *J* = 8.4, 2.1 Hz, 2H), 7.19 (dd, *J* = 7.6, 3.8 Hz, 3H), 7.05 – 7.03 (m, 1H), 6.98 – 6.86 (m, 5H), 5.30 (s, 1H). ^{13}C{^{1}H} NMR (100 MHz, $CDCl_3$) δ 199.6, 159.3, 140.0, 138.0, 135.5, 134.7, 132.7, 132.4, 132.2, 131.8, 131.8, 131.7, 130.0, 129.4, 128.9, 128.7, 126.9, 126.7, 125.3, 123.1, 120.6 (2C), 120.4, 120.2, 112.8, 112.4, 111.2, 70.7. HRMS (ESI-TOF) *m/z*: [M + H^+] Calcd for $C_{28}H_{17}Cl_4N_2O$ 537.0090, Found 537.0096.

5-Chloro-2-(5-chloro-2-phenyl-1*H*-indol-3-yl)-2-phenylindolin-3-one (±5j): Purification with petroleum ether: acetone (9/1) as eluent; yellow solid (150 mg, 64% yield, mp = 172-175 ºC). ^{1}H NMR (400 MHz, $CDCl_3$) δ 8.25 (s, 1H), 7.47 – 7.42 (m, 2H), 7.40 (dd, *J* = 8.6, 2.1 Hz, 1H), 7.32 (dd, *J* = 8.3, 4.8 Hz, 2H), 7.25 (dd, *J* = 5.4, 1.8 Hz, 3H), 7.21 (d, *J* = 9.4 Hz, 2H), 7.18 (s, 1H), 7.15 (s, 1H), 7.14 – 7.10 (m, 2H), 6.91 (d, *J* = 1.7 Hz, 1H), 6.65 (d, *J* = 8.6 Hz, 1H), 5.17 (s, 1H). ^{13}C{^{1}H} NMR (100 MHz, $CDCl_3$) δ 199.0,157.3, 139.6, 138.4, 137.2, 133.9, 132.7, 129.6 (2C), 128.7, 128.6 (2C), 128.3, 128.1, 127.9 (2C), 127.1 (2C), 125.7,

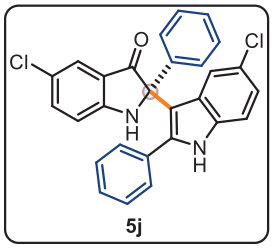

124.6, 124.4, 122.8, 121.2, 121.0, 113.4, 111.8, 111.5, 72.7. HRMS (ESI-TOF) *m/z*: [M + H^+] Calcd for $C_{28}H_{19}Cl_2N_2O$ 469.0869, Found 469.0873.

5-Bromo-2-(5-bromo-2-phenyl-1*H*-indol-3-yl)-2-phenylindolin-3-one (±5k): Purification with petroleum ether: acetone (9/1) as eluent; yellow solid (179 mg, 64% yield, mp = 181-183 °C). ^{1}H NMR (400 MHz, $CDCl_3$) δ 8.15 (s, 1H), 7.52 – 7.47 (m, 2H), 7.42 (dd, *J* = 6.5, 3.2 Hz, 2H), 7.34 – 7.28 (m, 1H), 7.26 – 7.17 (m, 7H), 7.16 – 7.11 (m, 2H), 7.04 (d, *J* = 1.4 Hz, 1H), 6.58 (d, *J* = 8.5 Hz, 1H), 5.13 (s, 1H). ^{13}C{^{1}H} NMR (100 MHz, $CDCl_3$) δ 198.6, 157.5, 139.7, 139.5, 138.1, 134.1, 132.6, 129.6 (2C), 128.9, 128.8, 128.6 (2C), 128.1, 127.9 (2C), 127.7, 127.1 (2C), 125.4, 124.1, 121.7, 113.7, 113.3, 112.1, 111.4, 111.2, 72.6. HRMS (ESI-TOF) *m/z*: [M + H^+] Calcd for $C_{28}H_{19}Br_2N_2O$ 556.9859, Found 556.9851.

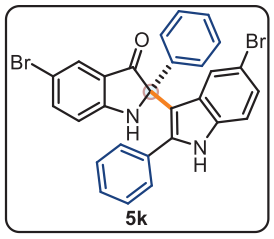

5k

5-Methyl-2-(5-methyl-2-(*p*-tolyl)-1*H*-indol-3-yl)-2-(*p*-tolyl)indolin-3-one (±5l): Purification with petroleum ether: acetone (9/1) as eluent; yellow solid (155 mg, 68% yield, mp = 205-207 °C). ^{1}H NMR (400 MHz, $CDCl_3$) δ 7.94 (s, 1H), 7.34 (d, *J* = 8.1 Hz, 2H), 7.27 (s, 1H), 7.21 (s, 1H), 7.18 (d, *J* = 8.2 Hz, 1H), 7.02 – 6.92 (m, 7H), 6.85 (s, 1H), 6.61 (d, *J* = 8.2 Hz, 1H), 5.01 (s, 1H), 2.33 (s, 3H), 2.28 (s, 3H), 2.26 (s, 6H). ^{13}C{^{1}H} NMR (100 MHz, $CDCl_3$) δ 200.0, 157.8, 138.3, 137.9, 137.8, 137.1, 137.0, 133.9, 130.6, 129.6 (2C), 128.9, 128.9 (2C), 128.5, 128.3 (2C), 127.8, 127.2 (2C), 124.7, 123.8, 121.3, 120.8, 112.3, 111.6, 110.3, 72.5, 21.7, 21.3, 21.0, 20.6. HRMS (ESI-TOF) *m/z*: [M + H^+] Calcd for $C_{32}H_{29}N_2O$ 457.2274, Found 457.2268.

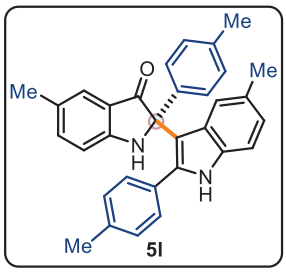

5l

2-(1*H*-Indol-3-yl)-2-phenylindolin-3-one (±16aa): Purification with petroleum ether: acetone (9/1) as eluent; yellow solid (113 mg, 70% yield, mp = 189-192 °C). ^{1}H NMR (400 MHz, $CDCl_3$) δ 8.25 (s, 1H), 7.69 (d, *J* = 7.7 Hz, 1H), 7.56 (d, *J* = 7.2 Hz, 2H), 7.50 (t, *J* = 7.7 Hz, 1H), 7.35 (d, *J* = 8.1 Hz, 1H), 7.29 (d, *J* = 6.8 Hz, 3H), 7.20 – 7.11 (m, 3H), 6.98 (t, *J* = 7.5 Hz, 1H), 6.94 – 6.86 (m, 2H), 5.40 (s, 1H). ^{13}C{^{1}H} NMR (10 MHz, $CDCl_3$) δ 200.6, 160.5, 139.5, 137.5, 136.9, 128.4 (2C), 127.7, 126.8 (2C), 125.6, 125.6, 123.8, 122.5, 120.0, 119.7, 119.6, 119.6, 115.5, 112.9, 111.6, 71.3. HRMS (ESI-TOF) *m/z*: [M + H^+] Calcd for $C_{22}H_{17}N_2O$ 325.1335, Found 325.1337.

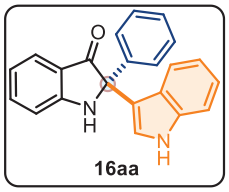

16aa

2-(5-Bromo-1*H*-indol-3-yl)-2-phenylindolin-3-one (±16ab): Purification with petroleum ether: acetone (9/1) as eluent; yellow solid (125 mg, 62% yield, mp = 206-209 ºC).

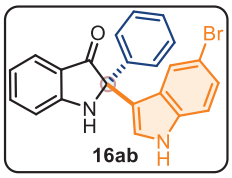

16ab

^{1}H NMR (400 MHz, $CDCl_3$) δ 8.42 (s, 1H), 7.70 (d, *J* = 7.8 Hz, 1H), 7.57 – 7.53 (m, 1H), 7.53 – 7.49 (m, 2H), 7.34 – 7.28 (m, 4H), 7.26 (dd, *J* = 8.6, 1.8 Hz, 1H), 7.22 (d, *J* = 8.6 Hz, 1H), 7.16 (s, 1H), 6.97 (d, *J* = 8.2 Hz, 1H), 6.92 (t, *J* = 7.4 Hz, 1H), 5.40 (s, 1H). ^{13}C{^{1}H} NMR (100 MHz, $CDCl_3$) δ 200.5, 160.5, 139.1, 137.8, 135.6, 128.6 (2C), 128.0, 127.3, 126.6 (2C), 125.6, 125.4, 125.0, 122.2, 119.8, 119.3, 115.1, 113.3, 113.1, 112.9, 71.1. HRMS (ESI-TOF) *m/z*: [M + H$^+$] Calcd for $C_{22}H_{16}BrN_2O$ 403.0441, Found 403.0447.

2-(5-Methoxy-1*H*-indol-3-yl)-2-phenylindolin-3-one (±16ac): Purification with petroleum ether: acetone (9/1) as eluent; yellow solid (129 mg, 73% yield, mp = 195-197 ºC).

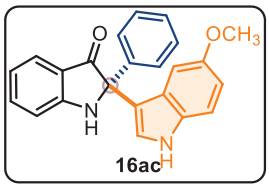

16ac

^{1}H NMR (400 MHz, $CDCl_3$) δ 8.14 (s, 1H), 7.72 (d, *J* = 7.7 Hz, 1H), 7.66 – 7.58 (m, 2H), 7.56 – 7.49 (m, 1H), 7.38 – 7.25 (m, 4H), 7.12 (d, *J* = 2.6 Hz, 1H), 6.96 (d, *J* = 8.2 Hz, 1H), 6.92 (t, *J* = 7.4 Hz, 1H), 6.85 (dd, *J* = 8.8, 2.4 Hz, 1H), 6.58 (d, *J* = 2.2 Hz, 1H), 5.39 (s, 1H), 3.63 (s, 3H). ^{13}C{^{1}H} NMR (100 MHz, $CDCl_3$) δ 200.7, 160.5, 154.0, 139.3, 137.5, 132.0, 128.4 (2C), 127.7, 126.8 (2C), 126.0, 125.5, 124.5, 119.8, 119.6, 115.5, 112.9, 112.3, 112.3, 100.9, 71.3, 55.6. HRMS (ESI-TOF) *m/z*: [M + H$^+$] Calcd for $C_{23}H_{19}N_2O_2$ 355.1441, Found 355.1447.

Dimethyl-2-(3-oxo-2-phenylindolin-2-yl)malonate (±16ad): Purification with petroleum ether: acetone (9/1) as eluent; yellow solid (119 mg, 70% yield, mp = 155-157 ºC).

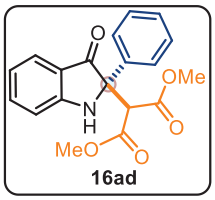

16ad

^{1}H NMR (400 MHz, $CDCl_3$) δ 7.58 – 7.54 (m, 1H), 7.53 – 7.48 (m, 2H), 7.48 – 7.44 (m, 1H), 7.33 – 7.30 (m, 1H), 7.28 (dd, *J* = 7.4, 1.4 Hz, 1H), 7.25 – 7.22 (m, 1H), 6.98 (dt, *J* = 8.1, 0.7 Hz, 1H), 6.81 (m, 1H), 6.05 (s, 1H), 4.75 (s, 1H), 3.57 (s, 3H), 3.49 (s, 3H). ^{13}C{^{1}H} NMR (100 MHz, $CDCl_3$) δ 197.9, 168.2, 166.5, 160.0, 137.3, 136.7, 128.9 (2C), 128.1, 125.4, 125.2(2C), 119.3, 119.2, 111.5, 70.2, 58.5, 52.6 (2C). HRMS (ESI-TOF) *m/z*: [M + H$^+$] Calcd for $C_{19}H_{18}NO_5$ 340.1179, Found. 340.1185.

Diethyl 2-(3-oxo-2-phenylindolin-2-yl)malonate (±16ae): Purification with petroleum ether: acetone (9/1) as eluent; yellow solid (138 mg, 75% yield, mp = 171-173 ºC).

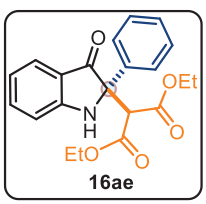

16ae

^{1}H NMR (400 MHz, $CDCl_3$) δ7.55 (d, *J* = 7.7 Hz, 1H), 7.52 – 7.48 (m, 2H), 7.45 (m, 1H), 7.29 (m, 2H), 7.25 – 7.20 (m, 1H), 6.95 (d, *J* = 8.2 Hz, 1H), 6.82

– 6.76 (m, 1H), 6.07 (s, 1H), 4.70 (s, 1H), 4.09 – 3.96 (m, 3H), 3.89 (m, 1H), 1.00 (t, *J* = 7.1 Hz, 3H), 0.84 (t, *J* = 7.1 Hz, 3H). $^{13}C\{^{1}H\}$ NMR (100 MHz, $CDCl_3$) δ 197.9, 167.7, 166.2, 160.0, 137.2, 136.9, 128.8 (2C), 128.0, 125.4, 125.3 (2C), 119.5, 119.1, 111.4, 70.2, 61.9, 61.6, 58.7, 13.7, 13.3. HRMS (ESI-TOF) *m/z*: [M + H^+] Calcd for $C_{21}H_{22}NO_5$ 368.1492, Found 368.1488.

Diisopropyl 2-(3-oxo-2-phenylindolin-2-yl)malonate (±16af): Purification with petroleum ether: acetone (9/1) as eluent; yellow solid (154 mg, 78% yield, mp = 168-171 °C). ^{1}H NMR (400 MHz, $CDCl_3$) δ 7.57 – 7.53 (m, 1H), 7.53 – 7.49 (m, 2H), 7.45 (m, 1H), 7.31 – 7.28 (m, 1H), 7.27 (t, *J* = 1.5 Hz, 1H), 7.25 – 7.20 (m, 1H), 6.95 (d, *J* = 8.2 Hz, 1H), 6.83 – 6.77 (m, 1H), 6.07 (s, 1H), 4.85 (m, 2H), 4.65 (s, 1H), 1.08 (d, *J* = 6.3 Hz, 3H), 1.05 (d, *J* = 6.3 Hz, 3H), 0.97 (d, *J* = 6.3 Hz, 3H), 0.72 (d, *J* = 6.3 Hz, 3H). $^{13}C\{^{1}H\}$ NMR (100 MHz, $CDCl_3$) δ 197.9, 167.3, 165.8, 160.1, 137.1, 137.1, 128.7 (2C), 127.9, 125.4, 125.3 (2C), 119.7, 119.0, 111.3, 70.2, 69.9, 69.2, 58.9, 21.3, 21.2, 21.2, 20.5. HRMS (ESI-TOF) *m/z*: [M + H^+] Calcd for $C_{23}H_{26}NO_5$ 396.1805, Found 396.1807.

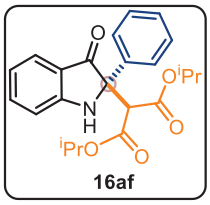

Ethyl 3-oxo-2-(3-oxo-2-phenylindolin-2-yl) butanoate (±16ag): Purification with petroleum ether: acetone (9/1) as eluent; yellow solid (101 mg, 60% yield, mp = 164-166 °C). ^{1}H NMR (400 MHz, $CDCl_3$) δ 7.54 (d, *J* = 7.7 Hz, 3H), 7.49 – 7.43 (m, 1H), 7.30 (t, *J* = 7.4 Hz, 2H), 7.22 (d, *J* = 7.3 Hz, 1H), 6.96 (d, *J* = 8.2 Hz, 1H), 6.79 (t, *J* = 7.4 Hz, 1H), 6.17 (s, 1H), 4.93 (s, 1H), 4.07 – 3.88 (m, 2H), 2.16 (s, 3H), 0.90 (t, *J* = 7.1 Hz, 3H). $^{13}C\{^{1}H\}$ NMR (100 MHz, $CDCl_3$) δ 203.4, 198.9, 166.3, 160.2, 137.3, 137.3, 128.9 (2C), 128.0, 125.3, 125.2 (2C), 119.4, 119.0, 111.5, 70.3, 63.0, 61.9, 32.9, 13.4. HRMS (ESI-TOF) *m/z*: [M + H^+] Calcd for $C_{20}H_{20}NO_4$ 338.1387, Found 338.1383.

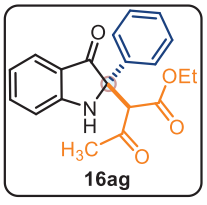

Ethyl 3-oxo-2-(3-oxo-2-phenylindolin-2-yl)-3-phenylpropionate (±16ah): Purification with petroleum ether: acetone (9/1) as eluent; yellow solid (146 mg, 73% yield, mp = 162-164 °C). ^{1}H NMR (400 MHz, $CDCl_3$) δ 7.88 (d, *J* = 7.5 Hz, 2H), 7.61 – 7.56 (m, 2H), 7.55 – 7.47 (m, 3H), 7.47 – 7.41 (m, 2H), 7.19 (t, *J* = 7.4 Hz, 2H), 7.13 (t, *J* = 7.2 Hz, 1H), 7.00 (d, *J* = 8.2 Hz, 1H), 6.80 (t, *J* = 7.4 Hz, 1H), 6.46 (s, 1H), 5.77 (s, 1H), 4.02 – 3.83 (m, 2H), 0.83 (t, *J* = 7.1 Hz, 3H). $^{13}C\{^{1}H\}$ NMR (100 MHz, $CDCl_3$) δ 199.0, 195.1, 166.6, 160.5, 137.4, 137.3, 136.9, 133.8, 128.8 (2C), 128.7 (2C), 128.4 (2C), 127.8, 125.4, 125.2 (2C), 119.3, 118.9, 111.6, 71.1, 61.9, 58.2, 13.3. HRMS (ESI-TOF) *m/z*: [M + H^+] Calcd for $C_{25}H_{22}NO_4$ 400.1543, Found 400.1539.

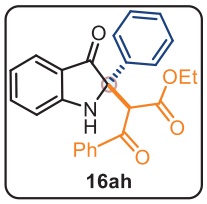

3-(3-Oxo-2-phenylindolin-2-yl)pentane-2,4-dione (±16ai): Purification with petroleum ether: acetone (9/1) as eluent; yellow solid (95 mg, 62% yield, mp = 148-150 °C). ^{1}H NMR (400 MHz, $CDCl_3$) δ 7.62 – 7.58 (m, 2H), 7.52 (d, *J* = 7.7 Hz, 1H), 7.47 (m, 1H), 7.32 (d, *J* = 7.0 Hz, 2H), 7.25 (d, *J* = 2.2 Hz, 1H), 6.98 (d, *J* = 8.3 Hz, 1H), 6.79 (t, *J* = 7.4 Hz, 1H), 6.29 (s, 1H), 5.08 (s, 1H), 2.13 (s, 3H), 2.04 (s, 3H). ^{13}C{^{1}H} NMR (100 MHz, $CDCl_3$) δ 203.5, 200.0, 199.5, 160.7, 138.0, 137.5, 128.9 (2C), 128.1, 125.4 (2C), 125.3, 119.3, 119.1, 112.2, 71.1, 71.1, 33.0, 31.3. HRMS (ESI-TOF) *m/z*: [M + H$^+$] Calcd for $C_{19}H_{18}NO_3$ 308.1281, Found 308.1287.

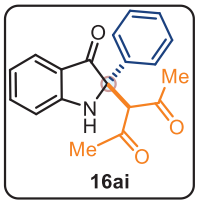

16ai

Methyl 2-cyano-2-(3-oxo-2-phenylindolin-2-yl)acetate (±16aj): Purification with petroleum ether: acetone (8/2) as eluent; yellow solid (dr = 1:1, 100 mg, 65% yield, mp = 145-147 °C). ^{1}H NMR (400 MHz, $CDCl_3$) δ 7.63 (d, *J* = 7.7 Hz, 1H), 7.55 (dt, *J* = 7.1, 3.7 Hz, 3H), 7.45 – 7.35 (m, 3H), 7.05 (d, *J* = 8.2 Hz, 1H), 6.93 (t, *J* = 7.5 Hz, 1H), 5.65 (s, 1H), 4.79 (s, 1H), 3.64 (s, 3H). ^{13}C{^{1}H} NMR (100 MHz, $CDCl_3$) δ 195.8, 163.4, 159.6, 137.7, 134.5, 129.4 (2C), 129.2, 125.6, 125.2 (2C), 120.6, 119.6, 114.5, 112.2, 70.1, 53.6, 46.7. HRMS (ESI-TOF) *m/z*: [M + H$^+$] Calcd for $C_{18}H_{15}N_2O_3$ 307.1077, Found 307.1085.

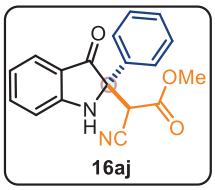

16aj

2-Allyl-2-phenylindolin-3-one (±16ak): Purification with petroleum ether: acetone (9/1) as eluent; yellow solid (83 mg, 67% yield, mp = 149-151 °C). ^{1}H NMR (400 MHz, $CDCl_3$) δ 7.64 – 7.59 (m, 2H), 7.57 (m, 1H), 7.48 (m, 1H), 7.37 – 7.34 (m, 1H), 7.33 (d, *J* = 1.5 Hz, 1H), 7.30 – 7.25 (m, 1H), 6.96 (dt, *J* = 8.3, 0.9 Hz, 1H), 6.83 (m, 1H), 5.59 (m, 1H), 5.16 (m, 1H), 5.12 (s, 1H), 5.07 (m, 1H), 3.08 – 3.02 (m, 1H), 2.65 (m, 1H). ^{13}C{^{1}H} NMR (100 MHz, $CDCl_3$) δ 201.1, 160.2, 138.5, 137.4, 132.5, 128.6 (2C), 127.6, 125.8 (2C), 125.4, 119.7, 119.5, 119.2, 112.2, 70.7, 42.8. HRMS (ESI-TOF) *m/z*: [M + H$^+$] Calcd for $C_{17}H_{16}NO$ 250.1226, Found 250.1230.

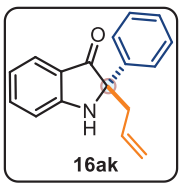

16ak

2-Phenyl-2-(1*H*-pyrrol-2-yl)indolin-3-one (±16al): Purification with petroleum ether: acetone (9/1) as eluent; yellow solid (85 mg, 62% yield, mp = 210-212 °C). ^{1}H NMR (400 MHz, $CDCl_3$) δ 8.84 (s, 1H), 7.64 (d, *J* = 7.7 Hz, 1H), 7.50 (m, 1H), 7.29 (q, *J* = 3.6 Hz, 3H), 7.24 (dd, *J* = 6.9, 3.0 Hz, 2H), 6.93 (d, *J* = 8.3 Hz, 1H), 6.88 (t, *J* = 7.5 Hz, 1H), 6.78 (q, *J* = 2.3 Hz, 1H), 6.28 – 6.24 (m, 1H), 6.20 (q, *J* = 2.9

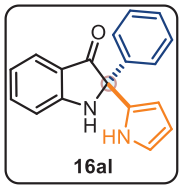

16al

Hz, 1H), 5.37 (s, 1H). $^{13}C\{^{1}H\}$ NMR (100 MHz, $CDCl_3$) δ 201.0, 160.9, 140.7, 137.9, 129.0, 128.7 (2C), 128.3, 126.6 (2C), 125.6, 119.8, 119.5, 118.5, 112.6, 108.4, 107.1, 70.8. HRMS (ESI-TOF) *m/z*: [M + H^+] Calcd for $C_{18}H_{15}N_2O$ 275.1179, Found 275.1173.

2-(3-Methoxyphenyl)-3-oxoindoline-2-carbonitrile (±16am): Purification with petroleum ether: acetone (7/3) as eluent; yellow solid (70 mg, 60% yield, mp = 136-138 °C). ^{1}H NMR (400 MHz, $CDCl_3$) δ 7.65 (d, *J* = 7.8 Hz, 1H), 7.63 – 7.58 (m, 1H), 7.54 (dd, *J* = 6.7, 2.9 Hz, 2H), 7.44 – 7.39 (m, 3H), 7.04 (d, *J* = 8.3 Hz, 1H), 7.00 (t, *J* = 7.5 Hz, 1H), 5.41 (s, 1H).$^{13}C\{^{1}H\}$ NMR (100 MHz, $CDCl_3$) δ 190.8, 160.2, 138.9, 133.1, 129.7, 129.4 (2C), 126.6, 125.3 (2C), 121.5, 116.9, 116.7, 112.7, 65.5. HRMS (ESI-TOF) *m/z*: [M + H^+] Calcd for $C_{15}H_{11}N_2O$ 235.0866, Found 235.0872.

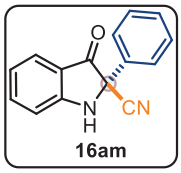

16am

Ethyl-2-(2-(4-fluoro-3-methylphenyl)-3-oxoindolin-2-yl)-3-oxo-3-phenylpropanoate (±16bh): Purification with petroleum ether: acetone (9/1) as eluent; yellow solid (142 mg, 66% yield, mp = 220-221°C). ^{1}H NMR (400 MHz, $CDCl_3$) δ 7.90 – 7.85 (m, 2H), 7.58 (t, *J* = 7.4 Hz, 2H), 7.52 – 7.42 (m, 3H), 7.37 – 7.28 (m, 2H), 7.00 (d, *J* = 8.2 Hz, 1H), 6.85 – 6.78 (m, 2H), 6.44 (s, 1H), 5.69 (s, 1H), 4.00 – 3.83 (m, 2H), 2.11 (d, *J* = 1.4 Hz, 3H), 0.84 (t, *J* = 7.1 Hz, 3H). $^{13}C\{^{1}H\}$ NMR (100 MHz, $CDCl_3$) δ 199.1, 195.1, 166.4, 160.7 (d, *J* = 245.7 Hz), 160.4, 137.5, 136.9, 133.9, 132.6 (d, *J* = 3.4 Hz), 128.8 (2C), 128.5 (d, *J* = 11.3 Hz), 128.4 (2C), 125.4, 125.1 (d, *J* = 17.6 Hz), 124.4 (d, *J* = 8.14 Hz), 119.2, 119.0, 115.3 (d, *J* = 22.7 Hz), 111.7, 70.5, 62.0, 58.2, 14.7 (d, *J* = 3.3 Hz), 13.3. ^{19}F NMR (376 MHz, $CDCl_3$) δ -118.9. HRMS (ESI-TOF) *m/z*: [M + H^+] Calcd for $C_{26}H_{23}FNO_4$ 432.1606, Found 432.1614.

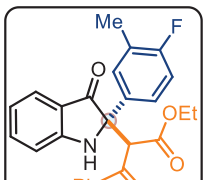

16bh

Ethyl-2-(2-(3-chlorophenyl)-3-oxoindolin-2-yl)-3-oxo-3-phenylpropanoate (±16ch): Purification with petroleum ether: acetone (9/1) as eluent; yellow solid (128 mg, 59% yield, mp = 160-162°C). ^{1}H NMR (400 MHz, $CDCl_3$) δ 7.90 – 7.85 (m, 2H), 7.61 – 7.54 (m, 3H), 7.52 – 7.47 (m, 1H), 7.47 – 7.42 (m, 3H), 7.14 – 7.09 (m, 2H), 7.01 (d, *J* = 8.3 Hz, 1H), 6.83 (t, *J* = 7.4 Hz, 1H), 6.47 (s, 1H), 5.69 (s, 1H), 3.99 – 3.83 (m, 2H), 0.83 (t, *J* = 7.1 Hz, 3H). $^{13}C\{^{1}H\}$ NMR (100 MHz, $CDCl_3$) δ 198.5, 194.8, 166.2, 160.4, 139.6, 137.7, 136.6, 134.7, 134.0, 130.0, 128.8 (2C), 128.4 (2C), 128.0, 125.7, 125.4, 123.7, 119.2, 119.1, 111.8, 70.6, 62.1, 58.3, 13.3. HRMS (ESI-TOF) *m/z*: [M + H^+] Calcd for $C_{25}H_{21}ClNO_4$ 434.1154, Found 434.1158.

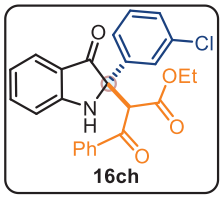

16ch

Ethyl-2-(2-(4-chlorophenyl)-3-oxoindolin-2-yl)-3-oxo-3-phenylpropanoate. (±16dh):

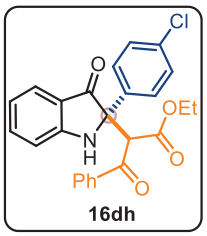

16dh

Purification with petroleum ether: acetone (8/2) as eluent; yellow solid (132 mg, 61% yield, mp = 145-147°C). ^{1}H NMR (400 MHz, $CDCl_3$) δ 7.87 (dd, *J* = 8.3, 1.0 Hz, 2H), 7.61 – 7.55 (m, 2H), 7.49 (m, 3H), 7.47 – 7.41 (m, 2H), 7.18 – 7.14 (m, 2H), 6.99 (d, *J* = 8.2 Hz, 1H), 6.85 – 6.78 (m, 1H), 6.51 (s, 1H), 5.71 (s, 1H), 4.00 – 3.83 (m, 2H), 0.83 (t, *J* = 7.1 Hz, 3H). ^{13}C{^{1}H} NMR (100 MHz, $CDCl_3$) δ 198.7, 194.8, 166.2, 160.4, 137.6, 136.6, 136.1, 134.0, 133.8, 128.9 (2C), 128.8 (2C), 128.4 (2C), 126.8 (2C), 125.3, 119.1, 119.1, 111.7, 70.6, 62.0, 58.2, 13.3. HRMS (ESI-TOF) *m/z*: [M + H$^+$] Calcd for $C_{25}H_{21}ClNO_4$ 434.1154, Found 434.1150.

Ethyl-2-(2-(4-bromophenyl)-3-oxoindolin-2-yl)-3-oxo-3-phenylpropanoate (±16eh):

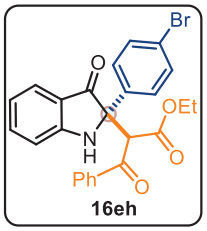

16eh

Purification with petroleum ether: acetone (8/2) as eluent; yellow solid (153 mg, 64% yield, mp = 159-161°C). ^{1}H NMR (400 MHz, $CDCl_3$) δ 7.88 (dt, *J* = 8.5, 1.5 Hz, 2H), 7.60 – 7.56 (m, 2H), 7.51 – 7.48 (m, 1H), 7.47 (s, 1H), 7.45 – 7.41 (m, 3H), 7.34 – 7.29 (m, 2H), 6.99 (d, *J* = 8.2 Hz, 1H), 6.86 – 6.78 (m, 1H), 6.47 (s, 1H), 5.69 (s, 1H), 3.99 – 3.83 (m, 2H), 0.83 (t, *J* = 7.1 Hz, 3H). ^{13}C{^{1}H} NMR (100 MHz, $CDCl_3$) δ 198.6, 194.8, 166.2, 160.4, 137.7, 136.7, 136.6, 134.1, 131.8 (2C), 128.9 (2C), 128.4 (2C), 127.1 (2C), 125.4, 122.1, 119.2, 119.1, 111.7, 70.7, 62.1, 58.2, 13.3. HRMS (ESI-TOF) *m/z*: [M + H$^+$] Calcd for $C_{25}H_{21}BrNO_4$ 478.0648, Found 478.0644.

Ethyl-3-oxo-2-(3-oxo-2-(*p*-tolyl)indolin-2-yl)-3-phenylpropanoate (±16fh): Purification with petroleum ether: acetone (9/1) as eluent; yellow solid (141 mg, 68% yield, mp = 180-182 °C). ^{1}H NMR (400 MHz, $CDCl_3$) δ 7.90 (d, *J* = 7.7 Hz, 2H), 7.57 (t, *J* = 7.6 Hz, 2H), 7.45 (m, 3H), 7.38 (d, *J* = 7.6 Hz, 2H), 6.99 (d, *J* = 7.9 Hz, 3H), 6.79 (t, *J* = 7.3 Hz, 1H), 6.43 (s, 1H), 5.77 (s, 1H), 3.91 (m, 2H), 2.18 (s, 3H), 0.82 (t, *J* = 7.0 Hz, 3H). ^{13}C{^{1}H} NMR (100 MHz, $CDCl_3$) δ 199.1, 195.1, 166.6, 160.5, 137.5, 137.3, 137.0, 134.3, 133.7, 129.6 (2C), 128.7 (2C), 128.5 (2C), 125.4, 125.1 (2C), 119.3, 118.8, 111.5, 71.0, 61.9, 58.0, 20.8, 13.3. HRMS (ESI-TOF) *m/z*: [M + H$^+$] Calcd for $C_{26}H_{24}NO_4$ 414.1700, Found 414.1704.

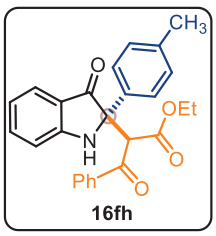

16fh

Ethyl-2-(2-(3-methoxyphenyl)-3-oxoindolin-2-yl)-3-oxo-3-phenylpropanoate (±16gh):

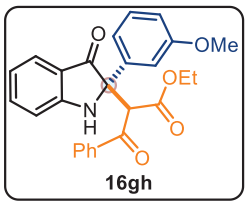

Purification with petroleum ether: acetone (9/1) as eluent; yellow solid (150 mg, 70% yield, mp = 190-192 °C). ^{1}H NMR (400 MHz, $CDCl_3$) δ 7.90 (d, *J* = 7.5 Hz, 2H), 7.57 (dd, *J* = 11.9, 7.5 Hz, 2H), 7.45 (dt, *J* = 15.3, 7.8 Hz, 3H), 7.08 (dd, *J* = 14.0, 7.7 Hz, 3H), 6.98 (d, *J* = 8.2 Hz, 1H), 6.80 (t, *J* = 7.4 Hz, 1H), 6.66 (dt, *J* = 6.4, 2.3 Hz, 1H), 6.44 (s, 1H), 5.77 (s, 1H), 3.92 (m, 2H), 3.63 (s, 3H), 0.82 (t, *J* = 7.1 Hz, 3H). ^{13}C{^{1}H} NMR (100 MHz, $CDCl_3$) δ 198.8, 195.0, 166.5, 160.5, 159.8, 138.9, 137.4, 136.9, 133.8, 129.8, 128.7 (2C), 128.4 (2C), 125.4, 119.2, 118.9, 117.5, 113.0, 111.5, 111.3, 71.1, 61.9, 58.0, 55.0, 13.3. HRMS (ESI-TOF) *m/z*: [M + H^{+}] Calcd for $C_{26}H_{24}NO_5$ 430.1649, Found 430.1655.

2-(3-Chlorophenyl)-3-oxoindoline-2-carbonitrile (±16dm): Purification with petroleum ether:

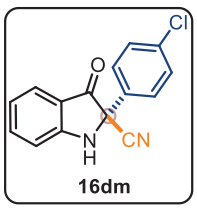

acetone (8/2) as eluent; yellow solid (77 mg, 57% yield, mp = 147-149 °C). ^{1}H NMR (400 MHz, $CDCl_3$ with few drops of DMSO-d_6) δ 8.90 (s, 1H), 7.69 (m, 1H), 7.56 (dt, *J* = 7.7, 2.5 Hz, 3H), 7.50 – 7.46 (m, 2H), 7.13 (d, *J* = 8.3 Hz, 1H), 6.99 – 6.92 (m, 1H). ^{13}C{^{1}H} NMR (100 MHz, $CDCl_3$ with few drops of DMSO-d_6) δ 189.3, 159.7, 137.8, 132.4, 130.2, 127.5 (2C), 125.1 (2C), 124.0, 118.4, 114.8, 112.7, 110.9, 62.4. HRMS (ESI-TOF) *m/z*: [M + H^{+}] Calcd for $C_{15}H_{10}ClN_2O$ 269.0476, Found 269.0474.

2-(3-Methoxyphenyl)-3-oxoindoline-2-carbonitrile (±16gm): Purification with petroleum

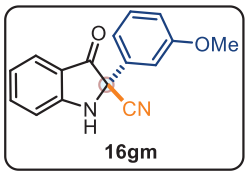

ether: acetone (9/1) as eluent; yellow solid (78 mg, 59% yield, mp = 155-157 °C). ^{1}H NMR (400 MHz, $CDCl_3$) δ 7.65 – 7.57 (m, 2H), 7.31 (t, *J* = 8.0 Hz, 1H), 7.13 – 7.09 (m, 1H), 7.07 (t, *J* = 2.0 Hz, 1H), 7.03 (s, 1H), 7.01 (d, *J* = 2.5 Hz, 1H), 6.92 (dd, *J* = 8.2, 2.0 Hz, 1H), 5.48 (s, 1H), 3.80 (s, 3H). ^{13}C{^{1}H} NMR (100 MHz, $CDCl_3$) δ 190.6, 160.2, 160.2, 138.9, 134.5, 130.5, 126.6, 121.4, 117.4, 116.8, 116.7, 115.0, 112.7, 111.2, 65.4, 55.4. HRMS (ESI-TOF) *m/z*: [M + H^{+}] Calcd for $C_{16}H_{13}N_2O_2$ 265.0972, Found 265.0978.

2-(4-Chlorophenyl)-2-(1H-indol-3-yl)indolin-3-one (±16da): Purification with petroleum

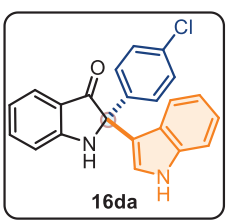

ether: acetone (9/1) as eluent; yellow solid (115 mg, 64% yield, mp = 178-180 °C). ^{1}H NMR (400 MHz, $CDCl_3$) δ 8.26 (s, 1H), 7.69 (d, *J* = 7.7 Hz, 1H), 7.54 – 7.47 (m, 3H), 7.37 (d, *J* = 8.2 Hz, 1H), 7.28 – 7.23 (m, 2H), 7.21

– 7.16 (m, 1H), 7.12 (m, 2H), 7.03 – 6.97 (m, 1H), 6.91 (t, *J* = 8.2 Hz, 2H), 5.35 (s, 1H). $^{13}C\{^{1}H\}$ NMR (100 MHz, $CDCl_3$) δ 200.2, 160.5, 138.1, 137.7, 136.9, 133.7, 128.5 (2C), 128.3 (2C), 125.6, 125.3, 123.7, 122.7, 120.2, 119.9, 119.5, 119.4, 115.2, 113.1, 111.7, 70.8. HRMS (ESI-TOF) *m/z*: [M + H^+] Calcd for $C_{22}H_{16}ClN_2O$ 359.0946, Found 359.0952.

2-(1*H*-Indol-3-yl)-2-(*p*-tolyl)indolin-3-one (±16fa): Purification with petroleum ether: acetone (9/1) as eluent; yellow solid (118 mg, 70% yield, mp = 189-191 °C). ^{1}H NMR (400 MHz, $CDCl_3$) δ 8.29 (s, 1H), 7.69 (d, *J* = 7.3 Hz, 1H), 7.49 (m, 1H), 7.43 (d, *J* = 8.2 Hz, 2H), 7.34 (d, *J* = 8.1 Hz, 1H), 7.20 – 7.13 (m, 2H), 7.10 (dd, *J* = 5.3, 2.6 Hz, 3H), 7.01 – 6.95 (m, 1H), 6.93 – 6.84 (m, 2H), 5.39 (s, 1H), 2.31 (s, 3H). $^{13}C\{^{1}H\}$ NMR (100 MHz, $CDCl_3$) δ 201.0, 160.6, 137.5, 137.5, 137.0, 136.5, 129.2 (2C), 126.7 (2C), 125.7, 125.6, 123.8, 122.5, 120.0, 119.8, 119.6, 119.5, 115.5, 112.9, 111.7, 71.2, 31.6. HRMS (ESI-TOF) *m/z*: [M + H^+] Calcd for $C_{23}H_{19}N_2O$ 339.1492, Found 339.1494.

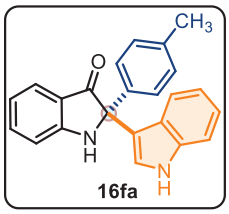

16fa

Dimethyl-2-(5-methyl-3-oxo-2-phenylindolin-2-yl)malonate (±16hd): Purification with petroleum ether: acetone (9/1) as eluent; yellow solid (127 mg, 72% yield, mp = 169-171 °C). ^{1}H NMR (400 MHz, $CDCl_3$) δ 7.52 – 7.46 (m, 2H), 7.35 (s, 1H), 7.32 – 7.27 (m, 3H), 7.24 (dd, *J* = 8.3, 6.0 Hz, 1H), 6.90 (d, *J* = 8.3 Hz, 1H), 5.92 (s, 1H), 4.75 (s, 1H), 3.56 (s, 3H), 3.50 (s, 3H), 2.26 (s, 3H). $^{13}C\{^{1}H\}$ NMR (100 MHz, $CDCl_3$) δ 198.0, 168.2, 166.5, 158.5, 138.7, 136.8, 128.8 (3C), 128.0, 125.2 (2C), 124.8, 119.4, 111.4, 70.6, 58.4, 52.6, 52.5, 20.5. HRMS (ESI-TOF) *m/z*: [M + H^+] Calcd for $C_{20}H_{20}NO_5$ 354.1336, Found 354.1332.

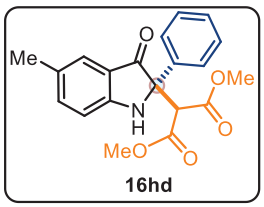

16hd

Ethyl 2-(5-methyl-3-oxo-2-phenylindolin-2-yl)-3-oxo-3-phenylpropanoate (±16hh): Purification with petroleum ether: acetone (9/1) as eluent; yellow solid (153 mg, 74% yield, mp = 160-162 °C). ^{1}H NMR (400 MHz, $CDCl_3$) δ 7.90 – 7.86 (m, 2H), 7.56 (tt, *J* = 6.9, 1.2 Hz, 1H), 7.52 – 7.48 (m, 2H), 7.43 (t, *J* = 7.7 Hz, 2H), 7.39 – 7.37 (m, 1H), 7.32 (dd, *J* = 8.3, 1.5 Hz, 1H), 7.20 – 7.15 (m, 2H), 7.14 – 7.09 (m, 1H), 6.93 (d, *J* = 8.3 Hz, 1H), 6.32 (s, 1H), 5.77 (s, 1H), 4.03 – 3.85 (m, 2H), 2.27 (s, 3H), 0.85 (t, *J* = 7.1 Hz, 3H). $^{13}C\{^{1}H\}$ NMR (100 MHz, $CDCl_3$ with few drops of DMSO-d_6) δ 197.0, 192.5, 165.1, 158.2, 136.9, 136.2, 135.0, 132.0, 127.2 (2C), 126.8 (2C), 126.4 (2C), 125.6, 125.4, 123.4 (2C), 121.8, 116.3, 110.4, 69.6, 59.5,

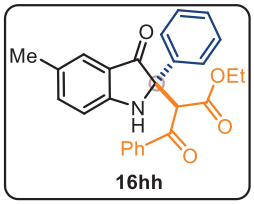

16hh

55.9, 18.3, 11.4. HRMS (ESI-TOF) *m/z*: [M + H^+] Calcd for $C_{26}H_{24}NO_4$ 414.1700, Found 414.1704.

Ethyl-2-(2-(4-chlorophenyl)-5-methyl-3-oxoindolin-2-yl)-3-oxo-3-phenylpropanoate

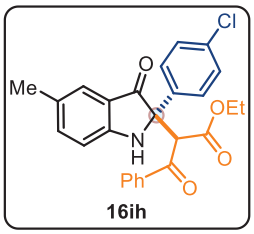

16ih

(±16ih): Purification with petroleum ether: acetone (9/1) as eluent; yellow solid (157 mg, 70% yield, mp = 188-190 °C). ^{1}H NMR (400 MHz, $CDCl_3$) δ 7.87 (d, *J* = 7.7 Hz, 2H), 7.58 (t, *J* = 7.5 Hz, 1H), 7.45 (q, *J* = 7.8 Hz, 4H), 7.38 (s, 1H), 7.32 (d, *J* = 8.4 Hz, 1H), 7.15 (d, *J* = 8.3 Hz, 2H), 6.92 (d, *J* = 8.3 Hz, 1H), 6.32 (s, 1H), 5.68 (s, 1H), 3.92 (m, 2H), 2.27 (s, 3H), 0.85 (t, *J* = 7.2 Hz, 3H). ^{13}C{^{1}H} NMR (100 MHz, $CDCl_3$) δ 198.8, 194.9, 166.3, 158.9, 139.1, 136.7, 136.3, 134.0, 133.8, 128.9 (2C), 128.8 (2C), 128.7, 128.4 (2C), 126.8 (2C), 124.7, 119.2, 111.6, 71.0, 62.0, 58.3, 20.5, 13.4. HRMS (ESI-TOF) *m/z*: [M + H^+] Calcd for $C_{26}H_{23}ClNO_4$ 448.1310, Found 448.1316.

Dimethyl-2-(2-(4-bromophenyl)-5-methyl-3-oxoindolin-2-yl)malonate (±16jd): Purification

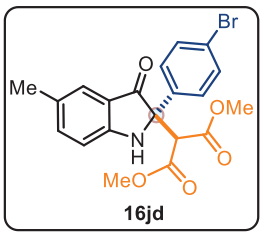

16jd

with petroleum ether: acetone (9/1) as eluent; yellow solid (149 mg, 69% yield, mp = 179-181 °C). ^{1}H NMR (400 MHz, $CDCl_3$) δ 7.44 – 7.38 (m, 4H), 7.35 (s, 1H), 7.31 (dd, *J* = 8.3, 1.6 Hz, 1H), 6.89 (d, *J* = 8.3 Hz, 1H), 5.93 (s, 1H), 4.66 (s, 1H), 3.59 (s, 3H), 3.49 (s, 3H), 2.26 (s, 3H). ^{13}C{^{1}H} NMR (100 MHz, $CDCl_3$) δ 197.6, 168.1, 166.2, 158.4, 138.9, 136.2, 131.9 (2C), 129.0, 127.1 (2C), 124.8, 122.4, 119.3, 111.5, 70.1, 58.3, 52.7, 52.7, 20.5. HRMS (ESI-TOF) *m/z*: [M + H^+] Calcd for $C_{20}H_{19}BrNO_5$ 432.0441, Found 432.0437.

Diethyl-2-(2-(4-bromophenyl)-5-methyl-3-oxoindolin-2-yl)malonate (±16je): Purification

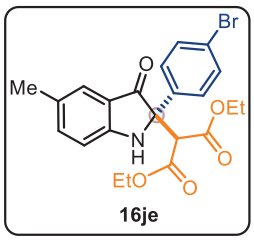

16je

with petroleum ether: acetone (9/1) as eluent; yellow solid (166 mg, 72% yield, mp = 175-177 °C). ^{1}H NMR (400 MHz, $CDCl_3$) δ 7.41 (s, 4H), 7.34 (d, *J* = 1.8 Hz, 1H), 7.32 – 7.27 (m, 1H), 6.87 (d, *J* = 8.3 Hz, 1H), 5.99 – 5.93 (m, 1H), 4.62 (s, 1H), 4.17 – 4.05 (m, 1H), 4.03 (dd, *J* = 7.4, 4.5 Hz, 1H), 4.01 – 3.95 (m, 1H), 3.95 – 3.86 (m, 1H), 2.25 (s, 3H), 1.07 (t, *J* = 7.1 Hz, 3H), 0.88 (t, *J* = 7.2 Hz, 3H). ^{13}C{^{1}H} NMR (100 MHz, $CDCl_3$) δ 197.6, 167.6, 165.9, 158.5, 138.8, 136.4, 131.8 (2C), 128.9, 127.2 (2C), 124.7, 122.3, 119.4, 111.4, 70.1, 62.0, 61.7, 58.5, 20.4, 13.7, 13.3. HRMS (ESI-TOF) *m/z*: [M + H^+] Calcd for $C_{22}H_{23}BrNO_5$ 460.0754, Found 460.0757.

Diisopropyl-2-(2-(4-bromophenyl)-5-methyl-3-oxoindolin-2-yl)malonate (±16jf): Purification

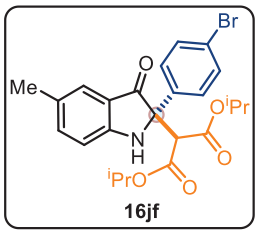

16jf

with petroleum ether: acetone (9/1) as eluent; yellow solid (159 mg, 65% yield, mp = 202-204 °C). ^{1}H NMR (400 MHz, $CDCl_3$) δ 7.40 (s, 4H), 7.34 (s, 1H), 7.31 – 7.27 (m, 1H), 6.87 (d, *J* = 8.3 Hz, 1H), 5.94 (s, 1H), 4.85 (m, 2H), 4.55 (s, 1H), 2.25 (s, 3H), 1.12 (d, *J* = 6.3 Hz, 3H), 1.05 (d, *J* = 6.3 Hz, 3H), 1.01 (d, *J* = 6.3 Hz, 3H), 0.75 (d, *J* = 6.2 Hz, 3H). ^{13}C{^{1}H} NMR (100 MHz, $CDCl_3$) δ 167.2, 165.5, 158.5, 138.7, 136.6, 131.7 (2C), 128.8, 127.3 (2C), 124.8, 122.2, 119.6, 111.4, 77.2, 70.1, 70.0, 69.4, 58.8, 21.4, 21.3, 21.2, 20.6, 20.4. HRMS (ESI-TOF) *m/z*: [M + H^{+}] Calcd for $C_{24}H_{27}BrNO_5$ 488.1067, Found 488.1061.

Ethyl-2-(2-(4-bromophenyl)-5-methyl-3-oxoindolin-2-yl)-3-oxo-3-phenylpropanoate

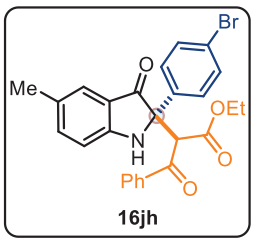

16jh

(±16jh): Purification with petroleum ether: acetone (9/1) as eluent; yellow solid (170 mg, 69% yield, mp = 201-203 °C). ^{1}H NMR (400 MHz, $CDCl_3$) δ 7.87 (d, *J* = 7.7 Hz, 2H), 7.58 (t, *J* = 7.4 Hz, 1H), 7.46 (s, 1H), 7.45 – 7.40 (m, 3H), 7.37 (s, 1H), 7.31 (t, *J* = 8.8 Hz, 3H), 6.92 (d, *J* = 8.3 Hz, 1H), 6.33 (s, 1H), 5.69 (s, 1H), 3.92 (m, 2H), 2.27 (s, 3H), 0.85 (t, *J* = 7.1 Hz, 3H). ^{13}C{^{1}H} NMR (100 MHz, $CDCl_3$) δ 198.7, 194.8, 166.3, 158.9, 139.1, 136.9, 136.7, 134.0, 131.8 (2C), 128.8 (2C), 128.7, 128.4 (2C), 127.1 (2C), 124.7, 122.0, 119.2, 111.6, 71.0, 62.0, 58.2, 20.5, 13.4. HRMS (ESI-TOF) *m/z*: [M + H^{+}] Calcd for $C_{26}H_{23}BrNO_4$ 492.0805, Found 492.0813.

3-(2-(4-Bromophenyl)-5-methyl-3-oxoindolin-2-yl)pentane-2,4-dione (±16jn): Purification

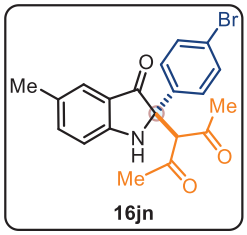

16jn

with petroleum ether: acetone (9/1) as eluent); yellow solid (130 mg, 65% yield, mp = 176-178 °C). ^{1}H NMR (400 MHz, $CDCl_3$) δ 7.50 (d, *J* = 8.5 Hz, 2H), 7.42 (d, *J* = 8.4 Hz, 2H), 7.31 (d, *J* = 10.8 Hz, 2H), 6.89 (d, *J* = 8.2 Hz, 1H), 6.16 (s, 1H), 5.00 (s, 1H), 2.25 (s, 3H), 2.13 (s, 3H), 2.04 (s, 3H). ^{13}C{^{1}H} NMR (100 MHz, $CDCl_3$) δ 203.3, 200.1, 199.5, 159.5, 140.1, 137.3, 132.2 (2C), 129.5, 127.7 (2C), 124.8, 122.6, 119.4, 112.7, 71.4, 71.3, 33.2, 31.7, 20.8. HRMS (ESI-TOF) *m/z*: [M + H^{+}] Calcd for $C_{20}H_{19}BrNO_3$ 400.0543, Found 400.0547.

Di-*tert*-butyl 2-(2-(4-bromophenyl)-5-methyl-3-oxoindolin-2-yl)malonate (±16jo):

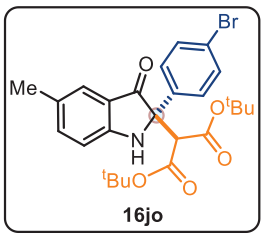

16jo

Purification with petroleum ether: acetone (8/2) as eluent); yellow solid (163 mg, 63% yield, mp = 189-191 °C). ^{1}H NMR (400 MHz, $CDCl_3$) δ 7.40 (d, *J* = 1.0 Hz, 4H), 7.33 (dd, *J* = 1.9, 0.9 Hz, 1H), 7.30 (dd, *J* = 8.3, 1.9 Hz, 1H), 6.86 (d, *J* = 8.3 Hz, 1H), 5.90 (s, 1H), 4.45 (s, 1H), 2.26 (s, 3H), 1.24 (s, 9H), 1.13 (s, 9H). ^{13}C{^{1}H} NMR (100 MHz, $CDCl_3$) δ 197.7, 167.0, 165.3, 158.5, 138.7, 137.0, 131.6 (2C), 128.7, 127.3 (2C), 124.9, 122.0, 119.6, 111.3, 83.2, 82.6, 70.4, 60.2, 27.6 (3C), 27.4 (3C), 20.5. HRMS (ESI-TOF) *m*/*z*: [M + H$^+$] Calcd for $C_{26}H_{31}BrNO_5$ 516.1380, Found 516.1376.

Diethyl 2-(5-chloro-3-oxo-2-phenylindolin-2-yl)malonate (±16ke): Purification with petroleum ether: acetone (9/1) as eluent); yellow solid (141 mg, 70% yield, mp = 151-154 °C). ^{1}H NMR (400 MHz, $CDCl_3$) δ 7.54 (d, *J* = 2.2 Hz, 1H), 7.53 – 7.49 (m, 2H), 7.43 (dd, *J* = 8.6, 2.2 Hz, 1H), 7.36 – 7.32 (m, 1H), 7.32 – 7.29 (m, 1H), 7.29 – 7.26 (m, 1H), 6.95 (d, *J* = 8.6 Hz, 1H), 6.17 (s, 1H), 4.72 (s, 1H), 4.12 – 3.93 (m, 4H), 1.04 (t, *J* = 7.1 Hz, 3H), 0.96 (t, *J* = 7.1 Hz, 3H). ^{13}C{^{1}H} NMR (100 MHz, $CDCl_3$) δ 196.8, 167.6, 166.0, 158.2, 137.0 (2C), 136.2, 128.8, 128.2 (2C), 125.2, 124.6, 124.2, 120.6, 112.5, 70.8, 62.0, 61.7, 58.6, 13.6, 13.4. HRMS (ESI-TOF) *m*/*z*: [M + H$^+$] Calcd for $C_{21}H_{21}ClNO_5$ 402.1103, Found 402.1107.

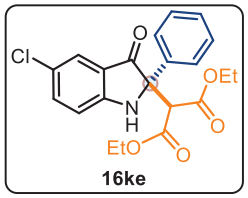

16ke

Diethyl 2-(5-bromo-3-oxo-2-phenylindolin-2-yl)malonate (±16le): Purification with petroleum ether: acetone (9/1) as eluent); yellow solid (141 mg, 67% yield, mp = 165-168 °C). ^{1}H NMR (400 MHz, $CDCl_3$) δ 7.66 (s, 1H), 7.56 – 7.51 (m, 1H), 7.48 (d, *J* = 7.9 Hz, 2H), 7.28 (m, 3H), 6.88 (d, *J* = 8.6 Hz, 1H), 6.15 (s, 1H), 4.69 (s, 1H), 4.10 – 3.90 (m, 4H), 1.01 (t, *J* = 7.1 Hz, 3H), 0.94 (t, *J* = 7.1 Hz, 3H). ^{13}C{^{1}H} NMR (100 MHz, $CDCl_3$) δ 196.7, 167.6, 166.0, 158.6, 139.7, 136.2, 128.9 (2C), 128.3, 127.8, 125.2 (2C), 121.2, 113.0, 111.1, 70.8, 62.1, 61.7, 58.7, 13.7, 13.5. HRMS (ESI-TOF) *m*/*z*: [M + H$^+$] Calcd for $C_{21}H_{21}BrNO_5$ 446.0598, Found 446.0606.

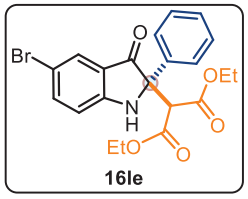

16le

Control experiment

To a 10 mL dried undivided reaction cell equipped with a stirring bar were added **1a** (0.5 mmol, 1.0 equiv), **13h** (1.5 mmol, 3.0 equiv), *n*-Bu_4NPF_6 (193 mg, 0.5 mmol, 1.0 equiv.), and TEMPO (15 mg, 0.1 mmol, 20 mol%), 2, 6-lutidine (1.0 mmol, 2.0 equiv), BHT (2.5 mmol) dissolved in CH_3CN: H_2O (10 mL, 9:1). Graphite-plate anode and Copper-plate cathode were

dipped into the reaction mixture and electrolyzed at a constant current condition (1.5 mA) under an air atmosphere at room temperature, and TLC monitored the reaction. The desired product **16ah** was not observed on TLC.

2-(1*H*-Indol-3-yl)-2-methylindolin-3-one (±16ka): Purification with petroleum ether: acetone (9/1) as eluent); yellow solid (85 mg, 65% yield, mp = 205-207 °C). ^{1}H NMR (400 MHz, $CDCl_3$) δ 8.39 (s, 1H), 7.72 (d, *J* = 6.7 Hz, 1H), 7.55 (m, 1H), 7.33 (d, *J* = 8.0 Hz, 1H), 7.28 (d, *J* = 7.4 Hz, 1H), 7.15 (m, 1H), 7.05 (d, *J* = 2.5 Hz, 1H), 6.99 (m, 1H), 6.94 – 6.87 (m, 2H), 5.06 (s, 1H), 1.80 (s, 3H). ^{13}C{^{1}H} NMR (100 MHz, $CDCl_3$) δ 203.6, 160.1, 137.6, 136.8, 125.4, 124.9, 122.7, 122.4, 120.0, 119.8, 119.7, 119.2, 115.5, 112.6, 111.5, 65.8, 24.0. HRMS (ESI-TOF) *m*/*z*: [M + H^{+}] Calcd for $C_{17}H_{15}N_2O$ 263.1179, Found 263.1185.

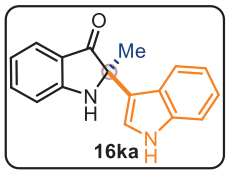

16ka

Gram-scale synthesis of 16ah: A 100 mL three-neck round bottom flask (as an undivided cell) was charged with **1a** (0.76 g, 3.93 mmol, 1.0 equiv), **13h** (2.26 g, 11.79 mmol, 3.0 equiv), *n*-Bu_4NPF_6 (1.52g, 3.93 mmol, 1.0 equiv), and TEMPO (0.122 g, 0.78 mmol, 20 mol%), 2, 6-lutidine (0.842 g, 7.86 mmol, 2.0 equiv) dissolved in CH_3CN: H_2O (36 mL, 9:1). Graphite plate anode and a Copper-plate cathode that was connected to a DC regulated power supply dipped into the reaction mixture and electrolyzed at a constant current condition (1.5 mA) under an air atmosphere at room temperature, and the reaction progress was monitored by TLC. The reaction solvent was evaporated under reduced pressure once the reaction was finished, after the usual workup and silica gel column chromatography purification furnished compound **16ah** (1.02 g) with 65% yield.

2-(3,5-Dimethyl-1*H*-pyrazol-4-yl)-2-phenylindolin-3-one (±18): To a stirred solution of **16ai** (100 mg, 0.32 mmol, 1.0 equiv) in ethanol (6.0 mL) in a dry 25 mL round-bottom flask was added hydrazine-hydrate (80%, 19 µL, 0.48 mmol, 1.5 equiv) dropwise over 10 min at room temperature. The resulting mixture was heated at 80°C using an oil bath for 4 h, and the reaction progress was monitored by TLC. Upon completion, the reaction mixture was cooled to 0 °C, and the resulting precipitate was filtered and washed with cold diethyl ether (5 mL). The crude solid was recrystallized from ethanol and afforded **18** (82% yield). Yellow solid (56 mg, 82% yield, mp = 230–232 °C). ^{1}H NMR (400 MHz, DMSO-d_6) δ 12.12 (s, 1H), 8.09 (s, 1H), 7.51 – 7.44 (m, 3H), 7.41 (d, *J* = 7.7 Hz, 1H), 7.36 – 7.25 (m, 3H), 6.91 (d, *J* = 8.3 Hz, 1H), 6.70 (t, *J*= 7.4 Hz, 1H), 1.64 (s, 6H).

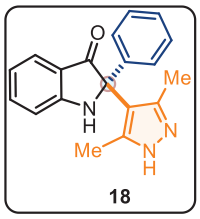

18

$^{13}C\{^{1}H\}$ NMR (100 MHz, DMSO-d_6) δ 201.1, 161.0, 140.8, 138.2, 128.7 (2C), 127.9, 127.1 (2C), 125.0, 118.1, 117.9 (2C), 114.9, 112.1 (2C), 70.2, 40.7, 40.5. HRMS (ESI-TOF) *m*/*z*: [M + H^+] Calcd for $C_{19}H_{18}N_3O$ 304.1444, Found 304.1432.

2-(4-Chlorophenyl)-2-(3-oxo-5-phenyl-2,3-dihydro-1*H*-pyrazol-4-yl)indolin-3-one (±19): To

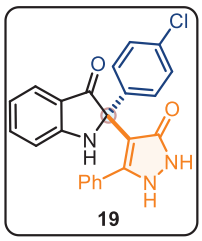

19

a stirred solution of **16dh** (100 mg, 0.23 mmol, 1 equiv) in ethanol (6.0 mL) in a dry 25 mL round-bottom flask was added hydrazine-hydrate (80% sol., 14 µL, 0.35 mmol, 1.5 equiv) dropwise over 10 min at room temperature. The resulting mixture was heated at 80°C using an oil bath for 4 h, and the reaction progress was monitored by TLC. Upon completion, the reaction mixture was cooled to 0 ºC; the resulting precipitate was filtered and washed with cold diethyl ether (5 mL). The crude solid was recrystallized from ethanol, yielding **19** (78%). ellow solid (82 mg, 78% yield, mp = 210-211 ºC). ^{1}H NMR (400 MHz, $CDCl_3$) δ 8.99 (s, 2H), 7.37 (t, *J* = 7.7 Hz, 1H), 7.32 (d, *J* = 7.6 Hz, 1H), 7.26 (d, *J* = 8.6 Hz, 2H), 7.16 (t, *J* = 7.3 Hz, 1H), 7.07 (t, *J* = 7.5 Hz, 2H), 7.01 – 6.94 (m, 4H), 6.76 (d, *J* = 8.2 Hz, 1H), 6.68 (t, *J* = 7.4 Hz, 1H), 6.09 (s, 1H). $^{13}C\{^{1}H\}$ NMR (100 MHz, $CDCl_3$ with few drops of DMSO-d_6) δ 201.1, 160.4, 138.2, 137.7, 133.2, 130.6, 129.1 (2C), 128.8, 128.5, 128.3 (3C), 128.1 (2C) 127.9 (2C), 125.4, 125.3, 119.0, 118.8, 112.3, 69.4. HRMS (ESI-TOF) *m*/*z*: [M + H^+] Calcd for $C_{23}H_{17}ClN_3O_2$ 402.1004, Found 402.0998.

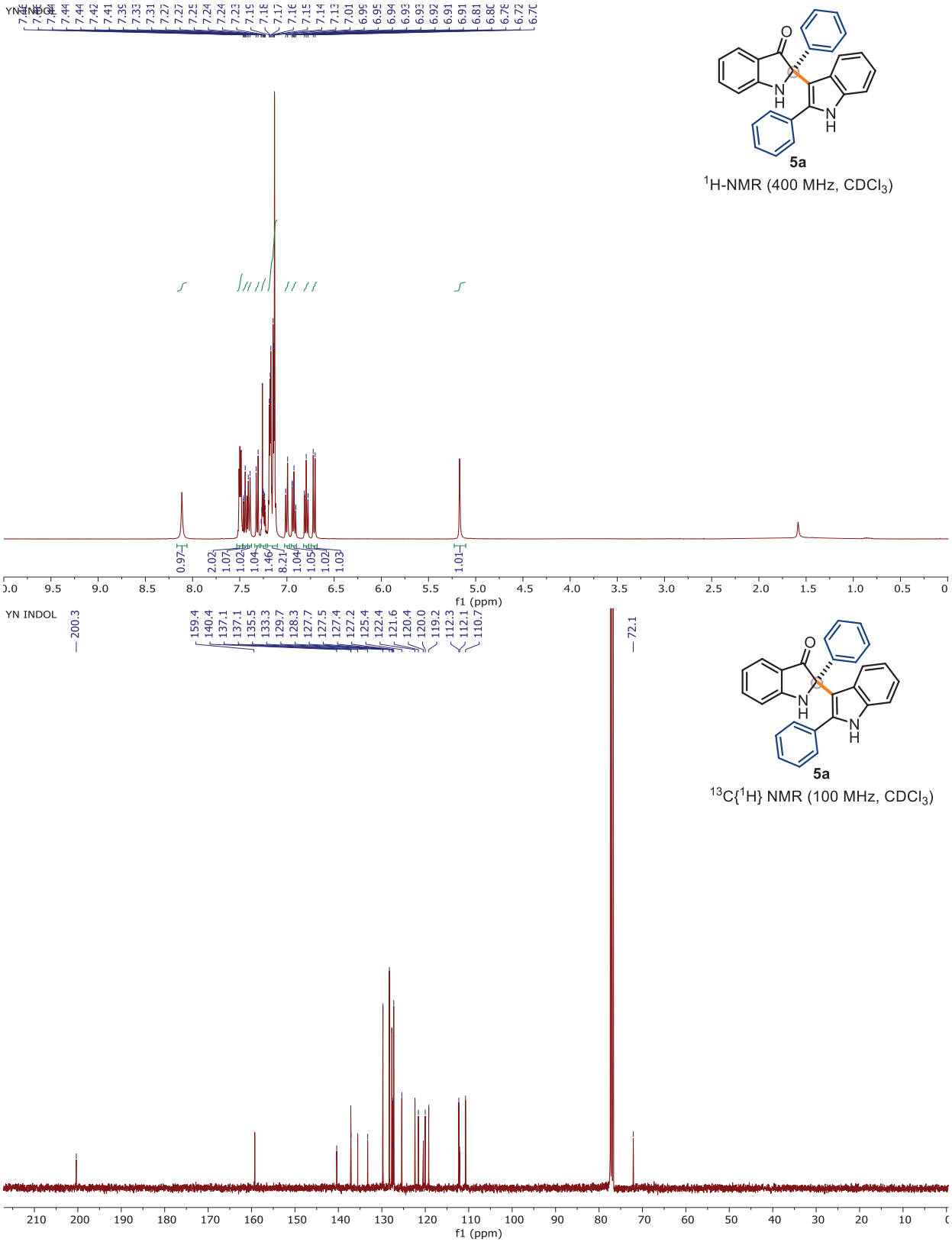

Figure 3.4: ^{1}H and ^{13}C NMR spectra of **5a**

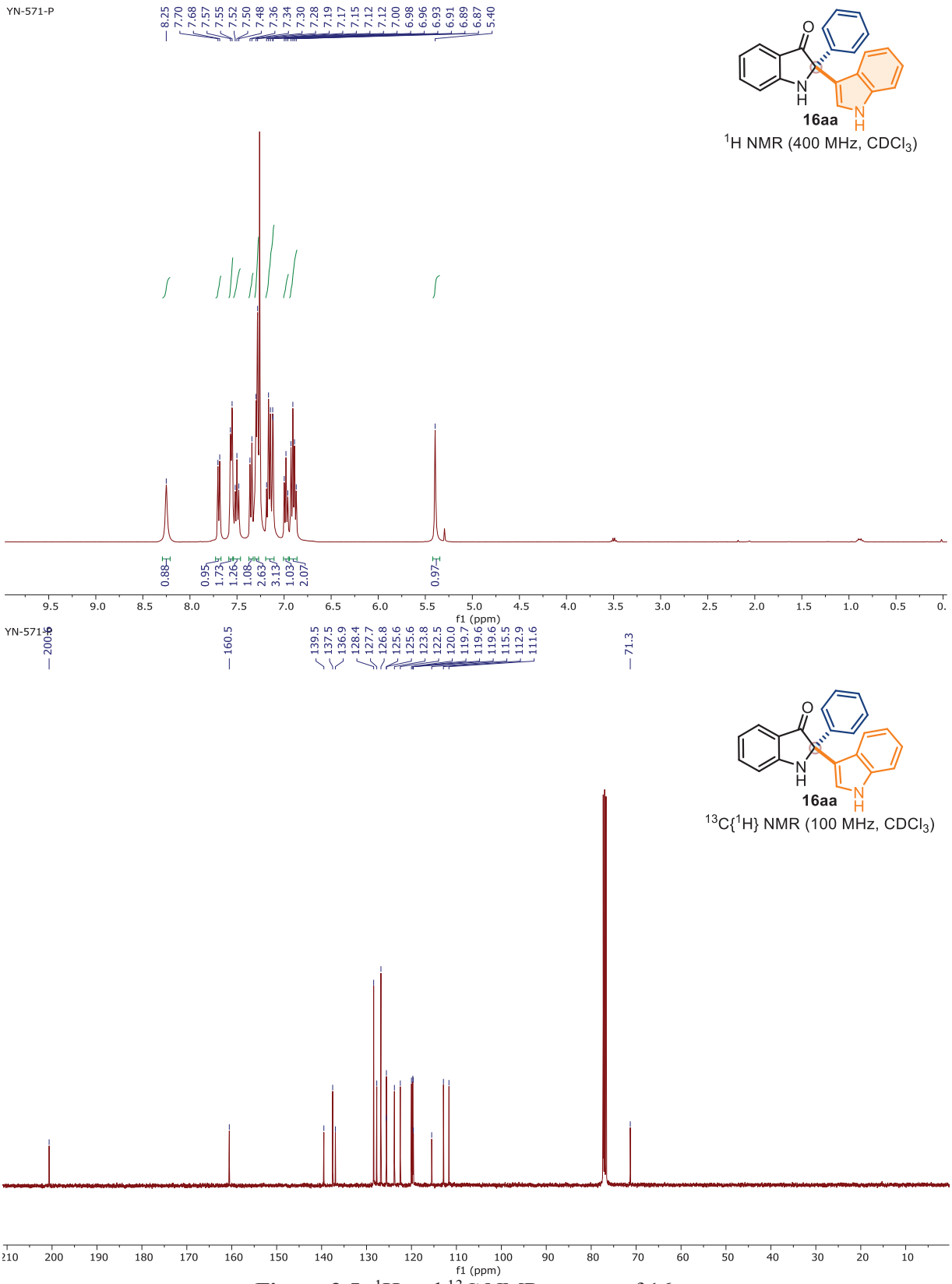

Figure 3.5: ^{1}H and ^{13}C NMR spectra of **16aa**

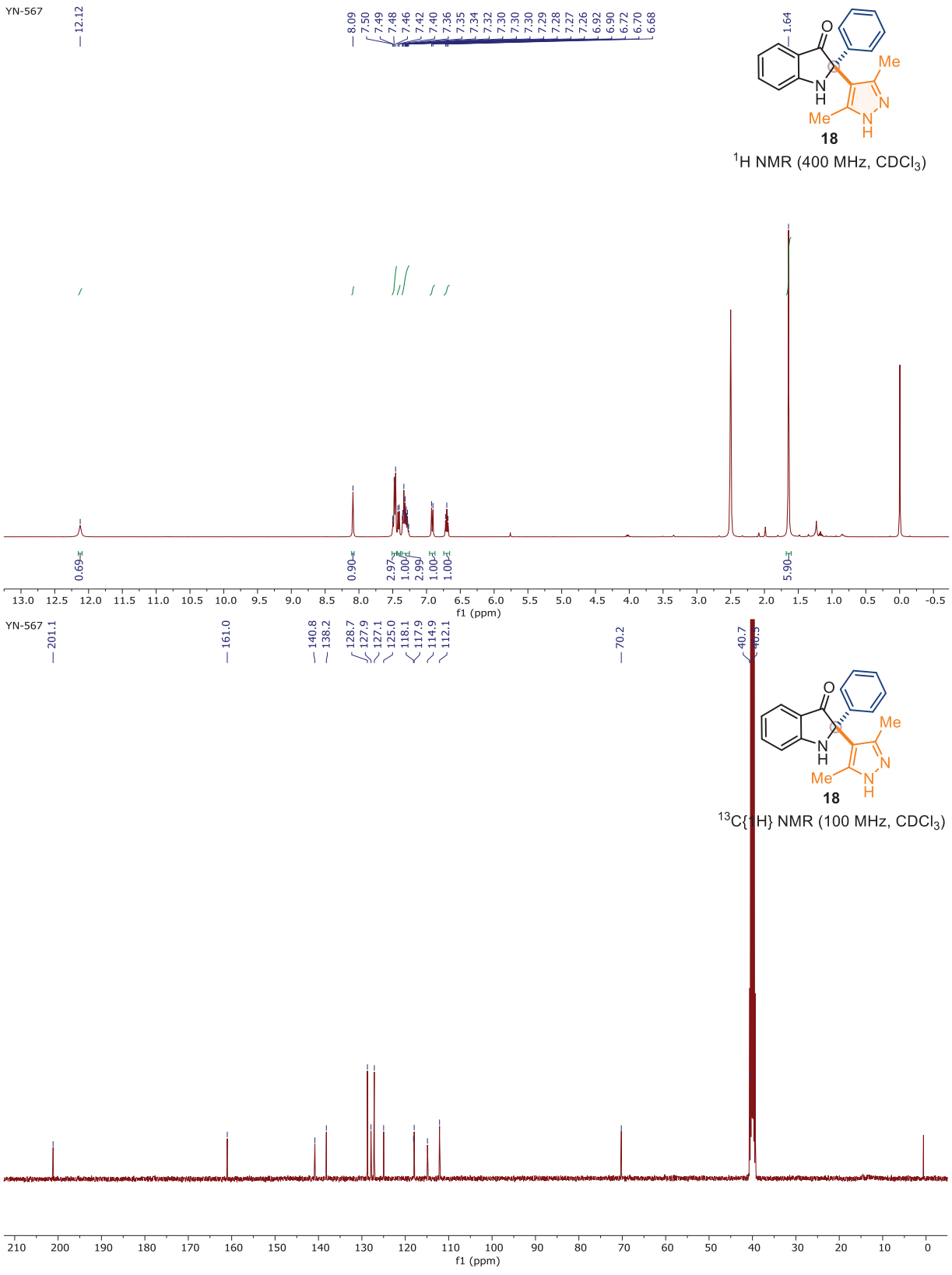

Figure 3.6: ^{1}H and ^{13}C NMR spectra of **18**

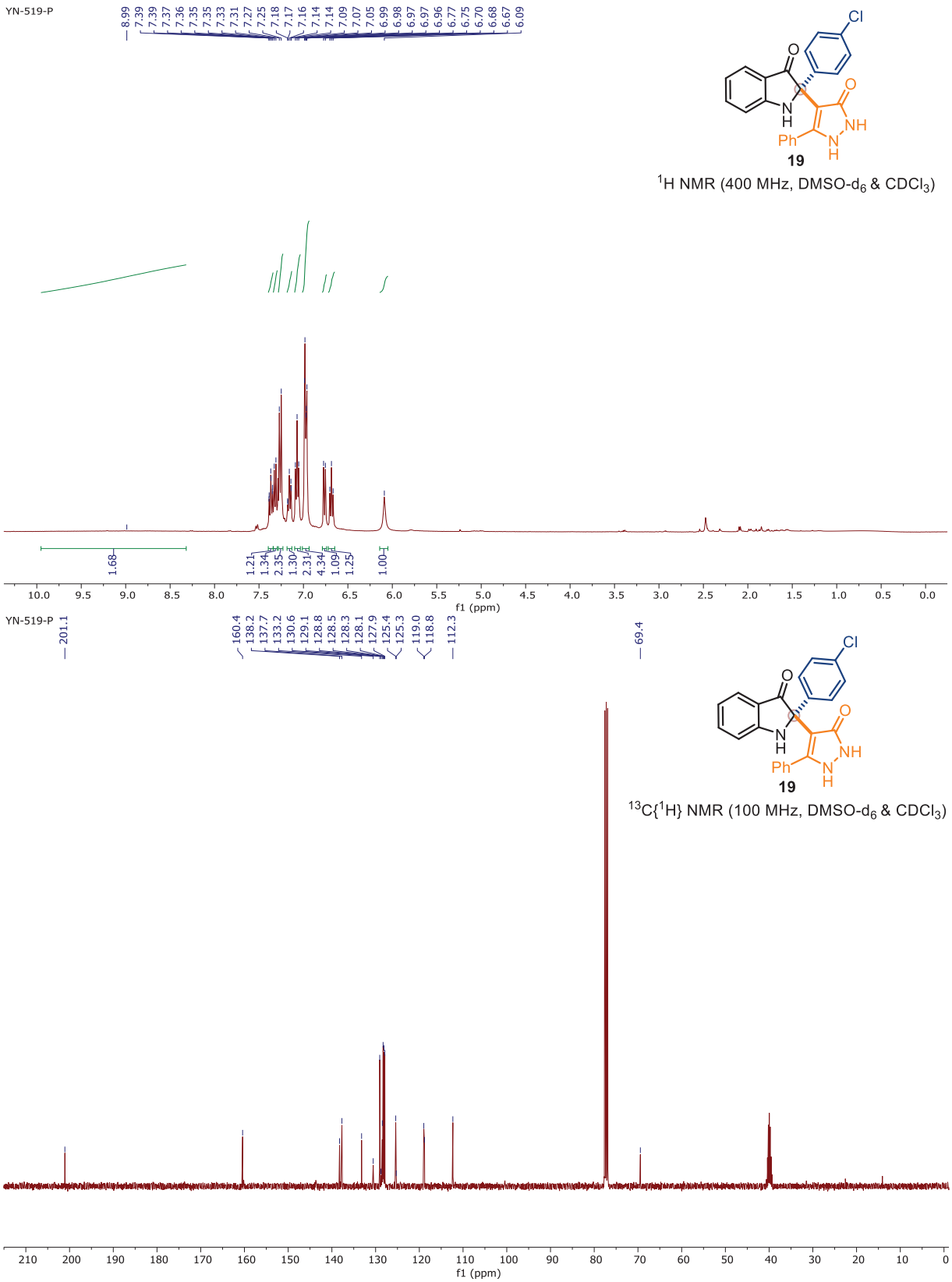

Figure 3.7: ^{1}H and ^{13}C NMR spectra of **19**

3.8 Single crystal X-ray diffraction experiment and analysis

3.8.1 Single crystal XRD experiments for (16ah):

The single crystal XRD data collection and data reduction were performed using CrysAlis PRO on a single crystal Rigaku Oxford XtaLab Pro Kappa dual home/near diffractometer. The crystals were kept at 93(2) K during data collection using CuKα (λ = 1.54184 Å) radiation. Using Olex2[1], the structure was solved with the ShelXT[2] structure solution program using Intrinsic Phasing and refined with the ShelXL[3] refinement package using Least Squares minimisation.

3.8.2 Single crystal structure, Cell parameters, and Structure data of compound (16ah) [exp_972_IK_YN-373_autored]

Single crystals of compound **16ah** $C_{26}H_{23}NO_4$ was obtained as brown blocks through the slow evaporation of (ethyl acetate + hexane) solvent mixture solution at room temperature. The compound **16ah** crystallized in a monoclinic, $P2_1/c$ space group with the following unit cell parameters: $C_{26}H_{23}NO_4$ (M =413.45 g/mol): monoclinic, space group $P2_1/c$ (no. 14), a = 9.86960(10) Å, b = 12.08520(10) Å, c = 18.1457(2) Å, β = 96.2890(10)°, V = 2151.32(4) Å^3, Z = 4, T = 93(2) K, μ(Cu Kα) = 0.696 mm^{-1}, *Dcalc* = 1.277 g/cm^3, 13553 reflections measured (8.808° ≤ 2Θ ≤ 159.594°), 4519 unique (R_{int} = 0.0361, R_{sigma} = 0.0379) which were used in all calculations. The final R_1 was 0.0433 (I > 2σ(I)) and wR_2 was 0.1215 (all data). The complete crystal structure and refinement information is deposited into the Cambridge Crystallographic Data Centre (**CCDC 2167742**) (**Table 3.5**). One molecular compound $C_{26}H_{23}NO_4$ appeared in an asymmetric unit during crystal structure solution, Z'=1. The ORTEP diagram of compound **16ah** and the atom number scheme is given in **Figure 3.8**. The compound obtained and crystallized as enantiomeric mixtures: four molecules (Z=4), two pairs of enantiomers, occupied per unit cell.

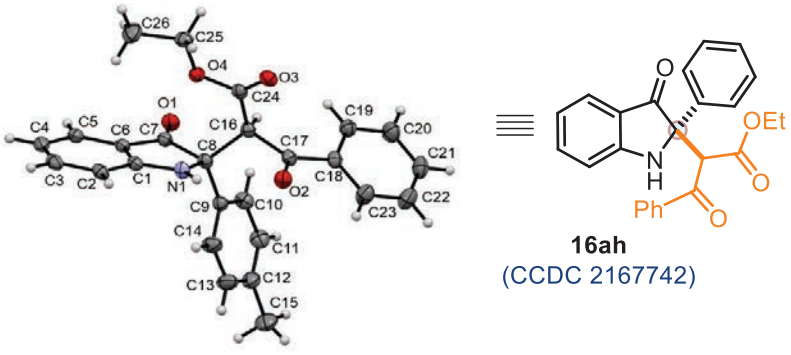

Figure 3.8 ORTEP diagram of compound **16ah** (CCDC **2167742**)

Table 3.5 Crystal data and structure refinement for (16ah) [Exp_972_IK_YN-373_autored.]

Identification code	exp_972_IK_YN-373_autored
Empirical formula	$C_{26}H_{23}NO_4$
Formula weight	413.45
Temperature/K	93(2)
Crystal system	monoclinic
Space group	$P2_1/c$
a/Å	9.86960(10)
b/Å	12.08520(10)
c/Å	18.1457(2)
α/°	90
β/°	96.2890(10)
γ/°	90
Volume/Å^3	2151.32(4)
Z	4
ρ_{calc}g/cm^3	1.277
μ/mm^{-1}	0.696
F(000)	872.0
Crystal size/mm^3	0.35 × 0.12 × 0.07
Radiation	Cu Kα (λ = 1.54184)
2Θ range for data collection/°	8.808 to 159.594
Index ranges	$-10 \leq h \leq 11$, $-14 \leq k \leq 14$, $-23 \leq l \leq 22$
Reflections collected	13553
Independent reflections	4519 [R_{int} = 0.0361, R_{sigma} = 0.0379]
Data/restraints/parameters	4519/0/282
Goodness-of-fit on F^2	1.077
Final R indexes [I>=2σ (I)]	R_1 = 0.0433, wR_2 = 0.1193
Final R indexes [all data]	R_1 = 0.0458, wR_2 = 0.1215

Largest diff. peak/hole / e $Å^{-3}$	0.25/-0.26

3.9 References

1. Kato, H.; Yoshida, T.; Tokue, T.; Nojiri, Y.; Hirota, H.; Ohta, T.; Williams R. M.; Tsukamoto, S. Notoamides A–D:. *Angew. Chem. Int. Ed*. **2007**, *46*, 2254–2256.
2. Steven A.; Overman, L. E. *Angew. Chem., Int. Ed*. **2007**, *46*, 5488–5508.
3. Wu, W.; Xiao, M.; Wang, J.; Li, Y.; Xie, Z. *Org. Lett*. **2012**, *14*, 1624–1627.
4. Lee, J.; Panek, J. S. Total Synthesis of (+)-Isatisine A. *Org. Lett*. **2011**, *13*, 502–505.
5. S. Arai, M. Nakajima and A. Nishida. *Angew. Chem., Int. Ed*. **2014**, *53*, 5569–5572.
6. Liu, J.-F.; Jiang, Z.-Y.; Wang, R.-R.; Zeng, Y.-T.; Chen, J.-J.; Zhang, X.-M.; Ma, Y.-B. Isatisine A. *Org. Lett.* **2007**, *9*, 4127–4129.
7. Li, Y.-J.; Yan, N.; Liu, C.-H.; Yu, Y.; Zhao, Y.-L. *Org. Lett*. **2017**, *19*, 1160–1168.
8. Abe, T.; Kukita, A.; Akiyama, K.; Naito, T.; Uemura. D. *Chem. Lett.* **2012**, *41*, 728–729.
9. Lee, J. H.; So, J.-H.; Jeon, J. H.; Choi, E. B.; Lee, Y.-R.; Chang, Y.-T.; Kim, C.-H.; Bae, M. A.; Ahn, J. H. *Chem. Commun*. **2011**, *47*, 7500–7502.
10. Wyrembak P. N.; Hamilton, A. D. *J. Am. Chem. Soc*. **2009**, *131*, 4566-4567.
11. Matsumoto, S.; Samata, D.; Akazome M.; Ogura, K. *Tetrahedron Lett*. **2009**, *50*, 111–114.
12. For a review article see; Chenga, D.-J.; Shao, Y.-D. *Adv. Synth. Catal*. **2018**, *360*, 3614–3616.
13. Liu, Y.; McWhorter, W. W. Jr. *J. Org. Chem.* **2003**, *68*, 2618–2622.
14. Li, L.; Han, M.; Xiao, M.; Xie, Z.; *Synlett* **2011**, *12*, 1727–1730.
15. Rueping, M.; Raja, S.; Núñez A. *Adv. Synth. Catal*. **2011**, *353*, 563–568.
16. Rueping, M; Rasappan, R.; Raja, S. *Helvetica Chimica Acta*, **2012**, *95*, 2296–2303.
17. Rueping, M.; Raja, S.; *Beilstein J. Org. Chem*. **2012**, *8*, 1819–1824.
18. Parra, A.; Alfaro, R.; Marzo, L.; Moreno-Carrasco, A.; García Ruano, J. L.; Alemán, J. *Chem. Commun*. **2012**, *48*, 9759–9761.
19. Nakamura, S.; Matsuda, N.; Ohara, M. *Chem.–Eur. J*. **2016**, *22*, 9478–9482.
20. Li, J.-S.; Liu, Y.-J.; Li, S.; Ma, J.-A. *Chem. Commun*. **2018**, *54*, 9151–9154.
21. Yuan, X.; Wu, X.; Zhang, P.; Peng, F.; Liu, C.; Yang, H.; Zhu, C.; Fu, H. *Org. Lett*. **2019**, *21*, 2498–2501.

22. Yuan, X.; Wu, X.; Peng, F.; Yang, H.; Zhub, C.; Fu, H. *Chem Commun.* **2020**, *56*, 12648.
23. Zhang, Q.-X.; Li, Y.; Wang, J.; Yang, C.; Liu, C.-J.; Li, X.; Cheng, J.-P. *Angew. Chem. Int. Ed*. **2020**, *59*, 4550–4554.
24. An, J.-X.; Yang, F.-F.; Wang, P.; Gu, Z.-C.; Li, Y.; Chen, L.; Zhao, Y.-L.; He, B. *RSC Adv.* **2022**, *12*, 7040–7043.
25. Sang, P.; Xie, Y.; Zou, J.; Zhang, Y. *Adv. Synth. Catal*. **2012**, *354*, 1873–1875.
26. Kong, Y.-B.; Zhu, J.-Y.; Chen, Z.-W.; Liu, L.-X. *Can. J. Chem.* **2014**, *92*, 269–272.
27. Lin, F.; Chen, Y.; Wang, B.; Qin, W.; Liu, L. *RSC Adv.* **2015**, *5*, 37018–37022.
28. Guchhait, S. K.; Chaudhary, V.; Rana, V. A.; Priyadarshani, G.; Kandekar, S.; Kashyap, M. *Org. Lett*. **2016**, 18, 1534–1536.
29. Kong, L.; Wang, M.; Zhang, F.; Xu, M.; Li, Y. *Org. Lett*. **2016**, *18*, 6124–6126.
30. Zhou, X.-Y.; Chen, X.; Wang, L.-G.; Yanga, D.; Li, J.-H. *Synlett* **2018**, *29*, 835–837.
31. Ding, X.; Dong, C.-L.; Guan, Z.; He, Y.-H. *Angew. Chem. Int. Ed*. **2019**, *58*, 118–124.
32. Jiang, X.; Zhu, B.; Lin, K.; Wang, G.; Su, W.-K.; Yu, C. *Org. Biomol. Chem*. **2019**, *17*, 2199–2203.
33. Liu, X.; Yan, X.; Yu, J.-H.; Tang, Y.; Wang, K.; Zhang, H. *Org. Lett*. **2019**, *21*, 5626–5629.
34. Liu, X.; Yan, X.; Tang, Y.; Jiang, C.-S.; Yu, J.-H.; Wang, K.; Zhang, H. *Chem. Commun*. **2019**, *55*, 6535–6538.
35. Singh, A.; Vanaparthi, S.; Choudhary, S.; Krishnan, R.; Kumar, I. *RSC Adv.* **2019**, *9*, 24050–24056.
36. Zhou, X.-Y.; Chen, X. *Can. J. Chem.* **2020**, *98*, 667–669.
37. Dong, C.-L.; Ding, X.; Huang, L.-Q.; He, Y.-H.; Guan, Z. *Org. Lett*. **2020**, *22*, 1076–1078.
38. Yan, X.; Tang, Y.-D.; Jiang, C.-S.; Liu, X.; Zhang, H. *Molecules* **2020**, *25*, 419–423.
39. Xu, F.; Smith, M. W. *Chem. Sci*. **2021**, *12*, 13756–13763.
40. Zhao, Y.-L.; An, J.-X.; Yang, F.-F.; Guan, X.; Fu, X.-Z.; Li, Z.-Q.; Wang, D.-P.; Zhou, M.; Yang, Y.-Y.; He, B. *Adv. Synth. Catal.* **2022**, *374*, 1277–1279.
41. Cremer, C.; Patureau, F. W.; *JACS Au* **2022**, *2*, 1318–1323.
42. Higuchi, K.; Sato, Y.; Kojima, S.; Tsuchimochi, M.; Sugiura, K.; Hatori, M.; Kawasaki, T. *Tetrahedron* **2010**, *66*, 1236–1243.
43. Yin Q.; You, S.-L. *Chem. Sci*. **2011**, *2*, 1344–1348.

44. Liu, R.-R.; Ye, S.-C.; Lu, C.-J.; Zhuang, G.-L.; Gaoand J.-R.; Jia, Y.-X. *Angew. Chem. Int. Ed*. **2015**, *54*, 11205–11208.
45. Zhao, Y.-L.; Fei, X.-H.; Tang, Y.-Q.; Xu, P.-F.; Yang, F.-F.; He, B.; Fu, X.-Z.; Yang, Y.-Y.; Zhou, M.; Mao, Y.-H.; Dong, Y.-X.; Li C. *J. Org. Chem*. **2019**, *84*, 8168–8176.
46. Chang, Y.-H.; Peng, W.-L.; Chen, I-C; Hsu, H.-Y.; Wu, Y.-K. *Chem. Commun*. **2020**, *56*, 4660–4663.
47. Xia, Z.; Hu, J.; Gao, Y. Q.; Yao, Q; Xie, W. *Chem. Commun*. **2017**, *53,* 7485–7488.
48. Wetzel, A.; Gagosz, F. *Angew. Chem., Int. Ed*. **2011**, *50*, 7354–7358.
49. Li, N.; Wang, T. Y.; Gong, L. Z.; Zhang, L. *Chem. –Eur. J*. **2015**, *21*, 3585–3588.
50. Liu, R. R.; Ye, S. C.; Lu, C. J.; Zhuang, G. L.; Gao, J. R.; Jia, Y. X. *Angew. Chem., Int. Ed*. **2015**, *54*, 11205–11208.
51. Fu, W.; Song, Q. *Org. Lett*. **2018**, *20*, 393–396.
52. Patel, P.; Ramana, C. V. *Org. Biomol. Chem*. **2011**, *9*, 7327–7334.
53. Zhang, X. X.; Li, P.; Lyu, C.; Yong, W. X.; Li, J.; Pan, X. Y.; Zhu, X. B.; Rao, W. D. *Adv. Synth. Catal*. **2017**, *359*, 4147–4152.
54. Zhang, T.; Qi, Z.; Zhang, X.; Wu, L.; Li, X. *Chem.–Eur. J*. **2014**, *20*, 3283–3288.
55. Mothe, S. R.; Novianti, M. L.; Ayers, B. J.; Chan, P. W. H. *Org. Lett*. **2014**, *16*, 4110–4113.
56. Chen, G.; Wang, Y.; Zhao, J.; Zhang, X.; Fan, X. *J. Org. Chem*. **2021**, *86*, 14652–14662.
57. Goriya, Y.; Ramana, C. V. *Chem. Commun*. **2013**, *49*, 6376–6378.
58. S. Lerch, L.-N. Unkel, and M. Brasholz. *Angew. Chem. Int. Ed*. **2014**, *53*, 6558–6562.
59. Ding, W.; Zhou, Q.-Q.; Xuan, J.; Li, T.- R.; Lu, L.-Q.; Xiao, W.-J. *Tetrahedron Lett*. **2014**, *55*, 4648–4652.
60. Bu, L.; Li, J.; Yin, Y.; Qiao, B.; Chai, G.; Zhao, X.; Jiang, Z. *Asian J*. **2018**, *13*, 2382–2387.
61. Kingston, C.; Palkowitz, M. D.; Takahira, Y.; Vantourout, J. C.; Peters, B. K.; Kawamata, Y.; Baran, P. S. *Acc. Chem. Res*. **2020**, *53*, 72–83.
62. Siu, J. C.; Fu, N.; Lin, S. *Acc. Chem. Res*. **2020**, *53*, 547–560.
63. Pollok, D.; Waldvogel, S. R. *Chem. Sci*. **2020**, *11*, 12386–12400.
64. Zhu, C.; Ang, N. W. J.; Meyer, T. H.; Qiu, Y.; Ackermann, L. *ACS Cent. Sci*. **2021**, *7*, 415–431.
65. Yuan, Y.; Yang, J.; Lei, A. *Chem. Soc. Rev*. **2021**, *50*, 10058–10086.

66. C. A. Malapit, M. B. Prater, J. R. Cabrera-Pardo, M. Li, T. D. Pham, T. P. McFadden, S. Blank, S. D. Minteer. *Chem. Rev*. **2022**, *122*, 3180–3218.
67. R. Francke, R. D. Little. *Chem. Soc. Rev*. **2014**, *43*, 2492–2521.
68. Waldvogel, S. R.; Lips, S.; Selt, M.; Riehl, B.; Kampf, C. J. *Chem. Rev*. **2018**, *118*, 6706–6765.
69. Ye, Z.; Ding, M.; Wu, Y.; Li, Y.; Hua, W.; Zhang, F. *Green Chem*. **2018**, *20*, 1732–1734.
70. Morofuji, T.; Shimizu, A.; Yoshida, J. I. *J. Am. Chem. Soc*. **2014**, *136*, 4496–4499.
71. Lu, F.-Y.; Chen, Y.-J.; Chen, Y.; Ding, X.; Guan, Z.; He, Y.-H. *Chem. Commun*. **2020**, *56*, 623–626.
72. Long, C.-J.; Cao, H.; Zhao, B.-K.; Tan, Y.-F.; He, Y.-H.; Huang, C.-S.; Zhi Guan, Z. *Angew Chem. Int. Ed*. **2022**, *61*, e202203666.
73. The X-ray crystallographic structure for **16ah** has been deposited at the Cambridge Crystallographic Data Centre (CCDC), under deposition number CCDC 2167742.
74. Slätt, J.; Bergman, J. *Tetrahedron* **2002**, *58*, 9187–9191.
75. Dolomanov, O.V., Bourhis, L.J., Gildea, R.J, Howard, J.A.K. & Puschmann, H. (**2009**), *J. Appl. Cryst.* 42, 339–341.
76. Sheldrick, G.M. (**2015**). *Acta Cryst*. A71, 3–8.

CHAPTER 4

Electrochemical Synthesis of 2-Aryl-3-(2-aminoaryl)quinoxalines via Oxidative Dearomatization/Ring-Opening/Cyclization Cascade Sequence of 2-Arylindoles with 1,2-Diaminoarenes

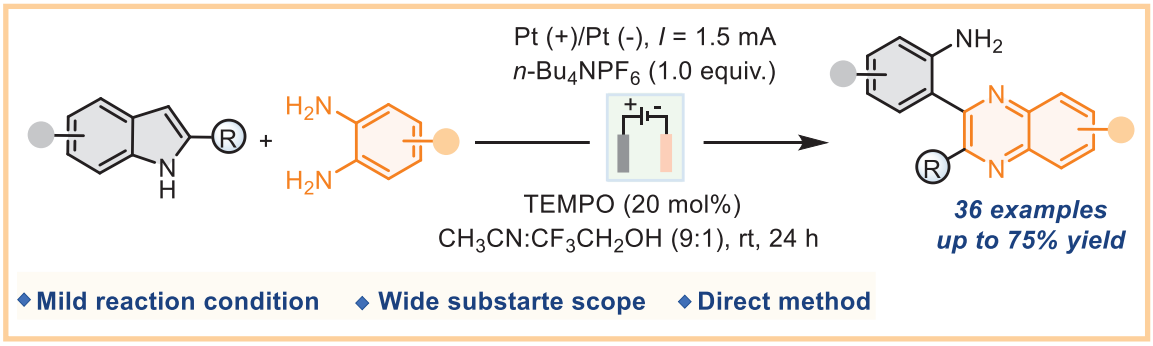

4.1 Introduction

Quinoxaline unit is an essential class of nitrogen-containing scaffolds commonly used in many areas of modern research, from drug discovery to material science. This versatile structure can be used to develop a wide range of products, from kinase inhibitors to antimicrobial agents and other bioactive compounds **(Figure 4.1)**.[1-6]

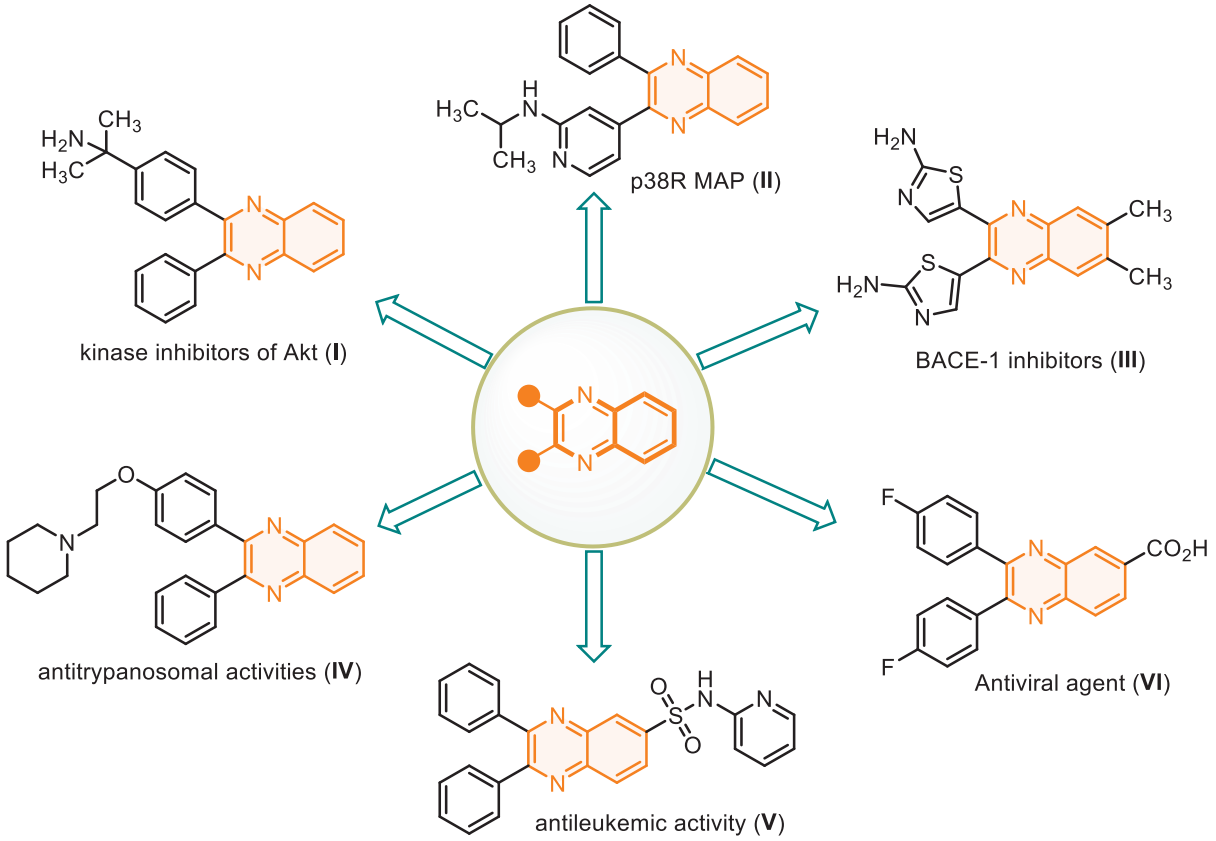

Figure 4.1 Selected bioactive compounds with the quinoxaline unit

Besides, the quinoxaline unit displayed a substantial role in DNA-cleaving agents,[7-8] and functional materials applications.[9-10] Consequently, several methods have been developed for synthesizing quinoxalines;[11-14] however, the condensation reaction between 1,2-phenylenediamines and 1,2-diketones is the most straightforward and explored method to access this unit.[15-19] Besides, condensation between 1,2-phenylenediamines and 1,2-diketones surrogates such as 1,2-diols,[20-23] α-hydroxy ketones,[24-25] α-haloketones,[26-30] or alkynes,[31-36] along with other methods.[37-38] However, these methods are practically tedious and provide poor regioselectivity during isomeric product formation with elaborately designed and unsymmetrically substituted reactants. Thus, developing more general and regioselective access

to quinoxalines is highly required.

4.2 General approach for the synthesis of quinoxaline

In this context, Hansen and co-workers developed a catalyst-free protocol for the synthesis of quinoxalines **(3)** via the classical cyclocondensation reaction between aryldiamines **(2)** and dicarbonyl compounds **(1) (Scheme 4.1)**. This transformation provides a novel route for accessing fused nitrogen-containing heterocycles. The cyclocondensation occurs fast under straightforward reaction conditions in medium to excellent chemical yields. In this reaction, methanol as solvent typically proceeds at room temperature, open to air, and with only 1 minute reaction time.[15]

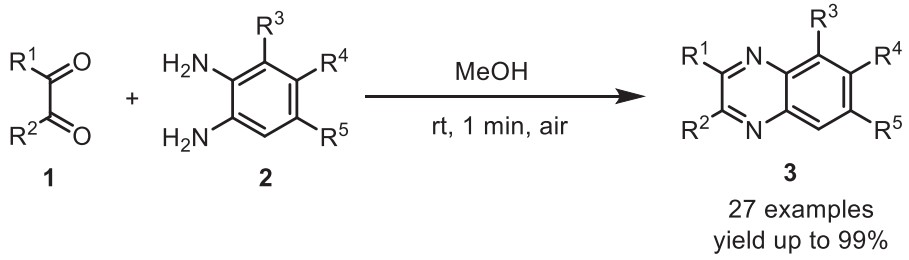

Scheme 4.1 Catalyst-free one-minute synthesis of quinoxalines

Domingo's group reported the ammonium bifluoride catalyzed cyclocondensation of 1,2-arylene-diamines **(4)** with 1,2-dicarbonyl compounds **(1)** at room temperature in methanol/water to desired product quinoxalines or pyrido[2,3-b]pyrazines **(5)** in excellent yields **(Scheme 4.2)**. Importantly, 2,8-disubstituted quinoxalines and 3-substituted pyrido[2,3-b]pyrazines were regioselectively formed by the reaction of arylglyoxals with 3-methylbenzene-1,2-diamine or pyridine-2,3-diamine respectively.[16]

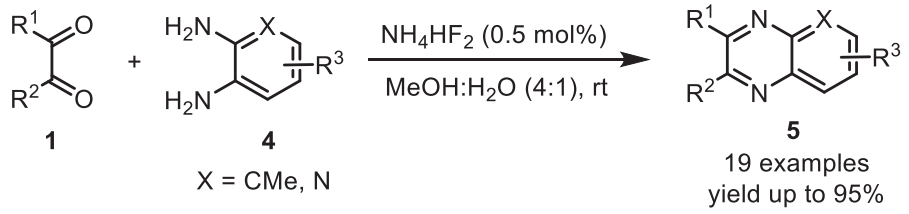

Scheme 4.2 Ammonium bifluoride catalyzed synthesis of quinoxalines

In 2008, Zhang and co-workers developed a Gallium(III) triflate-catalyzed reaction of phenylene-1,2-diamines **(7)** and 1,2-diketones **(6)** to produce quinoxalines **(8)** in excellent to quantitative yields **(Scheme 4.3)**. The reactions proceed with 1 mol % of Gallium(III) triflate in ethanol at room temperature. The catalyst can be recycled at least ten times.[17]

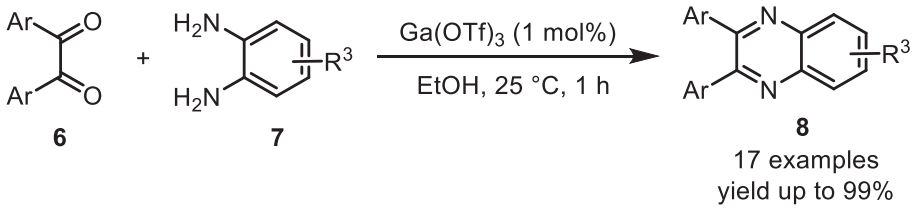

Scheme 4.3 Gallium(III) triflate catalyzed synthesis of quinoxalines

More *et al.* disclosed a simple, efficient, and eco-friendly method for the synthesis of quinoxalines **(9)** from various 1,2-diketones **(1)** and 1,2-diamines **(7)** using cheap and readily available CAN as a catalyst **(Scheme 4.4)**. This protocol shows high reaction rates, excellent product yields, and simple filtration, making this methodology an alternative platform to the conventional acid/base-catalyzed thermal processes. Still, it also becomes significant under environmentally greener and safer methods.[18]

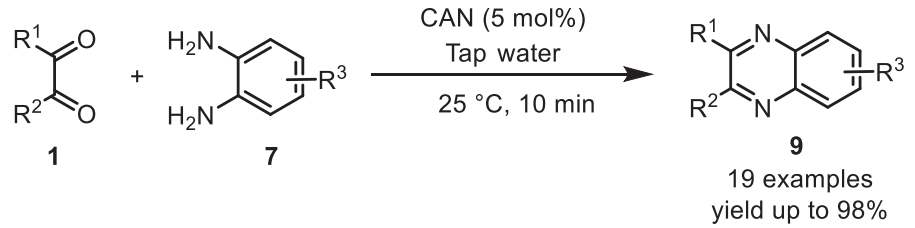

Scheme 4.4 Cerium (IV) ammonium nitrate catalyzed synthesis of quinoxalines

Petrini's group reported synthetic approaches for the quinoxalines **(9)**. The utilization of the NADES, ChCl/water (1 : 3.3), provides a remarkable green medium, enabling the fast activation of reactants and easy recovery of products to avoid further purification. This procedure has been utilized for the preparation of simple as well as functionalized quinoxalines embedding acetal protecting groups, which are unaffected by the reaction conditions (**Scheme 4.5**).[19]

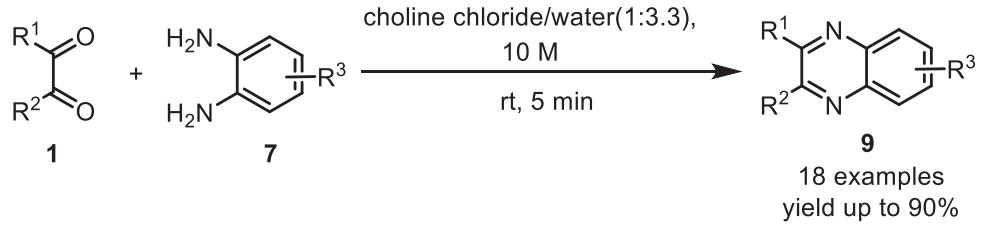

Scheme 4.5 Natural deep eutectic solvent (NADESs) promoted the synthesis of quinoxalines

4.2.1 Quinoxaline synthesis from 2-arylindoles

2-Arylindoles are central structural motifs in many pharmaceutically active compounds.[39] Due to the inherent electron-richness of 2-arylindoles, oxidative-dearomative ring-opening

transformations with different nucleophiles have recently been studied to access several heteroaromatic compounds.[40-46] Yan et al. recently developed an interesting approach for synthesizing 2,3-diarylquinoxalines **(12)** through NIS-mediated ring opening of 2-arylindoles **(10)** with 1,2-diamino benzenes **(11)** (**Scheme 4.6**). The key to this tandem reaction was the formation of 3-iodoindoles, which underwent Kornblum-type oxidation with DMSO to generate active 2-arylindole-3-ones. The active imines were captured *in situ* by 1,2-diaminoarenes to construct diverse quinoxalines. The protocol featured a broad range of tolerant functional groups and mild reaction conditions.[47]

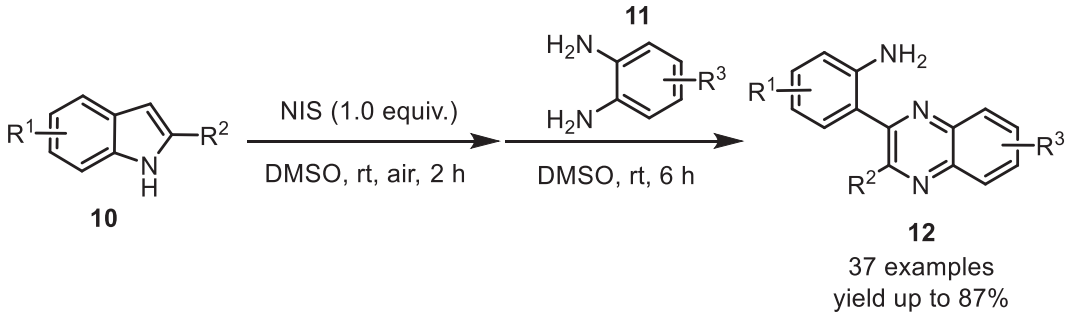

Scheme 4.6 NIS-mediated direct access to 2-aryl-3-(2-aminoaryl)quinoxalines

Besides, electrochemical organic transformations that use electrons as reagents for oxidative/reductive conversion and an excellent functional group tolerance under benign conditions have recently been influential in expanding modern organic synthesis.[48-53] Developing an environmentally benign organic-electrosynthesis approach for constructing privileged heterocycles has become a fascinating goal for synthetic chemists. In this direction, few electrochemical oxidative-dearomative transformations of 2-arylindoles have been developed; however, they are mainly limited to accessing 2,2-disubstituted indolin-3-ones.[54-56] Thus, developing an electrochemical method to synthesize 2,3-diarylquinoxalines via oxidative-dearomative conversions of 2-aryl indole will be highly interesting. This chapter presents our unprecedented results in synthesizing 2-aryl-3-(2-aminoaryl) quinoxalines **(12)** from 2-arylindoles **(10)** and 1,2-diaminoarenes **(11)** under mild electrochemical conditions. The reaction proceeds through *in situ* generations of 2-arylindole-3-ones under electrochemical oxidative dearomatization of 2-arylindoles, followed by a ring opening-cyclization sequence with 1,2-diaminoarenes **(Scheme 4.7).**

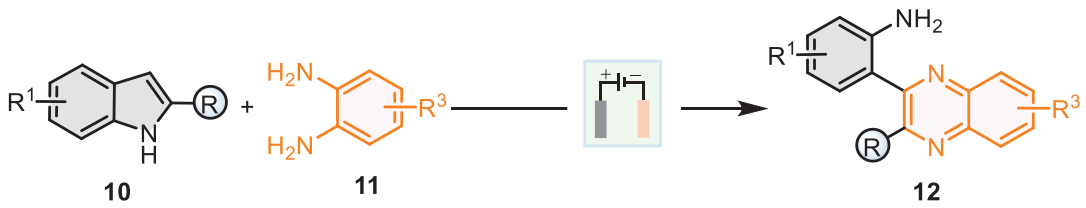

Scheme 4.7 Direct electrochemical synthesis of 2-aryl-3-(2-aminoaryl)quinoxalines

4.3 Results and discussion

We initiated our study for electrochemical oxidative dearomatization followed by a ring opening-cyclization sequence with 2-phenyl indole **10a** and o-phenylenediamine **11a** as suitable substrates (Table 4.1). Detailed studies concerning electrodes, electrolytes, catalysts, and solvents were carried out (Table 4.1) and led to the optimal reaction conditions. To our delight, 2-(3-phenylquinoxalin-2-yl)aniline **12aa** was obtained in 75% yield under optimized conditions (entry 1, Table 4.1). The reaction furnishes a trace amount of the product in the absence of TEMPO (entry 2, Table 4.1) and *n*-Bu_4NPF_6 (entry 3, Table 4.1), whereas no **12aa** was observed without current (entry 4, Table 4.1). Next, product **12aa** obtained a 45% yield and 60% when C(+)/C(-) and C(+)/Cu(-) electrodes were used under standard conditions (entries 5-6, Table 4.1). The reaction outcome did not improve either by decreasing (entry 7, Table 4.1) or increasing (entry 8, Table 4.1) the applied current. The product **12aa** was obtained with 63% yields when TEMPO (10 mol%) (entry 9, Table 4.1), whereas a trace amount of product **12aa** was observed with N_2 purging instead of air (entry 10, Table 4.1). Adding 2,6-Lutidine (1.0 equiv.) as a base under standard conditions (entry 11, Table 4.1) and lowering the amount of o-phenylenediamine **11a** (2.0 equiv) (entry 12, Table 4.1) didn't improve the reaction yield. By varying solvent mediums like CH_3CN/H_2O (9:1) and CH_3CN/HFIP (9:1) instead of CH_3CN/CF_3CH_2OH (9:1) (entries 13-14, Table 4.1) and other electrolytes were also tested, such as *n*-Bu_4NBF_4 and *n*-Bu_4NClO_4, but all gave inferior results compared to *n*-Bu_4NPF_6 (entries 15–16, Table 4.1). Therefore, we conducted our experiments under optimum conditions (entry 1, Table 4.1).

Table 4.1 Optimization of the reaction conditions[a]

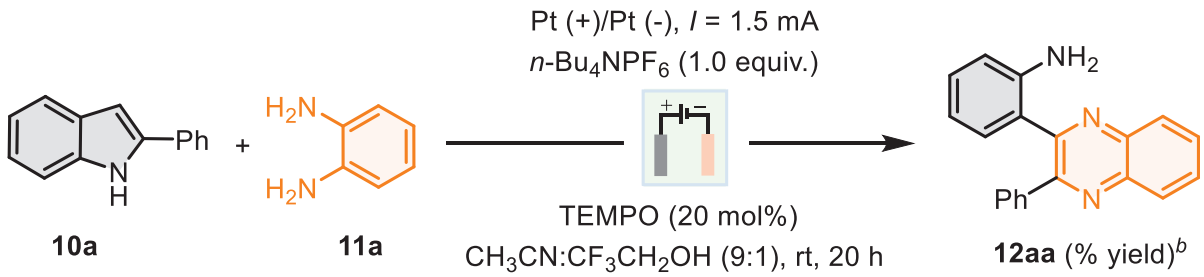

10a **11a** **12aa** (% yield)[b]

Entry	Variation from standard conditions	Yield (%)
1	none	75
2	without TEMPO	<5
3	without *n*-Bu_4NPF_6	<10
4	without current	-
5	C(+)/C(-) used instead of Pt(+)/Pt(-)	45
6	C(+)/Cu(-) used instead of Pt(+)/Pt(-)	60
7	*I* = 1.0 mA, instead of *I* = 1.5 mA	65
8	*I* = 2.0 mA, instead of *I* = 1.5 mA	58
9	TEMPO (10 mol%) instead of (20 mol%)	63
10	N_2 instead of air	<5
11	2,6-lutidine (1.0 equiv)	68
12	**11a** (2.0 equiv) was used	62
13	CH_3CN/H_2O (9:1) used instead of CH_3CN/CF_3CH_2OH (9:1)	58
14	CH_3CN/HFIP (9:1) used instead of CH_3CN/CF_3CH_2OH (9:1)	65
15	*n*-Bu_4NBF_4 (1.0 equiv.) used instead of *n*-Bu_4NPF_6 (1.0 equiv.)	58
16	*n*-Bu_4NClO_4 (1.0 equiv.) used instead of *n*-Bu_4NPF_6 (1.0 equiv.)	45

[a]**Reaction conditions**: **10a** (0.5 mmol, 1.0 equiv), **11a** (1.5 mmol, 3.0 equiv), *n*-Bu_4NPF_6 (0.5 mmol, 1.0 equiv), TEMPO (0.1 mmol, 20 mol%), CH_3CN/CF_3CH_2OH (9:1), Pt(+) | Pt(–), undivided cell, constant current = 1.5 mA, air, rt, 20 h. [b]All isolated yields of **12aa** after column chromatography were based on **10a**.

Having developed the optimized conditions for the electrochemical oxidative dearomatization/addition-cyclization sequence, we examine the method's scope with various 2-arylindoles **10** and o-amino-anilines **11 (Table 4.2)**. Initially, a series of 2-Arylindole **10a-10m** was tested by substituting with electron-withdrawing groups or electron-donating at the C2-aryl ring, producing corresponding products **12aa-12ma** (55-75%) under optimized conditions. When the C2-aryl ring was replaced with naphthyl **10n** and 5-bromo thienyl **10o,** complementary products **12na** (67%) and **12oa** (56%) were obtained, respectively. While having different substitutions at the indole-ring of 2-arylindole also furnished the complementary products **12pa-12ua** (67-74%). Next, we check the generality of 1,2-diaminoarenes **11b-11l** having different substitutions at ortho-, meta- or para-positions with 2-phenyl indole **10a** and furnished related products **12ab-12al** (57-73%) **(Table 4.2)**. In the case of unsymmetrically substituted 1,2-diaminoarenes such as **11b**, **11d**, **11f,** and **11i**, the corresponding regio-isomeric products were also observed as minor products (≤10% yields), whereas in the case of 1,2-diaminoarene **11aj**, an inseparable mixture (2:1) of regioisomeric product **12aj** was obtained.

Later, the developed method was expanded to the cross-combination of 2-arylindoles **10** with other 1,2-diaminoarenes **11**, and related products **12qg-12uk** were obtained with comparable yields (57–72%) **(Table 4.2)**. The single crystal X-ray analysis for compounds **12aa** (CCDC 2258070),[57] **12ag** (CCDC 2258074), **12ak** (CCDC 2258069), and **12al** (CCDC 2258072) confirmed the assigned structures.[58]

Table 4.2 Generality concerning various 2-substituted indoles

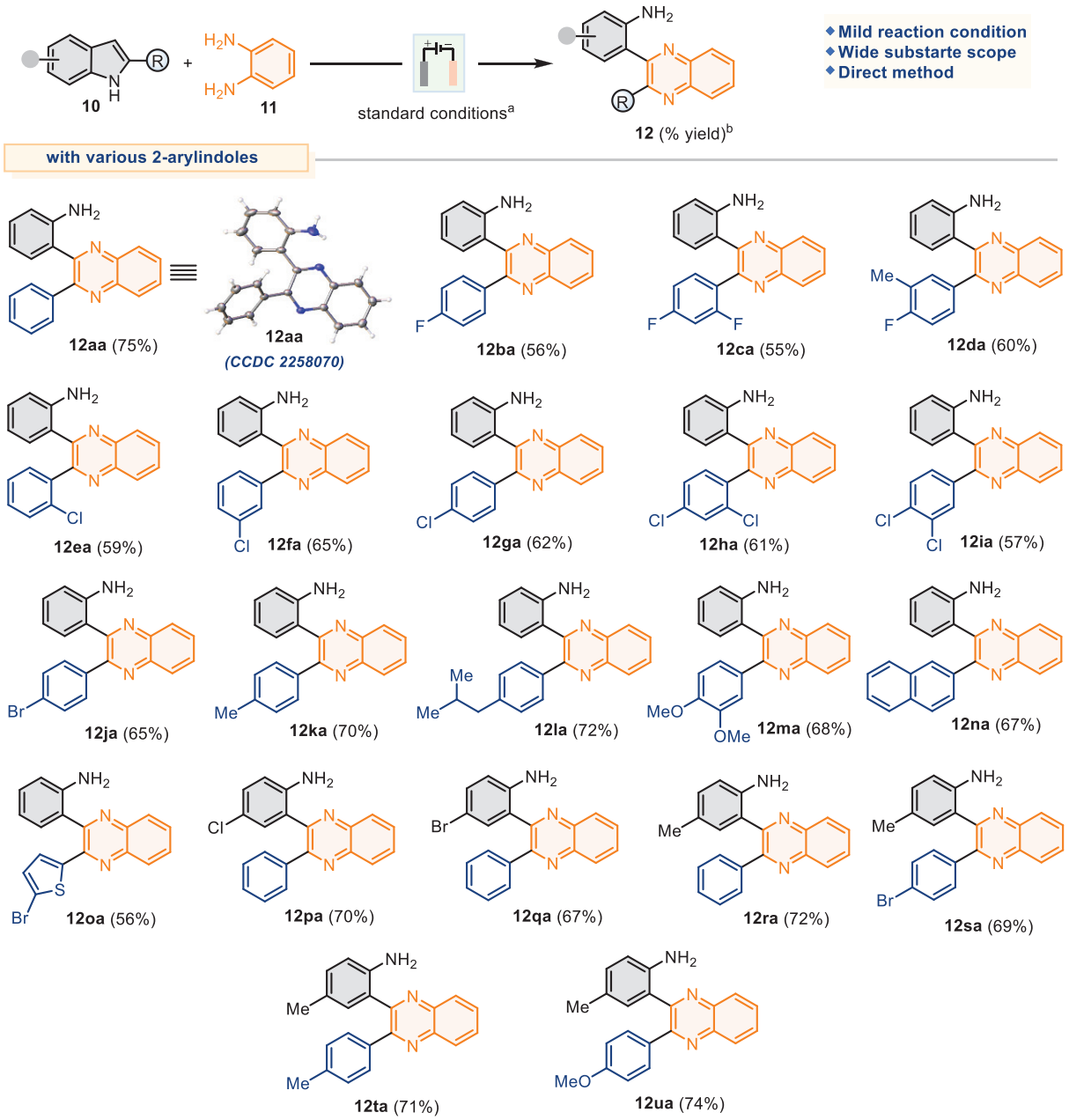

Reaction conditions: 10 (0.5 mmol, 1.0 equiv), **11** (1.5 mmol, 3.0 equiv), *n*-Bu_4NPF_6 (0.5 mmol, 1.0 equiv), TEMPO (0.1 mmol, 20 mol%), CH_3CN/CF_3CH_2OH (9:1), Pt(+) | Pt(–), undivided cell, constant current = 1.5 mA, air, rt, 20-25 h. [b]All isolated yields of **12** were based on **10**.

Table 4.3 Generality concerning various 1,2-diaminobenzene and 2-substituted indoles

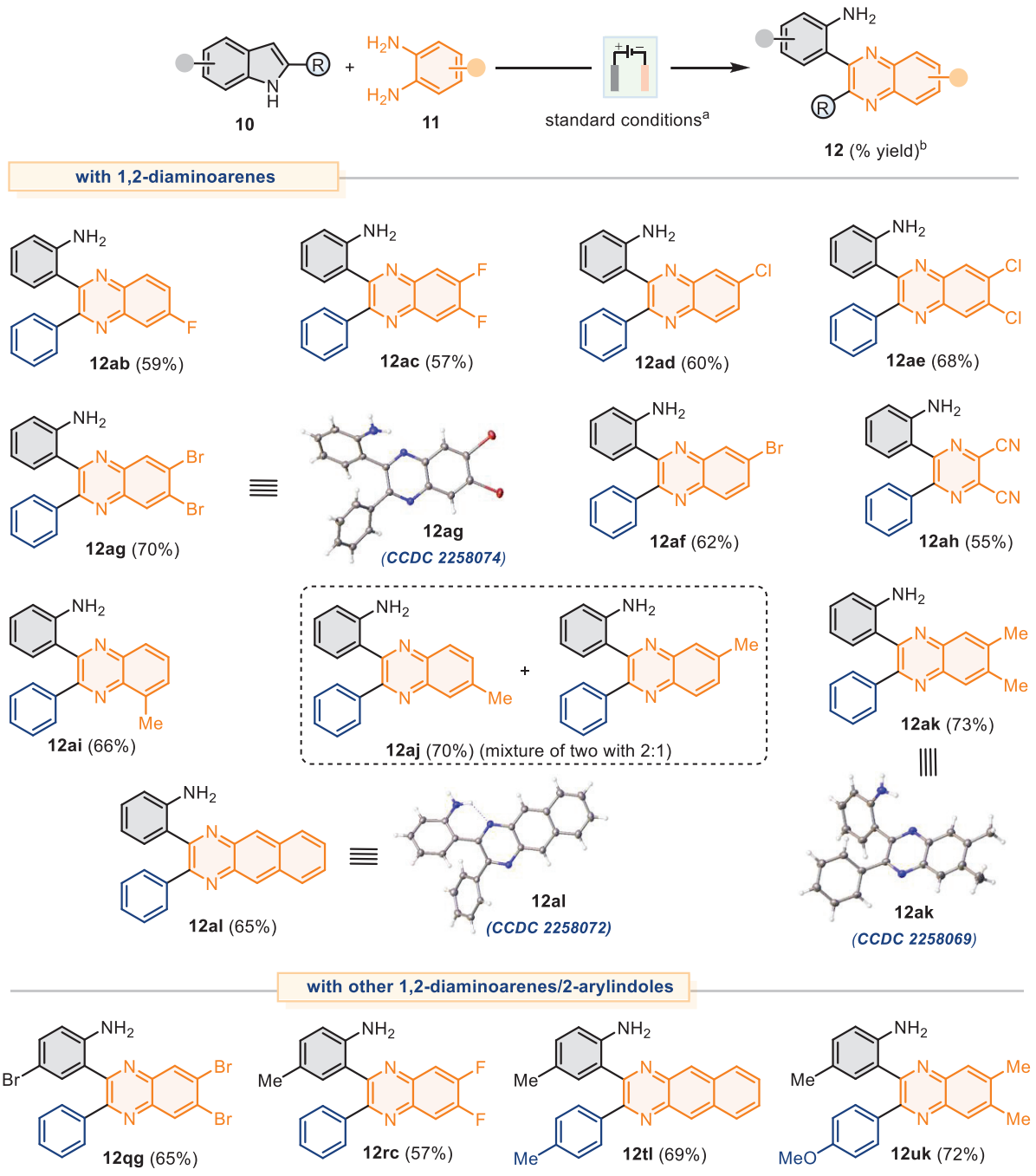

Reaction conditions: 10 (0.5 mmol, 1.0 equiv), **11** (1.5 mmol, 3.0 equiv), *n*-Bu_4NPF_6 (0.5 mmol, 1.0 equiv), TEMPO (0.1 mmol, 20 mol%), CH_3CN/CF_3CH_2OH (9:1), Pt(+) | Pt(–), undivided cell, constant current = 1.5 mA, air, rt, 20-25 h. [b]All isolated yields of **12** were based on **10**.

4.4 Cyclic voltammetry experiment

Cyclic voltammetry (CV) was performed using a three-electrodes cell (glassy carbon as the working electrode, Pt wire as the auxiliary electrode, and Ag/AgCl as reference electrode) in CH_3CN: CF_3CH_2OH (9:1) and *n*-Bu_4NPF_6 (0.02 M solution) as the supporting electrolyte at room temperature. The Ag/AgCl as the reference electrode, and the scan rate was 0.2 V/s, ranging from −1.0 V to +2.0 V. The oxidation potentials for **10a** (E_{ox} = +1.29 V vs Ag/AgCl as reference electrode), TEMPO (E_{ox} = +0.88 V vs Ag/AgCl as reference electrode), and **10a**+**11a**+TEMPO (E_{ox} = +1.12 V vs Ag/AgCl as reference electrode) were measured, respectively, as shown in Figure 4.2. The CV was plotted using the IUPAC convention.

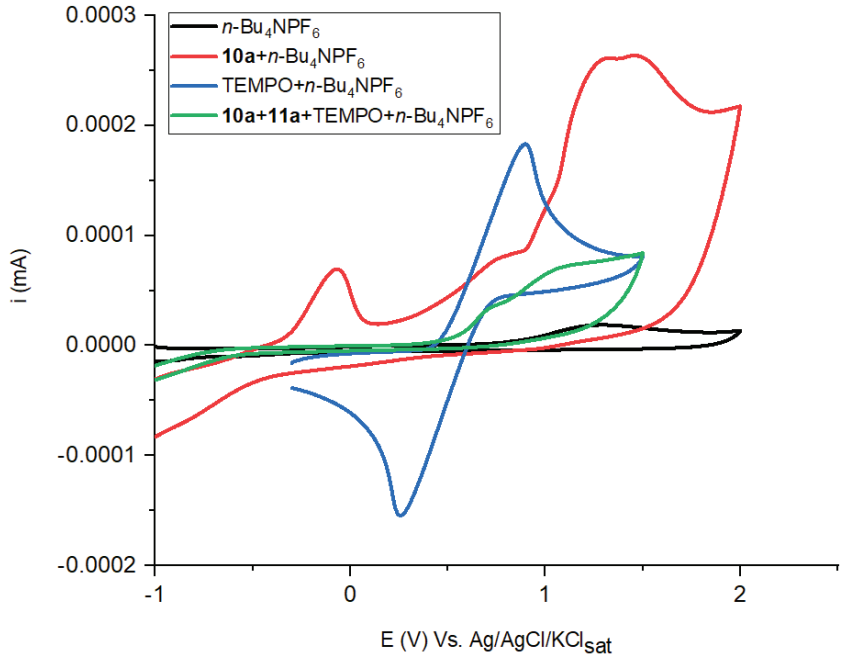

Figure 4.2 Cyclic voltammogram of: CH_3CN/CF_3CH_2OH/*n*-Bu_4NPF_6 (12 mL, 0.02M) (**black**), **10a** (2.0 mM) in CH_3CN/CF_3CH_2OH/*n*-Bu_4NPF_6 (12 mL, 0.02M) (**red**), TEMPO (2.0 mM) in CH_3CN/CF_3CH_2OH/*n*-Bu_4NPF_6 (12 mL, 0.02M) (**blue**), **10a** (2.0 mM), **11a** (2.0 mM), TEMPO (2.0 mM) in CH_3CN/CF_3CH_2OH/*n*-Bu_4NPF_6 (12 mL, 0.02M) (**green**), Reference electrode: Ag/AgCl (3M KCl), scan rate: 0.2 V/s. All experiments have been done at room temperature.

4.5 Control experiments, Reaction mechanism, Synthetic applications

The formation of product **12aa** was not observed with BHT as a radical scavenger under the standard electrochemical conditions, confirming the radical nature of the reaction at the intermediate step (**Scheme 4.8)**.

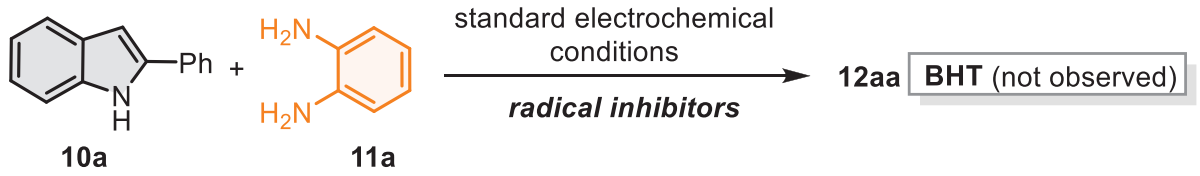

Scheme 4.8: Control experiment

A probable mechanism has been proposed based on our previous work and the available literature (Scheme 4.9). The anodic oxidation of TEMPO generates $TEMPO^+$ and oxidizes 2-arylindole **10** to radical cation **A**. The radical **B** and later **C**, generated through deprotonation of **A**, react with O_2 to create radical **D** and subsequently to radical **E** before generating indole-3-one **F** via the removal of hydroxyl radical. Later, the condensation of intermediate **F** and the 1,2-diaminoarenes **11** via intermediate **G** and **H** eventually generated **12** with an overall indole-ring opening reaction. *In situ* HRMS data also confirmed the formation of intermediate 2-arylindole-3-one F (Ar = Ph).

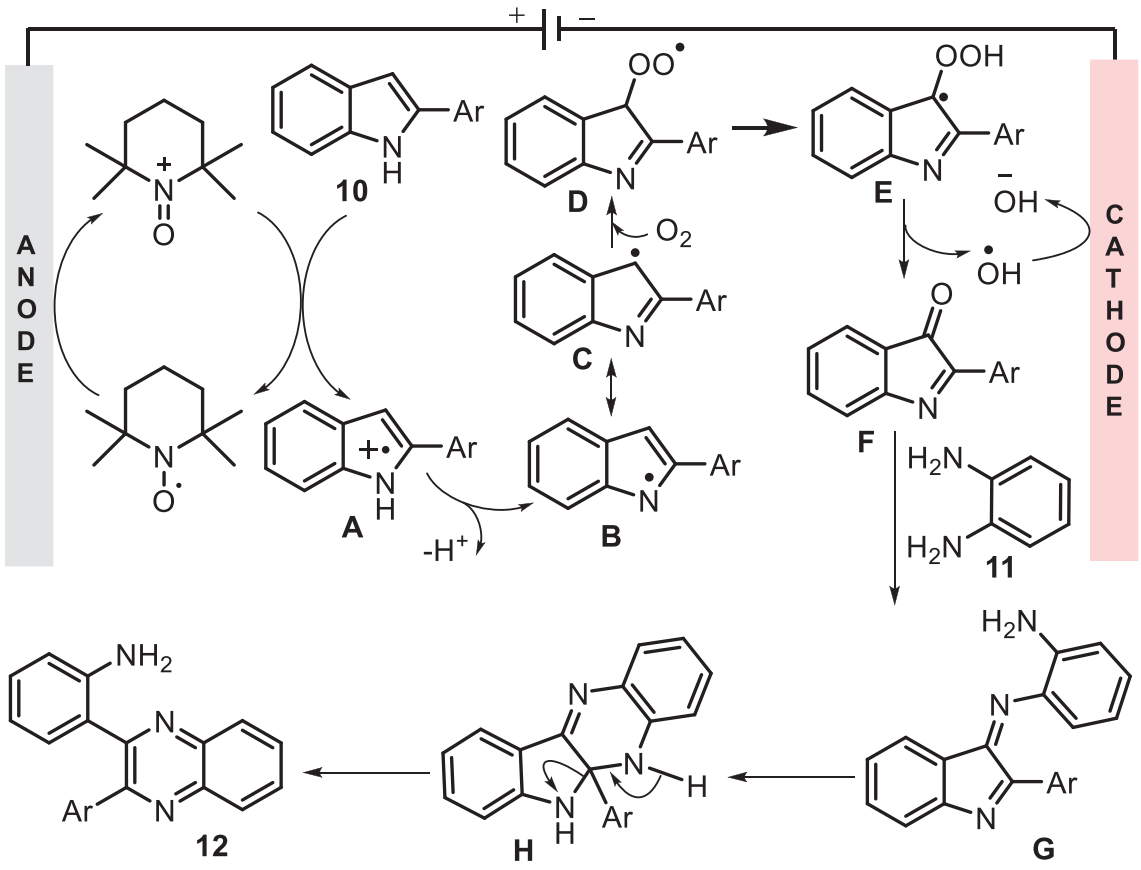

Scheme 4.9: A tentative mechanism for the electrochemical synthesis of 2-Aryl-3-(2-aminoaryl)quinoxalines **12**

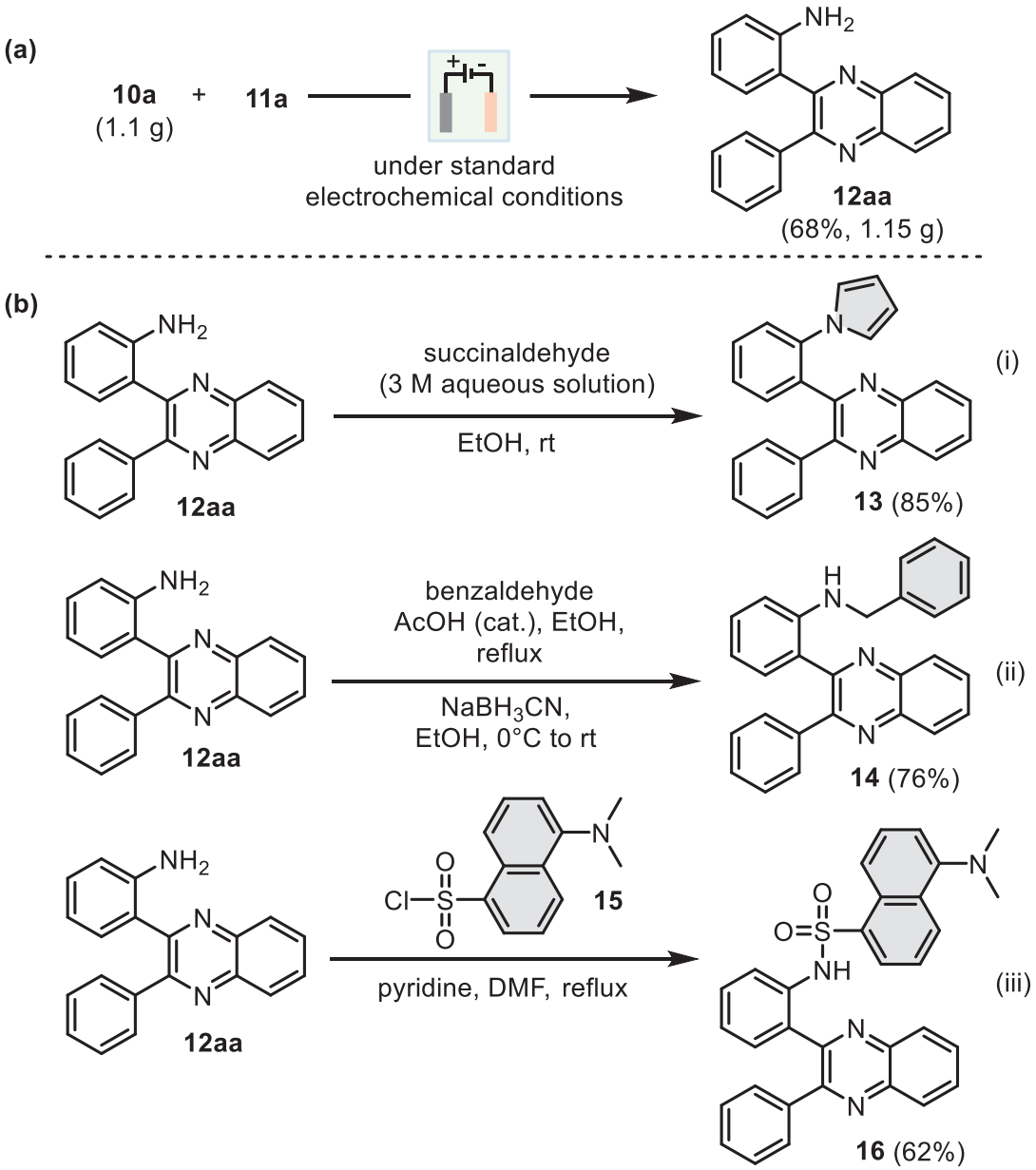

Scheme 4.10: Synthetic applications **(a)** gram-scale synthesis of **12aa**; **(b)** (i) synthesis of 2-(2-(1*H*-pyrrol-1-yl)phenyl)-3-phenyl quinoxaline **13**, (ii) *N*-benzyl-2-(3-phenylquinoxalin-2-yl)aniline **14**, (iii) 5-(dimethylamino)-*N*-(2-(3-phenylquinoxalin-2-yl)phenyl)naphthalene-1-sulfonamide **16**

The synthetic utility of the method was tested at the gram-scale synthesis of compound **12aa** (1.15 g, 68% yield) under optimized conditions (Scheme 4.10a). Next, the Paal-Knorr reaction of **12aa** was performed with aqueous succinaldehyde in ethanol at room temperature to access 2-(2-(1*H*-pyrrol-1-yl)phenyl)-3-phenyl quinoxaline **13** (85% yield) (Scheme 4.10b(i)). The reduction

amination of **12aa** with benzaldehyde was carried out to access *N*-benzyl-2-(3-phenylquinoxalin-2-yl)aniline **14** (76% yield) (Scheme 4.10b(ii)). Furthermore, **12aa** were treated with 5-(dimethylamino)naphthalene-1-sulfonyl chloride, *i.e.*, dansyl chloride in DMF under reflux conditions to furnish corresponding sulfonamide **16** ((62% yield) Scheme 4.10b(iii)); however, the resulting compound did not provide significant fluorescence.

4.6 Conclusion

In conclusion, we have developed an efficient electrochemical protocol for directly synthesizing 2-aryl-3-(2-aminoaryl) quinoxalines from 2-aryl indoles. The reaction proceeds through in situ generations of 2-arylindole-3-ones under electrochemical oxidative dearomatization of 2-arylindoles, followed by a ring opening-cyclization sequence with 1,2-diamino arenes to construct substituted quinoxaline compounds with good yields. Apart from gram-scale synthesis, the prepared compounds were tested for late-stage functionalization.

4.7 General experimental methods

All reactions were observed using thin-layer chromatography (on SiO_2 gel F254 plates) and performed on an IKA ElectroSyn 2.0 Pro instrument under standard conditions. The desired compounds were purified through flash column chromatography packed with silica gel (100−200 mesh size) as the stationary phase and a mixture of petroleum ether and acetone as the eluent. Melting points were determined in open capillary tubes on an EZMelt Automated melting point apparatus and are uncorrected. NMR spectra were recorded on a Bruker AV 400 spectrometer. The chemical shifts were reported in parts per million using a deuterated solvent as the internal standard. High-resolution mass spectra (HRMS-ESI) were recorded using a quadrupole time-of-flight (QTOF) mass spectrometer (Applied Biosystems). Cyclic voltammetry was performed using a CH Instruments electrochemical analyzer (model CHI1200B) with a three-electrodes cell [glassy carbon as the working electrode (3 mm diameter, circular), Pt wire as the auxiliary electrode, and Ag/AgCl as the reference electrode]. Before the experiments, the electrode was polished with Micro Polish Alumina Powder 0.05 μm using the following method. The alumina (0.05 μm) was mixed with water on the polishing pad to make a paste. The working electrode was then rubbed on the polishing pad with some alumina paste while ensuring that the face of the working electrode remained flat, and polishing was performed in figure eight so that grooves do not develop in the electrode surface. After being polished for ∼30 s, the electrode was sonicated in deionized water for ≤1 min. Finally, the electrode was washed with deionized water, and the

electrode surface was dried before use. All cyclic voltammetry experiments were performed after nitrogen purging for deoxygenation purposes. Cyclic voltammetry was performed using a CH Instruments electrochemical analyzer (model CHI1200B). All the chemicals were obtained from a commercial supplier and used without purification. All starting 2-arylindoles were prepared using the reported procedure,[59] oil baths were used for heating conditions.

4.7.1 General procedure for the synthesis of compound 12

A 10 mL dried undivided reaction cell with a stirring bar was charged with **1** (0.5 mmol, 1.0 equiv), *o*-amino-anilines **3** (1.5 mmol, 3.0 equiv), *n*-Bu_4NPF_6 (193 mg, 0.5 mmol, 1.0 equiv.), and TEMPO (15 mg, 0.1 mmol, 20 mol%), in CH_3CN/CF_3CH_2OH (10 mL, 9:1). Platinum-plate anode and Platinum-plate cathode were dipped into the reaction mixture and electrolyzed at a constant current condition (1.5 mA) under an air atmosphere at room temperature, and the reaction progress was monitored by TLC. Upon completion, the reaction mixture was evaporated under reduced pressure, and crude mass was stirred between ethyl acetate (10 mL) and NH_4Cl (10 mL, 10% solution) for five minutes. The organic phase was separated, dried over anhydrous Na_2SO_4, and evaporated under reduced pressure. Purification of crude mass on silica gel column chromatography using a mixture of petroleum ether and acetone as eluent furnished product **3** (45-75% yields).

4.7.2 Characterization data of synthesized compounds

2-(3-Phenylquinoxalin-2-yl)aniline (12aa). Purification with petroleum ether: acetone (9/1) as eluent; yellow solid (112 mg, 75% yield, mp = 152–154 °C). ^{1}H NMR (400 MHz, $CDCl_3$) δ 8.22 – 8.16 (m, 1H), 8.14 – 8.09 (m, 1H), 7.77 (qd, *J* = 6.8, 3.5 Hz, 2H), 7.59 (dt, *J* = 7.0, 2.3 Hz, 2H), 7.36 – 7.30 (m, 3H), 7.16 – 7.10 (m, 1H), 6.86 (dd, *J* = 7.8, 1.6 Hz, 1H), 6.80 (dd, *J* = 8.1, 1.0 Hz, 1H), 6.56 (td, *J* = 7.6, 1.1 Hz, 1H), 4.63 (s, 2H). ^{13}C{^{1}H} NMR (100 MHz, $CDCl_3$) δ 154.2, 152.9, 145.3, 141.0, 140.3, 138.9, 131.7, 129.9 (3C), 129.5 (2C), 129.2, 128.8, 128.6, 128.2 (2C), 123.1, 117.9, 116.8. **HRMS (ESI-TOF)** *m*/*z*: [M + H$^+$] Calcd for $C_{20}H_{16}N_3$ 298.1339, Found 298.1343.

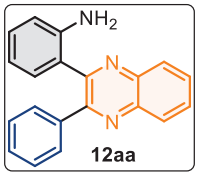

12aa

2-(3-(4-Fluorophenyl)quinoxalin-2-yl)aniline (12ba). Purification with petroleum ether: acetone (9/1) as eluent; yellow solid (88 mg, 56% yield, mp = 131–133 °C). ^{1}H NMR (400 MHz, $CDCl_3$) δ 8.21 – 8.17 (m, 1H), 8.14 – 8.09 (m, 1H), 7.78 (qd, *J* = 6.9, 3.5 Hz, 2H), 7.61 (m, 2H), 7.19 – 7.13 (m, 1H), 7.07 –

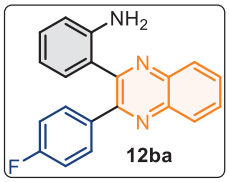

12ba

7.00 (m, 2H), 6.88 (dd, *J* = 7.7, 1.3 Hz, 1H), 6.84 – 6.80 (m, 1H), 6.63 – 6.58 (m, 1H), 4.64 (s, 2H). $^{13}C\{^{1}H\}$ NMR (100 MHz, $CDCl_3$) δ 163.0 (d, *J* = 248.7 Hz), 152.9, 152.6, 145.2, 140.8, 140.2, 134.8 (d, *J* = 3.1 Hz), 131.5 (2C), 131.4, 129.9 (d, *J* = 7.8 Hz), 129.9 (2C), 129.0, 128.5, 122.8, 117.9, 116.8 (2C), 115.1 (d, *J* = 21.2 Hz). HRMS (ESI-TOF) *m*/*z*: [M + H^+] Calcd for $C_{20}H_{15}FN_3$ 316.1245, Found 316.1248.

2-(3-(2,4-Difluorophenyl)quinoxalin-2-yl)aniline (12ca). Purification with petroleum ether: acetone (9/1) as eluent; yellow solid (92 mg, 55% yield, mp = 148–150 °C). ^{1}H NMR (400 MHz, $CDCl_3$) δ 8.19 – 8.11 (m, 2H), 7.83 – 7.78 (m, 2H), 7.64 – 7.58 (m, 1H), 7.14 – 7.08 (m, 1H), 6.97 (td, *J* = 8.5, 2.3 Hz, 1H), 6.82 – 6.77 (m, 2H), 6.73 (td, *J* = 9.6, 2.3 Hz, 1H), 6.51 (t, *J* = 7.5 Hz, 1H), 4.74 (s, 2H). $^{13}C\{^{1}H\}$ NMR (100 MHz, $CDCl_3$) δ 164.7 (d, *J* = 11.8 Hz), 162.2 (d, *J* = 11.8 Hz), 161.2 (d, *J* = 12.2 Hz), 158.7 (d, *J* = 12.2 Hz), 153.8, 149.5 (d, *J* = 1.4 Hz), 145.6, 140.7 (d, *J* = 12.4 Hz), 132.32 (dd, *J* = 9.8, 4.5 Hz), 130.5 (d, *J* = 5.9 Hz), 130.1 (2C), 129.2, 128.7, 123.87 (dd, *J* = 14.7, 3.9 Hz), 122.1 (d, *J* = 1.6 Hz), 117.6, 116.9, 111.83 (dd, *J* = 21.5, 3.6 Hz), 104.20 (t, *J* = 25.5 Hz). HRMS (ESI-TOF) *m*/*z*: [M + H^+] Calcd for $C_{20}H_{14}F_2N_3$ 334.1150, Found 334.1153.

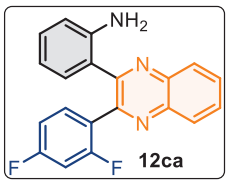

2-(3-(4-Fluoro-3-methylphenyl)quinoxalin-2-yl)aniline (12da). Purification with petroleum ether: acetone (9/1) as eluent; yellow solid (99 mg, 60% yield, mp = 173–175 °C). ^{1}H NMR (400 MHz, $CDCl_3$) δ 8.19 (dd, *J* = 6.3, 3.2 Hz, 1H), 8.12 (dd, *J* = 6.3, 3.2 Hz, 1H), 7.80 (q, *J* = 5.4, 3.8 Hz, 2H), 7.55 (d, *J* = 6.2 Hz, 1H), 7.30 (dd, *J* = 5.7, 2.8 Hz, 1H), 7.16 (t, *J* = 7.6 Hz, 1H), 6.93 (t, *J* = 9.0 Hz, 1H), 6.86 (dd, *J* = 19.6, 7.8 Hz, 2H), 6.61 (t, *J* = 7.4 Hz, 1H), 4.61 (s, 2H), 2.28 (s, 3H). $^{13}C\{^{1}H\}$ NMR (100 MHz, $CDCl_3$) δ 161.7 (d, *J* = 246.0 Hz), 153.3, 152.7, 145.2, 140.9, 140.3, 134.5 (d, *J* = 3.5 Hz), 132.8 (d, *J* = 5.6 Hz), 131.5, 130.0 (d, *J* = 4.1 Hz), 129.9, 129.1, 128.8 (d, *J* = 8.4 Hz), 128.6, 125.0, 124.8, 123.1, 118.0, 116.9 (2C), 114.7 (d, *J* = 22.2 Hz), 14.4. HRMS (ESI-TOF) *m*/*z*: [M + H^+] Calcd for $C_{21}H_{17}FN_3$ 330.1402, Found 330.1406.

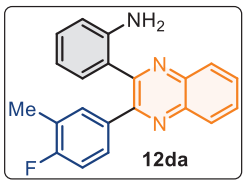

2-(3-(2-Chlorophenyl)quinoxalin-2-yl)aniline (12ea). Purification with petroleum ether: acetone (9/1) as eluent; yellow solid (98 mg, 59% yield, mp = 160–162 °C). ^{1}H NMR (400 MHz, $CDCl_3$) δ 8.22 – 8.17 (m, 1H), 8.14 (m, 1H), 7.83 – 7.77 (m, 2H), 7.55 – 7.51 (m, 1H), 7.36 – 7.27 (m, 3H), 7.10 – 7.04 (m, 1H), 6.80 (dd, *J* = 7.8, 1.2 Hz, 1H), 6.76 (d, *J* = 7.8 Hz, 1H), 6.47 – 6.41 (m, 1H), 4.87 (s, 2H).

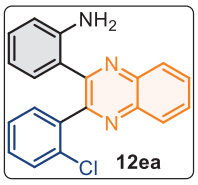

$^{13}C\{^{1}H\}$ NMR (100 MHz, $CDCl_3$) δ 153.6, 153.0, 145.9, 140.6, 140.4, 138.3, 133.0, 131.4, 130.8, 130.4, 130.0, 129.9, 129.8, 129.6, 129.2, 128.6, 126.8, 121.8, 117.2, 116.8. HRMS (ESI-TOF) *m/z*: [M + H^+] Calcd for $C_{20}H_{15}ClN_3$ 332.0950, Found 332.0954.

2-(3-(3-Chlorophenyl)quinoxalin-2-yl)aniline (12fa). Purification with petroleum ether: acetone (9/1) as eluent; yellow solid (108 mg, 65% yield, mp = 171–173 °C). ^{1}H NMR (400 MHz, $CDCl_3$) δ 8.17 (dp, *J* = 7.3, 2.9 Hz, 1H), 8.14 – 8.09 (m, 1H), 7.82 – 7.76 (m, 2H), 7.71 (t, *J* = 1.8 Hz, 1H), 7.36 – 7.30 (m, 2H), 7.20 (t, *J* = 7.9 Hz, 1H), 7.15 (td, *J* = 8.1, 1.5 Hz, 1H), 6.86 – 6.80 (m, 2H), 6.58 (td, *J* = 7.6, 0.9 Hz, 1H), 4.63 (s, 2H). $^{13}C\{^{1}H\}$ NMR (100 MHz, $CDCl_3$) δ 152.7, 152.7, 145.3, 140.9, 140.6, 140.5, 134.3, 131.6, 130.3, 130.2 (2C), 129.5, 129.3 (2C), 128.9, 128.6, 127.8, 122.6, 118.1, 117.0. HRMS (ESI-TOF) *m/z*: [M + H^+] Calcd for $C_{20}H_{15}ClN_3$ 332.0950, Found 332.0948.

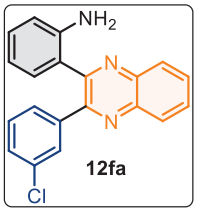

2-(3-(4-Chlorophenyl)quinoxalin-2-yl)aniline (12ga). Purification with petroleum ether: acetone (9/1) as eluent; yellow solid (103 mg, 62% yield, mp = 155–159 °C). ^{1}H NMR (400 MHz, $CDCl_3$) δ 8.19 – 8.15 (m, 1H), 8.13 – 8.08 (m, 1H), 7.82 – 7.75 (m, 2H), 7.53 (d, *J* = 8.5 Hz, 2H), 7.29 (s, 2H), 7.17 – 7.12 (m, 1H), 6.86 – 6.79 (m, 2H), 6.63 – 6.56 (m, 1H), 4.60 (s, 2H). $^{13}C\{^{1}H\}$ NMR (100 MHz, $CDCl_3$) δ 153.0, 152.7, 145.3, 141.0, 140.5, 137.4, 135.1, 131.6, 130.9 (2C), 130.1 (2C), 129.3, 128.7, 128.5, 123.0, 122.9 (2C) 118.2, 117.0. HRMS (ESI-TOF) *m/z*: [M + H^+] Calcd for $C_{20}H_{15}ClN_3$ 332.0950, Found 332.0947.

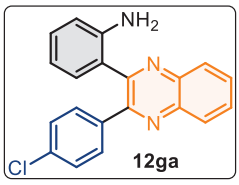

2-(3-(2,4-Dichlorophenyl)quinoxalin-2-yl)aniline (12ha). Purification with petroleum ether: acetone (9/1) as eluent; yellow solid (112 mg, 61% yield, mp = 181–183 °C). ^{1}H NMR (400 MHz, $CDCl_3$) δ 8.15 (m, 2H), 7.82 (m, 2H), 7.46 (d, *J* = 8.2 Hz, 1H), 7.38 – 7.36 (m, 1H), 7.34 – 7.29 (m, 1H), 7.10 (t, *J* = 7.6 Hz, 1H), 6.77 (d, *J* = 8.0 Hz, 2H), 6.49 (t, *J* = 7.5 Hz, 1H), 4.83 (s, 2H). $^{13}C\{^{1}H\}$ NMR (100 MHz, $CDCl_3$) δ 153.5, 152.0, 145.9, 140.7, 140.4, 137.0, 135.1, 133.9, 132.3, 130.7, 130.7, 130.2, 130.1, 129.6, 129.2, 128.7, 127.3, 121.6, 117.5, 116.9. HRMS (ESI-TOF) *m/z*: [M + H^+] Calcd for $C_{20}H_{14}Cl_2N_3$ 366.0560, Found 366.0566.

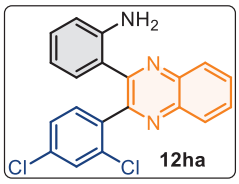

2-(3-(3,4-Dichlorophenyl)quinoxalin-2-yl)aniline (12ia). Purification with petroleum ether: acetone (9/1) as eluent; yellow solid (104 mg, 57% yield, mp = 180–183 °C). ^{1}H NMR (400 MHz, $CDCl_3$) δ 8.17 (d, *J* = 3.9 Hz, 1H), 8.11 (dd, *J* = 6.5, 2.9 Hz, 1H), 7.84 (s, 1H), 7.83 – 7.76 (m, 2H), 7.32 (q, *J* = 8.3 Hz, 2H), 7.18 (t, *J* = 7.5 Hz, 1H), 6.84 (t, *J* = 6.3 Hz, 2H), 6.63 (t, *J* = 7.4 Hz, 1H), 4.60 (s, 2H). ^{13}C{^{1}H} NMR (100 MHz, $CDCl_3$) δ 152.4, 151.5, 145.1, 140.8, 140.5, 138.7, 133.1, 132.5, 131.4, 131.3, 130.4, 130.3, 130.2, 129.9, 129.1, 128.8, 128.6, 122.4, 118.2, 117.0. HRMS (ESI-TOF) *m*/*z*: [M + H$^+$] Calcd for $C_{20}H_{14}Cl_2N_3$ 366.0560, Found 366.0565.

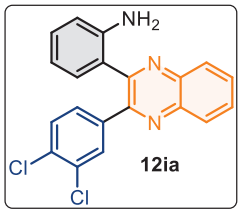

2-(3-(4-Bromophenyl)quinoxalin-2-yl)aniline (12ja). Purification with petroleum ether: acetone (9/1) as eluent; yellow solid (122 mg, 65% yield, mp = 155–159 °C). ^{1}H NMR (400 MHz, $CDCl_3$) δ 8.19 – 8.13 (m, 1H), 8.13 – 8.07 (m, 1H), 7.81 – 7.74 (m, 2H), 7.49 – 7.43 (m, 4H), 7.17 – 7.12 (m, 1H), 6.83 (m, 2H), 6.59 (td, *J* = 7.6, 1.0 Hz, 1H), 4.61 (s, 2H). ^{13}C{^{1}H} NMR (100 MHz, $CDCl_3$) δ 152.9, 152.6, 145.2, 140.9, 140.4, 137.8, 131.6, 131.3 (2), 131.1 (2C), 130.1 (3C), 129.2, 128.6, 123.4, 122.8, 118.2, 117.0. HRMS (ESI-TOF) *m*/*z*: [M + H$^+$] Calcd for $C_{20}H_{15}BrN_3$ 376.0444, Found 376.0445.

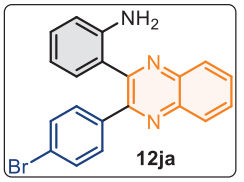

2-(3-(*p*-Tolyl)quinoxalin-2-yl)aniline (12ka). Purification with petroleum ether: acetone (9/1) as eluent; yellow solid (109 mg, 70% yield, mp = 155–159 °C). ^{1}H NMR (400 MHz, $CDCl_3$) δ 8.19 – 8.14 (m, 1H), 8.12 – 8.07 (m, 1H), 7.79 – 7.72 (m, 2H), 7.48 (d, *J* = 8.1 Hz, 2H), 7.16 – 7.11 (m, 3H), 6.89 (dd, *J* = 7.7, 1.4 Hz, 1H), 6.83 – 6.79 (m, 1H), 6.58 (td, *J* = 7.6, 1.1 Hz, 1H), 4.58 (s, 2H), 2.35 (s, 3H). ^{13}C{^{1}H} NMR (100 MHz, $CDCl_3$) δ 154.2, 152.9, 145.2, 141.1, 140.3, 138.9, 136.0, 131.7, 129.9 (2C), 129.7, 129.4 (2C), 129.2, 129.0 (2C), 128.6, 123.5, 118.1, 116.9, 21.3. HRMS (ESI-TOF) *m*/*z*: [M + H$^+$] Calcd for $C_{21}H_{18}N_3$ 312.1495, Found 312.1496.

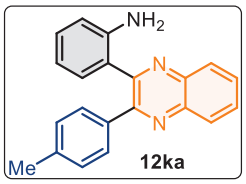

2-(3-(4-Isobutylphenyl)quinoxalin-2-yl)aniline (12la). Purification with petroleum ether: acetone (9/1) as eluent; yellow solid (127 mg, 72% yield, mp = 152–154 °C). ^{1}H NMR (400 MHz, $CDCl_3$) δ 8.21 – 8.15 (m, 1H), 8.13 – 8.07 (m, 1H), 7.79 – 7.71 (m, 2H), 7.49 (d, *J* = 8.2 Hz, 2H), 7.15 – 7.08 (m, 3H), 6.87 (dd, *J* = 7.7, 1.4 Hz, 1H), 6.82 – 6.77 (m, 1H), 6.55 (td, *J* = 7.6, 1.0 Hz, 1H), 4.63 (s, 2H), 2.47 (d, *J* = 7.2 Hz, 2H), 1.86 (dh, *J* = 13.6, 7.2 Hz, 1H),

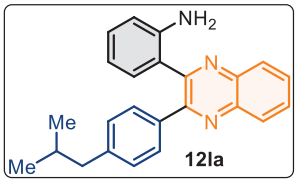

0.89 (d, J = 6.6 Hz, 6H). $^{13}C\{^1H\}$ NMR (100 MHz, $CDCl_3$) δ 154.3, 153.0, 145.3, 142.6, 141.0, 140.3, 136.2, 131.7, 129.8, 129.8, 129.7, 129.3 (2C), 129.1, 129.0 (2C), 128.6, 123.3, 117.9, 116.9, 45.1, 30.1, 22.3 (2C). HRMS (ESI-TOF) m/z: [M + H^+] Calcd for $C_{24}H_{24}N_3$ 354.1965, Found 354.1966.

2-(3-(3,4-Dimethoxyphenyl)quinoxalin-2-yl)aniline (12ma). Purification with petroleum ether: acetone (9/1) as eluent; yellow solid (122 mg, 68% yield, mp = 211–213 °C). ^1H NMR (400 MHz, $CDCl_3$) δ 8.17 – 8.14 (m, 1H), 8.10 – 8.06 (m, 1H), 7.74 (m, 2H), 7.30 (dd, J = 8.3, 2.1 Hz, 1H), 7.13 (m, 1H), 7.07 (d, J = 2.0 Hz, 1H), 6.93 (dd, J = 7.7, 1.4 Hz, 1H), 6.84 (d, J = 8.4 Hz, 1H), 6.81 – 6.78 (m, 1H), 6.62 (td, J = 7.6, 1.1 Hz, 1H), 3.88 (s, 3H), 3.66 (s, 3H). $^{13}C\{^1H\}$ NMR (100 MHz, $CDCl_3$) δ 153.5, 152.7, 149.7, 148.3, 145.0, 141.1, 140.2, 131.3, 131.0, 129.9, 129.8, 129.6, 129.0, 128.6, 123.9, 122.6, 118.3, 116.8, 112.7, 110.8, 55.8, 55.6. HRMS (ESI-TOF) m/z: [M + H^+] Calcd for $C_{22}H_{20}N_3O_2$ 358.1551, Found 358.1555.

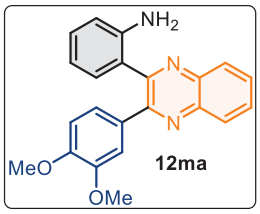

2-(3-(Naphthalen-2-yl)quinoxalin-2-yl)aniline (12na). Purification with petroleum ether: acetone (9/1) as eluent; yellow solid (116 mg, 67% yield, mp = 155–159 °C). ^1H NMR (400 MHz, $CDCl_3$) δ 8.26 – 8.20 (m, 2H), 8.17 – 8.12 (m, 1H), 7.80 (m, 4H), 7.75 (d, J = 8.6 Hz, 1H), 7.62 (dd, J = 8.5, 1.7 Hz, 1H), 7.52 – 7.45 (m, 2H), 7.14 – 7.09 (m, 1H), 6.90 (dd, J = 7.7, 1.4 Hz, 1H), 6.84 – 6.80 (m, 1H), 6.49 (td, J = 7.7, 0.9 Hz, 1H), 4.67 (s, 2H). $^{13}C\{^1H\}$ NMR (100 MHz, $CDCl_3$) δ 154.0, 153.1, 145.3, 141.1, 140.4, 136.4, 133.3, 133.1, 131.7, 130.0 (2C), 129.9, 129.5, 129.2, 128.7, 128.6, 127.6 (2C), 126.8, 126.7, 126.1, 123.2, 118.1, 116.9. HRMS (ESI-TOF) m/z: [M + H^+] Calcd for $C_{24}H_{18}N_3$ 348.1495, Found 348.1497.

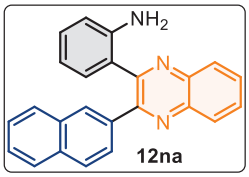

2-(3-(5-Bromothiophen-2-yl)quinoxalin-2-yl)aniline (12oa). Purification with petroleum ether: acetone (9/1) as eluent; yellow solid (107 mg, 56% yield, mp = 153–155 °C). ^1H NMR (400 MHz, $CDCl_3$) δ 8.12 (d, J = 7.8 Hz, 1H), 8.07 (d, J = 7.7 Hz, 1H), 7.79 – 7.69 (m, 2H), 7.41 (d, J = 4.8 Hz, 1H), 7.33 – 7.27 (m, 1H), 7.20 (d, J = 7.4 Hz, 1H), 6.96 (d, J = 3.3 Hz, 1H), 6.92 – 6.89 (m, 1H), 6.86 (dd, J = 7.6, 4.9 Hz, 1H), 4.03 (s, 2H). $^{13}C\{^1H\}$ NMR (100 MHz, $CDCl_3$) δ 150.9, 147.5, 144.7, 142.5, 141.1, 140.3, 130.5, 130.5, 130.3, 129.6 (2C), 128.8, 128.8 (2C), 128.0, 124.1, 118.8, 116.9. HRMS (ESI-TOF) m/z: [M + H^+] Calcd for $C_{18}H_{13}BrN_3S$ 382.0009, Found 382.0015.

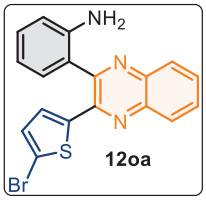

4-Chloro-2-(3-phenylquinoxalin-2-yl)aniline (12pa). Purification with petroleum ether: acetone (9/1) as eluent; yellow solid (116 mg, 70% yield, mp = 155–157 °C). ^{1}H NMR (400 MHz, $CDCl_3$) δ 8.23 – 8.16 (m, 1H), 8.14 – 8.08 (m, 1H), 7.80 (m, 2H), 7.58 (dd, *J* = 7.4, 1.7 Hz, 2H), 7.37 (q, *J* = 5.5, 5.0 Hz, 3H), 7.09 (dd, *J* = 8.6, 2.3 Hz, 1H), 6.87 (d, *J* = 2.3 Hz, 1H), 6.72 (d, *J* = 8.6 Hz, 1H), 4.53 (s, 2H). ^{13}C{^{1}H} NMR (100 MHz, $CDCl_3$) δ 154.0, 151.5, 143.9, 141.2, 140.4, 138.4, 131.1, 130.4, 130.2, 129.8, 129.4 (2C), 129.3, 129.2, 128.7, 128.4 (2C), 124.5, 122.6, 118.1. HRMS (ESI-TOF) *m*/*z*: [M + H$^+$] Calcd for $C_{20}H_{15}ClN_3$ 332.0950, Found 332.0955.

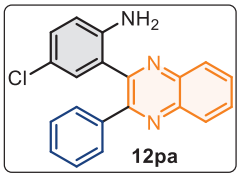

4-Bromo-2-(3-phenylquinoxalin-2-yl)aniline (12qa). Purification with petroleum ether: acetone (9/1) as eluent; yellow solid (126 mg, 67% yield, mp = 165–167 °C). ^{1}H NMR (400 MHz, $CDCl_3$) δ 8.19 (dd, *J* = 6.6, 2.8 Hz, 1H), 8.10 (dd, *J* = 6.4, 3.0 Hz, 1H), 7.78 (m, 2H), 7.61 – 7.55 (m, 2H), 7.37 (d, *J* = 6.7 Hz, 3H), 7.20 (dd, *J* = 8.6, 2.1 Hz, 1H), 7.01 (d, *J* = 2.0 Hz, 1H), 6.65 (d, *J* = 8.6 Hz, 1H), 4.55 (s, 2H). ^{13}C{^{1}H} NMR (100 MHz, $CDCl_3$) δ 153.9, 151.3, 144.3, 141.1, 140.3, 138.3, 134.0, 132.6, 130.3, 130.1, 129.4 (2C), 129.3, 129.1, 128.6, 128.4 (2C), 124.8, 118.3, 109.4. HRMS (ESI-TOF) *m*/*z*: [M + H$^+$] Calcd for $C_{20}H_{15}BrN_3$ 376.0444, Found 376.0448.

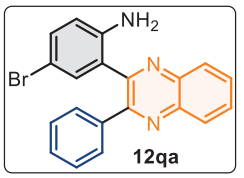

4-Methyl-2-(3-phenylquinoxalin-2-yl)aniline (12ra). Purification with petroleum ether: acetone (9/1) as eluent; yellow solid (112 mg, 72% yield, mp = 144–146 °C). ^{1}H NMR (400 MHz, $CDCl_3$) δ 8.18 (dd, *J* = 7.4, 2.1 Hz, 1H), 8.12 (dd, *J* = 7.1, 2.4 Hz, 1H), 7.76 (p, *J* = 6.2 Hz, 2H), 7.63 – 7.58 (m, 2H), 7.37 – 7.30 (m, 3H), 6.94 (d, *J* = 7.6 Hz, 1H), 6.72 (s, 1H), 6.69 (d, *J* = 8.1 Hz, 1H), 4.31 (s, 2H), 2.03 (s, 3H). ^{13}C{^{1}H} NMR (100 MHz, $CDCl_3$) δ 154.1, 153.0, 142.6, 140.9, 140.4, 138.8, 131.9, 130.5, 129.8, 129.8, 129.4 (2C), 129.1, 128.7, 128.6, 128.1 (2C), 127.2, 123.4, 116.9, 20.1. HRMS (ESI-TOF) *m*/*z*: [M + H$^+$] Calcd for $C_{21}H_{18}N_3$ 312.1495, Found 312.1496.

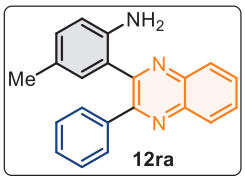

2-(3-(4-Bromophenyl)quinoxalin-2-yl)-4-methylaniline (12sa). Purification with petroleum ether: acetone (9/1) as eluent; yellow solid (135 mg, 69% yield, mp = 186–188 °C). ^{1}H NMR (400 MHz, $CDCl_3$) δ 8.15 (m, 1H), 8.13 – 8.08 (m, 1H), 7.79 (dd, *J* = 3.4, 1.3 Hz, 1H), 7.78 – 7.75 (m, 1H), 7.49 (d, *J* = 8.9 Hz, 2H), 7.45 (d, *J* = 8.9 Hz, 2H), 6.97 (dd, *J* = 8.1, 1.6 Hz, 1H), 6.72 (s,

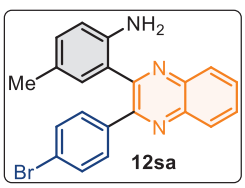

1H), 6.70 (s, 1H), 4.31 (s, 2H), 2.07 (s, 3H). $^{13}C\{^{1}H\}$ NMR (100 MHz, $CDCl_3$) δ 152.9, 152.8, 142.6, 141.0, 140.6, 137.8, 131.7, 131.3 (2C), 131.1 (2C), 130.8, 130.1, 130.1, 129.2, 128.7, 127.6, 123.4, 123.3, 117.1, 20.3. HRMS (ESI-TOF) *m/z*: [M + H^+] Calcd for $C_{21}H_{17}BrN_3$ 390.0600, Found 390.0608.

4-Methyl-2-(3-(*p*-tolyl)quinoxalin-2-yl)aniline (12ta). Purification with petroleum ether: acetone (9/1) as eluent; yellow solid (116 mg, 71% yield, mp = 206–208 °C). ^{1}H NMR (400 MHz, $CDCl_3$) δ 8.21 – 8.16 (m, 1H), 8.15 – 8.10 (m, 1H), 7.78 (p, *J* = 6.9 Hz, 2H), 7.52 (d, *J* = 7.8 Hz, 2H), 7.15 (d, *J* = 7.7 Hz, 2H), 6.98 (d, *J* = 7.9 Hz, 1H), 6.79 (s, 1H), 6.72 (d, *J* = 8.1 Hz, 1H), 4.29 (s, 2H), 2.37 (s, 3H), 2.08 (s, 3H). $^{13}C\{^{1}H\}$ NMR (100 MHz, $CDCl_3$) δ 154.1, 153.0, 142.5, 141.1, 140.5, 138.9, 136.0, 131.8, 130.6, 129.8, 129.7, 129.4 (2C), 129.2, 128.9 (2C), 128.7, 127.4, 123.9, 117.0, 21.3, 20.3. HRMS (ESI-TOF) *m/z*: [M + H^+] Calcd for $C_{22}H_{20}N_3$ 326.1652, Found 326.1654.

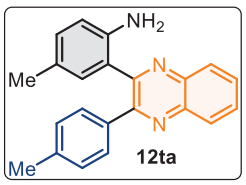

2-(3-(4-Methoxyphenyl)quinoxalin-2-yl)-4-methylaniline (12ua). Purification with petroleum ether: acetone (9/1) as eluent; yellow solid (126 mg, 74% yield, mp = 198–200 °C). ^{1}H NMR (400 MHz, $CDCl_3$) δ 8.14 (dd, *J* = 22.0, 7.2 Hz, 2H), 7.76 (p, *J* = 7.1 Hz, 2H), 7.60 (d, *J* = 8.3 Hz, 2H), 6.98 (d, *J* = 7.6 Hz, 1H), 6.87 (d, *J* = 8.3 Hz, 2H), 6.82 (s, 1H), 6.72 (d, *J* = 8.0 Hz, 1H), 4.28 (s, 2H), 3.83 (s, 3H), 2.11 (s, 3H). $^{13}C\{^{1}H\}$ NMR (100 MHz, $CDCl_3$) δ 160.2, 153.5, 152.8, 142.4, 141.1, 140.3, 131.6, 131.1, 130.9 (2C), 130.5, 129.8, 129.5, 129.0, 128.6, 127.4, 124.0, 117.0, 113.6 (2C), 55.2, 20.3. HRMS (ESI-TOF) *m/z*: [M + H^+] Calcd for $C_{22}H_{20}N_3O$ 342.1601, Found 342.1606.

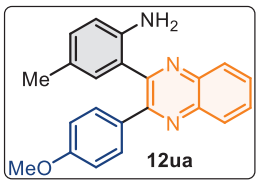

2-(6-Fluoro-3-phenylquinoxalin-2-yl)aniline (12ab). Purification with petroleum ether: acetone (9/1) as eluent; yellow solid (93 mg, 59% yield, mp = 152–155 °C). ^{1}H NMR (400 MHz, $CDCl_3$) δ 8.20 (dd, *J* = 9.2, 5.7 Hz, 1H), 7.75 (dd, *J* = 9.1, 2.7 Hz, 1H), 7.62 – 7.55 (m, 3H), 7.36 (qd, *J* = 5.1, 1.9 Hz, 3H), 7.19 – 7.13 (m, 1H), 6.87 (dd, *J* = 7.8, 1.4 Hz, 1H), 6.85 – 6.81 (m, 1H), 6.61 – 6.55 (m, 1H), 4.66 (s, 2H). $^{13}C\{^{1}H\}$ NMR (100 MHz, $CDCl_3$) δ 162.8 (d, *J* = 246.0 Hz), 153.2, 153.6 (d, *J* = 3.3 Hz), 145.3, 141.1 (d, *J* = 12.8 Hz), 138.6, 138.2 (d, *J* = 0.7 Hz), 131.7, 131.3 (d, *J* = 9.8 Hz), 130.2, 129.5 (2C), 128.9, 128.3 (2C), 122.7, 120.6 (d, *J* = 26.4 Hz), 118.0, 117.0,

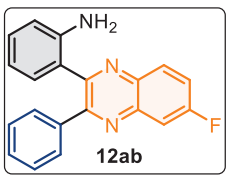

112.1 (d, *J* = 21.2 Hz). HRMS (ESI-TOF) *m/z*: [M + H$^+$] Calcd for $C_{20}H_{15}FN_3$ 316.1245, Found 316.1248.

2-(6,7-Difluoro-3-phenylquinoxalin-2-yl)aniline (12ac). Purification with petroleum ether: acetone (9/1) as eluent; yellow solid (95 mg, 57% yield, mp = 127–130 °C). ^{1}H NMR (400 MHz, $CDCl_3$) δ 7.91 (t, *J* = 9.3 Hz, 1H), 7.84 (t, *J* = 9.3 Hz, 1H), 7.56 (d, *J* = 6.3 Hz, 2H), 7.34 (q, *J* = 6.1 Hz, 3H), 7.14 (t, *J* = 7.6 Hz, 1H), 6.82 (dd, *J* = 15.6, 7.9 Hz, 2H), 6.56 (t, *J* = 7.5 Hz, 1H), 4.58 (s, 2H). ^{13}C{^{1}H} NMR (100 MHz, $CDCl_3$) δ 154.4 (d, *J* = 2.3 Hz), 153.7 (dd, *J* = 17.9, 1.8 Hz), 153.2 (d, *J* = 2.3 Hz), 151.1 (dd, *J* = 17.4, 1.8 Hz), 145.2, 138.3, 138.2(d, *J* = 2.3 Hz), 137.6 (dd, *J* = 8.9, 2.9 Hz), 131.7, 130.2, 129.4 (2C), 129.1, 128.3 (2C), 122.5, 118.1, 117.0, 114.7 (dd, *J* = 15.5, 3.2 Hz), 114.2 (dd, *J* = 12.7, 5.6 Hz). HRMS (ESI-TOF) *m/z*: [M + H$^+$] Calcd for $C_{20}H_{14}F_2N_3$ 334.1151, Found 334.1150.

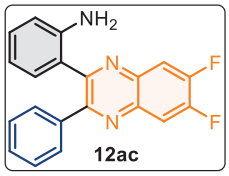

2-(6-Chloro-3-phenylquinoxalin-2-yl)aniline (12ad). Purification with petroleum ether: acetone (9/1) as eluent; yellow solid (100 mg, 60% yield, mp = 178–180 °C). ^{1}H NMR (400 MHz, $CDCl_3$) δ 8.11 (d, *J* = 6.0 Hz, 1H), 8.09 (s, 1H), 7.71 (dd, *J* = 9.0, 2.2 Hz, 1H), 7.58 – 7.54 (m, 2H), 7.38 – 7.30 (m, 3H), 7.13 (m, 1H), 6.84 (dd, *J* = 7.8, 1.4 Hz, 1H), 6.82 – 6.79 (m, 1H), 6.54 (td, *J* = 7.7, 1.1 Hz, 1H), 4.66 (s, 2H). ^{13}C{^{1}H} NMR (100 MHz, $CDCl_3$) δ 154.4, 153.9, 145.4, 140.6, 139.5, 138.6, 135.7, 131.8, 130.9, 130.5, 130.2, 129.5 (2C), 129.0, 128.3 (2C), 127.5, 122.6, 118.0, 117.0. HRMS (ESI-TOF) *m/z*: [M + H$^+$] Calcd for $C_{20}H_{15}ClN_3$ 332.0950, Found 332.0956.

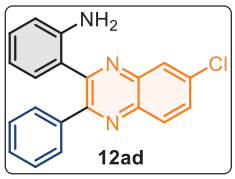

2-(6,7-Dichloro-3-phenylquinoxalin-2-yl)aniline (12ae). Purification with petroleum ether: acetone (9/1) as eluent; yellow solid (125 mg, 68% yield, mp = 175–177 °C). ^{1}H NMR (400 MHz, $CDCl_3$) δ 8.28 (s, 1H), 8.21 (s, 1H), 7.58 – 7.56 (m, 1H), 7.56 – 7.54 (m, 1H), 7.39 – 7.30 (m, 3H), 7.14 (td, *J* = 8.1, 1.5 Hz, 1H), 6.82 (td, *J* = 8.0, 1.0 Hz, 2H), 6.54 (td, *J* = 7.7, 1.0 Hz, 1H), 4.66 (s, 2H). ^{13}C{^{1}H} NMR (100 MHz, $CDCl_3$) δ 155.3, 154.1, 145.4, 139.7, 139.0, 138.3 (2C), 134.4, 131.8, 130.4, 129.8, 129.5 (2C), 129.3, 129.1, 128.3 (2C), 122.3, 118.0, 117.1. HRMS (ESI-TOF) *m/z*: [M + H$^+$] Calcd for $C_{20}H_{14}Cl_2N_3$ 366.0560, Found 366.0565.

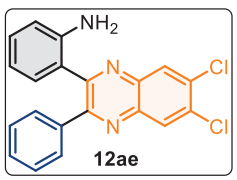

2-(6-Bromo-3-phenylquinoxalin-2-yl)aniline (12af). Purification with petroleum ether: acetone (9/1) as eluent; yellow solid (117 mg, 62% yield, mp = 195–197 °C). ^{1}H NMR (400 MHz, $CDCl_3$) δ 8.28 (d, *J* = 1.9 Hz, 1H), 8.03 (d, *J* = 8.9 Hz, 1H), 7.84 (dd, *J* = 8.9, 1.9 Hz, 1H), 7.60 – 7.53 (m, 2H), 7.33 (q, *J* = 5.6 Hz, 3H), 7.16 – 7.10 (m, 1H), 6.82 (dd, *J* = 11.6, 8.0 Hz, 2H), 6.54 (t, *J* = 7.4 Hz, 1H), 4.67 (s, 2H). ^{13}C{^{1}H} NMR (100 MHz, $CDCl_3$) δ 154.6, 153.9, 145.5, 140.9, 139.7, 138.6, 133.5, 131.8, 130.8, 130.5, 130.2, 129.5 (2C), 129.1, 128.3 (2C), 123.8, 122.6, 118.0, 117.0. HRMS (ESI-TOF) *m*/*z*: [M + H^{+}] Calcd for $C_{20}H_{15}BrN_3$ 376.0444, Found 376.0446.

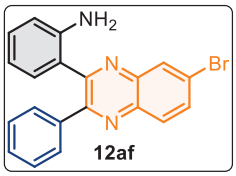

2-(6,7-Dibromo-3-phenylquinoxalin-2-yl)aniline (12ag). Purification with petroleum ether: acetone (9/1) as eluent; yellow solid (159 mg, 70% yield, mp = 216–219 °C). ^{1}H NMR (400 MHz, $CDCl_3$) δ 8.47 (s, 1H), 8.39 (s, 1H), 7.59 – 7.53 (m, 2H), 7.39 – 7.30 (m, 3H), 7.16 – 7.11 (m, 1H), 6.85 – 6.78 (m, 2H), 6.56 – 6.51 (m, 1H), 4.68 (s, 2H). ^{13}C{^{1}H} NMR (100 MHz, $CDCl_3$) δ 155.4, 154.2, 145.5, 140.1, 139.5, 138.3, 133.2, 132.5, 131.8, 130.4, 129.5 (2C), 129.3, 128.3 (2C), 126.4 (2C), 122.2, 118.0, 117.1. HRMS (ESI-TOF) *m*/*z*: [M + H^{+}] Calcd for $C_{20}H_{14}Br_2N_3$ 455.9529, Found 455.9532.

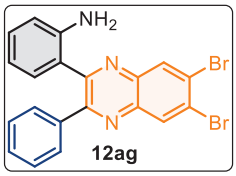

5-(2-Aminophenyl)-6-phenylpyrazine-2,3-dicarbonitrile (12ah). Purification with petroleum ether: acetone (9/1) as eluent; yellow solid (82 mg, 55% yield, mp = 221–222 °C). ^{1}H NMR (400 MHz, DMSO-d_6 & $CDCl_3$) δ 7.52 (d, *J* = 7.4 Hz, 2H), 7.37 (t, *J* = 7.2 Hz, 1H), 7.29 (d, *J* = 7.6 Hz, 2H), 7.09 (t, *J* = 7.4 Hz, 1H), 6.79 (d, *J* = 7.6 Hz, 1H), 6.74 (d, *J* = 8.2 Hz, 1H), 6.43 (t, *J* = 7.4 Hz, 1H), 5.13 (s, 2H). ^{13}C{^{1}H} NMR (100 MHz, DMSO-d_6 & $CDCl_3$) δ 155.0, 154.9, 145.7, 134.6, 130.8, 130.0, 129.8, 128.3 (2C), 128.2, 127.5 (2C), 117.7, 116.1 (2C), 116.0, 112.1, 112.6. HRMS (ESI-TOF) *m*/*z*: [M + H^{+}] Calcd for $C_{18}H_{12}N_5$ 298.1088, Found 298.1085.

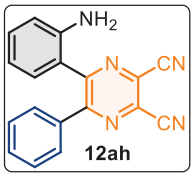

2-(5-Methyl-3-phenylquinoxalin-2-yl)aniline (12ai). Purification with petroleum ether: acetone (9/1) as eluent; yellow solid (103 mg, 66% yield, mp = 160–162 °C). ^{1}H NMR (400 MHz, $CDCl_3$) δ 8.03 – 7.99 (m, 1H), 7.66 (dd, *J* = 8.3, 7.1 Hz, 1H), 7.59 (m, 3H), 7.34 (t, *J* = 2.2 Hz, 2H), 7.33 – 7.31 (m, 1H), 7.12 (m, 1H), 6.86 (dd, *J* = 7.8, 1.4 Hz, 1H), 6.83 (dd, *J* = 8.1, 0.9 Hz, 1H), 6.52 (td, *J* = 7.7, 1.1 Hz, 1H), 4.96 (s, 2H), 2.82 (s, 3H). ^{13}C{^{1}H} NMR (100 MHz, $CDCl_3$) δ 153.7, 151.4, 145.8, 140.9,

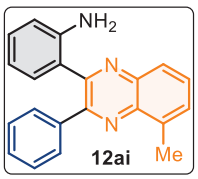

139.3, 136.7, 132.2, 129.9, 129.8, 129.7, 129.6 (2C), 128.7, 128.2 (2C), 128.1, 127.1, 123.0, 117.7, 117.0, 17.3. HRMS (ESI-TOF) *m/z*: [M + H^+] Calcd for $C_{21}H_{18}N_3$ 312.1495, Found. 312.1491.

2-(6-Methyl-3-phenylquinoxalin-2-yl)aniline/2-(7-methyl-3-phenylquinoxalin-2-yl)aniline

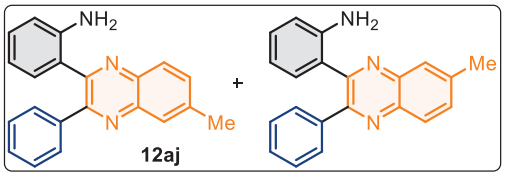

12aj

(12aj). Purification with petroleum ether: acetone (9/1) as eluent; yellow solid (2:1 by NMR) (109 mg, 70% yield, mp = 156–159 °C). ^{1}H NMR (400 MHz, $CDCl_3$) δ 8.03 (dd, *J* = 29.8, 8.5 Hz, 1H), 7.92 (d, *J* = 31.8 Hz, 1H), 7.63 – 7.55 (m, 3H), 7.35 – 7.28 (m, 3H), 7.14 – 7.08 (m, 1H), 6.86 (dd, *J* = 7.7, 1.2 Hz, 1H), 6.79 (d, *J* = 8.0 Hz, 1H), 6.58 – 6.52 (m, 1H), 4.62 (s, 2H), 2.62 (s, 1H), 2.61 (s, 2H). ^{13}C{^{1}H} NMR (100 MHz, $CDCl_3$) δ 153.3, 152.7, 145.3, 140.4, 139.5, 139.0, 132.2, 132.2, 131.7, 129.8, 129.7, 129.5, 129.5, 128.7, 128.7, 128.6, 128.1, 128.1, 128.0, 127.4, 123.2, 117.9, 117.9, 116.8, 21.8. HRMS (ESI-TOF) *m/z*: [M + H^+] Calcd for $C_{21}H_{18}N_3$ 312.1495, Found 312.1497.

2-(6,7-Dimethyl-3-phenylquinoxalin-2-yl)aniline (12ak). Purification with petroleum ether: acetone (9/1) as eluent; yellow solid (119 mg, 73% yield, mp = 169–172 °C). ^{1}H NMR (400 MHz, $CDCl_3$) δ 7.95 (s, 1H), 7.87 (s, 1H), 7.61 – 7.56 (m, 2H), 7.36 – 7.32 (m, 3H), 7.13 (m, 1H), 6.87 (dd, *J* = 7.7, 1.4 Hz, 1H), 6.81 (dd, *J* = 8.1, 0.9 Hz, 1H), 6.57 (td, *J* = 7.6, 1.1 Hz, 1H), 4.61 (s, 2H), 2.54 (d, *J* = 1.1 Hz, 3H), 2.53 (s, 3H). ^{13}C{^{1}H} NMR (100 MHz, $CDCl_3$) δ 153.2, 151.8, 145.2, 140.5, 140.4, 140.0, 139.4, 139.2, 131.7, 129.6, 129.5 (2C), 128.5, 128.2, 128.1 (2C), 127.6, 123.5, 117.9, 116.8, 20.3 (2C). HRMS (ESI-TOF) *m/z*: [M + H^+] Calcd for $C_{22}H_{20}N_3$ 326.1652, Found 326.1655.

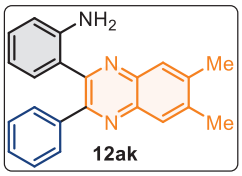

12ak

2-(3-Phenylbenzo[*g*]quinoxalin-2-yl)aniline (12al). Purification with petroleum ether: acetone (9/1) as eluent; yellow solid (113 mg, 65% yield, mp = 180–183 °C). ^{1}H NMR (400 MHz, $CDCl_3$) δ 8.74 (s, 1H), 8.66 (s, 1H), 8.12 (tq, *J* = 6.8, 3.3 Hz, 2H), 7.66 – 7.61 (m, 2H), 7.58 (dq, *J* = 6.6, 3.4 Hz, 2H), 7.36 (dq, *J* = 6.6, 3.2 Hz, 3H), 7.17 – 7.11 (m, 1H), 6.88 (dd, *J* = 7.8, 1.3 Hz, 1H), 6.84 (d, *J* = 8.0 Hz, 1H), 6.58 – 6.53 (m, 1H), 4.83 (s, 2H). ^{13}C{^{1}H} NMR (100 MHz, $CDCl_3$) δ 155.0, 153.8, 145.6, 139.1, 137.7, 137.1, 134.1, 134.0, 131.9, 130.1, 129.5 (2C), 129.0, 128.6, 128.5

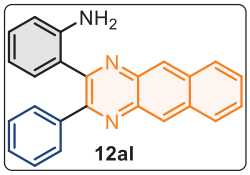

12al

(2C), 128.2, 127.6, 126.8 (2C), 126.7, 122.9, 117.8, 117.0. HRMS (ESI-TOF) *m/z*: [M + H^+] Calcd for $C_{24}H_{18}N_3$ 348.1495, Found 348.1493.

4-Bromo-2-(6,7-dibromo-3-phenylquinoxalin-2-yl)aniline (12qg). Purification with petroleum ether: acetone (9/1) as eluent; yellow solid (174 mg, 65% yield, mp = 165–167 °C). ^{1}H NMR (400 MHz, $CDCl_3$) δ 8.50 (s, 1H), 8.42 (s, 1H), 7.57 (dt, *J* = 6.6, 1.5 Hz, 2H), 7.47 – 7.43 (m, 1H), 7.43 – 7.41 (m, 1H), 7.40 – 7.37 (m, 1H), 7.24 (dd, *J* = 8.6, 2.3 Hz, 1H), 6.99 (d, *J* = 2.3 Hz, 1H), 6.69 (d, *J* = 8.6 Hz, 1H), 4.64 (s, 2H). ^{13}C{^{1}H} NMR (100 MHz, $CDCl_3$) δ 155.1, 152.7, 144.4, 140.3, 139.4, 137.7, 134.0, 133.3, 133.1, 132.6, 129.7, 129.4 (2C), 128.5 (2C), 126.9, 126.7, 123.9, 118.6, 109.4. HRMS (ESI-TOF) *m/z*: [M + H^+] Calcd for $C_{20}H_{13}Br_3N_3$ 531.8654, Found 531.8657.

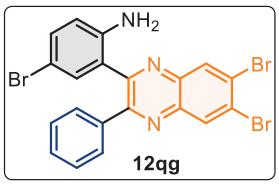

2-(6,7-Difluoro-3-phenylquinoxalin-2-yl)-4-methylaniline (12rc). Purification with petroleum ether: acetone (9/1) as eluent; yellow solid (99 mg, 57% yield, mp = 189–191 °C). ^{1}H NMR (400 MHz, $CDCl_3$) δ 7.91 (dd, *J* = 10.2, 8.4 Hz, 1H), 7.84 (dd, *J* = 10.1, 8.4 Hz, 1H), 7.57 (dq, *J* = 6.2, 2.2 Hz, 2H), 7.39 – 7.30 (m, 3H), 6.95 (dd, *J* = 8.2, 1.5 Hz, 1H), 6.71 – 6.67 (m, 2H), 4.32 (s, 2H), 2.03 (s, 3H). ^{13}C{^{1}H} NMR (100 MHz, $CDCl_3$) δ 154.4 (d, *J* = 2.8 Hz), 153.7 (dd, *J* = 17.9, Hz), 153.2 (d, *J* = 2.8 Hz), 151.1 (d, *J* = 17.8 Hz), 142.6, 138.3, 138.2 (d, *J* = 2.3 Hz), 137.6 (dd, *J* = 8.9, 2.9 Hz), 131.8, 130.9, 129.4 (2C), 129.1, 128.2 (2C), 127.4, 122.9, 117.1, 114.7(dd, *J* = 15.5, 3.2 Hz), 114.2 (dd, *J* = 12.7, 5.6 Hz), 20.1. HRMS (ESI-TOF) *m/z*: [M + H^+] Calcd for $C_{21}H_{16}F_2N_3$ 348.1307, Found 348.1308.

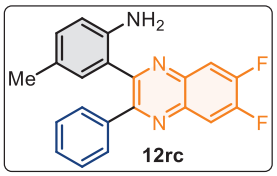

4-Methyl-2-(3-(*p*-tolyl)benzo[g]quinoxalin-2-yl)aniline (12tl). Purification with petroleum ether: acetone (9/1) as eluent; yellow solid (130 mg, 69% yield, mp = 190–193 °C). ^{1}H NMR (400 MHz, $CDCl_3$) δ 8.72 (s, 1H), 8.64 (s, 1H), 8.09 (m, 2H), 7.55 (dd, *J* = 7.3, 2.6 Hz, 4H), 7.16 (d, *J* = 7.9 Hz, 2H), 6.97 (dd, *J* = 8.1, 1.5 Hz, 1H), 6.81 – 6.78 (m, 1H), 6.72 (d, *J* = 8.1 Hz, 1H), 4.49 (s, 2H), 2.37 (s, 3H), 2.06 (s, 3H). ^{13}C{^{1}H} NMR (100 MHz, $CDCl_3$) δ 154.8, 153.9, 142.8, 139.0, 137.8, 137.2, 136.1, 133.9, 133.8, 131.9, 130.7, 129.4 (2C), 128.8 (2C), 128.5, 128.4, 127.4, 127.1, 126.8, 126.6 (2C), 123.6, 117.0, 21.3, 20.2. HRMS (ESI-TOF) *m/z*: [M + H^+] Calcd for $C_{26}H_{22}N_3$ 376.1809, Found 376.1811.

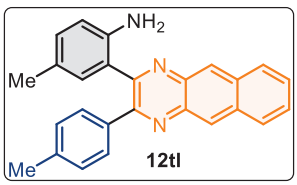

2-(3-(4-Methoxyphenyl)-6,7-dimethylquinoxalin-2-yl)-4-methylaniline (12uk). Purification with petroleum ether: acetone (9/1) as eluent; yellow solid (133 mg, 72% yield, mp = 219–221 °C). ^{1}H NMR (400 MHz, $CDCl_3$) δ 7.89 (s, 1H), 7.83 (s, 1H), 7.54 (d, *J* = 8.7 Hz, 2H), 6.94 (dd, *J* = 8.1, 1.7 Hz, 1H), 6.84 (s, 2H), 6.78 (s, 1H), 6.67 (d, *J* = 8.1 Hz, 1H), 4.20 (s, 2H), 3.79 (s, 3H), 2.50 (s, 3H), 2.49 (s, 3H), 2.08 (s, 3H). ^{13}C{^{1}H} NMR (100 MHz, $CDCl_3$) δ 160.0, 152.6, 151.7, 142.4, 140.3, 140.1, 140.0, 139.3, 131.7, 131.5, 130.8 (2C), 130.3, 128.1, 127.7, 127.4, 124.4, 116.9, 113.5 (2C), 55.2, 20.3, 20.3, 20.3. HRMS (ESI-TOF) *m/z*: [M + H$^+$] Calcd for $C_{24}H_{24}N_3O$ 370.1914, Found 370.1911.

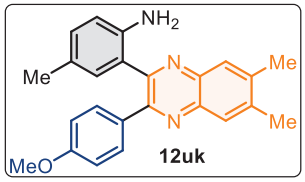

Controlled Experiments: To a 10 mL dried undivided reaction cell equipped with a stirring bar were added **10a** (0.5 mmol, 1.0 equiv), **11a** (1.5 mmol, 3.0 equiv), *n*-Bu_4NPF_6 (193 mg, 0.5 mmol, 1.0 equiv.), and TEMPO (15 mg, 0.1 mmol, 20 mol%), BHT (2.5 mmol) dissolved in CH_3CN: CF_3CH_2OH (10 mL, 9:1). Platinum-plate anode and Platinum-plate cathode were dipped into the reaction mixture and electrolyzed at a constant current condition (1.5 mA) under standard conditions. The desired product **12aa** formation was not observed on TLC.

Gram-Scale synthesis of 12aa. A 100 mL three-neck round bottom flask (as an undivided cell) was charged with **10a** (1.1 g, 5.69 mmol, 1.0 equiv), **11a** (1.84 g, 17.07 mmol, 3.0 equiv), *n*-Bu_4NPF_6 (2.2 g, 5.69 mmol, 1.0 equiv), and TEMPO (0.177 g, 1.13 mmol, 20 mol%), in CH_3CN/CF_3CH_2OH (36 mL, 9:1). Platinum-plate anode and Platinum-plate cathode that was connected to a DC regulated power supply dipped into the reaction mixture and electrolyzed at a constant current condition (1.5 mA) under an air atmosphere at room temperature, and the reaction progress was monitored by TLC. The reaction solvent was evaporated under reduced pressure once the reaction was finished, after the usual workup and silica gel column chromatography purification furnished compound **12aa** (1.15 g) with 68% yield.

2-(2-(1*H*-Pyrrol-1-yl)phenyl)-3-phenyl quinoxaline (13). To a stirred solution of **12aa** (100 mg, 0.33 mmol, 1.0 equiv) in ethanol (6.0 mL) in a dry 25 mL round-bottom flask was added succinaldehyde (3.0 M sol., 0.50 mmol, 170 µL, 1.5 equiv) at room temperature under an N_2 atmosphere. The mixture was stirred at rt for 10 h, and the reaction progress was monitored by TLC. The reaction mixture was concentrated under reduced pressure and diluted with EtOAc (10 mL). The resultant mixture was washed with H_2O (3×5.0 mL). The organic layer was separated, dried over anhydrous Na_2SO_4,

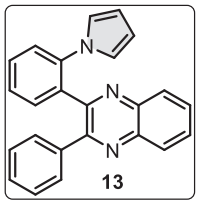

and concentrated under reduced pressure. Purification by column chromatography using petroleum ether/EtOAc (9/1) as the eluent afforded **13** as yellow solid (97 mg, 85% yield, mp = 168-170 ° C). ^{1}H NMR (400 MHz, $CDCl_3$) δ 8.24 – 8.19 (m, 1H), 8.16 – 8.12 (m, 1H), 8.05 (d, *J* = 2.3 Hz, 1H), 7.85 – 7.80 (m, 2H), 7.61 (dd, *J* = 8.6, 2.3 Hz, 1H), 7.29 – 7.24 (m, 2H), 7.16 (t, *J* = 7.7 Hz, 2H), 7.02 (dd, *J* = 7.1, 1.6 Hz, 2H), 6.99 (d, *J* = 8.5 Hz, 1H), 5.87 (t, *J* = 2.2 Hz, 2H), 5.76 (t, *J* = 2.2 Hz, 2H). ^{13}C{^{1}H} NMR (100 MHz, $CDCl_3$) δ 152.7, 150.1, 140.5, 140.0, 137.5, 135.7, 134.2, 133.7, 132.3, 129.5, 129.1, 128.4, 128.1, 127.7, 127.6 (2C), 126.9 (2C), 125.4, 120.1 (2C), 119.3, 109.1 (2C). HRMS (ESI-TOF) *m*/*z*: [M + H^+] Calcd for $C_{24}H_{18}N_3$ 348.1495, Found 348.1499.

***N*-Benzyl-2-(3-phenylquinoxalin-2-yl)aniline (14).** To a stirred solution of **12aa** (100 mg, 0.33 mmol, 1.0 equiv) in ethanol (6.0 mL) in a dry 25 mL round-bottom flask was added benzaldehyde (35 mg, 0.33 mmol, 1 equiv), and a few drops of acetic acid at room temperature under an N_2 atmosphere. The resulting mixture was stirred at reflux temperature for 6 h. The precipitate was formed, which was further cooled to 0 °C, and sodium cyanoborohydride was added portion-wise over 10 min and then stirred for 2-3 h. The reaction progress was monitored by TLC. The reaction mixture was concentrated under reduced pressure and diluted with EtOAc (10 mL). The resultant mixture was washed with H_2O (3×5.0 mL). The organic layer was separated, dried over anhydrous Na_2SO_4, and concentrated under reduced pressure. Purification by column chromatography using petroleum ether/acetone (8/2) as the eluent afforded **14** as yellow solid (97 mg, 76% yield, mp = 230–233 ºC). ^{1}H NMR (400 MHz, $CDCl_3$) δ 8.20 – 8.16 (m, 1H), 8.10 – 8.06 (m, 1H), 7.80 – 7.73 (m, 2H), 7.60 – 7.57 (m, 2H), 7.38 – 7.33 (m, 3H), 7.32 – 7.28 (m, 4H), 7.24 (dd, *J* = 6.2, 2.7 Hz, 1H), 7.19 – 7.15 (m, 1H), 6.96 (dd, *J* = 7.6, 1.5 Hz, 1H), 6.71 (d, *J* = 8.1 Hz, 1H), 6.56 (td, *J* = 7.5, 0.9 Hz, 1H), 5.88 (t, 1H), 4.36 (d, *J* = 4.9 Hz, 2H). ^{13}C{^{1}H} NMR (100 MHz, $CDCl_3$) δ 154.3,153.0, 146.2, 141.1, 140.4, 139.2, 139.0, 131.8, 130.3, 130.0, 129.9, 129.5 (2C), 129.2, 128.9, 128.6 (3C), 128.2 (2C), 127.2 (2C), 127.0, 122.9, 116.8, 111.9, 47.8. HRMS (ESI-TOF) *m*/*z*: [M + H^+] Calcd for $C_{27}H_{22}N_3$ 388.1808, Found 388.1813.

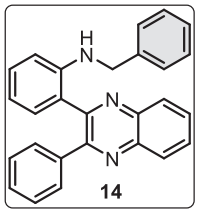

14

5-(Dimethylamino)-*N*-(2-(3-phenylquinoxalin-2-yl)phenyl)naphthalene-1-sulfonamide (16). To a stirred solution of **12aa** (100 mg, 0.33 mmol, 1.0 equiv) in DMF (5.0 mL) in a dry 25 mL round-bottom flask was added dansyl chloride (108 mg, 0.4 mmol, 1.2 equiv), and pyridine (133 μL, 1.66 mmol, 5 equiv) at room temperature under an N_2 atmosphere. The resulting mixture was stirred at reflux temperature overnight, and the reaction progress was monitored by TLC. Upon completion, the reaction mixture was quenched with H_2O (5.0 mL) and stirred with EtOAc (10 mL). The organic layer was separated, dried over anhydrous Na_2SO_4, and concentrated under reduced pressure. Purification by column chromatography using petroleum ether/EtOAc (9/1) as the eluent afforded **16** as yellow solid (110 mg, 62% yield, mp = 205-207 °C). ^{1}H NMR (400 MHz, $CDCl_3$) δ 10.26 (s, 1H), 8.25 – 8.21 (m, 2H), 8.19 (dd, *J* = 7.3, 1.2 Hz, 1H), 8.11 – 8.08 (m, 1H), 8.00 – 7.96 (m, 1H), 7.93 – 7.86 (m, 2H), 7.51 (d, *J* = 8.6 Hz, 1H), 7.36 (dd, *J* = 8.4, 7.4 Hz, 1H), 7.31 – 7.27 (m, 1H), 7.18 – 7.12 (m, 1H), 6.96 (t, *J* = 7.8 Hz, 2H), 6.73 (td, *J* = 7.7, 1.1 Hz, 1H), 6.60 (dd, *J* = 7.8, 1.4 Hz, 1H), 6.49 (d, *J* = 7.5 Hz, 1H), 6.27 – 6.21 (m, 2H), 6.03 – 5.95 (m, 1H), 2.38 (s, 6H). ^{13}C{^{1}H} NMR (100 MHz, $CDCl_3$) δ 151.7, 150.1, 140.9, 139.6, 137.7, 135.0, 134.3, 131.8, 131.0, 130.6, 130.5, 130.1, 130.0, 129.6, 129.4, 129.3 (2C), 129.2, 128.6, 128.5, 128.5, 127.7 (2C), 127.1, 125.5, 124.3, 122.6, 117.6, 114.6, 44.7 (2C). HRMS (ESI-TOF) *m*/*z*: [M + H$^+$] Calcd for $C_{32}H_{27}N_4O_2S$ 531.1849, Found. 531.1852.

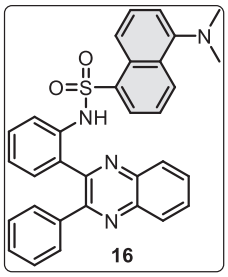

16

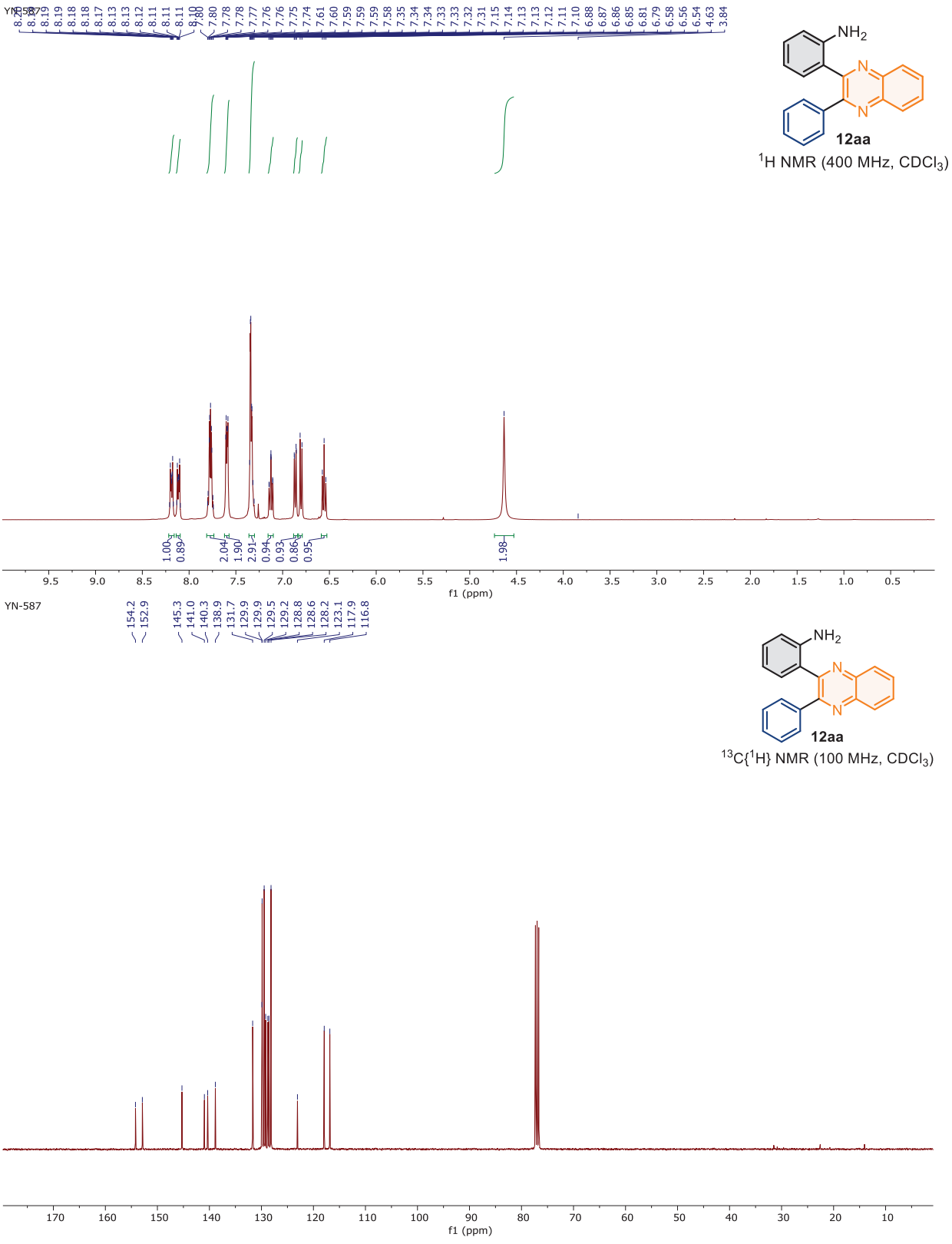

Figure 4.3. ^{1}H and ^{13}C NMR spectra of **12aa**

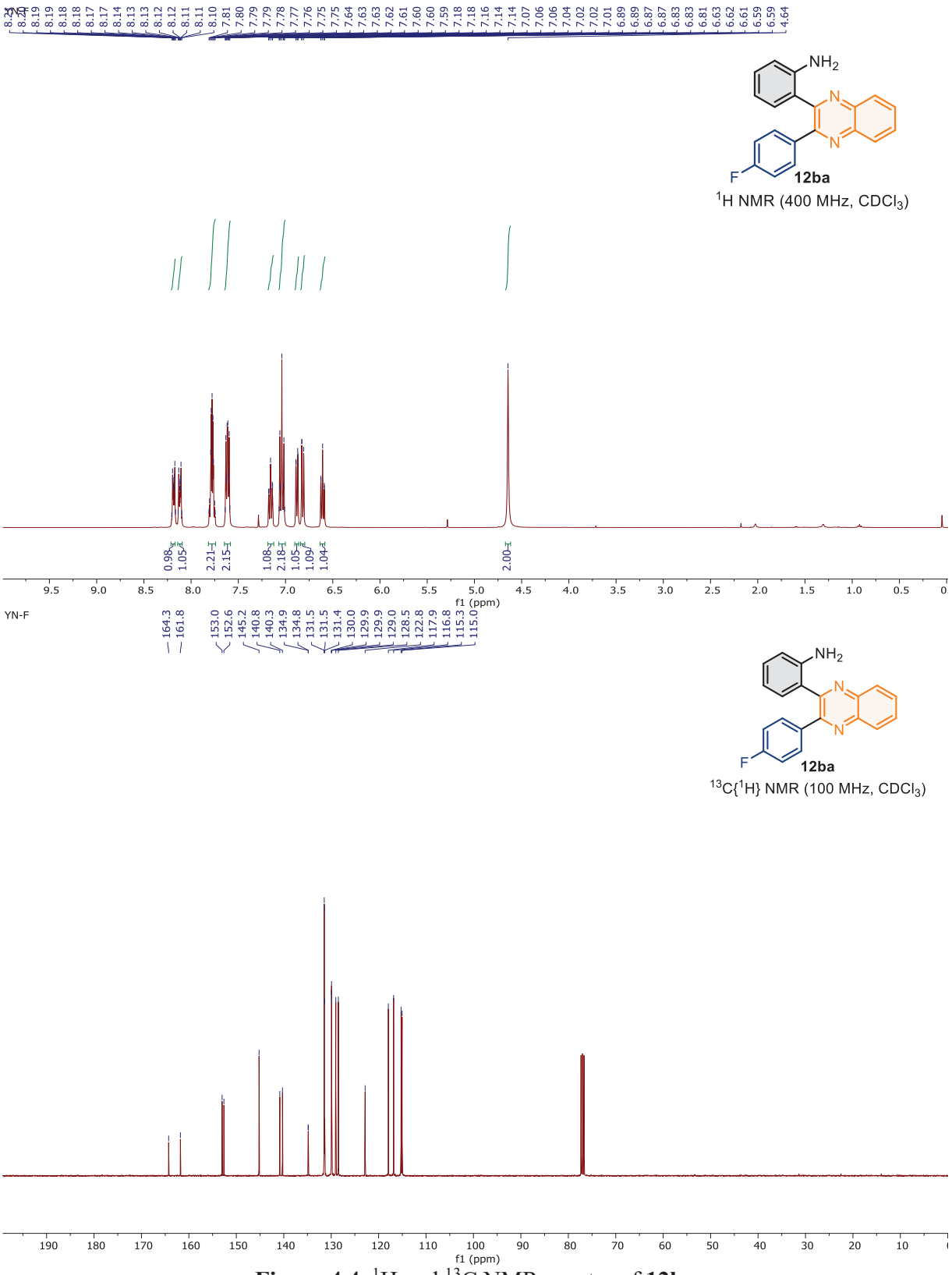

Figure 4.4. ^{1}H and ^{13}C NMR spectra of **12ba**

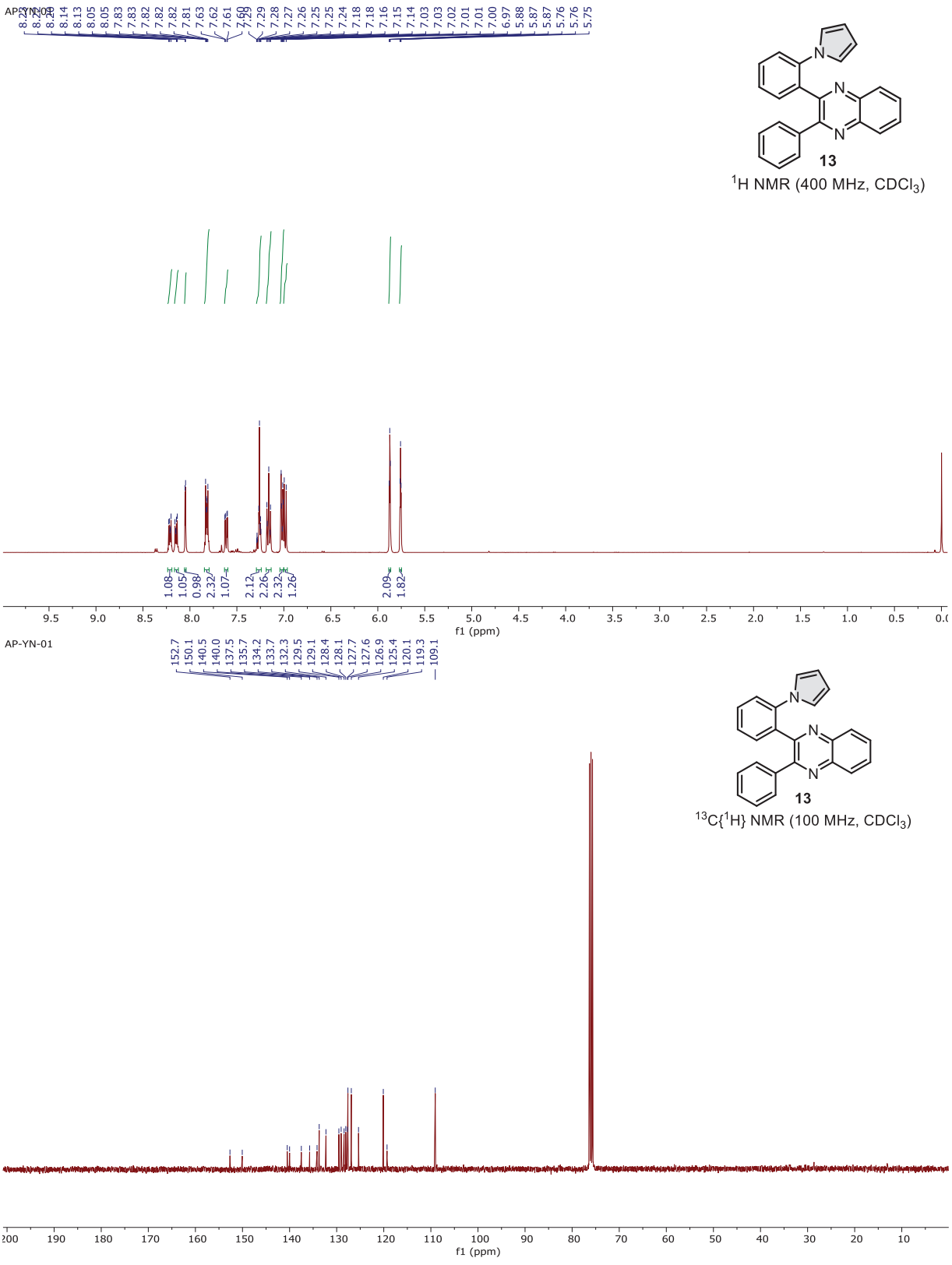

Figure 4.5. ^{1}H and ^{13}C NMR spectra of **13**

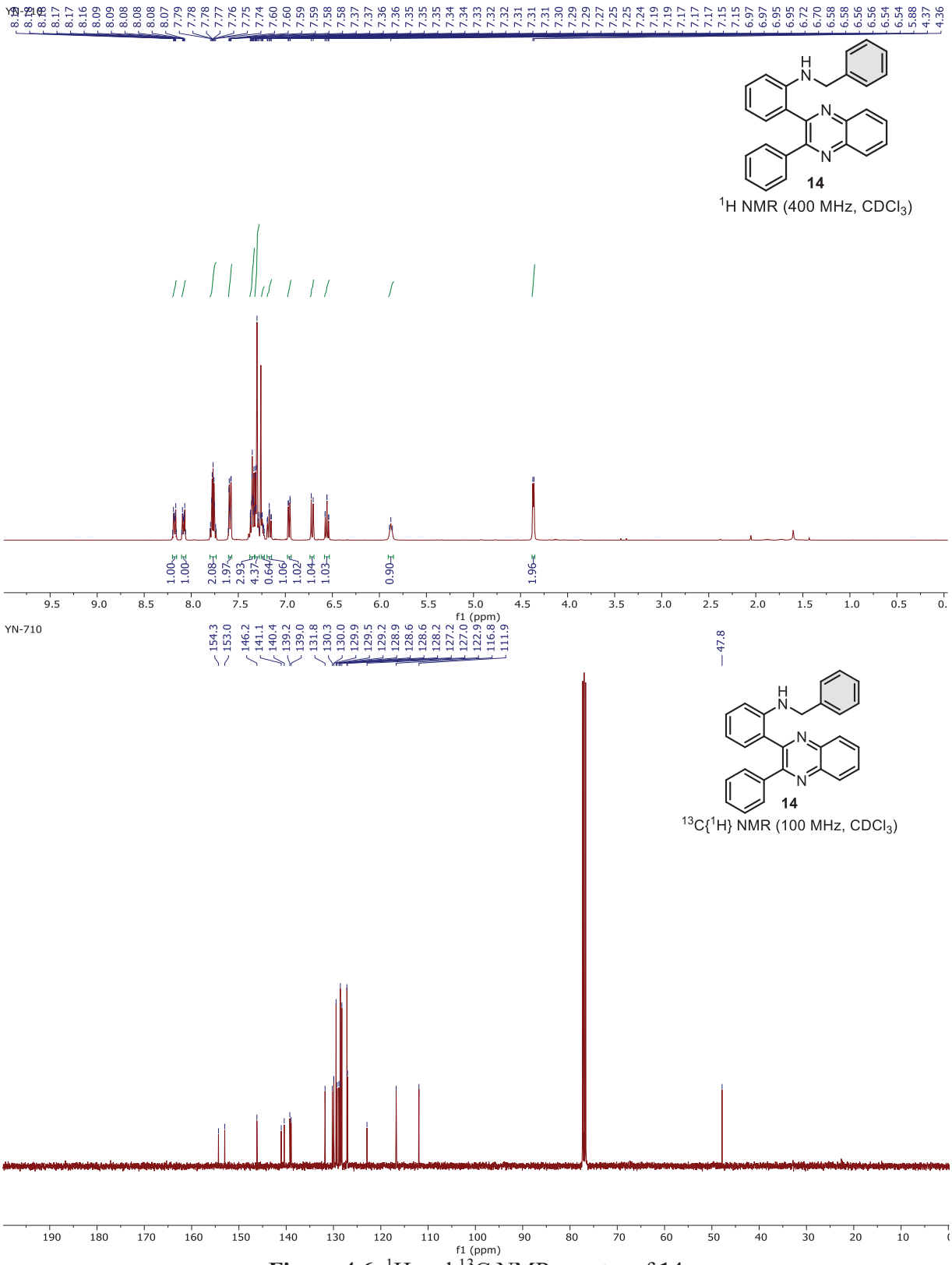

Figure 4.6. ^{1}H and ^{13}C NMR spectra of **14**

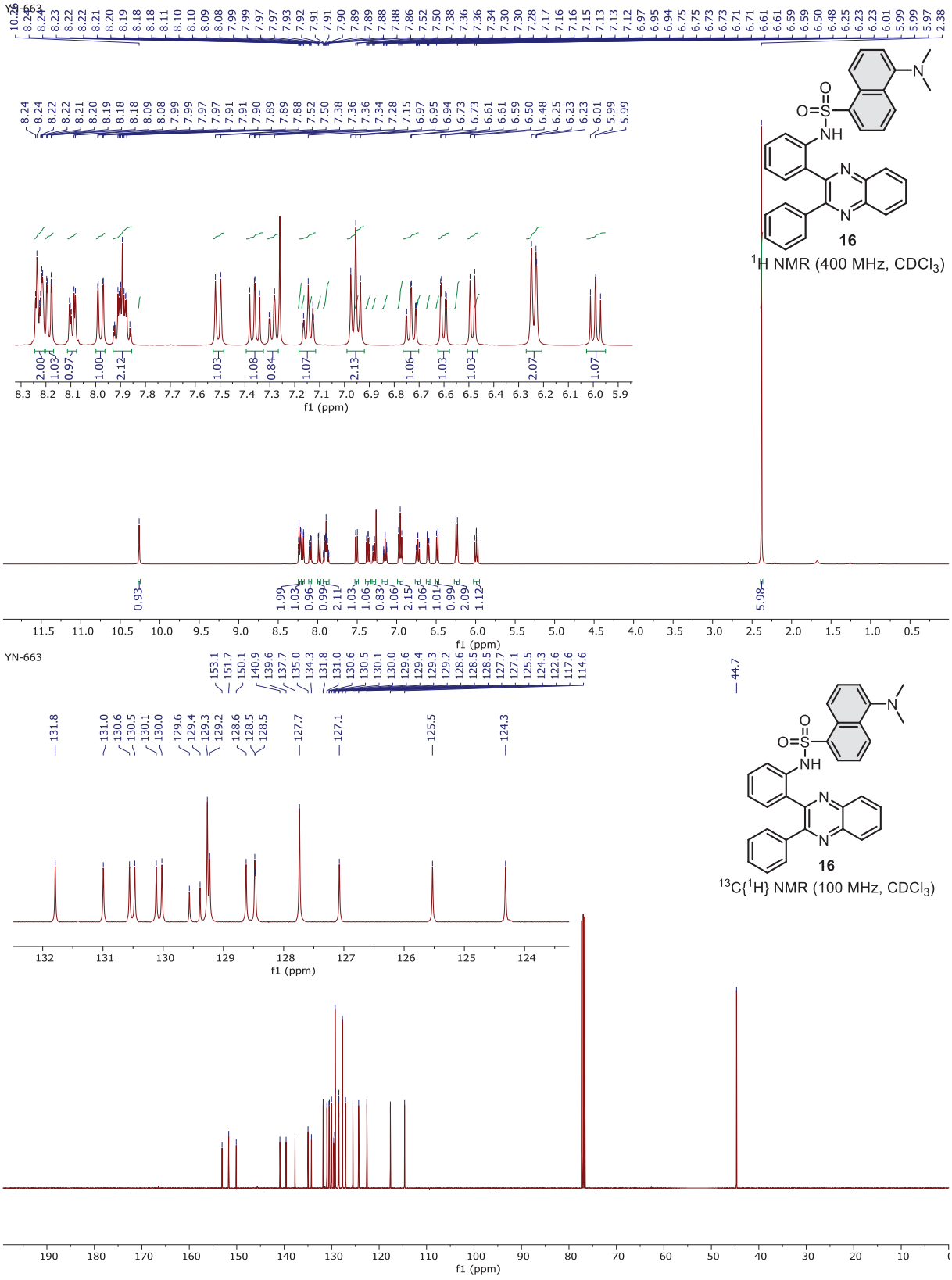

Figure 4.7. ^{1}H and ^{13}C NMR spectra of **16**

4.8 Single crystal X-ray diffraction experiment and analysis

4.8.1 Single crystal XRD experiments:

The single crystal XRD data collection and data reduction were performed using CrysAlis PRO on a single crystal Rigaku Oxford XtaLab Pro Kappa dual home/near diffractometer. The crystals were kept at 123(2) K during data collection using CuKα (λ = 1.54184 Å) radiation. Using Olex2[60], the structure was solved with the ShelXT[61] structure solution program using Intrinsic Phasing and refined with the ShelXL[62] refinement package using Least Squares minimization.

4.8.2 Single crystal structure, Cell parameters, and Structure data of compound 12aa (exp_1208_YN-587_20220910):

The compound **12aa** (**exp_1208_YN-587_20220910),** $C_{20}H_{15}N_3$, crystallized as a yellow block from the slow evaporation of the solution of this compound in $CHCl_3$:Hexane mixed solvents. The compound crystallized in a monoclinic system, $P2_1/n$ space group with following crystal data parameters, **crystal data** for $C_{20}H_{15}N_3$ (M =297.35 g/mol): monoclinic, space group $P2_1/n$ (no. 14), a = 14.4369(3) Å, b = 6.69760(10) Å, c = 16.4090(3) Å, β = 103.040(2)°, V = 1545.71(5) Å^3, Z = 4, T = 133(2) K, μ(Cu Kα) = 0.602 mm^{-1}, *Dcalc* = 1.278 g/cm^3, 8829 reflections measured (9.266° ≤ 2Θ ≤ 159.898°), 3267 unique (R_{int} = 0.0308, R_{sigma} = 0.0360) which were used in all calculations. The final R_1 was 0.0429 (I > 2σ(I)) and wR_2 was 0.1260 (all data). The crystallographic details of the compound **12aa** (**exp_1208_YN-587_20220910)** are deposited to the Cambridge Crystallographic (CCDC 2258070). The crystal data and structure refinement for compound **12aa** are shown in **Table 4.4.** The ORTEP diagram as the crystal structure of compound **12aa** (**exp_1208_YN-587_20220910)** is illustrated in **Figure 4.8**.

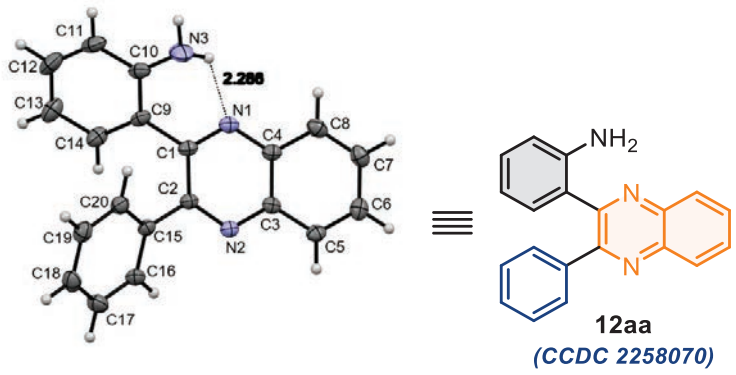

Figure 4.8. ORTEP diagram of compound **12aa** (**exp_1208_YN-587_20220910)**.

Table 4.4: Crystal data and structure refinement for compound 12aa (exp_1208_YN-587_20220910).

Identification code	exp_1208_YN-587_20220910
Empirical formula	$C_{20}H_{15}N_3$
Formula weight	297.35
Temperature/K	133(2)
Crystal system	monoclinic
Space group	$P2_1/n$
a/Å	14.4369(3)
b/Å	6.69760(10)
c/Å	16.4090(3)
α/°	90
β/°	103.040(2)
γ/°	90
Volume/Å^3	1545.71(5)
Z	4
ρ_{calc}g/cm^3	1.278
μ/mm^{-1}	0.602
F(000)	624.0
Crystal size/mm^3	0.23 × 0.14 × 0.11
Radiation	Cu Kα (λ = 1.54184)
2Θ range for data collection/°	9.266 to 159.898
Index ranges	-18 ≤ h ≤ 17, -8 ≤ k ≤ 8, -20 ≤ l ≤ 17
Reflections collected	8829
Independent reflections	3267 [R_{int} = 0.0308, R_{sigma} = 0.0360]
Data/restraints/parameters	3267/0/209
Goodness-of-fit on F^2	1.058
Final R indexes [I>=2σ (I)]	R_1 = 0.0429, wR_2 = 0.1224
Final R indexes [all data]	R_1 = 0.0465, wR_2 = 0.1260

Largest diff. peak/hole / e Å^{-3} 0.23/-0.24

4.8.3 Single crystal structure, Cell parameters, and Structure data of compound 12ag (exp_1380_YN-593_20230316):

The compound **12ag** (**exp_1380_YN-593_20230316),** $C_{20}H_{13}Br_2N_3$, crystallized as brown colour blocks from the slow evaporation of a solution of this compound in $CHCl_3$:Hexane mixed solvents. The compound crystallized in an orthorhombic system, *Pbcn* space group with following crystal data parameters, **crystal data** for $C_{20}H_{13}Br_2N_3$ (M =455.15 g/mol): orthorhombic, space group *Pbcn* (no. 60), a = 7.78610(10) Å, b = 15.7236(2) Å, c = 28.1772(4) Å, V = 3449.61(8) Å^3, Z = 8, T = 133(2) K, μ(Cu Kα) = 6.012 mm^{-1}, *Dcalc* = 1.753 g/cm^3, 12473 reflections measured (6.274° ≤ 2Θ ≤ 159.74°), 3665 unique (R_{int} = 0.0286, R_{sigma} = 0.0262) which were used in all calculations. The final R_1 was 0.0369 (I > 2σ(I)), and wR_2 was 0.0970 (all data). The crystallographic details of compound **12ag** (**exp_1380_YN-593_20230316)** are deposited to the Cambridge Crystallographic (CCDC 2258074). The crystal data and structure refinement for compound **12ag** are shown in **Table 4.5**. The ORTEP diagram as the crystal structure of compound **12ag** (**exp_1380_YN-593_20230316)** is illustrated in **Figure 4.9**.

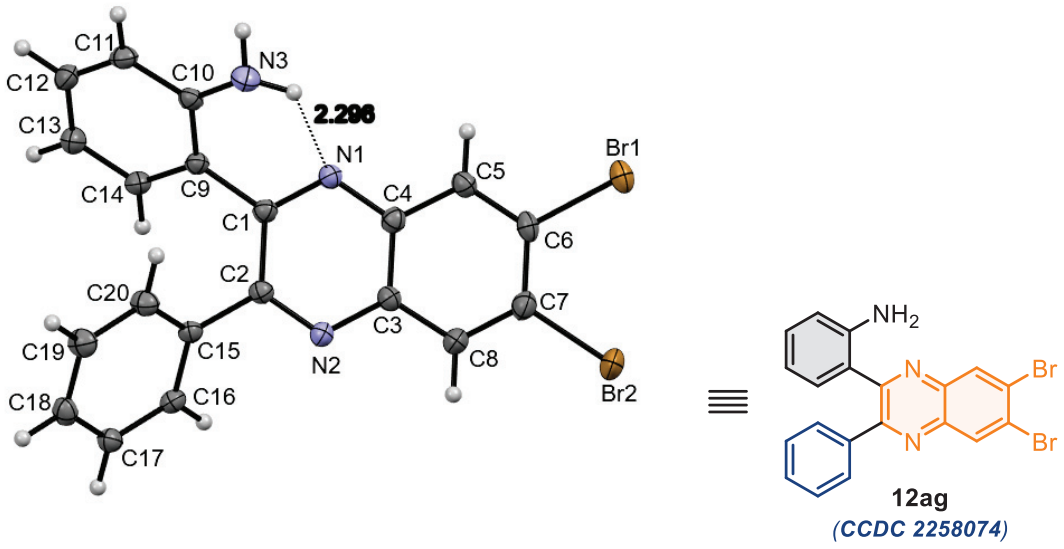

Figure 4.9. ORTEP diagram of compound **12ag** (**exp_1380_YN-593_20230316)**. The thermal ellipsoids are drawn at a 50 % probability level (CCDC 2258074).

Table 4.5: Crystal data and structure refinement for exp_1380_YN-593_20230316.

Identification code	exp_1380_YN-593_20230316
Empirical formula	$C_{20}H_{13}Br_2N_3$
Formula weight	455.15
Temperature/K	133(2)
Crystal system	orthorhombic
Space group	Pbcn
a/Å	7.78610(10)
b/Å	15.7236(2)
c/Å	28.1772(4)
α/°	90
β/°	90
γ/°	90
Volume/Å^3	3449.61(8)
Z	8
ρ_{calc}g/cm^3	1.753
μ/mm^{-1}	6.012
F(000)	1792.0
Crystal size/mm^3	0.15 × 0.1 × 0.08
Radiation	Cu Kα (λ = 1.54184)
2Θ range for data collection/°	6.274 to 159.74
Index ranges	$-9 \leq h \leq 9$, $-18 \leq k \leq 19$, $-35 \leq l \leq 28$
Reflections collected	12473
Independent reflections	3665 [R_{int} = 0.0286, R_{sigma} = 0.0262]
Data/restraints/parameters	3665/0/231
Goodness-of-fit on F^2	1.059
Final R indexes [I>=2σ (I)]	R_1 = 0.0369, wR_2 = 0.0958
Final R indexes [all data]	R_1 = 0.0384, wR_2 = 0.0970
Largest diff. peak/hole / e Å^{-3}	0.88/-0.96

4.8.4 Single crystal structure, Cell parameters, and Structure data of compound 12ak (exp_1196_YN-600_20220822):

The compound **12ak** (**exp_1196_YN-600_20220822),** $C_{22}H_{19}N_3$, crystallized as a yellow block from the slow evaporation of a solution of this compound in Hexane:DCM: Acetone mixed solvents. The compound crystallized in orthorhombic system, *Pbcn* space group with following crystal data parameters, **crystal data** for $C_{22}H_{19}N_3$ (M =325.40 g/mol): orthorhombic, space group Pbcn (no. 60), a = 7.9836(2) Å, b = 15.5913(3) Å, c = 27.5447(5) Å, V = 3428.62(12) Å^3, Z = 8, T = 133(2) K, μ(Cu Kα) = 0.585 mm^{-1}, *Dcalc* = 1.261 g/cm^3, 12029 reflections measured (6.418° ≤ 2Θ ≤ 159.162°), 3637 unique (R_{int} = 0.0366, R_{sigma} = 0.0390) which were used in all calculations. The final R_1 was 0.0461 (I > 2σ(I)) and wR_2 was 0.1286 (all data). The crystallographic details of the compound **12ak** (**exp_1196_YN-600_20220822)** are deposited to the Cambridge Crystallographic (CCDC 2258069). The crystal data and structure refinement for compound **12ak** are shown in **Table 4.6.** The ORTEP diagram as the crystal structure of compound **12ak** (**exp_1196_YN-600_20220822)** is illustrated in **Figure 4.10**.

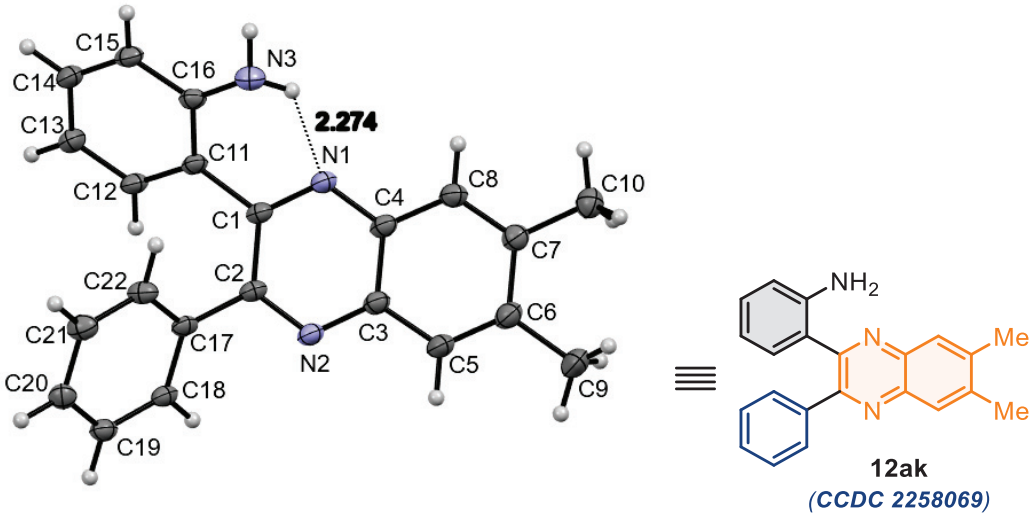

Figure 4.10. ORTEP diagram of compound **12ak** (**exp_1196_YN-600_20220822)**. The thermal ellipsoids are drawn at a 50 % probability level (CCDC 2258069).

Table 4.6: Crystal data and structure refinement for 12ak (exp_1196_YN-600_20220822).

Identification code	exp_1196_YN-600_20220822
Empirical formula	$C_{22}H_{19}N_3$

Formula weight	325.40
Temperature/K	133(2)
Crystal system	orthorhombic
Space group	Pbcn
a/Å	7.9836(2)
b/Å	15.5913(3)
c/Å	27.5447(5)
α/°	90
β/°	90
γ/°	90
Volume/Å^3	3428.62(12)
Z	8
ρ_{calc}g/cm^3	1.261
μ/mm^{-1}	0.585
F(000)	1376.0
Crystal size/mm^3	0.24 × 0.12 × 0.04
Radiation	Cu Kα (λ = 1.54184)
2Θ range for data collection/°	6.418 to 159.162
Index ranges	-10 ≤ h ≤ 8, -19 ≤ k ≤ 17, -35 ≤ l ≤ 35
Reflections collected	12029
Independent reflections	3637 [R_{int} = 0.0366, R_{sigma} = 0.0390]
Data/restraints/parameters	3637/0/229
Goodness-of-fit on F^2	1.065
Final R indexes [I>=2σ (I)]	R_1 = 0.0461, wR_2 = 0.1250
Final R indexes [all data]	R_1 = 0.0513, wR_2 = 0.1286
Largest diff. peak/hole / e Å^{-3}	0.28/-0.27

4.8.5 Single crystal structure, Cell parameters, and Structure data of compound 12al (exp_1356_YN-596_20230208):

The compound **12al** (**exp_1356_YN-596_20230208),** $C_{24}H_{17}N_3$, crystallized as a yellow block from the slow evaporation of solution of this compound in $CHCl_3$:Hexane mixed solvents. The compound crystallized in monoclinic system, $P2_1/c$ space group with following crystal data parameters, **crystal data** for $C_{24}H_{17}N_3$ (M =347.40 g/mol): monoclinic, space group $P2_1/c$ (no. 14), a = 14.8628(3) Å, b = 8.07630(10) Å, c = 15.5078(3) Å, β = 107.770(2)°, V = 1772.69(6) Å^3, Z = 4, T = 133(2) K, μ(Cu Kα) = 0.606 mm^{-1}, *Dcalc* = 1.302 g/cm^3, 9743 reflections measured (11.704° ≤ 2Θ ≤ 159.726°), 3733 unique (R_{int} = 0.0329, R_{sigma} = 0.0369) which were used in all calculations. The final R_1 was 0.0399 (I > 2σ(I)), and wR_2 was 0.1081 (all data). The crystallographic details of the compound **12al** (**exp_1356_YN-596_20230208)** are deposited to the Cambridge Crystallographic (CCDC 2258072). The crystal data and structure refinement for compound **12al** are shown in **Table 4.7.** The ORTEP diagram as the crystal structure of compound **12al** (**exp_1356_YN-596_20230208)** is illustrated in **Figure 4.11.**

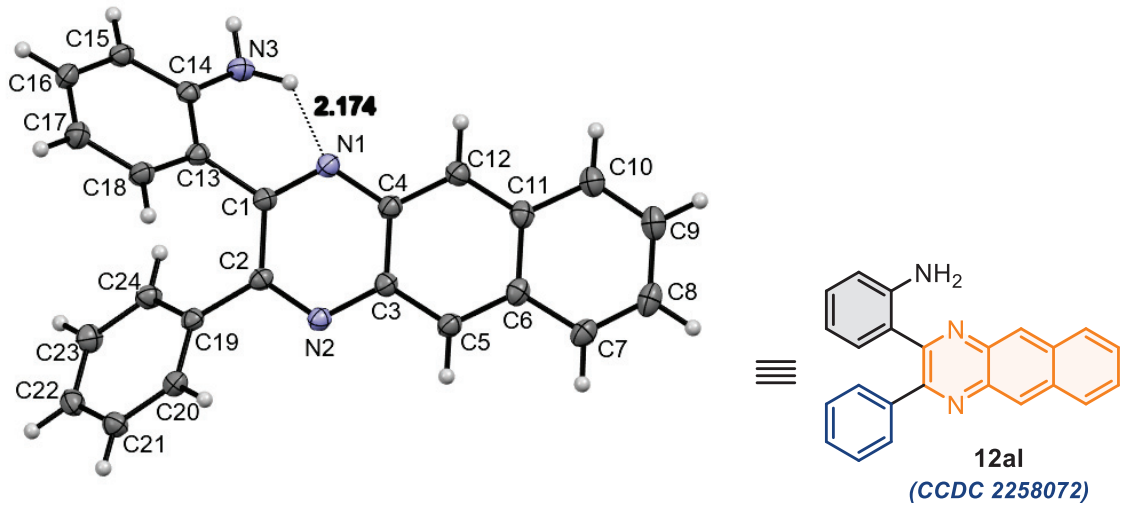

Figure 4.11. ORTEP diagram of compound **12al** (**exp_1356_YN-596_20230208)**. The thermal ellipsoids are drawn at 50 % probability level (CCDC 2258072).

Table 4.7: Crystal data and structure refinement for 12al (exp_1356_YN-596_20230208).

Identification code	exp_1356_YN-596_20230208
Empirical formula	$C_{24}H_{17}N_3$
Formula weight	347.40
Temperature/K	133(2)

Crystal system	monoclinic
Space group	$P2_1/c$
a/Å	14.8628(3)
b/Å	8.07630(10)
c/Å	15.5078(3)
α/°	90
β/°	107.770(2)
γ/°	90
Volume/Å^3	1772.69(6)
Z	4
ρ_{calc}g/cm^3	1.302
μ/mm^{-1}	0.606
F(000)	728.0
Crystal size/mm^3	0.16 × 0.09 × 0.06
Radiation	Cu Kα (λ = 1.54184)
2Θ range for data collection/°	11.704 to 159.726
Index ranges	-18 ≤ h ≤ 18, -9 ≤ k ≤ 9, -17 ≤ l ≤ 19
Reflections collected	9743
Independent reflections	3733 [R_{int} = 0.0329, R_{sigma} = 0.0369]
Data/restraints/parameters	3733/0/249
Goodness-of-fit on F^2	1.066
Final R indexes [I>=2σ (I)]	R_1 = 0.0399, wR_2 = 0.1050
Final R indexes [all data]	R_1 = 0.0442, wR_2 = 0.1081
Largest diff. peak/hole / e Å^{-3}	0.14/-0.24

4.9 References

1. Lindsley, C. W.; Zhao, Z.; Leister, W. H.; Robinson, R. G.; Barnett, S. F.; Defeo-Jones, D.; Jones, R. E.; Hartman, G. D.; Huff, J. R.; Huber, H. E.; Duggan, M. E. *Bioorg. Med. Chem. Lett*. **2005**, *15*, 761–764.

2. Dolle, R. E.; Le Bourdonnec,B.; Morales, G. A.; Moriarty, K. J.; Salvino, J. M. 2005. *J. Comb. Chem*. **2006**, *8*, 597–635.
3. Koch, P.; Jahns, H.; Schattel, V.; Goettert, M.; Laufer, S. *J. Med. Chem*. **2010**, *53*, 1128–1137.
4. Cogo, J.; Kaplum, V.; Sangi, D. P.; Ueda-Nakamura, T.; Corrêa, A. G.; Nakamura, C. V. *Eur. J. Med. Chem*. **2015**, *90*, 107–123.
5. Sagar, S. R.; Singh, D. P.; Das, R. D.; Panchal, N. B.; Sudarsanam, V.; Nivsarkar, M.; Vasu, K. K. *Bioorg. Chem*. **2019**, *89*, 102992–102999.
6. Ingle, R.; Marathe, R.; Magar, D.; Patel, H. M.; Surana, S. J. *Eur. J. Med. Chem*. **2013**, *65*, 168–186.
7. Kazunobu, T.; Ryusuke, T.; Tomohiro, O.; Shuichi, M. *Chem. Commun*. **2002**, 212–213.
8. Hegedus, L. S.; Greenberg, M. M.; Wendling, J. J.; Bullock, J. P. *J. Org, Chem*. **2003**, *68*, 4179–4188.
9. Yuan, J.; Ouyang, J.; Cimrová, V.; Leclerc, M.; Najari, A.; Zou, Y. *J. Mater. Chem. C* **2017**, *5*, 1858–1879.
10. Jung, C. Y.; Song, C. J.; Yao, W.; Park, J. M.; Hyun, I. H.; Seong, D. H.; Jaung, J. Y. *Cell. Dyes Pigm*. **2015**, *121*, 204–210.
11. Yashwantrao, G.; Saha, S. *Org. Chem. Front.* **2021**, *8*, 2812–2820.
12. Kumar, A.; Dhameliya, T. M.; Shar.ma, K.; Patel, K. A.; Hirani, R. V.; Bhatt, A. J. *J. Mol. Stru.* **2021**, *1259*, 132732–132738.
13. Borah, B.; Chowhan, L. R. *RSC Adv*., **2021**, *11*, 37325–37353.
14. Biesen, L.; Müller, T. J. J. *Adv. Synth. Catal*., **2021**, *363*, 980–1006.
15. Elumalai, V.; Hansen, J. H. *SynOpen* **2021**, *5*, 43–48.
16. Lassagne, F.; Chevallier, F.; Roisnel, T.; Dorcet, V.; Mongin, F.; Domingo, L. R. *Synthesis* **2015**, *47*, 2680–2689.
17. Cai, J.-J.; Zou, J.-P.; Pan, X.-Q.; Zhang, W. *Tetrahedron Lett.* **2008**, *49*, 7386–7390.
18. More, S. V.; Sastry, M. N. V.; Yao, C.-F. *Green Chem.* **2006**, *8*, 91–95.
19. Lupidi, G.; Palmieri, A.; Petrini, M. *Green Chem*., **2022**, *24*, 3629–3633.
20. Wu, J.; Darcel, C. *J. Org. Chem*. **2021**, *86*, 1023–1036.

21. Wang, Y.-B.; Shi, L.; Zhang, X.; Fu, L.-R.; Hu, W.; Zhang, W.; Zhu, X.; Hao, X.-Q.; Song, M.-P. *J. Org. Chem.* **2021**, *86*, 947–958.
22. Shee, S.; Panja, D.; Kundu, S. *J. Org. Chem*. **2020**, *85*, 2775–2784.
23. Climent, M. J.; Corma, A.; Hernández, J. C.; Hungría, A. B.; Iborra, S.; Martínez-Silvestre, S. *J. Catal*. **2012**, *292*, 118–129.
24. Paul, S.; Basu, B. *Tetrahedron Lett.* **2011**, *52*, 6597–6602.
25. Sithambaram, S.; Ding, Y.; Li, W.; Shen, X.; Gaenzler, F.; Suib, S. L. *Green Chem*. **2008**, *10*, 1029–1032.
26. Wadavrao, S. B.; Ghogare, R. S.; Narsaiah, A. V. *Org. Commun*. **2013**, *6*, 23–30.
27. Wan, J.-P.; Gan, S.-F.; Wu, J.-M.; Pan, Y. *Green Chem*. **2009**, *11*, 1633–1637.
28. Nagarapu, L.; Mallepalli, R.; Arava, G.; Yeramanchi, L. *Eur. J. Chem*. **2010**, *1*, 228–231.
29. Ghosh, P.; Mandal, A. *Tetrahedron Lett*. **2012**, *53*, 6483–6488.
30. Madhav, B.; Murthy, S. N.; Reddy, V. P.; Rao, K. R.; Nageswar, Y. V. D. *Tetrahedron Lett*. **2009**, *50*, 6025–6028.
31. Wang, W.; Shen, Y.; Meng, X.; Zhao, M.; Chen, Y.; Chen, B. *Org. Lett.* **2011**, *13*, 4514–4517.
32. Okumura, S.; Takeda, Y.; Kiyokawa, K.; Minakata, S. *Chem. Commun*. **2013**, *49*, 9266–9268.
33. Shi, S.; Wang, T.; Yang, W.; Rudolph, M.; Hashmi, A. S. K. *Chem. - Eur. J*. **2013**, *19*, 6576–6580.
34. Chen, C.-Y.; Hu, W.-P.; Liu, M.-C.; Yan, P.-C.; Wang, J.-J.; Chung, M.-I. *Tetrahedron* **2013**, *69*, 9735–9741.
35. Viswanadham, K. K. D. R.; Reddy, M. P.; Sathyanarayana, P.; Ravi, O.; Kant, R.; Bathula, S. R. *Chem. Commun*. **2014**, *50*, 13517–13520.
36. Wang, Z.; Hu, G.; Liu, J.; Liu, W.; Zhang, H.; Wang, B. *Chem. Commun.* **2015**, *51*, 5069–5070.
37. Venkatesh, C.; Singh, B.; Mahata, P. K.; Ila, H.; Junjappa, H. *Org. Lett*. **2005**, *7*, 2169–2172.
38. Suzuki, Y.; Takehara, R.; Miura, K.; Ito, R.; Suzuki, N. *J. Org. Chem*. **2021**, *86*, 16892–16900.
39. Lal, S.; Snape, T. J. *Curr. Med. Chem.* **2012**, *19*, 4828–4837.

40. Yamashita, M.; Iida, A. *Tetrahedron Lett.* **2014**, *55*, 2991–2993.
41. Cao, W. B.; Chu, X. Q.; Zhou, Y.; Yin, L.; Xu, X. P.; Ji, S. J. *Chem. Commun.* **2017**, *53*, 6601–6604.
42. Cao, W.-B.; Liu, B.-B.; Xu, X.-P.; Ji, S.-J. *Org. Chem. Front.* **2018**, *5*, 1194–1201.
43. Xu, M. M.; Cao, W. B.; Xu, X. P.; Ji, S. J. *Chem. Commun.* **2018**, *54*, 12602–12605.
44. Chen, Y.-H.; Yang, J.; Lu, Z.-H.; Zhao, K.-H.; Xie, Q.-Y.; Yan, S.-J. *Chem. Commun*. **2023**, *59*, 1217–1220.
45. Patel, O. P. S.; Dhiman, S.; Khan, S.; Shinde, V. N.; Jaspal, S.; Srivathsa, M. R.; Jha, P. N.; Kumar, A. *Org. Biomol. Chem*. **2019**, *17*, 5962–5970.
46. Zhang, L.-L.; Cao, W.-B.; Xu, X.-P.; Ji, S.-J. *Org. Chem. Front*. **2019**, *6*, 1787–1795.
47. Yan, J.; Zheng, L.; Wang, J.; Liu, X.; Hu. Y. *J. Org. Chem*. **2022**, *87*, 6347–6351.
48. Kingston, C.; Palkowitz, M. D.; Takahira, Y.; Vantourout, J. C.; Peters, B. K.; Kawamata, Y.; Baran, P. S. *Acc. Chem. Res*. **2020**, *53*, 72–83.
49. Siu, J. C.; Fu, N.; Lin, S. *Acc. Chem. Res*. **2020**, *53*, 547–560.
50. Pollok, D.; Waldvogel, S. R. *Chem. Sci*. **2020**, *11*, 12386–12400.
51. Zhu, C.; Ang, N. W. J.; Meyer, T. H.; Qiu, Y.; Ackermann, L. *ACS Cent. Sci*. **2021**, *7*, 415–431.
52. Yuan, Y.; Yang, J.; Lei, A. *Chem. Soc. Rev*. **2021**, *50*, 10058–10086.
53. (a) C. A. Malapit, M. B. Prater, J. R. Cabrera-Pardo, M. Li, T. D. Pham, T. P. McFadden, S. Blank, S. D. Minteer, *Chem. Rev*. **2022**, *122*, 3180–3218. (b) Wan, Q.; Zhang, Z.; Hou, Z.-W.; Wang, L. **2023**, 10, 2830–2848. (c) Zhang, Z.; Hou, Z.-W.; Chen, H.; Li, P.; Wang, L. *Green Chem*., **2023**, 25, 3543–3548.
54. Lu, F.-Y.; Chen, Y.-J.; Chen, Y.; Ding, X.; Guan, Z.; He, Y.-H. *Chem. Commun*. **2020**, *56*, 623–626.
55. Long, C.-J.; Cao, H.; Zhao, B.-K.; Tan, Y.-F.; He, Y.-H.; Huang, C.-S.; Zhi Guan, Z. *Angew Chem. Int. Ed*. **2022**, *61*, e202203666.
56. Nagare, Y. K.; Shah, I. A.; Yadav, J.; Pawar, A. P.; Rangan, K.; Choudhary, R.; Iype, E.; Kumar, I. *J. Org. Chem*. **2022**, *87*, 15771–15782.

57. An identical X-ray structure was reported: Aksenov, A.V.; Arutiunov, N.A.; Aksenov, D.A.; Samovolov, A.V.; Kurenkov, I.A.; Aksenov, N.A.; Aleksandrova, E.A.; Momotova, D.S.; Rubin, M. *Int. J. Mol. Sci*. **2022**, *23*, 11120.
58. The X-ray crystallographic structure for compounds **12aa**, **12ag**, **12ak**, and **12al** have been deposited at the Cambridge Crystallographic Data Centre (CCDC) under deposition numbers (CCDC 2258070, 2258074, 2258069, and 2258072), respectively.
59. Slätt, J.; Bergman, J. *Tetrahedron* **2002**, *58*, 9187–9191.
60. Dolomanov, O.V., Bourhis, L.J., Gildea, R.J, Howard, J.A.K. & Puschmann, H. (**2009**), *J. Appl. Cryst*. *42*, 339–341.
61. Sheldrick, G.M. (**2015**). *Acta Cryst*. A71, 3–8.
62. Sheldrick, G.M. (**2015**). *Acta Cryst*. C71, 3–8.

CHAPTER 5

Electrochemical Oxidative [4 + 2] Annulation between Cyclic Ketimines and Tertiary Anilines for the Synthesis of Dihydroindolo[1,2-*c*]quinazolin-12(6*H*)-one

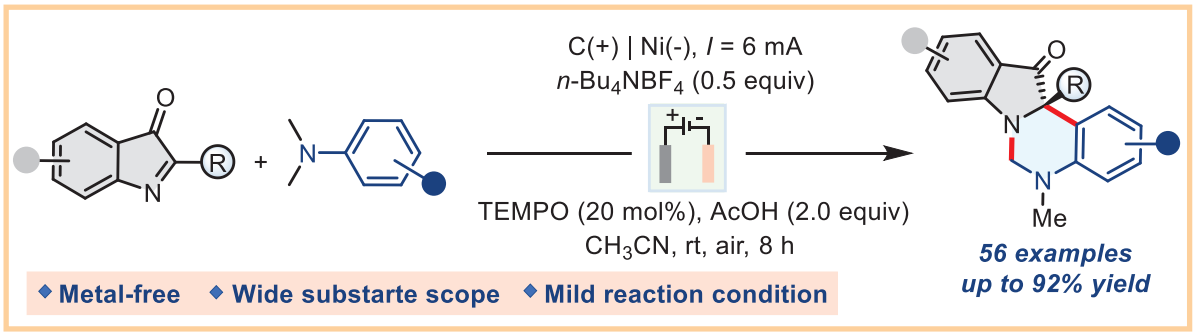

5.1 Introduction

Poly-Heterocycles are frequently found in bioactive natural products and have been intensively studied as drug candidates, such as indolo[1,2-*c*]quinazoline, a kind of tetracyclic heterocycle, features a fusion of indole and quinazoline rings. The indolo[1,2-c]quinazoline is the core structure of various natural products and artificial compounds possessing potent anticancer, anti-inflammatory, antimalarial, antiviral activities, and organic photoelectric properties.[1-12] Some representative examples of this aspect are shown in **Figure 5.1**.

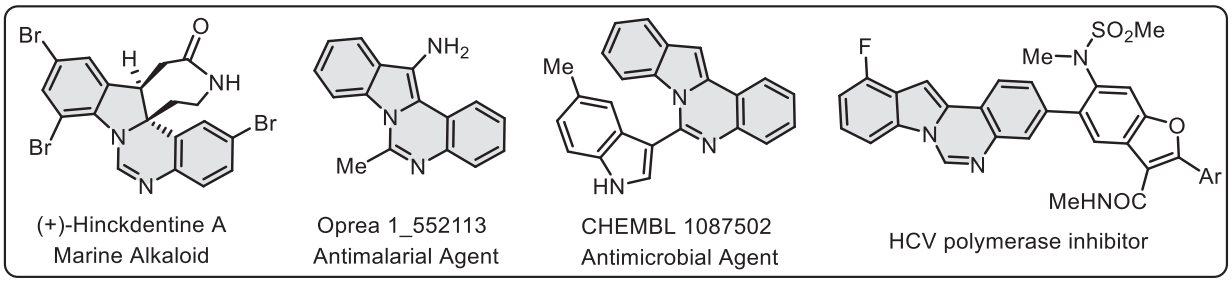

Figure 5.1: Selected natural products and bioactive compounds having indolo[1,2-c]quinazoline as a core unit

Due to the high synthetic and biological importance of indolo[1,2-*c*]quinazoline, several methods have been developed to access this scaffold. The indolo[1,2-*c*]quinazoline can be prepared in two forms: *(i) unsaturated and (ii) saturated* ones **(Figure 5.2)**. The synthesis of unsaturated indolo[1,2-*c*]quinazoline moieties is well-explored, but no report has been found for saturated indolo[1,2-*c*]quinazoline unit.

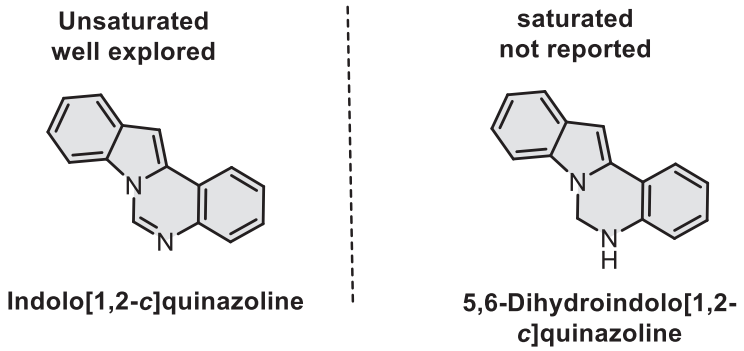

Figure 5.2 Two forms of indolo[1,2-*c*]quinazoline unit

5.2 Synthesis of unsaturated indolo[1,2-*c*]quinazoline unit

In this direction, Wu and colleagues discovered an effective two-step procedure for the synthesis of substituted 6-trifluoro methyl indolo[1,2-*c*]quinazolines from *N*-(2-iodophenyl) trifluoro

acetimidoyl chlorides and indoles *via* addition-elimination and subsequent palladium-catalyzed arylation. When the 2-position of indole was blocked by substitutions, a seven-membered ring was created instead. This methodology's application was proved by the quick synthesis of additional trifluoromethylated polyheterocycles by Friedel-Crafts reaction/C-H bond functionalization utilizing *N*-(2-iodophenyl)trifluoroacetimidoyl chlorides as building blocks **(Scheme 5.1)**.[13]

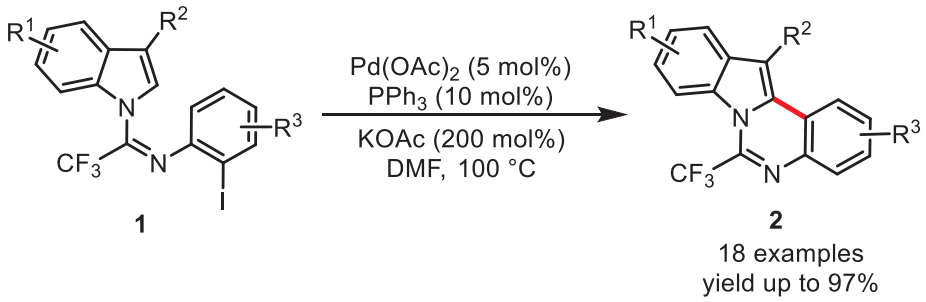

Scheme 5.1 Pd-catalyzed synthesis of 6-trifluoromethylindolo[1,2-*c*]quinazolines

Zhang and co-workers developed a simple and efficient copper-catalyzed method for the synthesis of indolo[1,2-*c*]quinazoline derivatives **(5)**. In this protocol, air acts as the oxidant, cheap $Cu(OAc)_2$ as the catalyst, and readily available 2-(2-halophenyl)-1*H*-indoles **(3)** and (aryl)methanamines **(4)** as the starting materials without the use of ligands. The accessibility and generality of this process make it highly valuable because of the medicinal importance of these polyheterocycles **(Scheme 5.2)**.[14]

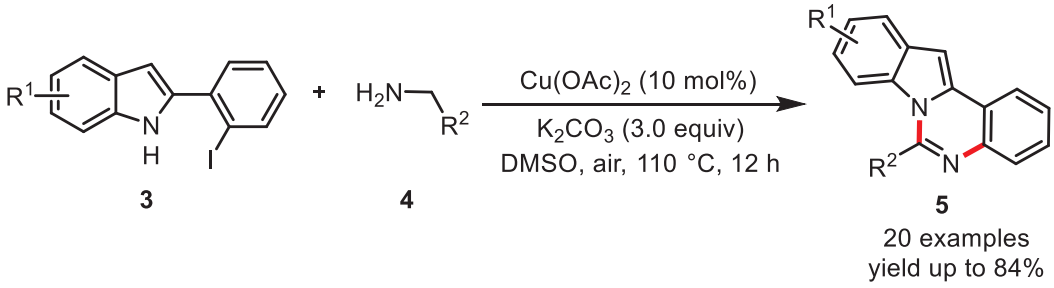

Scheme 5.2 Cu-catalyzed synthesis of indolo[1,2-*c*]quinazoline

Yao's groups reported an alternative methodology to construct the indolo[1,2-*c*]quinazoline framework based on a zinc bromide-promoted domino sequence involving 5-*endo-dig* hydroamination and intramolecular cyclization between the indole nitrogen with an amide group. The procedure includes mild conditions, benign functional group tolerance, and non-

indole starting materials to create a variety of indolo[1,2-*c*]quinazoline derivatives **(Scheme 5.3)**.[15]

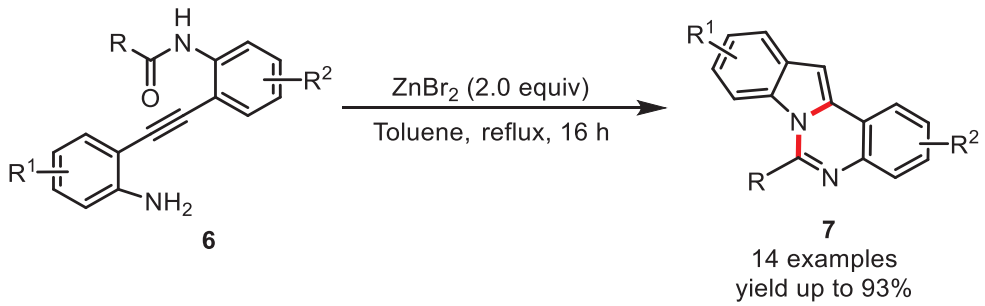

Scheme 5.3 $ZnBr_2$-promoted synthesis of indolo[1,2-c]quinazoline

Guo *et al.* developed an efficient and general strategy for the selective synthesis of indolo[1,2-*c*]quinazoline derivatives *via* copper-catalyzed one-pot sequential reactions of 2-(2-bromoaryl)-1*H*-indoles, aldehydes, and aqueous ammonia. This synthetic route exhibits high efficiency and regioselectivity, readily obtainable starting materials, and operational simplicity **(Scheme 5.4)**.[16]

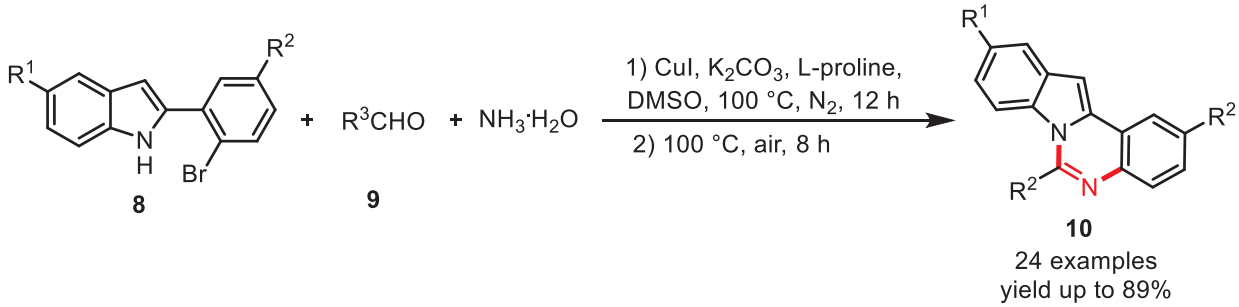

Scheme 5.4 Cu-catalyzed synthesis of indolo[1,2-c]quinazoline

Fan and co-workers reported a protocol for the selective synthesis of indolo[1,2-*c*]quinazolines *via* the copper-catalyzed intramolecular *N*-cyclization reaction under acidic conditions. Notably, the selectivity of the reaction is exclusively dependent on the reaction solvents. With DMF as the reaction solvent, the indole substrates undergo a selective C3-oxygenation reaction to give 3*H*-indol-3-ones as the main products, whereas, with 1,4-dioxane as the reaction medium, indolo[1,2-*c*]quinazolines are selectively obtained *via* an intramolecular indolyl N1-cyclization **(Scheme 5.5)**.[17]

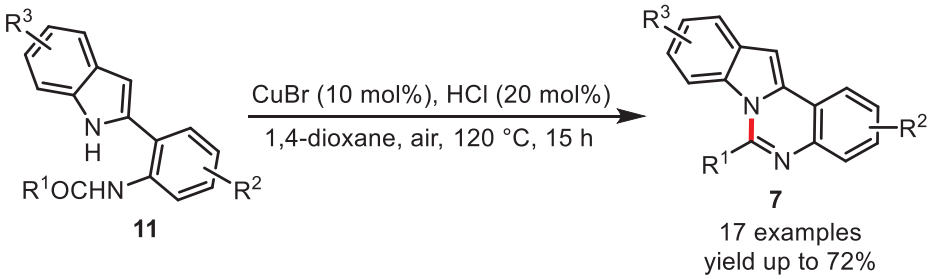

Scheme 5.5 Cu-catalyzed intramolecular indolyl N1-cyclization for indolo[1,2-*c*]quinazoline synthesis

Szostak's groups reported an Rh-catalyzed synthesis of indolo[1,2-*c*]quinazolines through direct C–H amidation and intramolecular N–H/N–C(O) cyclization of broadly available 2-aryl-1*H*-indoles with dioxazolones. This mild and effective method provides the most straightforward platform for the synthesis of indolo[1,2-*c*]quinazolines discovered to date. The reaction had a broad scope concerning 2-arylindoles **(12)** and dioxazolone **(13)**. The reaction occurs with excellent atom economy, producing H_2O and CO_2 as byproducts while avoiding substrate prefunctionalization **(Scheme 5.6)**.[18]

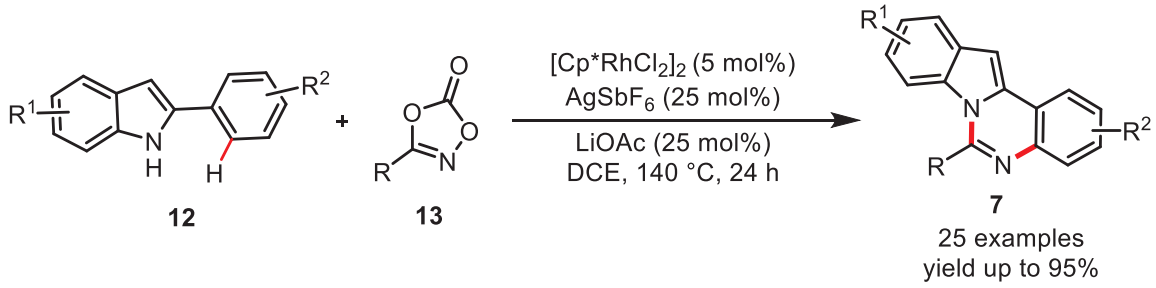

Scheme 5.6 Rh-catalyzed synthesis of indolo[1,2-*c*]quinazolines

Fan and co-workers reported a reaction condition-controlled selective synthesis of indolo[1,2-*c*]quinazolines **(16)** through the cascade reaction of 2-(1*H*-indol-2-yl)anilines **(14)** with sulfoxonium ylides **(15)**. The formation of products involves the generation of a carbene species from sulfoxonium ylide and its N–H bond insertion reaction with 2-(1*H*-indol-2-yl)aniline followed by deoxygenative imine formation, intramolecular nitrogen or carbon nucleophilic addition and deoxygenative aromatization **(Scheme 5.7)**.[19]

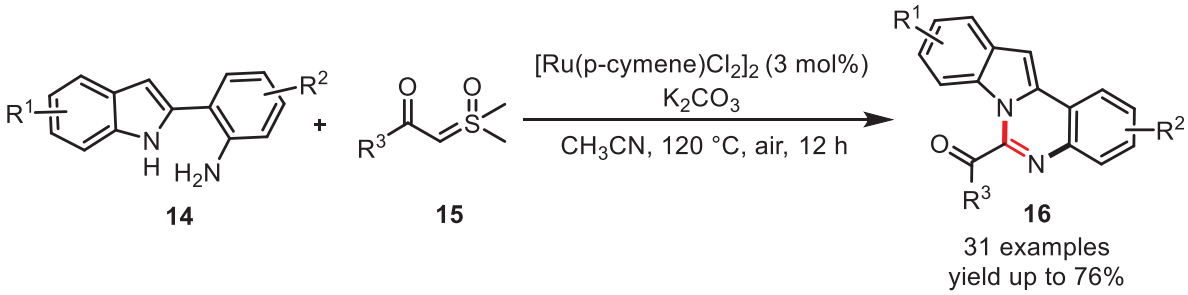

Scheme 5.7 Ru-catalyzed synthesis of indolo[1,2-*c*]quinazolines

5.3 Photo-/electro-induced [4 + 2] annulation of tertiary anilines with dienophiles (alkene)

5.3.1 Photo-induced [4 + 2] annulation

In this context, in 2012, Bian and co-workers demonstrated the $Ru(bpy)_3Cl_2$-mediated visible light irradiation method for the preparation of tetrahydroquinoline **(19)** compounds from tertiary anilines **(17)** and *N*-arylmaleimides **(18)**. This protocol is advantageous in terms of high catalytic efficiency and easy operation. This reaction is initiated by the single electron transfer from amine **(17)** to the photo-excited $Ru(bpy)_3Cl_2$, which generates the α-aminoalkyl radical. $Ru(bpy)_3(II)^*$ is reduced to $Ru(bpy)_3(I)$ at the same time. Then, α-aminoalkyl radical is reacted with *N*-phenyl maleimide **(18)** via a radical addition process, and the latter then undergoes cyclization followed by aerobic oxidation, finally providing the annulated tetrahydroisoquinoline **(19)** product **(Scheme 5.8)**. The catalyst $Ru(bpy)_3(II)$ is regenerated from $Ru(bpy)_3(I)$ via aerobic oxidation. This work serves as a new illustration that visible light photocatalysis will enhance the value of α-aminoalkyl radicals in organic synthesis.[20]

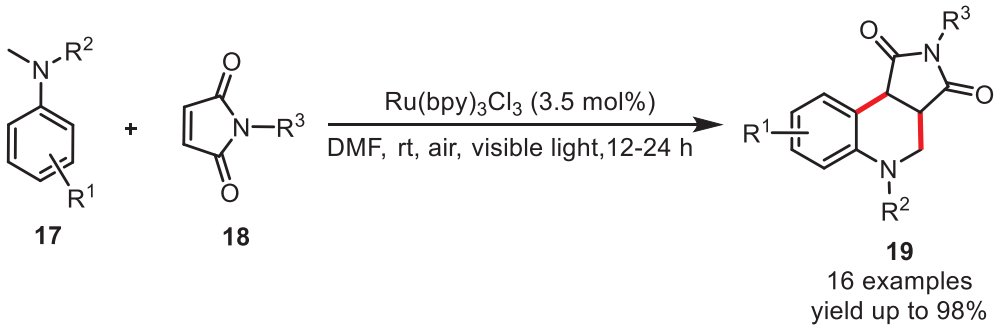

Scheme 5.8 Ruthenium-catalyzed visible-light-mediated synthesis of tetrahydroquinolines

Zhu *et al.* have explored visible light photoredox-catalyzed intermolecular C–H functionalization reactions of tertiary amines **(17)**. In this reaction, oxygen acts as a chemical switch to trigger a radical addition/cyclization reaction that resulted in the formation of

tetrahydroquinoline **(21)** derivatives in good yields under mild reaction conditions **(Scheme 5.9)**.[21] This reaction follows the same mechanism pathway as discussed in **Scheme 5.1.**

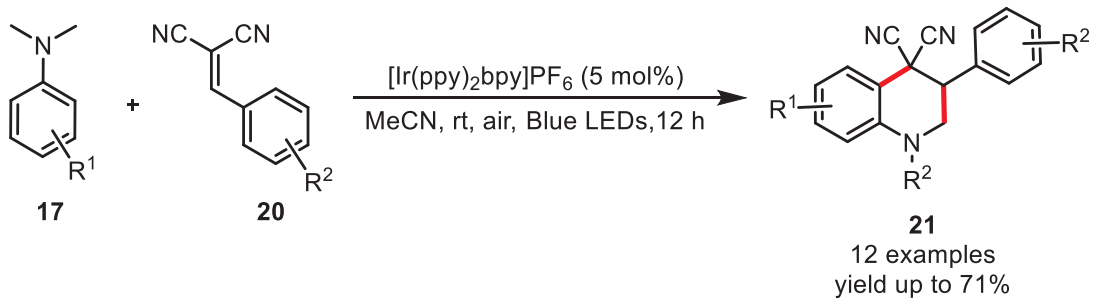

Scheme 5.9 Visible-light promoted iridium-catalyzed synthesis of tetrahydroquinolines

In 2015, Shen's group discovered a surface-modified titanium dioxide (TiO_2/NiO) which acts as an excellent visible light-responsive photocatalyst in sp^3 C-H bond activation in tertiary amines to execute direct cyclization between a wide variety of tertiary anilines **(17)** and maleimides **(18)**. This is the first time that surface-modified TiO_2 has been used for a purpose other than environmental protection to selectively accelerate synthetic organic processes. As per previously reported TiO_2-catalyzed organic reactions that typically use a stoichiometric amount of conventional unmodified TiO_2 (Degussa P25) in combination with UVA light, the extended absorption in the visible light region and the reduced hole–electron pair recombination of the NiO surface-modified catalysts allow them to be used in a catalytic amount as small as 1 mol % together with visible light irradiation to achieve high catalytic efficiency **(Scheme 5.10)**. Furthermore, the high thermal and photochemical stability of these modified photocatalysts enables them to be quickly recovered by centrifugation and reused at least nine times without significant decay of the catalytic activity.[22]

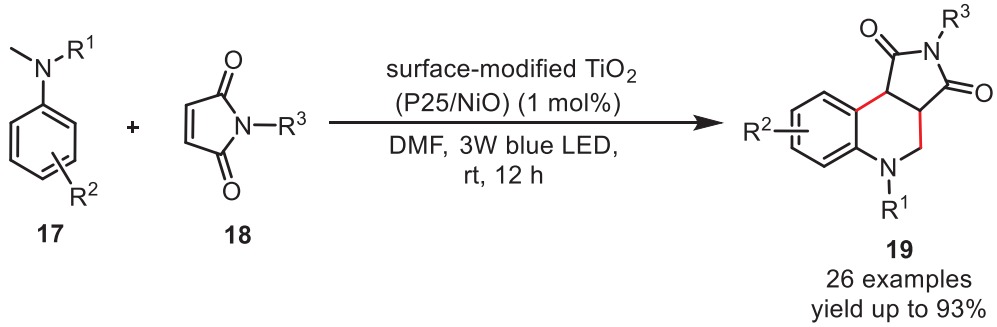

Scheme 5.10 Visible-light mediated cyclization of tertiary anilines with maleimides

Zhang and colleagues developed a metal-free approach for the synthesis of tetrahydroquinolines **(19)** from *N, N*-dimethylanilines **(17)**, and maleimides **(18)** using molecular oxygen as an oxidant and Eosin Y as a catalyst under visible light irradiation. This methodology is green because it uses visible light and atmospheric oxygen as the greenest reagents and metal-free, low-cost Eosin Y as the photocatalyst to deliver the product at ambient temperature in a simple one-pot operation. This metal-free strategy uses aerobic oxidative cyclization via the sp^3 C-H bond functionalization process to achieve good yields in a one-pot procedure under mild conditions **(Scheme 5.11)**.[23]

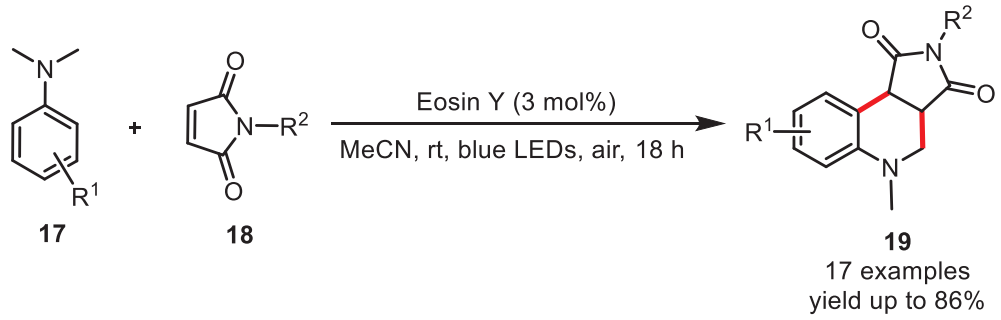

Scheme 5.11 Eosin Y-catalyzed visible-light mediated synthesis of tetrahydroquinolines

Bissember and co-workers demonstrated the first example of the direct functionalization of *α*-amino C–H bonds promoted by a copper-based visible light photocatalyst. This chemistry enables the rapid synthesis of complex and essential heterocyclic scaffolds, including novel octahydroisoquinolino[2,1-*a*]pyrrolo[3,4-*c*]quinoline frameworks as single diastereoisomers and a novel aglycone analogue of the natural product incargranine B. Trifluoroacetic acid (TFA) is crucial in mediating the aerobic oxidative quenching of a putative photoexcited copper(I) species involved in the catalytic cycle. As such, this process appears to be a rare example of a Brønsted acid-mediated radical reaction in organic synthesis. The outcomes of this research will contribute to expanding the scope and applications of visible light Cu(I) photocatalysis in organic synthesis in the future **(Scheme 5.12)**.[24]

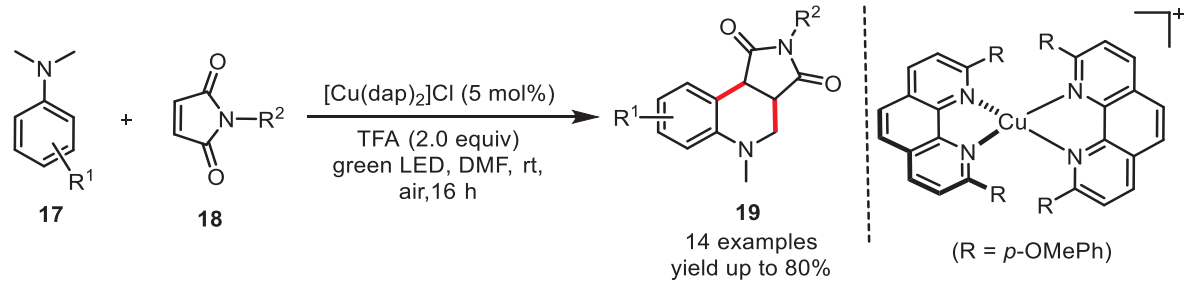

Scheme 5.12 Copper-catalyzed reactions of electron-deficient olefins with tertiary anilines

Zhang's team revealed in 2016 that a precise bandgap engineering technique of conjugated nanoporous poly-benzobisthiadiazole networks as metal-free, heterogeneous photocatalysts allows for adequate photoredox potential justification and optimized catalytic performance. Via copolymerization with an optimal composition of electron-withdrawing benzobisthiadiazole moiety, the resulting valence and conduction band positions of the polymers can be strategically aligned to bracket the redox potential of targeted individual reactions. The polymers' enhanced visible light-active photocatalytic activity was utilized in the oxidative cyclization of *N, N*-dimethylanilines **(17)** with maleimides **(18)** to yield tetrahydroquinoline **(19)** products, common structural motifs found in numerous pharmacologically relevant compounds **(Scheme 5.13)**.[25]

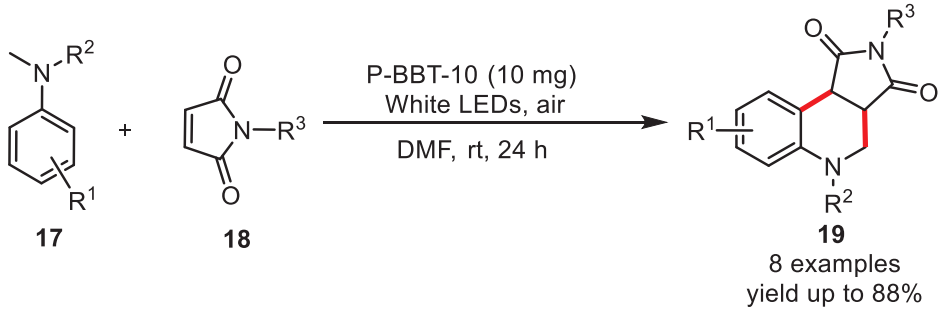

Scheme 5.13 The direct coupling of various tertiary anilines with N-substituted maleimides using P-BBT-10 as photocatalyst

Xin *et al*. have explored a metal-free visible-light-driven reaction for the synthesis of tetrahydroquinoline **(21)** derivatives via tandem radical cyclization of *N,N*-dimethylanilines **(17)** with 2-benzylidene malononitrile **(20)**. The mild conditions enable moderate yields using cheap and commercially available Rose Bengal instead of previous transition metal photocatalysts and a household light bulb instead of a high-intensity monochromatic LED light source. The yields obtained with this method can match the previously reported results, and twenty new tetrahydroquinoline derivatives were synthesized. This work demonstrates a synergistic benefit

of combining TFA with Rose Bengal, and it might provide a promising protocol for synthesizing tetrahydroquinoline derivatives **(Scheme 5.14)**.[26]

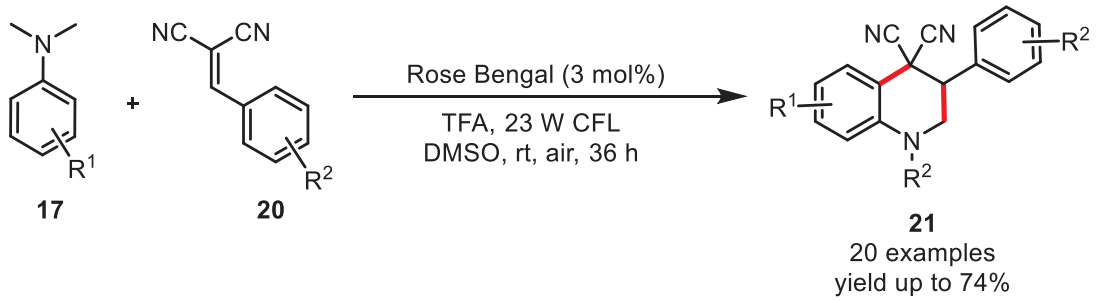

Scheme 5.14 Rose bengal-catalyzed visible-light mediated synthesis of tetrahydroquinolines

Yadav and co-workers developed a simple metal-free [4+2] radical cyclization of *N*,*N*-dimethylanilines with maleimides to produce tetrahydroquinolines utilizing *N*-hydroxyphthalimides as an organophotoredox catalyst in visible light. At room temperature, C(sp^3)-H activation of *N*,*N*-dimethylanilines results in the formation of α-amino radicals without the need of an oxidant. This method explains how to efficiently manufacture tricyclic heterocycles with acceptable to good yields under mild reaction conditions **(Scheme 5.15)**.[27]

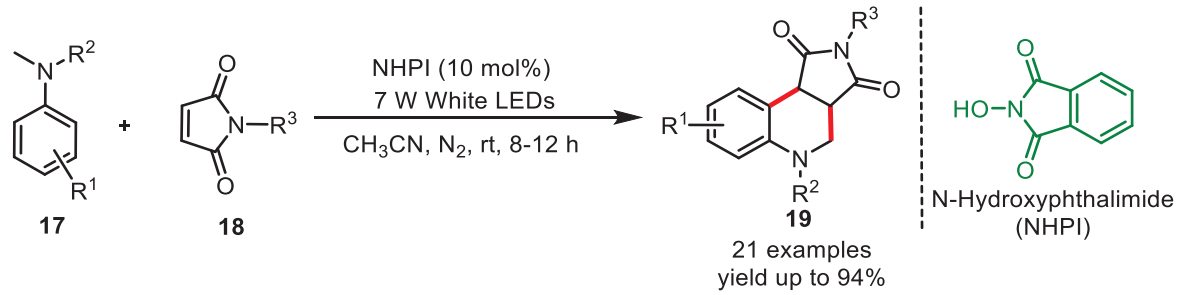

Scheme 5.15 NHPI-catalyzed visible-light mediated synthesis of tetrahydroquinolines

Guo *et al*. have developed a green, facile, and efficient method for synthesizing tetrahydroquinolines from *N*,*N*-dimethylanilines, and maleimides **(Scheme 5.16)**. This methodology is notably green since it uses visible light and atmospheric oxygen as the greenest reagents and natural pigment chlorophyll as the photosensitizer in a straightforward procedure to deliver the products at ambient temperature. This approach allows for direct cyclization via an sp^3 C-H bond functionalization process, resulting in tetrahydroquinoline frameworks useful in medical and pharmaceutical chemistry. Under mild circumstances, several substrates yielded moderate to high yields (61-98 %). This new approach is an example of investigating an

ecologically friendly, simple, and convenient synthesis pathway in organic chemistry that uses chlorophyll and light energy.[28]

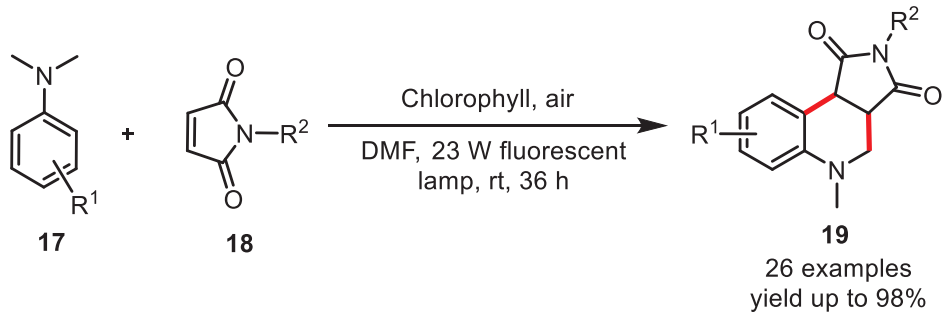

Scheme 5.16 Chlorophyll-catalyzed visible-light mediated synthesis of tetrahydroquinolines

In 2018, Wu's team successfully developed a redox-neutral reaction to achieve oxidative cyclization synthesis of tetrahydroquinolines in conjunction with hydrogenation. Various tetrahydroquinolines **(19)** were produced from tertiary anilines **(17)** and maleimides **(18)** in good to excellent yields by irradiating a catalytic quantity of photocatalyst $Ru(bpy)_3Cl_2$ and cobaloxime catalyst $Co(dmgH)_2pyCl$ with visible light. Simultaneously, the electron and proton removed from tertiary anilines are trapped by a cobaloxime catalyst, allowing for *in-situ* hydrogen transfer to maleimides **(Scheme 5.17)**.[29]

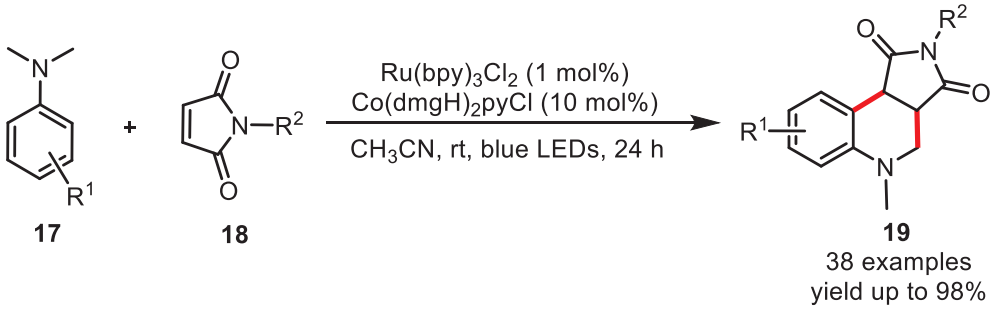

Scheme 5.17 Ru-catalyzed visible-light mediated synthesis of tetrahydroquinolines

Sunden and co-workers developed a catalyst-free, photochemical oxidative annulation reaction between dialkylanilines **(17)** and maleimides **(18)** to generate tetrahydroquinolines **(19) (Scheme 5.18)**. This reaction is driven by the photochemical activity of an electron donor–acceptor (EDA) complex. It has a broad substrate scope and isolates the relevant products in good to excellent yields. Optimization has revealed that the wavelength of the light source must overlap with the absorption spectrum of the EDA complex, that atmospheric oxygen serves as an external oxidant, and that EDA complex concentration is critical for high reaction turnovers.[30]

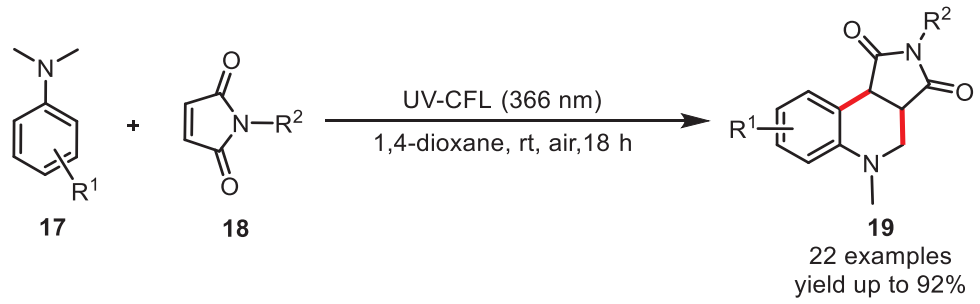

Scheme 5.18 Light-induced α-aminoalkyl radical addition to maleimides

Zhang and co-workers developed a versatile template-directed synthesis approach to prepare new types of photocatalyst-encapsulating metal–organic frameworks (photocatalyst@MOFs) with zeolite-like structures. Photocatalyst@MOFs showed remarkable heterogeneous catalytic activity for the reaction of aerobic oxidation of tertiary anilines **(17)** followed by cyclization with maleimides **(18)** under visible light due to the high robustness, permeant porosity, and protective effect of MOF matrixes **(Scheme 5.19)**. Interestingly, photocatalyst@MOFs demonstrated increased photocatalytic activity when compared to homogeneous photocatalyst counterparts. The pores of MOFs may efficiently disperse the photocatalyst and enable the movement of reactants and products, which is required for high catalytic activity. This study reveals a novel approach for creating highly effective heterogeneous photocatalysts and expanding the catalytic applications of MOF materials.[31]

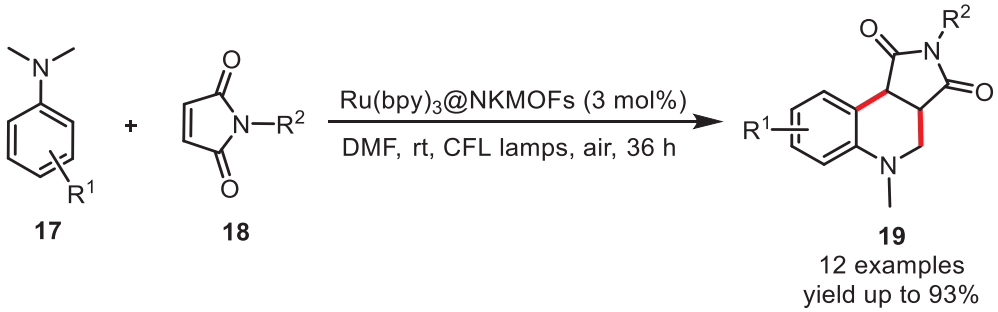

Scheme 5.19 Ru@MOFs-catalyzed visible-light mediated synthesis of tetrahydroquinolines

Sarkar and colleagues reported a macrocyclic mesotetraphenylporphyrin ligand coordinated Ni(II) complex (NiTPP) with excellent synthetic utility as a photoredox catalyst. This catalyst is superior to the known non-precious metal-based photocatalysts in ready availability and excited state redox properties. NiTPP also exhibits the dual activity of both excited state photo-oxidant and photo-reductant, as shown in maleimide annulation **(Scheme 5.20)**. Considering the earth-

abundant, less-toxic core metal and readily accessible ligand framework, mild reaction conditions, and high catalytic efficiency, this system is anticipated to offer new scope to promote green and economical synthesis using visible light photoredox catalysis.[32]

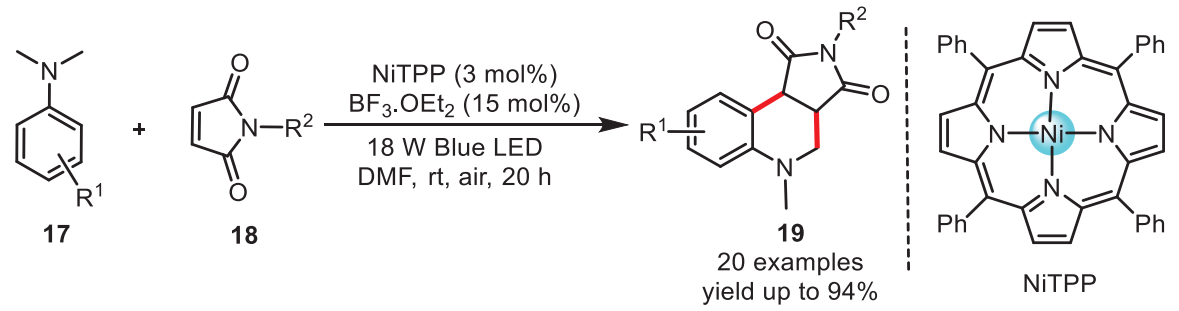

Scheme 5.20 NiTPP-catalyzed visible-light mediated synthesis of tetrahydroquinolines

Runemark *et al*. have developed a protocol for the visible-light-mediated synthesis of substituted tetrahydroquinolines **(23) (Scheme 5.21)**. This reaction didn't require any photocatalyst and relies on photoexcitation of an EDA complex formed between *N*-alkyl-*N*-methylaniline **(17)** and 1,2-dibenzoyl ethylene **(22)**, where atmospheric oxygen functions as the terminal oxidant. A broad substrate scope indicates the reaction's tolerance for common functional groups. The resultant 3,4-dibenzoyl-THQ structure is further derivatized and demonstrated to be a helpful building block for the synthesis of fused heterocycles.[33]

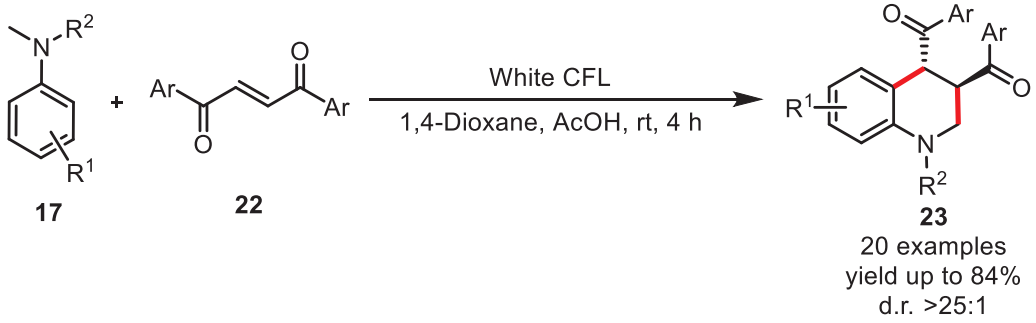

Scheme 5.21 Light-induced construction of tetrahydroquinolines

Kokotos and co-workers developed a protocol for the synthesis of tricyclic cores from *N*,*N*-dimethylanilines, and *N*-substituted maleimides utilizing benzaldehyde as the photoinitiator and cheap household lamps as the source of irradiation **(Scheme 5.22)**. The various substituted *N*,*N*-dimethylanilines **(17)**, and *N*-substituted maleimides **(18)** were converted into the corresponding product **(19)** in moderate to high yields. Initially, upon excitation, benzaldehyde (PC) advances to its triplet state, and then, a radical pair is formed between an excited molecule of

benzaldehyde and a ground state molecule of benzaldehyde. This radical pair can react with oxygen to form peroxy radicals. One of these radicals, belonging to the radical pair or the peroxy radicals, can perform a hydrogen atom abstraction from the alpha position of the nitrogen of the dialkyl aniline, namely from the methyl substituent of the aniline forming the α-amino radical. Then, this radical reacts with the electrophilic double bond of the maleimide, forming a radical. Subsequently, an intramolecular annulation takes place, forming the main scaffold and then undergoing oxidation from the air's oxygen, which is essential for the reaction to form the product.[34]

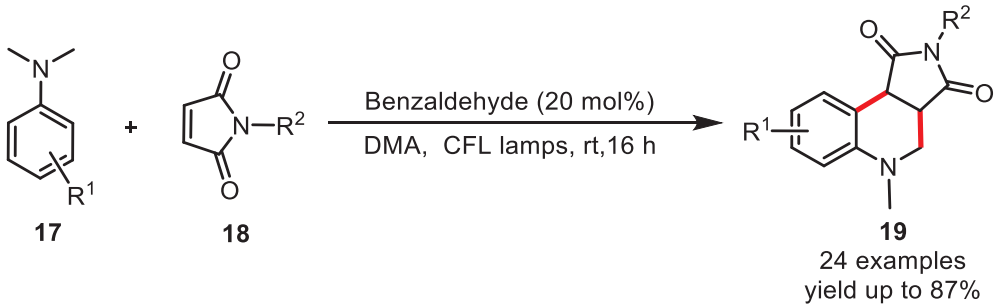

Scheme 5.22 Benzaldehyde-catalyzed visible-light mediated construction of tetrahydroquinolines

In 2022, Sunden's team successfully developed a visible light-induced aerobic oxidative annulation reaction protocol between dialkylanilines **(17)** and activated alkenes **(18)** to deliver the desired product **(19)**. This reaction is postulated to proceed *via* the excitation of an EDA complex formed between the catalyst 1,2-dibenzoyl ethylene and the amine reaction partner. The simple and available 1,2-dibenzoyl ethylene makes the developed protocol attractive as an alternative to the use of complex photoredox catalysts **(Scheme 5.23)**.[35]

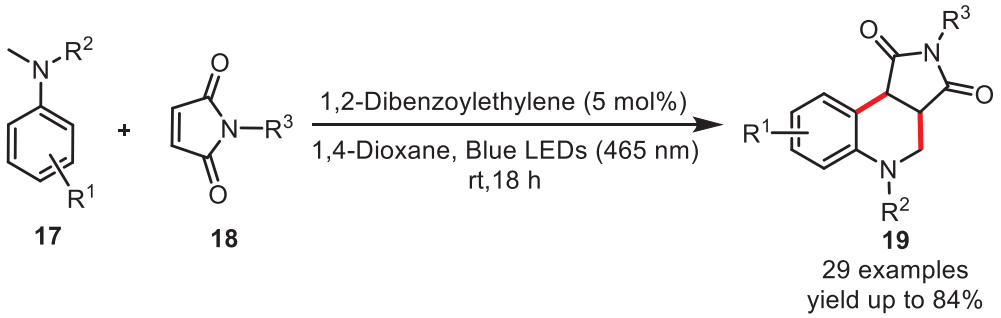

Scheme 5.23 EDA catalysis for visible light-mediated synthesis of tetrahydroquinolines

5.3.2 Electro-induced [4 + 2] annulation

In this context, Lei and co-workers reported an electrochemical oxidative [4 + 2] annulation between alkenes **(24)** and tertiary anilines **(17)** for the synthesis of tetrahydroquinoline derivatives **(25)** (yields of up to 72%) **(Scheme 5.24)**.[36] The undivided cell was equipped with platinum electrodes, *n*-Bu_4NBF_4 as the electrolyte, and MeCN : AcOH (4 : 1) as a solvent mixture under a constant current (3mA) at room temperature. The methodology presented a broad reaction scope for electron-donating groups and electron-withdrawing groups. Additionally, heterocyclic enamines were well tolerated (naphthyl, thiophene, tetrahydrofuran, pyridine, and pyrrolidinone). The authors propose that the mechanism involves anodic oxidation of **17** to generate the radical cation stabilized by acetic acid, which, after deprotonation, would deliver the tertiary α-amino carbon radical. This radical would react with **24** *via* radical addition, followed by intramolecular cyclization and anodic oxidation, to form the final product **25**.

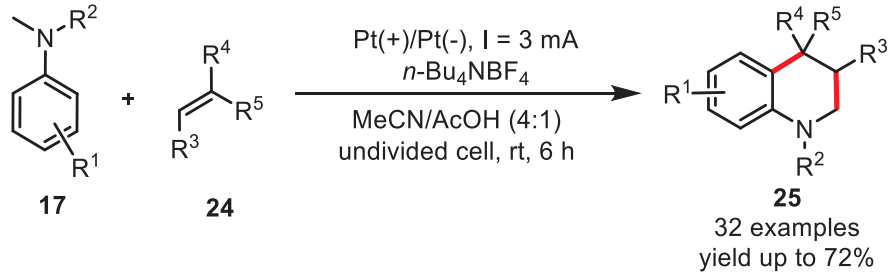

Scheme 5.24 Electrochemical oxidative [4 + 2] annulation between alkenes and tertiary anilines

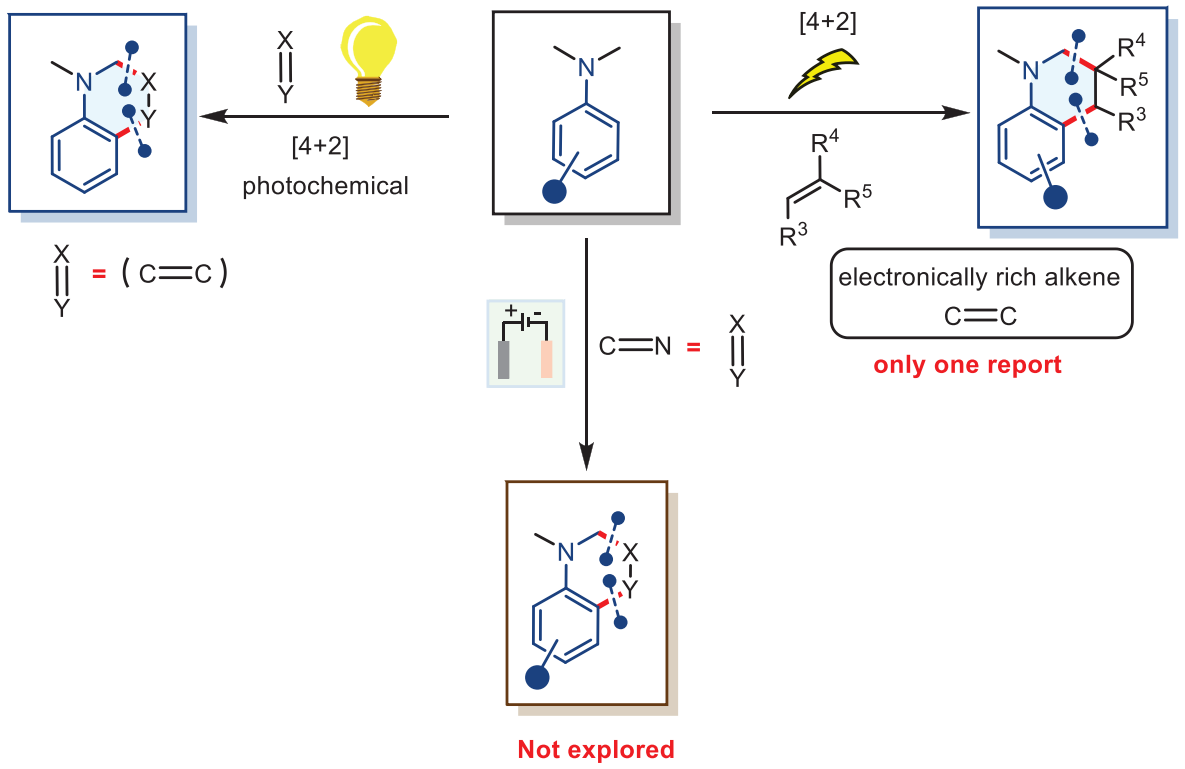

Figure 5.3 The gap in the literature for utilization of tertiary aniline in [4 + 2] annulation reaction

Despite these graceful photo/electrochemical methods, these strategies are mainly limited to the electronically rich alkenes (C=C) as dienophiles, whereas, the utilization of electron-deficient imines for oxidative [4 + 2] annulation remained unexplored (Figure 5.3). In this chapter, we present our first-time results in synthesizing dihydroindolo[1,2-*c*]quinazolin-12(6*H*)-one **(27)** from 2-aryl-3*H*-indol-3-one **(26)** and tertiary anilines **(17)** under mild electrochemical conditions. In this strategy, one partner loses only two hydrogen atoms while another partner reduces one degree of unsaturation, accompanied by hydrogen generation **(Scheme 5.25)**.

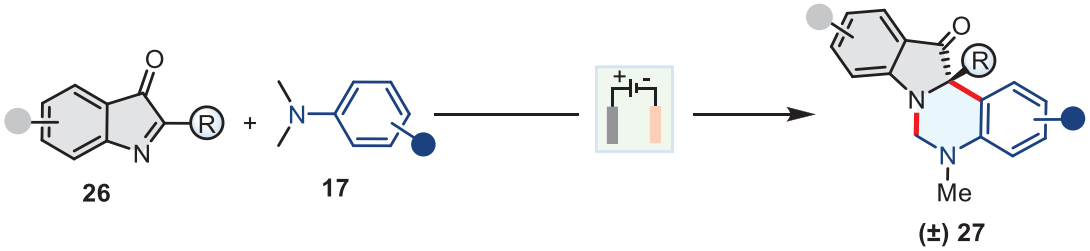

Scheme 5.25 Electrochemical oxidative [4 + 2] annulation between cyclic ketimine and tertiary anilines

5.4 Results and discussion

To evaluate the feasibility of our proposed synthetic pathway, initially, we examined the model reaction; 2-phenyl-3*H*-indol-3-one **26a** and *N, N*-dimethylaniline **17a** were employed as model substrates (Table 5.1). Extensive experiments for finding suitable reaction parameters such as electrodes, electrolytes, catalysts, and solvents (Table 5.1) were performed and led to identifying the optimal reaction conditions. To our delight, desired 5-methyl-12a-phenyl-5,12a-dihydroindolo[1,2-*c*]quinazolin-12(*6H*)-one **27aa** was obtained in 81% yield under optimized conditions (entry 1, Table 5.1). The reaction furnishes 70 % product yield without TEMPO (entry 2, Table 5.1). For instance, no desired product was found without *n*-Bu_4NBF_4 (entry 3, Table 5.1) and current (entry 4, Table 5.1). Next, product **27aa** obtained a 63% yield and 57% when C(+)/C(-) and C(+)/Pt(-) electrodes were used under standard conditions (entries 5-6, Table 5.1). The reaction outcome did not improve either by decreasing (entry 7, Table 5.1) or increasing (entry 8, Table 5.1) the applied current. The product **27aa** was obtained with 55% yields when TEMPO (10 mol%) (entry 9, Table 5.1), whereas a 69 % yield was observed of **27aa** with N_2 purging instead of air (entry 10, Table 5.1). Moreover, other electrolytes were also tested, such as *n*-Bu_4NPF_6 and *n*-Bu_4NClO_4, but all gave inferior results compared to *n*-Bu_4NBF_4 (entries 11-12, Table 5.1). The addition of HCl (1.0 equiv.) under standard conditions (entries 13, Table 5.1) and NaOAc (1.0 equiv.) (entries 14, Table 5.1) did not improve the reaction yields. Furthermore, increasing the *N, N*-dimethylaniline **17a** (2.0 equiv) (entry 15, Table 5.1) decreased the reaction yield. The choice of solvent is crucial to the reaction. DCE and MeOH were ineffective for this reaction (entries 16-17, Table 5.1). Thus, we prefer to perform the reaction under optimized conditions.

After confirming the optimized conditions for the electrochemical oxidative [4+2] annulation between cyclic ketimine and tertiary anilines, we examine the method's scope with various 2-aryl-3*H*-indol-3-one **26** and *N,N*-dimethylaniline **17 (Table 5.2)**. Initially, a series of 2-aryl-3*H*-indol-3-one **26a-26l** was tested by substituting with electron-withdrawing groups or electron-donating at the C2-aryl ring, producing corresponding products **27aa**-**27la** (70-86%) under optimized conditions. When the C2-aryl ring was replaced with naphthyl **26m**, thienyl **26n,** and 5-bromo thienyl **26o,** complementary products **27ma** (70%), **27na** (75%), and **27oa** (72%) were obtained, respectively.

Table 5.1: Optimization of the reaction conditions[a]

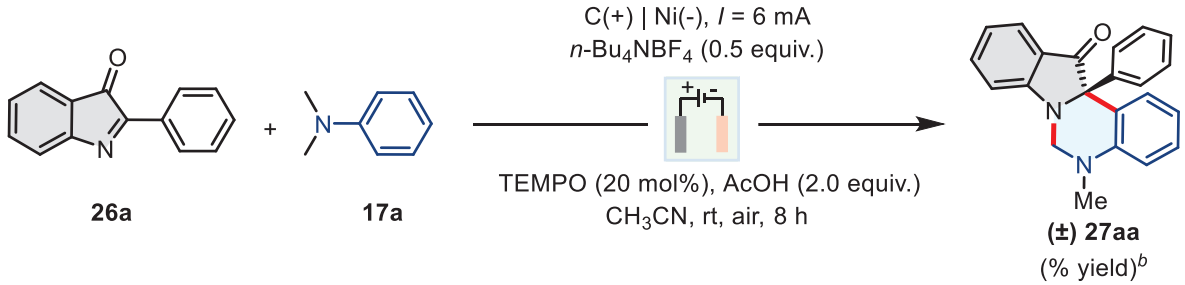

Entry	Variation from standard conditions	Yield (%)
1	none	81
2	without TEMPO	70
3	without *n*-Bu_4NBF_4	-
4	without current	-
5	C(+)/C(-) used instead of C(+)/Ni(-)	63
6	C(+)/Pt(-) used instead of C(+)/Ni(-)	57
7	3 mA, 15 h	46
8	10 mA, 5 h	58
9	TEMPO (10 mol%)	55
10	N_2 instead of air	69
11	*n*-Bu_4NPF_6 (1.0 equiv.) used instead of *n*-Bu_4NBF_4 (1.0 equiv.)	50
12	*n*-Bu_4NClO_4 (1.0 equiv.) used instead of *n*-Bu_4NBF_4 (1.0 equiv.)	45
13	HCl (1.0 mmol)	20
14	NaOAC (1.0 mmol)	40
15	17a (1.0 mmol) was used	60
16	DCE	44
17	MeOH	30

[a]**Reaction conditions**: **26a** (0.5 mmol, 1.0 equiv), **17a** (0.5 mmol, 1.0 equiv), *n*-Bu_4NBF_4 (0.25 mmol, 0.5 equiv), TEMPO (0.1 mmol, 20 mol%), AcOH (1.0 mmol, 2.0 equiv), CH_3CN (8.0 mL), in an Undivided cell with C(+) | Ni(-), constant current = 6 mA, air, rt, 8 h. [b]All isolated yields of 3 after column chromatography were based on **26a**.

Table 5.2: Electrochemical oxidative [4 + 2] annulation of 2-aryl-3*H*-indol-3-ones and *N*,*N*-dimethylaniline

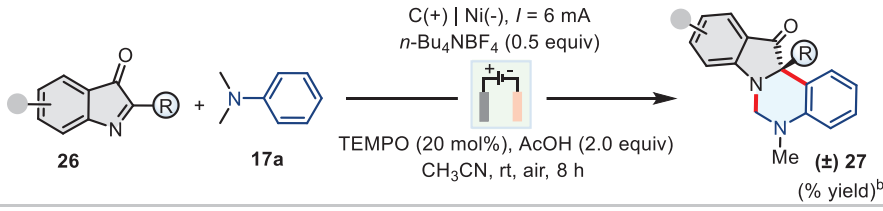

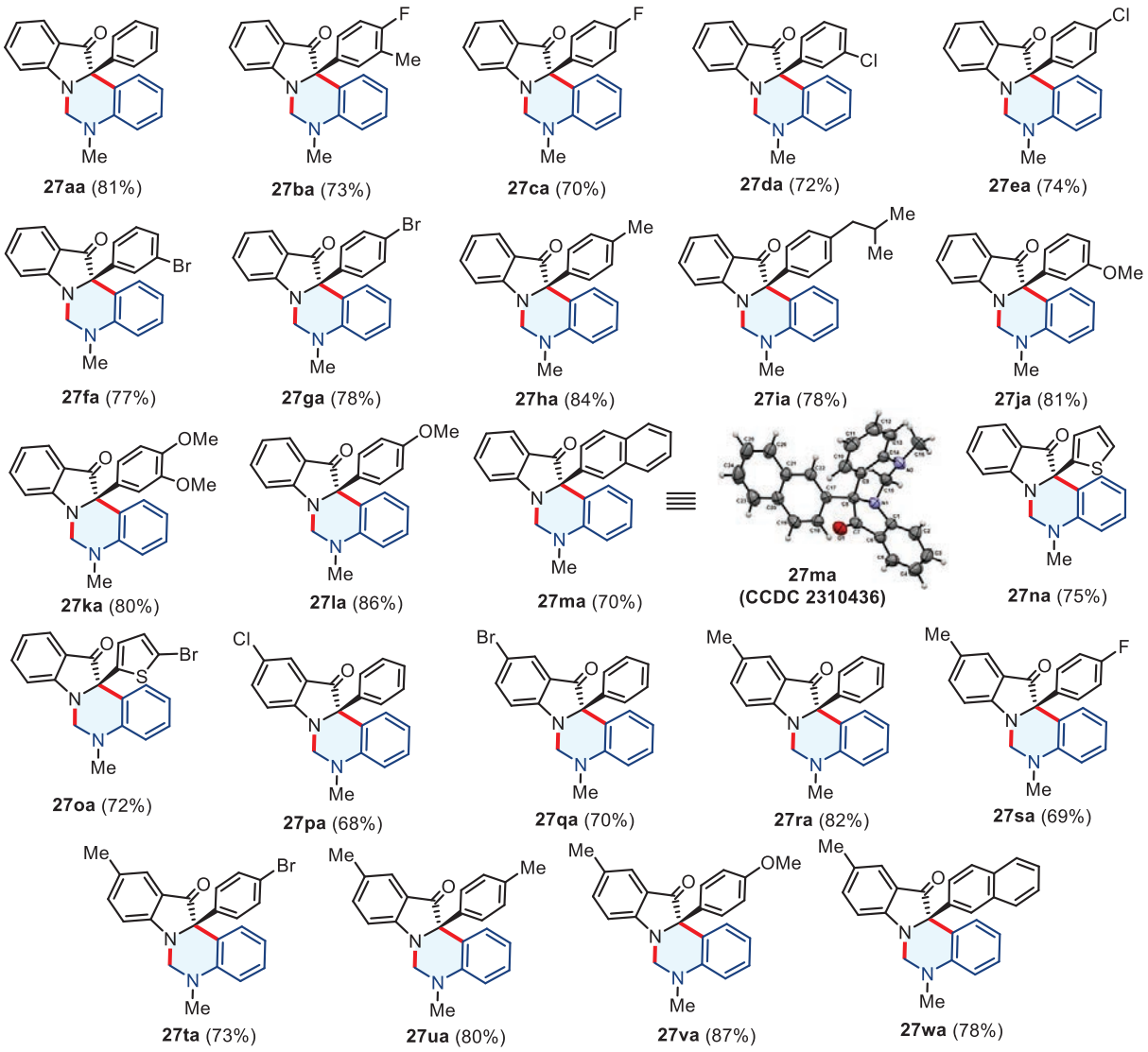

[a]**Reaction conditions**: **26** (0.5 mmol, 1.0 equiv), **17a** (0.5 mmol, 1.0 equiv), *n*-Bu_4NBF_4 (0.25 mmol, 0.5 equiv), TEMPO (0.1 mmol, 20 mol%), AcOH (1.0 mmol, 2.0 equiv), CH_3CN (8.0 mL), in an Undivided cell with C(+) | Ni(-), constant current = 6 mA, air, rt, 8 h. [a]All isolated yields of **27** after column chromatography were based on **26**.

Table 5.3: Electrochemical oxidative [4 + 2] annulation of 2-phenyl-3*H*-indol-3-one and tertiary anilines

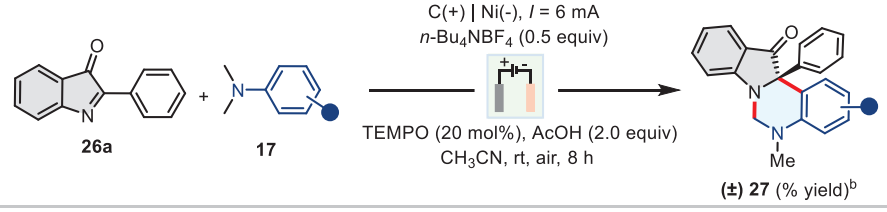

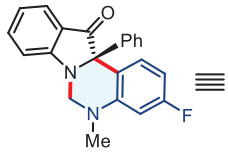
27ab (68%)

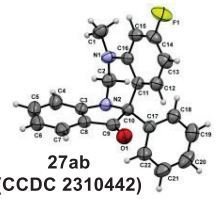
27ab
(CCDC 2310442)

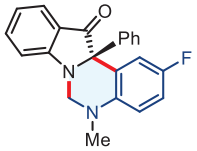
27ac (70%)

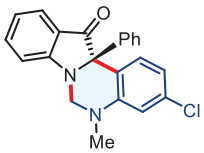
27ad (76%)

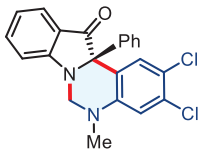
27ae (65%)

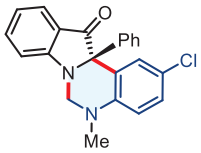
27af (77%)

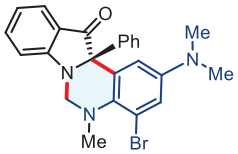
27ag (78%)

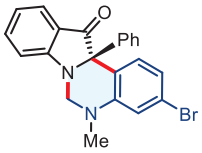
27ah (76%)

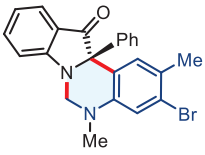
27ai (81%)

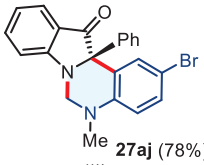
27aj (78%)

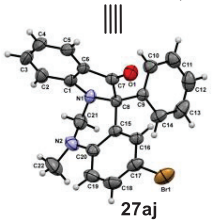
27aj
(CCDC 2310439)

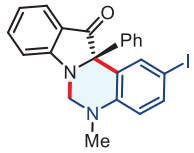
27ak (80%)

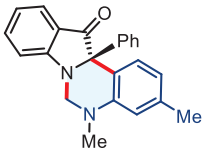
27al (86%)

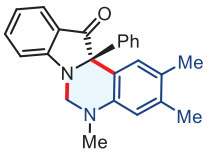
27am (90%)

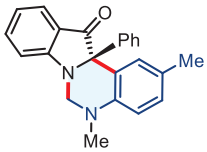
27an (92%)

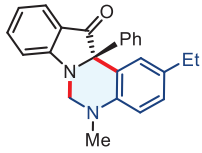
27ao (88%)

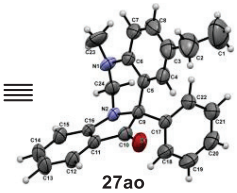
27ao
(CCDC 2310469)

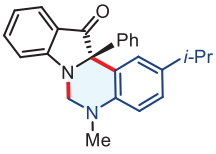
27ap (84%)

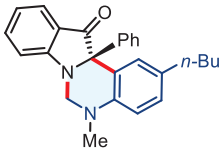
27aq (83%)

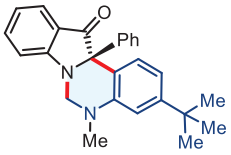
27ar (86%)

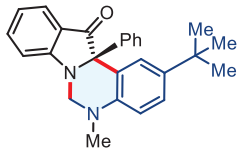
27as (87%)

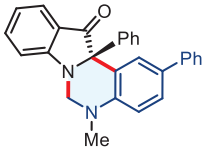
27at (85%)

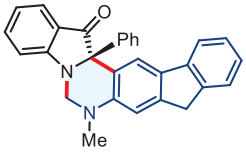
27au (81%)

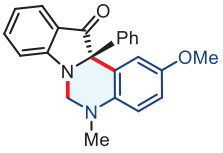
27av (89%)

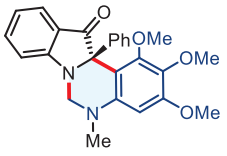
27aw (78%)

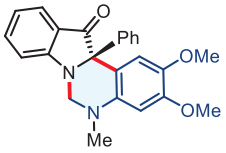
27ax (83%)

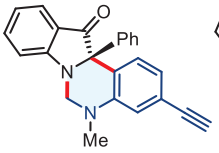
27ay (88%)

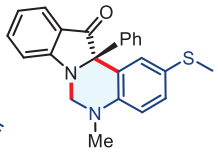
27az (79%)

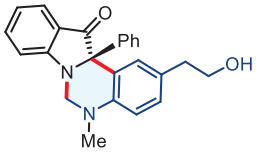
27aaa (77%)

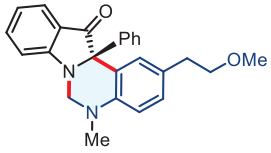
27aab (80%)

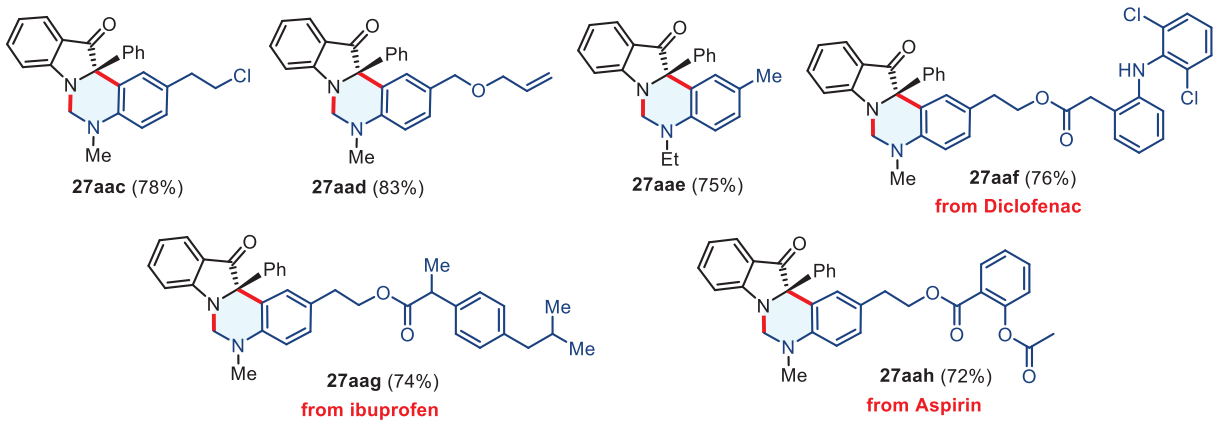

[a]**Reaction conditions**: **26a** (0.5 mmol, 1.0 equiv), **17** (0.5 mmol, 1.0 equiv), *n*-Bu_4NBF_4 (0.25 mmol, 0.5 equiv), TEMPO (0.1 mmol, 20 mol%), AcOH (1.0 mmol, 2.0 equiv), CH_3CN (8.0 mL), in an Undivided cell with C(+) | Ni(-), constant current = 6 mA, air, rt, 8 h. [b]All isolated yields of **27** after column chromatography were based on **26a**.

While having different substitutions at the indole ring of 2-aryl-3*H*-indol-3-one also furnished the complementary products **27pa-27ra** (68-82%). Next, a series of 2-aryl-3*H*-indol-3-one with substitutions like- Me, F, Br, and OMe were examined on both the aryl rings. A series of related products, **27sa-27va** (68-87% yields), were obtained with *N*,*N*- dimethylaniline **17a** as a second coupling partner. When the C2-aryl ring was replaced with a naphthyl ring and methyl substitute at the indole ring was tested under the optimized condition, the corresponding product **27wa** was obtained with 78% yield.

Next, we check the generality of *N*,*N*-dimethyl arylamine **17b-17ah** having different substitutions at ortho-, meta- or para-positions with 2-phenyl-3*H*-indol-3-one **26a** and furnished related products **27ab-27aah** (65-92%) **(Table 5.3)**. The single crystal X-ray analysis for compounds **27ma** (CCDC 2310436), **27ab** (CCDC 2310442), **27aj** (CCDC 2310439) and **27ao** (CCDC 2310469) confirmed the assigned structures.

5.5 Cyclic voltammetry experiment

Cyclic voltammetry (CV) was performed using a three-electrodes cell (glassy carbon as the working electrode, Pt wire as the auxiliary electrode, and Ag/AgCl as reference electrode) in CH_3CN/*n*-Bu_4NBF_4 (12 mL, 0.02M) as the supporting electrolyte at room temperature. The Ag/AgCl as the reference electrode, and the scan rate was 0.2 V/s, ranging from +1.8 V to +2.0 V. The oxidation potentials for **26a** (E_{ox} = -0.62 V vs. Ag/AgCl as reference electrode), **17a** (E_{ox}

= +1.12 V vs. Ag/AgCl as reference electrode), TEMPO (E_{ox} = +0.1.36 V vs. Ag/AgCl as reference electrode), and **26a**+**17a**+TEMPO+AcOH (E_{ox} = +1.32 V and +1.50 V vs. Ag/AgCl as reference electrode) were measured, respectively, as shown in Figure 5.2. The CV was plotted using the IUPAC convention.

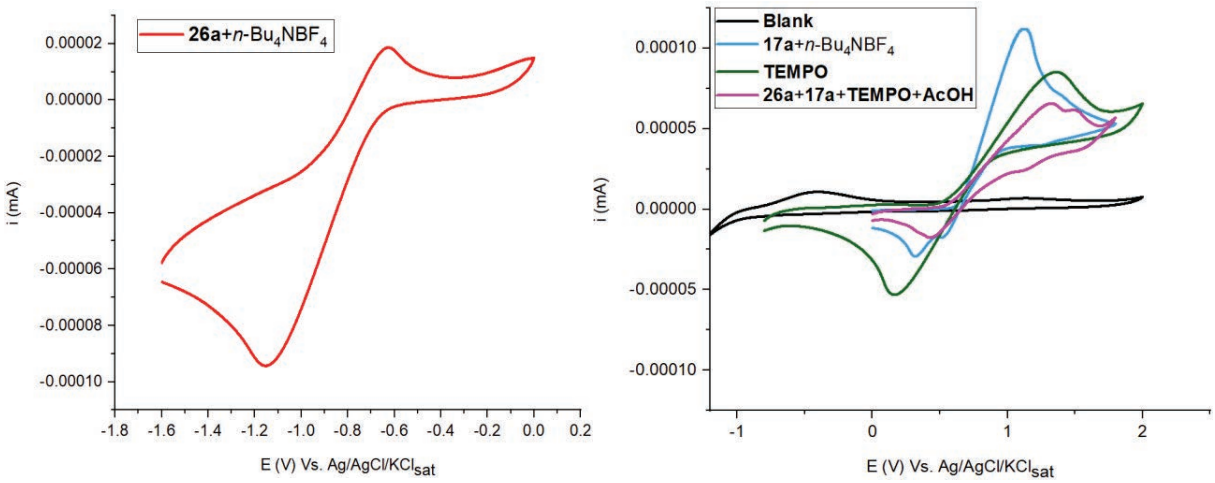

Figure 5.4 Cyclic voltammogram of CH_3CN/*n*-Bu_4NBF_4 (12 mL, 0.02M) (**black**), **26a** (2.0 mM) in CH_3CN/*n*-Bu_4NBF_4 (12 mL, 0.02M) (**red**), **17a** (2.0 mM) in CH_3CN/*n*-Bu_4NBF_4 (12 mL, 0.02M) (**blue**), **TEMPO** (2.0 mM) in CH_3CN/*n*-Bu_4NBF_4 (12 mL, 0.02M) (**green**), **26a** (2.0 mM), **17a** (2.0 mM), TEMPO (2.0 mM), AcOH (2.0 mM) in CH_3CN/*n*-Bu_4NBF_4 (12 mL, 0.02M) (**pink**), Reference electrode: Ag/AgCl (3M KCl), scan rate: 0.2 V/s. all experiments were done at room temperature

5.6 Control experiments, Reaction mechanism, Synthetic applications

The formation of product **27aa** was not observed with BHT or TEMPO as a radical scavenger under the standard electrochemical conditions, confirming the radical nature of the reaction at the intermediate step **(Scheme 5.26)**.

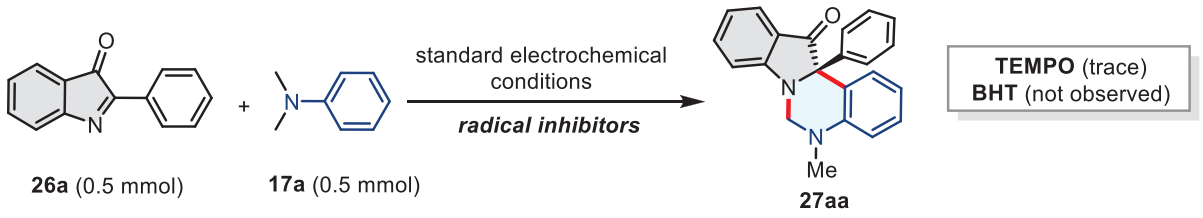

Scheme 5.26: Control experiment

A probable mechanism has been proposed based on the literature available in this direction. As shown in **Scheme 5.27**, TEMPO underwent oxidation at the anode to generate $TEMPO^+$, which could oxidize **17a** to a radical cation that can be stabilized by acetic acid. Afterward, the radical

cation resonates and deprotonates to get the tertiary α-amino carbon radical **A**; the radical intermediate **A** can react with **26a** via a radical addition process, forming intermediate **B**. The subsequent radical **B** species could engage in an intramolecular cyclization reaction, followed by anodic oxidation, which produces the desired product **27aa,** and another possible way could be the intermediate **B** again undergoes anodic oxidation that forms carbocation **C,** which follows the intramolecular Friedel crafts reaction to access the desired product **27aa.**

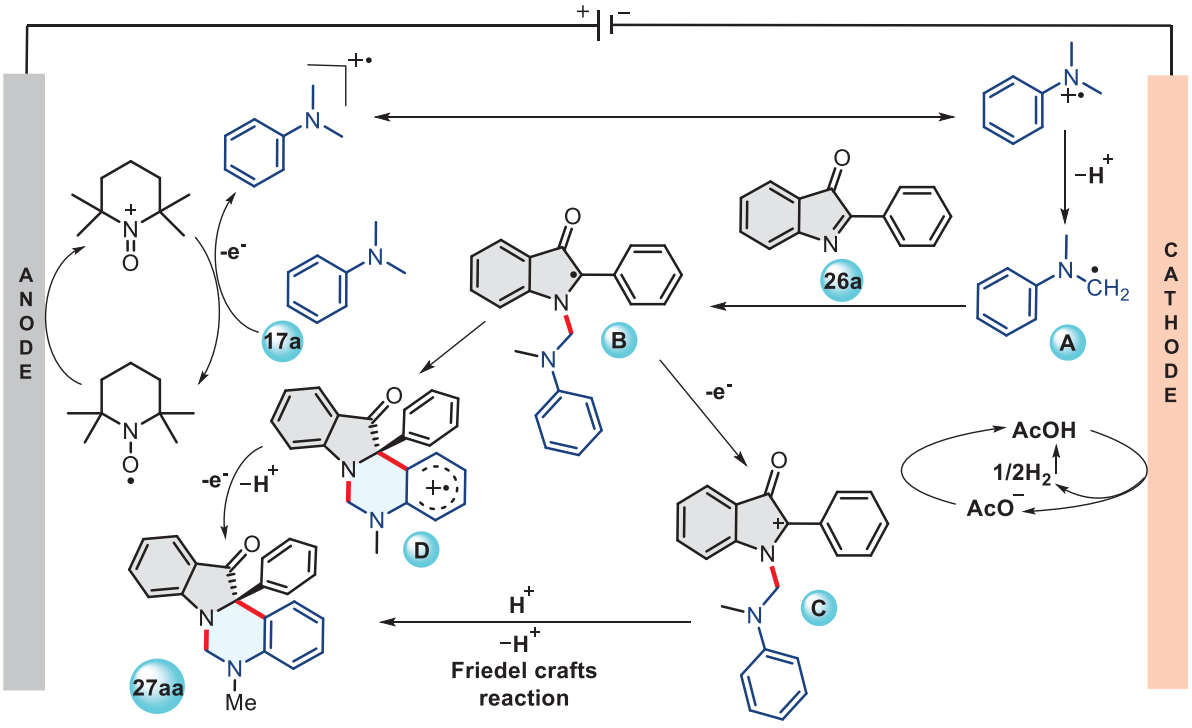

Scheme 5.27: A tentative mechanism for the electrochemical oxidative [4+2] annulation

The practicality of the developed method was shown at the gram-scale preparation of compound **27aa** (1.3 g, 78% yield) under optimized conditions **(Scheme 5.28a)**. Next, the developed method was applied successfully for the synthesis of 2,5-dimethyl-12a-phenyl-5,6,12,12a-tetrahydroindolo[1,2-*c*]quinazolin-12-ol **28** (81%, **(Scheme 5.28b)**), respectively, when compound **27aa** were treated with sodium borohydride and lithium bromide as an additive in 1, 4-dioxane at 0 °C to rt conditions.

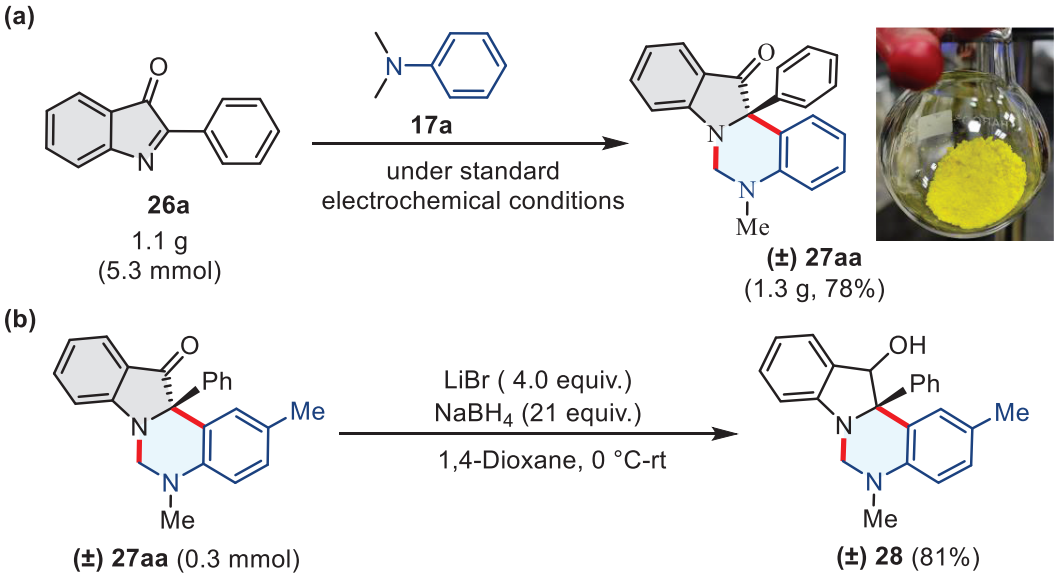

Scheme 5.28: Synthetic applications **(a)** gram-scale synthesis of **27aa**; **(b)** synthesis of 2,5-dimethyl-12a-phenyl-5,6,12,12a-tetrahydroindolo[1,2-*c*]quinazolin-12-ol **28**

5.7 Conclusions

In conclusion, we have developed a novel method for the electrochemical oxidative intermolecular [4+2] annulation of tertiary aryl amines and cyclic ketimines to access functionalized dihydroindolo[1,2-*c*]quinazolin-12(6*H*)-one moiety. This developed protocol can occur under air and metal-free conditions at room temperature, and a wide range of functional groups proved to be compatible under our optimized conditions. Notably, the reaction conditions were consistent with some drug structure derivatives. Further studies on the reaction's scope and application are ongoing in our laboratory.

5.8 General experimental methods

All reactions were observed using Thin-layer chromatography (on SiO_2 gel F254 plates) and performed on IKA ElectroSyn 2.0 Pro under standard conditions. The desired compounds were purified through Flash column chromatography packed with silica gel (100-200 meshes size) as the stationary phase and a mixture of petroleum ether-acetone as eluent. Melting points were determined in open capillary tubes on an EZ-Melt Automated melting point apparatus and are uncorrected. NMR spectra were recorded on a Bruker AV 400 spectrometer. The chemical shifts were reported in parts per million (ppm) using deuterated solvent as the internal standard. High-resolution mass spectra (HRMS-ESI) were recorded using a quadrupole time-of-flight (Q-TOF) mass spectrometer (Applied Biosystems). The cyclic voltammetry was performed using CH

Instruments Electrochemical Analyzer (Model CHI1200B) with a three-electrodes cell (glassy carbon as the working electrode (3-mm diameter, circular), Pt wire as the auxiliary electrode, and Ag/AgCl as the reference electrode). Before experimenting, the electrode was polished with Micro Polish Alumina Powder 0.05 μm as per the following method: The alumina (0.05 μm) was mixed with water on the polishing pad to make a paste. The working electrode was then rubbed on the polishing pad with some alumina paste while ensuring that the face of the working electrode remained flat, and polishing was performed in a figure-8 so that grooves do not develop in the electrode surface. After polishing for about 30 seconds, the electrode was sonicated in deionized water for no more than 1 minute. Finally, the electrode was washed with deionized water, and the electrode surface was dried before use. All cyclic voltammetry experiments were performed after nitrogen purging for deoxygenation purposes. The cyclic voltammetry was performed using CH Instruments electrochemical Analyzer (Model CHI1200B). All the chemicals were obtained from the commercial supplier and were used without Purification. The 2-arylindoles,[37] 2-aryl substituted 3*H*-indol-3-ones[38] **26**, and tertiary aniline **17** were prepared according to the reported procedures.[39] Oil baths were used for heating conditions.

5.8.1 General procedure for the synthesis of compound 27

A 10 mL dried undivided reaction cell with a stirring bar was charged with **26** (0.5 mmol, 1.0 equiv.), N, N-Dimethylaniline **17** (0.5 mmol, 1.0 equiv.), *n*-Bu_4NBF_4 (82 mg, 0.25 mmol, 0.5 equiv.), TEMPO (16 mg, 0.1 mmol, 20 mol%) and AcOH (60 mg, 1.0 mmol, 2.0 equiv.) in CH_3CN (10 mL). The carbon-plate anode and nickel-plate cathode were dipped into the reaction mixture and electrolyzed at a constant current condition (6 mA) under an air atmosphere at room temperature. The reaction progress was monitored by TLC. Upon completion, the reaction mixture was evaporated under reduced pressure, and crude mass was stirred between ethyl acetate (10 mL) and NH_4Cl (10 mL, 10% solution) for five minutes. The organic phase was separated, dried over anhydrous Na_2SO_4, and evaporated under reduced pressure. Purification of crude mass on silica gel column chromatography using a mixture of petroleum ether and acetone as eluent furnished product **27** (65-92% yields).

5.8.2 Characterization data of synthesized compounds

5-Methyl-12a-phenyl-5, 12a-dihydroindolo[1,2-*c*]quinazolin-12(6*H*)-one (±27aa):

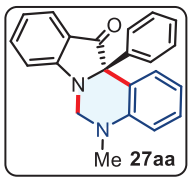

Purification with petroleum ether: acetone (8/2) as eluent); yellow solid (132 mg, 81% yield, mp = 210-215 °C). ^{1}H NMR (400 MHz, $CDCl_3$) δ 7.73 – 7.69 (m, 1H), 7.67 (dd, *J* = 7.9, 1.5 Hz, 1H), 7.57 (m, 1H), 7.30 (dt, *J* = 4.6, 2.3 Hz, 3H), 7.23 – 7.17 (m, 3H), 7.14 (d, *J* = 8.3 Hz, 1H), 6.98 – 6.93 (m, 1H), 6.85 – 6.80 (m, 1H), 6.70 (d, *J* = 8.3 Hz, 1H), 4.68 (d, *J* = 11.9 Hz, 1H), 4.27 (d, *J* = 12.0 Hz, 1H), 2.93 (s, 3H). ^{13}C{^{1}H} NMR (100 MHz, $CDCl_3$) δ 200.1, 160.7, 145.7, 142.2, 136.8, 130.0, 128.7, 128.6 (2C), 128.4 (2C), 128.0, 125.8, 123.0, 120.5, 118.3, 117.2, 112.5, 111.3, 74.4, 59.7, 36.8. HRMS (ESI-TOF) *m*/*z*: [M + H^{+}] Calcd for $C_{22}H_{19}N_2O$ 327.1492, found. 327.1493.

12a-(4-Fluoro-3-methyl phenyl)-5-methyl-5, 12a-dihydroindolo[1,2-*c*]quinazolin-12(6*H*)-one (±27ba):

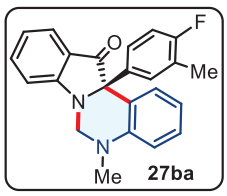

Purification with petroleum ether: acetone (8/2) as eluent); yellow solid (131 mg, 73% yield, mp = 152-154 °C). ^{1}H NMR (400 MHz, $CDCl_3$) δ 7.73 – 7.69 (m, 1H), 7.64 (dd, *J* = 7.9, 1.5 Hz, 1H), 7.58 (m, 1H), 7.20 (m, 1H), 7.15 (d, *J* = 8.3 Hz, 1H), 7.02 – 6.88 (m, 4H), 6.85 – 6.79 (m, 1H), 6.73 – 6.67 (m, 1H), 4.68 (d, *J* = 11.9 Hz, 1H), 4.25 (d, *J* = 12.0 Hz, 1H), 2.93 (s, 3H), 2.21 (s, 3H). ^{13}C{^{1}H} NMR (100 MHz, $CDCl_3$) δ 200.1, 160.6, 145.6, 137.6 (d, *J* = 3.5 Hz), 136.9, 131.6 (d, *J* = 5.4 Hz), 131.5, 130.0, 128.8, 128.0 (d, *J* = 8.3 Hz), 125.8, 125.0 (d, *J* = 17.6 Hz), 122.9, 120.6, 118.3, 117.0, 114.8 (d, *J* = 22.6 Hz), 112.6, 111.4, 74.0, 59.7, 36.8, 14.7. HRMS (ESI-TOF) *m*/*z*: [M + H^{+}] Calcd for $C_{23}H_{20}FN_2O$ 359.1554, Found. 359.1556.

12a-(4-Fluorophenyl)-5-methyl-5, 12a-dihydroindolo[1,2-*c*]quinazolin-12(6*H*)-one (±27ca):

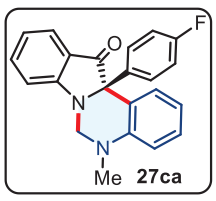

Purification with petroleum ether: acetone (8/2) as eluent); yellow solid (121 mg, 70% yield, mp = 173-175 °C). ^{1}H NMR (400 MHz, $CDCl_3$) δ 7.71 (m, 1H), 7.64 (dd, *J* = 7.9, 1.6 Hz, 1H), 7.58 (m, 1H), 7.22 – 7.16 (m, 3H), 7.14 (d, *J* = 8.3 Hz, 1H), 7.02 – 6.94 (m, 3H), 6.82 (td, *J* = 7.9, 1.2 Hz, 1H), 6.70 (dd, *J* = 8.3, 1.0 Hz, 1H), 4.68 (d, *J* = 11.9 Hz, 1H), 4.24 (d, *J* = 12.0 Hz, 1H), 2.93 (s, 3H). ^{13}C{^{1}H} NMR (100 MHz, $CDCl_3$) δ 199.9, 162.4 (d, *J* = 247.5 Hz), 160.6, 145.6, 137.9 (d, *J* = 3.3 Hz), 136.9, 130.5, 130.4, 129.9, 128.8, 125.8, 122.8, 120.6, 118.3, 116.9, 115.3, 115.1, 112.6, 111.3, 73.8, 59.7, 36.8. HRMS (ESI-TOF) *m*/*z*: [M + H^{+}] Calcd for $C_{22}H_{18}FN_2O$ 345.1398, Found. 345.1399.

12a-(3-Chlorophenyl)-5-methyl-5, 12a-dihydroindolo[1,2-*c*]quinazolin-12(6*H*)-one (±27da):

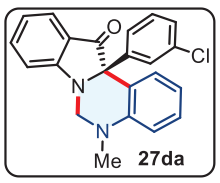

Purification with petroleum ether: acetone (8/2) as eluent); yellow solid (130 mg, 72% yield, mp = 160-163 ºC). ^{1}H NMR (400 MHz, $CDCl_3$) δ 7.71 (d, *J* = 7.7 Hz, 1H), 7.66 (dd, *J* = 7.9, 1.5 Hz, 1H), 7.58 (m, 1H), 7.28 (dt, *J* = 8.0, 1.7 Hz, 1H), 7.25 – 7.22 (m, 1H), 7.20 (m, 2H), 7.15 (d, *J* = 8.3 Hz, 1H), 7.12 (dt, *J* = 7.3, 1.6 Hz, 1H), 6.97 (t, *J* = 7.4 Hz, 1H), 6.87 – 6.81 (m, 1H), 6.72 – 6.68 (m, 1H), 4.69 (d, *J* = 12.0 Hz, 1H), 4.25 (d, *J* = 12.0 Hz, 1H), 2.93 (s, 3H). ^{13}C{^{1}H} NMR (100 MHz, $CDCl_3$) δ 199.3, 160.6, 145.6, 144.0, 137.0, 134.3, 129.8, 129.6, 128.9, 128.7, 128.2, 126.8, 125.9, 122.7, 120.7, 118.4, 116.3, 112.6, 111.4, 73.8, 59.8, 36.7. HRMS (ESI-TOF) *m*/*z*: [M + H^+] Calcd for $C_{22}H_{18}ClN_2O$ 361.1102, Found. 361.1105.

12a-(4-Chlorophenyl)-5-methyl-5, 12a-dihydroindolo[1,2-*c*]quinazolin-12(6*H*)-one (±27ea):

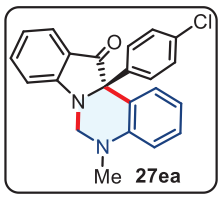

Purification with petroleum ether: acetone (8/2) as eluent); yellow solid (134 mg, 74% yield, mp = 158-160 ºC). ^{1}H NMR (400 MHz, $CDCl_3$) δ 7.70 (d, *J* = 7.7 Hz, 1H), 7.66 – 7.62 (m, 1H), 7.61 – 7.55 (m, 1H), 7.28 (d, *J* = 8.6 Hz, 2H), 7.23 – 7.17 (m, 1H), 7.17 – 7.13 (m, 3H), 6.96 (t, *J* = 7.4 Hz, 1H), 6.82 (t, *J* = 7.3 Hz, 1H), 6.70 (d, *J* = 8.2 Hz, 1H), 4.69 (d, *J* = 12.0 Hz, 1H), 4.23 (d, *J* = 12.0 Hz, 1H), 2.93 (s, 3H). ^{13}C{^{1}H} NMR (100 MHz, $CDCl_3$) δ 199.6, 160.6, 145.6, 140.6, 137.0, 134.0, 130.1 (2C), 129.8, 128.9, 128.5 (2C), 125.8, 122.8, 120.7, 118.3, 116.7, 112.6, 111.4, 73.8, 59.7, 36.8. HRMS (ESI-TOF) *m*/*z*: [M + H^+] Calcd for $C_{22}H_{18}ClN_2O$ 361.1102, Found. 361.1105.

12a-(3-Bromophenyl)-5-methyl-5, 12a-dihydroindolo[1,2-*c*]quinazolin-12(6*H*)-one (±27fa):

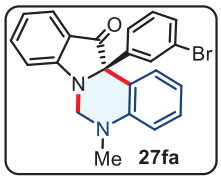

Purification with petroleum ether: acetone (8/2) as eluent); yellow solid (156 mg, 77% yield, mp = 108-110 ºC). ^{1}H NMR (400 MHz, $CDCl_3$) δ 7.68 (dd, *J* = 18.4, 6.3 Hz, 2H), 7.62 – 7.53 (m, 1H), 7.43 (s, 1H), 7.35 (s, 1H), 7.17 (t, *J* = 12.8 Hz, 4H), 7.03 – 6.93 (m, 1H), 6.89 – 6.79 (m, 1H), 6.70 (d, *J* = 6.5 Hz, 1H), 4.69 (d, *J* = 11.3 Hz, 1H), 4.25 (d, *J* = 11.6 Hz, 1H), 2.93 (s, 3H). ^{13}C{^{1}H} NMR (100 MHz, $CDCl_3$) δ 199.2, 160.6, 145.6, 144.2, 137.0, 131.5, 131.2, 129.9, 129.8, 129.0, 127.4, 125.9, 122.7, 122.6, 120.7, 118.4, 116.3, 112.6, 111.4, 73.8, 59.8, 36.7. HRMS (ESI-TOF) *m*/*z*: [M + H^+] Calcd for $C_{22}H_{18}BrN_2O$ 405.0597, Found. 405.0598.

12a-(4-Bromophenyl)-5-methyl-5, 12a-dihydroindolo[1,2-*c*]quinazolin-12(6*H*)-one (±27ga):

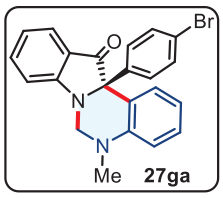

Purification with petroleum ether: acetone (8/2) as eluent); yellow solid (158 mg, 78% yield, mp = 120-123 °C). ^{1}H NMR (400 MHz, $CDCl_3$) δ 7.70 (d, *J* = 7.6 Hz, 1H), 7.63 (d, *J* = 7.7 Hz, 1H), 7.58 (t, *J* = 7.6 Hz, 1H), 7.43 (d, *J* = 8.3 Hz, 2H), 7.20 (t, *J* = 7.6 Hz, 1H), 7.14 (d, *J* = 8.3 Hz, 1H), 7.09 (d, *J* = 8.3 Hz, 2H), 6.96 (t, *J* = 7.4 Hz, 1H), 6.82 (t, *J* = 7.5 Hz, 1H), 6.70 (d, *J* = 8.3 Hz, 1H), 4.68 (d, *J* = 12.0 Hz, 1H), 4.23 (d, *J* = 12.0 Hz, 1H), 2.92 (s, 3H). ^{13}C{^{1}H} NMR (100 MHz, $CDCl_3$) δ 199.5, 160.6, 145.6, 141.1, 137.0, 131.5 (2C), 130.4 (2C), 129.8, 128.9, 125.8, 122.8, 122.3, 120.7, 118.3, 116.6, 112.6, 111.4, 73.8, 59.7, 36.8. **HRMS (ESI-TOF)** *m*/*z*: [M + H$^+$] Calcd for $C_{22}H_{18}BrN_2O$ 405.0597, Found. 405.0598.

5-Methyl-12a-(*p*-tolyl)-5, 12a-dihydroindolo[1,2-*c*]quinazolin-12(6*H*)-one (±27ha):

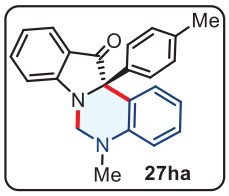

Purification with petroleum ether: acetone (8/2) as eluent); yellow solid (143 mg, 84% yield, mp = 180-183 °C). ^{1}H NMR (400 MHz, $CDCl_3$) δ 7.73 – 7.69 (m, 1H), 7.66 (dd, *J* = 7.9, 1.5 Hz, 1H), 7.56 (m, 1H), 7.19 (m, 1H), 7.15 – 7.10 (m, 3H), 7.10 – 7.06 (m, 2H), 6.97 – 6.92 (m, 1H), 6.81 (td, *J* = 8.0, 1.1 Hz, 1H), 6.72 – 6.68 (m, 1H), 4.67 (d, *J* = 11.9 Hz, 1H), 4.27 (d, *J* = 11.9 Hz, 1H), 2.92 (s, 3H), 2.33 (s, 3H). ^{13}C{^{1}H} NMR (100 MHz, $CDCl_3$) δ 200.3, 160.6, 145.7, 139.3, 137.8, 136.8, 130.0, 129.1 (2C), 128.6, 128.5 (2C), 125.7, 123.1, 120.4, 118.2, 117.3, 112.4, 111.3, 74.2, 59.7, 36.8, 21.1. HRMS (ESI-TOF) *m*/*z*: [M + H$^+$] Calcd for $C_{23}H_{21}N_2O$ 341.1648, Found. 341.1649.

12a-(4-Isobutylphenyl)-5-methyl-5, 12a-dihydroindolo[1,2-*c*]quinazolin-12(6*H*)-one (±27ia):

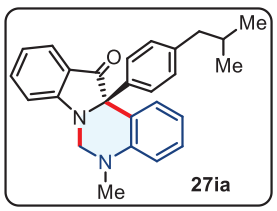

Purification with petroleum ether: acetone (8/2) as eluent); yellow solid (150 mg, 78% yield, mp = 100-103 °C). ^{1}H NMR (400 MHz, $CDCl_3$) δ 7.75 – 7.72 (m, 1H), 7.70 (dd, *J* = 7.9, 1.6 Hz, 1H), 7.59 (m, 1H), 7.21 (m, 1H), 7.17 – 7.14 (m, 1H), 7.11 (d, *J* = 1.0 Hz, 4H), 6.97 (m, 1H), 6.84 (m, 1H), 6.72 (dd, *J* = 8.3, 1.2 Hz, 1H), 4.70 (d, *J* = 11.9 Hz, 1H), 4.31 (d, *J* = 11.9 Hz, 1H), 2.95 (s, 3H), 2.47 (d, *J* = 7.2 Hz, 2H), 1.84 (dp, *J* = 13.6, 6.8 Hz, 1H), 0.93 (d, *J* = 1.2 Hz, 3H), 0.91 (d, *J* = 1.2 Hz, 3H). ^{13}C{^{1}H} NMR (100 MHz, $CDCl_3$) δ 200.3, 160.6, 145.7, 141.5, 139.5, 136.8, 130.0, 129.1 (2C), 128.6, 128.3 (2C), 125.7, 123.1, 120.4, 118.2, 117.4, 112.4, 111.3, 74.3, 59.7, 45.0, 36.8, 30.1, 22.4, 22.4. HRMS (ESI-TOF) *m*/*z*: [M + H$^+$] Calcd for $C_{26}H_{27}N_2O$ 383.2118, Found. 383.2119.

12a-(3-Methoxyphenyl)-5-methyl-5, 12a-dihydroindolo[1,2-*c*]quinazolin-12(6*H*)-one

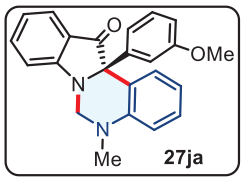

(±27ja): Purification with petroleum ether: acetone (8/2) as eluent); yellow solid (144 mg, 81% yield, mp = 170-173 ºC). ^{1}H NMR (400 MHz, $CDCl_3$) δ 7.72 – 7.69 (m, 1H), 7.68 (dd, *J* = 7.9, 1.5 Hz, 1H), 7.56 (m, 1H), 7.23 (t, *J* = 8.0 Hz, 1H), 7.18 (m, 1H), 7.13 (d, *J* = 8.3 Hz, 1H), 6.97 – 6.92 (m, 1H), 6.86 – 6.78 (m, 3H), 6.76 – 6.74 (m, 1H), 6.70 – 6.67 (m, 1H), 4.68 (d, *J* = 11.9 Hz, 1H), 4.29 (d, *J* = 11.9 Hz, 1H), 3.73 (s, 3H), 2.92 (s, 3H). ^{13}C{^{1}H} NMR (100 MHz, $CDCl_3$) δ 199.8, 160.6, 159.5, 145.6, 143.6, 136.8, 130.0, 129.4, 128.7, 125.8, 122.9, 121.0, 120.4, 118.2, 117.0, 115.0, 113.0, 112.5, 111.3, 74.2, 59.7, 55.2, 36.8. HRMS (ESI-TOF) *m*/*z*: [M + H^{+}] Calcd for $C_{23}H_{21}N_2O_2$ 357.1598, Found. 357.1598.

12a-(3,4-Dimethoxyphenyl)-5-methyl-5, 12a-dihydroindolo[1,2-*c*]quinazolin-12(6*H*)-one

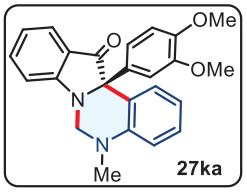

(±27ka): Purification with petroleum ether: acetone (8/2) as eluent); yellow solid (155 mg, 80% yield, mp = 160-162 ºC). ^{1}H NMR (400 MHz, $CDCl_3$) δ 7.71 (d, *J* = 7.6 Hz, 1H), 7.66 (d, *J* = 7.6 Hz, 1H), 7.57 (t, *J* = 7.6 Hz, 1H), 7.22 – 7.12 (m, 2H), 6.95 (t, *J* = 7.4 Hz, 1H), 6.77 (m, 3H), 6.69 (d, *J* = 8.3 Hz, 1H), 6.66 (s, 1H), 4.68 (d, *J* = 11.9 Hz, 1H), 4.29 (d, *J* = 11.9 Hz, 1H), 3.85 (s, 3H), 3.75 (s, 3H), 2.93 (s, 3H). ^{13}C{^{1}H} NMR (100 MHz, $CDCl_3$) δ 200.1, 160.6, 148.9, 145.5, 136.8, 134.5, 130.0, 128.7, 125.8, 122.9, 121.9, 120.4, 118.1, 117.2, 112.4, 111.4, 111.3 (2C), 110.5, 74.4, 59.6, 55.9 (2C), 36.8. HRMS (ESI-TOF) *m*/*z*: [M + H^{+}] Calcd for $C_{24}H_{23}N_2O_3$ 387.1703, Found. 387.1705.

12a-(4-Methoxyphenyl)-5-methyl-5, 12a-dihydroindolo[1,2-*c*]quinazolin-12(6*H*)-one

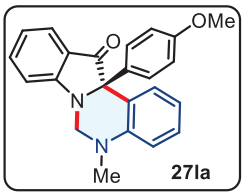

(±27la): Purification with petroleum ether: acetone (8/2) as eluent); yellow solid (153 mg, 86% yield, mp = 175-177 ºC). ^{1}H NMR (400 MHz, $CDCl_3$) δ 7.71 (d, *J* = 7.7 Hz, 1H), 7.67 – 7.63 (m, 1H), 7.56 (t, *J* = 7.6 Hz, 1H), 7.21 – 7.15 (m, 1H), 7.15 – 7.09 (m, 3H), 6.94 (t, *J* = 7.4 Hz, 1H), 6.82 (dd, *J* = 14.2, 8.1 Hz, 3H), 6.69 (d, *J* = 8.3 Hz, 1H), 4.67 (d, *J* = 11.9 Hz, 1H), 4.27 (d, *J* = 11.9 Hz, 1H), 3.78 (s, 3H), 2.92 (s, 3H). ^{13}C{^{1}H} NMR (100 MHz, $CDCl_3$) δ 200.4, 160.5, 159.3, 145.6, 136.8, 134.4, 129.9 (3C), 128.6, 125.7, 123.0, 120.4, 118.2, 117.4, 113.7 (2C), 112.4, 111.3, 74.1, 59.6, 55.3, 36.8. HRMS (ESI-TOF) *m*/*z*: [M + H^{+}] Calcd for $C_{23}H_{21}N_2O_2$ 357.1598, Found. 357.1598.

5-Methyl-12a-(naphthalen-2-yl)-5, 12a-dihydroindolo[1,2-*c*]quinazolin-12(6*H*)-one

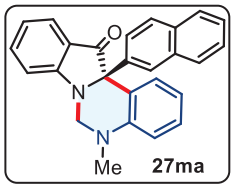

(±27ma): Purification with petroleum ether: acetone (8/2) as eluent); yellow solid (132 mg, 70% yield, mp = 156-158 ºC). ^{1}H NMR (400 MHz, $CDCl_3$) δ 7.85 – 7.72 (m, 5H), 7.68 (s, 1H), 7.60 (t, *J* = 7.6 Hz, 1H), 7.47 (dq, *J* = 11.9, 6.9 Hz, 2H), 7.27 (d, *J* = 4.2 Hz, 1H), 7.24 (s, 1H), 7.18 (d, *J* = 8.2 Hz, 1H), 6.99 (t, *J* = 7.4 Hz, 1H), 6.89 (t, *J* = 7.4 Hz, 1H), 6.76 (d, *J* = 8.2 Hz, 1H), 4.70 (d, *J* = 12.0 Hz, 1H), 4.29 (d, *J* = 12.0 Hz, 1H), 2.95 (s, 3H). ^{13}C{^{1}H} NMR (100 MHz, $CDCl_3$) δ 200.1, 160.8, 145.8, 139.5, 136.8, 133.0, 132.9, 130.1, 128.9, 128.8, 128.4, 128.2, 127.5, 126.3, 126.1, 125.8, 125.6, 123.1, 120.6, 118.3, 116.8, 112.6, 111.4, 74.6, 59.7, 36.8. HRMS (ESI-TOF) *m*/*z*: [M + H^{+}] Calcd for $C_{26}H_{21}N_2O$ 377.1648, Found. 377.1650.

5-Methyl-12a-(thiophen-2-yl)-5, 12a-dihydroindolo[1,2-*c*]quinazolin-12(6*H*)-one (±27na):

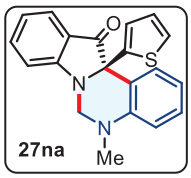

Purification with petroleum ether: acetone (8/2) as eluent); yellow solid (125 mg, 75% yield, mp = 140-143 ºC). ^{1}H NMR (400 MHz, $CDCl_3$) δ 7.87 (dd, *J* = 7.9, 1.4 Hz, 1H), 7.70 (d, *J* = 7.7 Hz, 1H), 7.61 – 7.55 (m, 1H), 7.29 – 7.27 (m, 1H), 7.22 – 7.15 (m, 2H), 7.12 – 7.09 (m, 1H), 7.01 – 6.93 (m, 2H), 6.87 – 6.82 (m, 1H), 6.67 (d, *J* = 8.2 Hz, 1H), 4.78 (d, *J* = 12.0 Hz, 1H), 4.52 (d, *J* = 12.1 Hz, 1H), 2.93 (s, 3H). ^{13}C{^{1}H} NMR (100 MHz, $CDCl_3$) δ 197.4, 159.8, 145.5, 144.9, 137.0, 129.2, 128.8, 127.2, 126.9, 126.0, 125.8, 122.3, 120.8, 118.6, 118.3, 112.4, 111.5, 71.2, 60.1, 36.7. HRMS (ESI-TOF) *m*/*z*: [M + H^{+}] Calcd for $C_{20}H_{17}N_2OS$ 333.1056, Found. 333.1058.

12a-(5-Bromothiophen-2-yl)-5-methyl-5, 12a-dihydroindolo[1,2-*c*]quinazolin-12(6*H*)-one

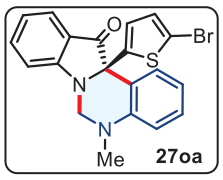

(±27oa): Purification with petroleum ether: acetone (8/2) as eluent); yellow solid (148 mg, 72% yield, mp = 128-130 ºC). ^{1}H NMR (400 MHz, $CDCl_3$) δ 7.85 (d, *J* = 7.4 Hz, 1H), 7.69 (d, *J* = 7.3 Hz, 1H), 7.58 (t, *J* = 7.2 Hz, 1H), 7.18 (t, *J* = 8.8 Hz, 2H), 7.08 (s, 1H), 7.02 – 6.92 (m, 2H), 6.83 (t, *J* = 7.0 Hz, 1H), 6.66 (d, *J* = 7.8 Hz, 1H), 4.77 (d, *J* = 12.0 Hz, 1H), 4.51 (d, *J* = 11.9 Hz, 1H), 2.93 (s, 3H). ^{13}C{^{1}H} NMR (100 MHz, $CDCl_3$) δ 197.4, 159.8, 145.6, 145.0, 137.0, 129.2, 128.9, 127.3, 126.9, 126.1, 125.9, 122.4, 120.8, 118.6, 118.4, 112.4, 111.5, 71.2, 60.1, 36.8. HRMS (ESI-TOF) *m*/*z*: [M + H^{+}] Calcd for $C_{20}H_{16}BrN_2OS$ 411.0161, Found. 411.0162.

10-Chloro-5-methyl-12a-phenyl-5, 12a-dihydroindolo[1,2-*c*]quinazolin-12(6*H*)-one (±27pa):

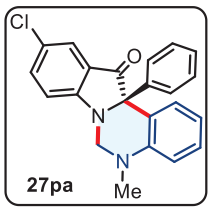

Purification with petroleum ether: acetone (8/2) as eluent); yellow solid (123 mg, 68% yield, mp = 122-124 ºC). ^{1}H NMR (400 MHz, $CDCl_3$) δ 7.81 (d, *J* = 1.9 Hz, 1H), 7.62 (m, 2H), 7.34 – 7.29 (m, 3H), 7.23 – 7.20 (m, 1H), 7.18 (dt, *J* = 6.1, 2.1 Hz, 2H), 7.04 (d, *J* = 8.7 Hz, 1H), 6.86 – 6.80 (m, 1H), 6.71 (d, *J* = 8.3 Hz, 1H), 4.62 (d, *J* = 12.0 Hz, 1H), 4.25 (d, *J* = 12.0 Hz, 1H), 2.92 (s, 3H). ^{13}C{^{1}H} NMR (100 MHz, $CDCl_3$) δ 198.7, 159.3, 145.6, 141.6, 139.3, 130.0, 129.0, 128.6 (2C), 128.5 (2C), 128.3, 128.2, 124.9, 118.5, 116.6, 113.1, 112.9, 112.6, 75.0, 59.7, 36.8. HRMS (ESI-TOF) *m*/*z*: [M + H^{+}] Calcd for $C_{22}H_{18}ClN_2O$ 361.1102, Found. 361.1104.

10-Bromo-5-methyl-12a-phenyl-5, 12a-dihydroindolo[1,2-*c*]quinazolin-12(6*H*)-one (±27qa):

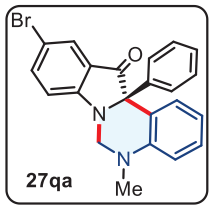

Purification with petroleum ether: acetone (8/2) as eluent); yellow solid (142 mg, 70% yield, mp = 150-153 ºC). ^{1}H NMR (400 MHz, $CDCl_3$) δ 7.81 (d, *J* = 2.0 Hz, 1H), 7.62 (m, 2H), 7.33 – 7.29 (m, 3H), 7.23 – 7.16 (m, 3H), 7.04 (d, *J* = 8.7 Hz, 1H), 6.86 – 6.81 (m, 1H), 6.73 – 6.69 (m, 1H), 4.62 (d, *J* = 12.0 Hz, 1H), 4.25 (d, *J* = 12.0 Hz, 1H), 2.92 (s, 3H). ^{13}C{^{1}H} NMR (100 MHz, $CDCl_3$) δ 198.6, 159.3, 145.6, 141.6, 139.3, 130.0, 128.9, 128.6 (2C), 128.5 (2C), 128.2, 128.2, 124.8, 118.5, 116.5, 113.1, 112.9, 112.6, 75.0, 59.7, 36.8. HRMS (ESI-TOF) *m*/*z*: [M + H^{+}] Calcd for $C_{22}H_{18}BrN_2O$ 405.0597, Found. 405.0598.

5,10-dimethyl-12a-phenyl-5, 12a-dihydroindolo[1,2-*c*]quinazolin-12(6*H*)-one (±27ra):

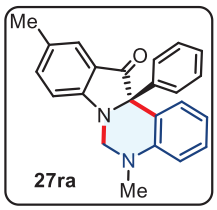

Purification with petroleum ether: acetone (8/2) as eluent); yellow solid (140 mg, 82% yield, mp = 180-183 ºC). ^{1}H NMR (400 MHz, $CDCl_3$) δ 8.22 – 7.66 (dd, *J* = 7.9, 1.5 Hz, 1H), 7.53 – 7.50 (m, 1H), 7.40 (dd, *J* = 8.4, 1.5 Hz, 1H), 7.31 (qd, *J* = 4.5, 1.7 Hz, 3H), 7.23 – 7.16 (m, 3H), 7.07 (d, *J* = 8.4 Hz, 1H), 6.82 (td, *J* = 7.5, 1.2 Hz, 1H), 6.69 (dd, *J* = 8.3, 1.2 Hz, 1H), 4.65 (d, *J* = 11.9 Hz, 1H), 4.24 (d, *J* = 12.0 Hz, 1H), 2.92 (s, 3H), 2.31 (s, 3H). ^{13}C{^{1}H} NMR (100 MHz, $CDCl_3$) δ 200.1, 159.1, 145.7, 142.4, 138.1, 130.1 (2C), 128.7 (2C), 128.6, 128.3 (2C), 127.9, 125.2, 123.3, 118.2, 117.2, 112.4, 111.3, 74.7, 60.0, 36.8, 20.5. HRMS (ESI-TOF) *m*/*z*: [M + H^{+}] Calcd for $C_{23}H_{21}N_2O$ 341.1648, Found. 341.1649.

12a-(4-fluorophenyl)-5, 10-dimethyl-5, 12a-dihydroindolo[1,2-*c*]quinazolin-12(6*H*)-one

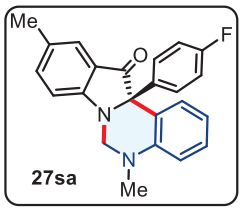

(±27sa): Purification with petroleum ether: acetone (8/2) as eluent); yellow solid (124 mg, 69% yield, mp = 108-110 °C). ^{1}H NMR (400 MHz, $CDCl_3$) δ 7.62 (dd, *J* = 7.9, 1.5 Hz, 1H), 7.50 (p, *J* = 0.9 Hz, 1H), 7.41 (dd, *J* = 8.4, 1.5 Hz, 1H), 7.21 – 7.15 (m, 3H), 7.07 (d, *J* = 8.4 Hz, 1H), 7.02 – 6.95 (m, 2H), 6.83 – 6.78 (m, 1H), 6.68 (dd, *J* = 8.3, 0.9 Hz, 1H), 4.65 (d, *J* = 11.9 Hz, 1H), 4.21 (d, *J* = 12.0 Hz, 1H), 2.92 (s, 3H), 2.31 (s, 3H). ^{13}C{^{1}H} NMR (100 MHz, $CDCl_3$) δ 199.9, 162.4 (d, *J* = 247.1 Hz), 159.0, 145.6, 138.2, 138.2 (d, *J* = 3.2 Hz), 130.5, 130.5, 130.3, 129.9, 128.7, 125.2, 123.1, 118.3, 117.1, 115.3, 115.1, 112.5, 111.3, 74.1, 59.9, 36.8, 20.5. HRMS (ESI-TOF) *m*/*z*: [M + H^{+}] Calcd for $C_{23}H_{20}FN_2O$ 359.1554, Found. 359.1555.

12a-(4-Bromophenyl)-5, 10-dimethyl-5, 12a-dihydroindolo[1,2-*c*]quinazolin-12(6*H*)-one

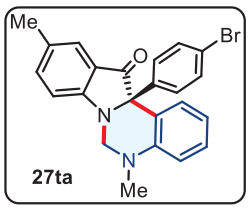

(±27ta): Purification with petroleum ether: acetone (8/2) as eluent); yellow solid (153 mg, 73% yield, mp = 160-163 °C). ^{1}H NMR (400 MHz, $CDCl_3$) δ 7.63 – 7.58 (m, 1H), 7.49 (s, 1H), 7.41 (t, *J* = 7.0 Hz, 3H), 7.21 – 7.15 (m, 1H), 7.10 – 7.04 (m, 3H), 6.81 (t, *J* = 7.4 Hz, 1H), 6.68 (d, *J* = 8.3 Hz, 1H), 4.64 (d, *J* = 11.9 Hz, 1H), 4.19 (d, *J* = 12.0 Hz, 1H), 2.91 (s, 3H), 2.31 (s, 3H). ^{13}C{^{1}H} NMR (100 MHz, $CDCl_3$) δ 199.5, 159.0, 145.6, 141.3, 138.3, 131.5 (2C), 130.4 (3C), 129.9, 128.8, 125.3, 123.1, 122.2, 118.3, 116.7, 112.5, 111.3, 74.2, 60.0, 36.8, 20.6. HRMS (ESI-TOF) *m*/*z*: [M + H^{+}] Calcd for $C_{23}H_{20}BrN_2O$ 419.0754, Found. 419.0755.

5, 10-Dimethyl-12a-(p-tolyl)-5, 12a-dihydroindolo[1,2-*c*]quinazolin-12(6*H*)-one (±27ua):

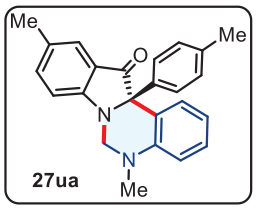

Purification with petroleum ether: acetone (8/2) as eluent); yellow solid (142 mg, 80% yield, mp = 176-178 °C). ^{1}H NMR (400 MHz, $CDCl_3$) δ 7.66 – 7.62 (m, 1H), 7.51 (s, 1H), 7.39 (d, *J* = 8.3 Hz, 1H), 7.21 – 7.15 (m, 1H), 7.09 (dt, *J* = 16.7, 8.3 Hz, 6H), 6.80 (t, *J* = 7.4 Hz, 1H), 6.68 (d, *J* = 8.2 Hz, 1H), 4.63 (d, *J* = 11.9 Hz, 1H), 4.24 (d, *J* = 11.9 Hz, 1H), 2.91 (s, 3H), 2.33 (s, 3H), 2.31 (s, 3H). ^{13}C{^{1}H} NMR (100 MHz, $CDCl_3$) δ 200.3, 159.0, 145.7, 139.5, 138.1, 137.7, 130.1 (2C), 129.1 (2C), 128.6 (2C), 128.5, 125.1, 123.3, 118.2, 117.5, 112.4, 111.3, 74.6, 60.0, 36.8, 21.1, 20.6. HRMS (ESI-TOF) *m*/*z*: [M + H^{+}] Calcd for $C_{24}H_{23}N_2O$ 355.1805, Found. 355.1806.

12a-(4-Methoxyphenyl)-5, 10-dimethyl-5, 12a-dihydroindolo[1,2-*c*]quinazolin-12(6*H*)-one (±27va): 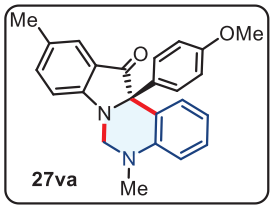

Purification with petroleum ether: acetone (8/2) as eluent); yellow solid (162 mg, 87% yield, mp = 170-172 ºC). ^{1}H NMR (400 MHz, $CDCl_3$) δ 7.63 (dd, *J* = 7.9, 1.5 Hz, 1H), 7.50 (d, *J* = 0.9 Hz, 1H), 7.39 (dd, *J* = 8.4, 1.7 Hz, 1H), 7.17 (m, 1H), 7.14 – 7.09 (m, 2H), 7.06 (d, *J* = 8.4 Hz, 1H), 6.83 (dt, *J* = 8.5, 2.4 Hz, 2H), 6.81 – 6.78 (m, 1H), 6.70 – 6.66 (m, 1H), 4.64 (d, *J* = 11.9 Hz, 1H), 4.24 (d, *J* = 11.9 Hz, 1H), 3.78 (s, 3H), 2.91 (s, 3H), 2.31 (s, 3H). ^{13}C{^{1}H} NMR (100 MHz, $CDCl_3$) δ 200.4, 159.2, 158.9, 145.6, 138.1, 134.6, 130.1, 130.0, 129.9 (2C), 128.5, 125.1, 123.2, 118.2, 117.5, 113.7 (2C), 112.4, 111.3, 74.4, 59.9, 55.3, 36.8, 20.5. HRMS (ESI-TOF) *m*/*z*: [M + H$^+$] Calcd for $C_{24}H_{23}N_2O_2$ 371.1754, Found. 371.1755.

5, 10-dimethyl-12a-(naphthalen-2-yl)-5, 12a-dihydroindolo[1,2-*c*]quinazolin-12(6*H*)-one (±27wa): 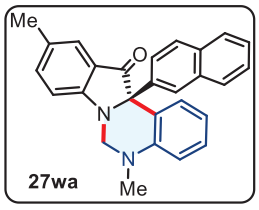

Purification with petroleum ether: acetone (8/2) as eluent); yellow solid (152 mg, 78% yield, mp = 133-135 ºC). ^{1}H NMR (400 MHz, $CDCl_3$) δ 7.80 (dd, *J* = 9.4, 2.2 Hz, 2H), 7.77 – 7.75 (m, 1H), 7.75 – 7.72 (m, 1H), 7.67 – 7.65 (m, 1H), 7.54 (s, 1H), 7.45 (m, 3H), 7.25 – 7.20 (m, 2H), 7.09 (d, *J* = 8.4 Hz, 1H), 6.89 – 6.83 (m, 1H), 6.76 – 6.71 (m, 1H), 4.66 (d, *J* = 11.9 Hz, 1H), 4.25 (d, *J* = 12.0 Hz, 1H), 2.93 (s, 3H), 2.33 (s, 3H). ^{13}C{^{1}H} NMR (100 MHz, $CDCl_3$) δ 200.2, 159.2, 145.8, 139.7, 138.2, 133.0, 132.9, 130.3, 130.2, 128.9, 128.7, 128.4, 128.2, 127.5, 126.3, 126.1, 125.7, 125.2, 123.3, 118.3, 116.9, 112.5, 111.4, 75.0, 60.0, 36.8, 20.6. HRMS (ESI-TOF) *m*/*z*: [M + H$^+$] Calcd for $C_{27}H_{23}N_2O$ 391.1805, Found. 391.1806.

3-Fluoro-5-methyl-12a-phenyl-5, 12a-dihydroindolo[1,2-*c*]quinazolin-12(6*H*)-one (±27ab): 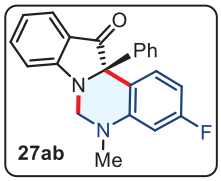

Purification with petroleum ether: acetone (8/2) as eluent); yellow solid (117 mg, 68% yield, mp = 102-104 ºC). ^{1}H NMR (400 MHz, $CDCl_3$) δ 7.74 – 7.70 (m, 1H), 7.62 (dd, *J* = 8.7, 6.6 Hz, 1H), 7.59 – 7.56 (m, 1H), 7.32 (dd, *J* = 5.1, 1.9 Hz, 3H), 7.20 – 7.16 (m, 2H), 7.13 (d, *J* = 8.3 Hz, 1H), 7.00 – 6.95 (m, 1H), 6.51 (td, *J* = 8.5, 2.6 Hz, 1H), 6.38 (dd, *J* = 11.7, 2.5 Hz, 1H), 4.69 (d, *J* = 12.0 Hz, 1H), 4.28 (d, *J* = 12.1 Hz, 1H), 2.91 (s, 3H). ^{13}C{^{1}H} NMR (100 MHz, $CDCl_3$) δ 199.9, 163.3 (d, *J* = 244.7 Hz), 160.4, 147.1 (d, *J* = 10.6 Hz), 141.8, 136.9, 131.5 (d, *J* = 10.0 Hz), 128.5 (2C), 128.4 (2C), 128.1, 125.8, 122.8, 120.7, 112.6 (d, *J* = 2.6 Hz), 111.2, 105.0 (d, *J* = 21.8 Hz), 99.3 (d, *J* = 26.2 Hz), 73.8, 59.3, 36.7. HRMS (ESI-TOF) *m*/*z*: [M + H$^+$] Calcd for $C_{22}H_{18}FN_2O$ 345.1398, Found. 345.1399.

2-Fluoro-5-methyl-12a-phenyl-5, 12a-dihydroindolo[1,2-*c*]quinazolin-12(6*H*)-one (±27ac):

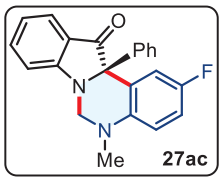

Purification with petroleum ether: acetone (8/2) as eluent); yellow solid (121 mg, 70% yield, mp = 105-107 ºC). ^{1}H NMR (400 MHz, $CDCl_3$) δ 7.73 (d, *J* = 7.5 Hz, 1H), 7.61 – 7.56 (m, 1H), 7.45 (dd, *J* = 9.6, 3.0 Hz, 1H), 7.32 (dd, *J* = 5.1, 1.9 Hz, 3H), 7.21 – 7.17 (m, 2H), 7.15 (d, *J* = 8.3 Hz, 1H), 6.97 (t, *J* = 7.4 Hz, 1H), 6.92 (m, 1H), 6.65 (dd, *J* = 9.1, 4.7 Hz, 1H), 4.67 (d, *J* = 11.9 Hz, 1H), 4.22 (d, *J* = 12.0 Hz, 1H), 2.90 (s, 3H). ^{13}C{^{1}H} NMR (100 MHz, $CDCl_3$) δ 199.6, 160.7, 155.7 (d, *J* = 238.1 Hz), 142.3 (d, *J* = 2.0 Hz), 141.7, 137.1, 128.5 (4C), 128.2, 125.7, 122.9, 120.6, 118.6 (d, *J* = 6.8 Hz), 116.2 (d, *J* = 23.5 Hz), 115.7 (d, *J* = 22.4 Hz), 113.6 (d, *J* = 7.3 Hz), 111.4, 74.2 (d, *J* = 1.8 Hz), 59.9, 37.2. HRMS (ESI-TOF) *m*/*z*: [M + H^{+}] Calcd for $C_{22}H_{18}FN_2O$ 345.1398, Found. 345.1399.

3-Chloro-5-methyl-12a-phenyl-5, 12a-dihydroindolo[1,2-*c*]quinazolin-12(6*H*)-one (±27ad):

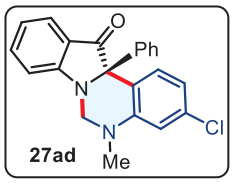

Purification with petroleum ether: acetone (8/2) as eluent); yellow solid (137 mg, 76% yield, mp = 112-114 ºC). ^{1}H NMR (400 MHz, $CDCl_3$) δ 7.72 (d, *J* = 7.6 Hz, 1H), 7.58 (t, *J* = 7.5 Hz, 2H), 7.34 – 7.29 (m, 3H), 7.20 – 7.15 (m, 2H), 7.12 (d, *J* = 8.3 Hz, 1H), 6.97 (t, *J* = 7.4 Hz, 1H), 6.81 – 6.75 (m, 1H), 6.68 – 6.64 (m, 1H), 4.68 (d, *J* = 12.1 Hz, 1H), 4.29 (d, *J* = 12.1 Hz, 1H), 2.92 (s, 3H). ^{13}C{^{1}H} NMR (100 MHz, $CDCl_3$) δ 199.7, 160.4, 146.5, 141.6, 137.0, 134.8, 131.1, 128.5 (4C), 128.2, 125.8, 122.8, 120.7, 118.1, 115.4, 112.2, 111.2, 73.9, 59.3, 36.7. HRMS (ESI-TOF) *m*/*z*: [M + H^{+}] Calcd for $C_{22}H_{18}ClN_2O$ 361.1102, Found. 361.1103.

2,3-Dichloro-5-methyl-12a-phenyl-5, 12a-dihydroindolo[1,2-*c*]quinazolin-12(6*H*)-one

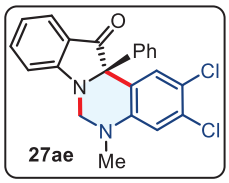

(±27ae): Purification with petroleum ether: acetone (8/2) as eluent); yellow solid (128 mg, 65% yield, mp = 142-144 ºC). ^{1}H NMR (400 MHz, $CDCl_3$) δ 7.74 – 7.71 (m, 2H), 7.59 (m, 1H), 7.35 – 7.31 (m, 3H), 7.18 – 7.14 (m, 2H), 7.11 (d, *J* = 8.3 Hz, 1H), 7.01 – 6.97 (m, 1H), 6.74 (s, 1H), 4.68 (d, *J* = 12.1 Hz, 1H), 4.29 (d, *J* = 12.1 Hz, 1H), 2.92 (s, 3H). ^{13}C{^{1}H} NMR (100 MHz, $CDCl_3$) δ 199.2, 160.3, 144.9, 141.1, 137.2, 132.9, 131.0, 128.7 (2C), 128.5 (2C), 128.4, 126.0, 122.6, 121.2, 120.9, 117.1, 113.8, 111.2, 73.6, 59.2, 36.7. HRMS (ESI-TOF) *m*/*z*: [M + H^{+}] Calcd for $C_{22}H_{17}Cl_2N_2O$ 395.0712, Found. 395.0712.

2-Chloro-5-methyl-12a-phenyl-5, 12a-dihydroindolo[1,2-*c*]quinazolin-12(6*H*)-one (±27af):

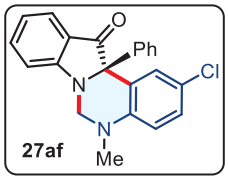

Purification with petroleum ether: acetone (8/2) as eluent); yellow solid (139 mg, 77% yield, mp = 152-154 ºC). ^{1}H NMR (400 MHz, $CDCl_3$) δ 7.73 (d, *J* = 7.7 Hz, 1H), 7.67 (d, *J* = 2.2 Hz, 1H), 7.58 (t, *J* = 7.6 Hz, 1H), 7.32 (d, *J* = 3.8 Hz, 3H), 7.22 – 7.16 (m, 2H), 7.14 (s, 2H), 6.97 (t, *J* = 7.4 Hz, 1H), 6.61 (d, *J* = 8.9 Hz, 1H), 4.68 (d, *J* = 12.0 Hz, 1H), 4.25 (d, *J* = 12.0 Hz, 1H), 2.91 (s, 3H). ^{13}C{^{1}H} NMR (100 MHz, $CDCl_3$) δ 199.5, 160.5, 144.2, 141.5, 137.0, 129.3, 128.7, 128.5 (4C), 128.2, 125.8, 123.2, 122.7, 120.7, 118.6, 113.7, 111.3, 74.0, 59.5, 36.8.HRMS (ESI-TOF) *m*/*z*: [M + H^+] Calcd for $C_{22}H_{18}ClN_2O$ 361.1102, Found. 361.1103.

10-Methoxy-5-methyl-12a-phenyl-5, 12a-dihydroindolo[1,2-*c*]quinazolin-12(6*H*)-one

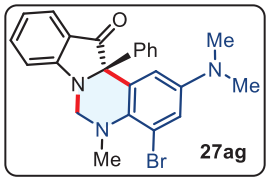

(±27ag): Purification with petroleum ether: acetone (8/2) as eluent); yellow solid (175 mg, 78% yield, mp = 162-165 ºC). ^{1}H NMR (400 MHz, $CDCl_3$) δ 7.72 – 7.67 (m, 1H), 7.54 (m, 1H), 7.34 (m, 3H), 7.25 (dd, *J* = 5.4, 1.9 Hz, 2H), 7.07 (d, *J* = 8.3 Hz, 1H), 6.98 – 6.91 (m, 1H), 6.52 (s, 1H), 6.39 (s, 1H), 4.54 (d, *J* = 11.9 Hz, 1H), 4.18 (d, *J* = 12.0 Hz, 1H), 2.94 (s, 3H), 2.22 (d, *J* = 16.5 Hz, 6H). ^{13}C{^{1}H} NMR (100 MHz, $CDCl_3$) δ 199.7, 159.5, 147.4, 142.2, 140.8, 137.8, 136.5, 128.4 (2C), 128.3, 127.7, 125.5, 124.4 (2C), 124.2, 120.5, 111.8, 111.3 (2C), 76.2, 59.6, 38.0, 22.7, 21.3. HRMS (ESI-TOF) *m*/*z*: [M + H^+] Calcd for $C_{24}H_{23}BrN_3O$ 448.1019, Found. 448.1020.

3-Bromo-5-methyl-12a-phenyl-5, 12a-dihydroindolo[1,2-*c*]quinazolin-12(6*H*)-one (±27ah):

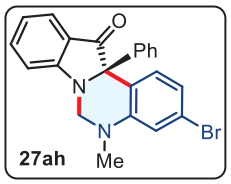

Purification with petroleum ether: acetone (8/2) as eluent); yellow solid (154 mg, 76% yield, mp = 110-113 ºC). ^{1}H NMR (400 MHz, $CDCl_3$) δ 7.74 – 7.69 (m, 1H), 7.58 (m, 1H), 7.52 (d, *J* = 8.4 Hz, 1H), 7.34 – 7.29 (m, 3H), 7.20 – 7.14 (m, 2H), 7.12 (d, *J* = 8.3 Hz, 1H), 7.00 – 6.95 (m, 1H), 6.92 (dd, *J* = 8.4, 1.9 Hz, 1H), 6.81 (d, *J* = 1.9 Hz, 1H), 4.68 (d, *J* = 12.1 Hz, 1H), 4.29 (d, *J* = 12.1 Hz, 1H), 2.92 (s, 3H). ^{13}C{^{1}H} NMR (100 MHz, $CDCl_3$) δ 199.6, 160.4, 146.6, 141.5, 137.0, 131.4, 128.6 (2C), 128.5 (2C), 128.2, 125.9, 123.1, 122.8, 121.0, 120.7, 115.9, 115.1, 111.2, 74.0, 59.3, 36.7. HRMS (ESI-TOF) *m*/*z*: [M + H^+] Calcd for $C_{22}H_{18}BrN_2O$ 405.0597, Found. 405.0598.

3-Bromo-2,5-dimethyl-12a-phenyl-5, 12a-dihydroindolo[1,2-*c*]quinazolin-12(6*H*)-one

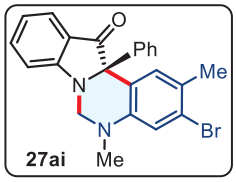

(±27ai): Purification with petroleum ether: acetone (8/2) as eluent); yellow solid (170 mg, 81% yield, mp = 162-163 °C). ^{1}H NMR (400 MHz, $CDCl_3$) δ 7.71 (d, *J* = 7.7 Hz, 1H), 7.57 (t, *J* = 7.6 Hz, 1H), 7.50 (s, 1H), 7.34 – 7.29 (m, 3H), 7.17 (dd, *J* = 6.4, 2.8 Hz, 2H), 7.12 (d, *J* = 8.3 Hz, 1H), 6.97 (t, *J* = 7.4 Hz, 1H), 6.88 (s, 1H), 4.64 (d, *J* = 12.0 Hz, 1H), 4.25 – 4.20 (m, 1H), 2.89 (s, 3H), 2.28 (s, 3H). ^{13}C{^{1}H} NMR (100 MHz, $CDCl_3$) δ 199.9, 160.5, 144.7, 141.7, 137.0, 131.5, 128.6 (2C), 128.5 (2C), 128.2, 127.2, 125.8, 125.5, 122.8, 120.7, 116.4, 116.1, 111.3, 74.1, 59.5, 36.8, 21.8. HRMS (ESI-TOF) *m*/*z*: [M + H$^+$] Calcd for $C_{23}H_{20}BrN_2O$ 419.0754, Found. 419.0756.

2-Bromo-5-methyl-12a-phenyl-5, 12a-dihydroindolo[1,2-*c*]quinazolin-12(6*H*)-one (±27aj):

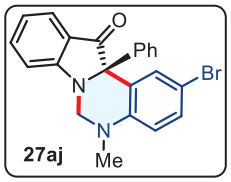

Purification with petroleum ether: acetone (8/2) as eluent); yellow solid (158 mg, 78% yield, mp = 122-125 °C). ^{1}H NMR (400 MHz, $CDCl_3$) δ 7.79 (d, *J* = 2.4 Hz, 1H), 7.75 – 7.72 (m, 1H), 7.59 (m, 1H), 7.35 – 7.28 (m, 3H), 7.27 (s, 1H), 7.21 – 7.16 (m, 2H), 7.13 (d, *J* = 8.3 Hz, 1H), 7.01 – 6.95 (m, 1H), 6.56 (d, *J* = 8.9 Hz, 1H), 4.68 (d, *J* = 12.0 Hz, 1H), 4.26 (d, *J* = 12.1 Hz, 1H), 2.91 (s, 3H). ^{13}C{^{1}H} NMR (100 MHz, $CDCl_3$) δ 199.4, 160.4, 144.6, 141.5, 137.0, 132.1, 131.6, 128.5 (4C), 128.2, 125.8 (2C), 122.7, 120.7, 119.0, 114.1, 111.2, 110.3, 73.9, 59.4, 36.7. HRMS (ESI-TOF) *m*/*z*: [M + H$^+$] Calcd for $C_{22}H_{18}BrN_2O$ 405.0597, Found. 405.0598.

2-Iodo-5-methyl-12a-phenyl-5, 12a-dihydroindolo[1,2-*c*]quinazolin-12(6*H*)-one (±27ak):

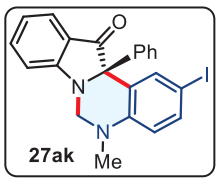

Purification with petroleum ether: acetone (8/2) as eluent); yellow solid (181 mg, 80% yield, mp = 162-164 °C). ^{1}H NMR (400 MHz, $CDCl_3$) δ 7.92 (d, *J* = 1.8 Hz, 1H), 7.72 (d, *J* = 7.6 Hz, 1H), 7.58 (t, *J* = 7.5 Hz, 1H), 7.47 – 7.42 (m, 1H), 7.36 – 7.29 (m, 3H), 7.21 – 7.15 (m, 2H), 7.12 (d, *J* = 8.3 Hz, 1H), 6.97 (t, *J* = 7.4 Hz, 1H), 6.44 (d, *J* = 8.7 Hz, 1H), 4.67 (d, *J* = 12.0 Hz, 1H), 4.26 (d, *J* = 12.1 Hz, 1H), 2.90 (s, 3H). ^{13}C{^{1}H} NMR (100 MHz, $CDCl_3$) δ 199.4, 160.4, 145.1, 141.5, 137.7, 137.4, 137.0, 128.5 (4C), 128.2, 125.8, 122.7, 120.7, 119.4, 114.6, 111.2, 79.5, 73.7, 59.3, 36.6. HRMS (ESI-TOF) *m*/*z*: [M + H$^+$] Calcd for $C_{22}H_{18}IN_2O$ 453.0458, Found. 453.0460.

3,5-Dimethyl-12a-phenyl-5, 12a-dihydroindolo[1,2-*c*]quinazolin-12(6*H*)-one (±27al):

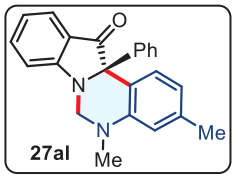

Purification with petroleum ether: acetone (8/2) as eluent); yellow solid (146 mg, 86% yield, mp = 178-180 °C). ^{1}H NMR (400 MHz, $CDCl_3$) δ 7.74 (d, *J*

= 7.5 Hz, 1H), 7.58 (t, *J* = 7.0 Hz, 2H), 7.33 (d, *J* = 5.5 Hz, 3H), 7.28 – 7.22 (m, 2H), 7.16 (d, *J* = 8.3 Hz, 1H), 6.97 (t, *J* = 7.3 Hz, 1H), 6.69 (d, *J* = 7.6 Hz, 1H), 6.55 (s, 1H), 4.69 (d, *J* = 11.9 Hz, 1H), 4.28 (d, *J* = 11.9 Hz, 1H), 2.94 (s, 3H), 2.32 (s, 3H).$^{13}C\{^{1}H\}$ NMR (100 MHz, $CDCl_3$) δ 200.2, 160.6, 145.5, 142.1, 138.6, 136.7, 129.8, 128.6 (2C), 128.3 (2C), 127.9, 125.7, 123.0, 120.4, 119.3, 114.2, 113.1, 111.3, 74.3, 59.7, 36.8, 21.6. HRMS (ESI-TOF) *m/z*: [M + H^+] Calcd for $C_{23}H_{21}N_2O$ 341.1648, Found. 341.1650.

2,3,5-Trimethyl-12a-phenyl-5, 12a-dihydroindolo[1,2-*c*]quinazolin-12(6*H*)-one (±27am):

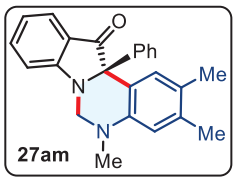

Purification with petroleum ether: acetone (8/2) as eluent); yellow solid (160 mg, 90% yield, mp = 192-194 ºC). ^{1}H NMR (400 MHz, $CDCl_3$) δ 7.74 – 7.70 (m, 1H), 7.56 (m, 1H), 7.43 (s, 1H), 7.32 (m, 3H), 7.25 – 7.21 (m, 2H), 7.14 (d, *J* = 8.3 Hz, 1H), 6.97 – 6.92 (m, 1H), 6.53 (s, 1H), 4.64 (d, *J* = 11.8 Hz, 1H), 4.20 (d, *J* = 11.9 Hz, 1H), 2.90 (s, 3H), 2.22 (s, 3H), 2.18 (s, 3H). $^{13}C\{^{1}H\}$ NMR (100 MHz, $CDCl_3$) δ 200.3, 160.7, 143.9, 142.3, 137.2, 136.7, 130.5, 128.6 (2C), 128.3 (2C), 127.9, 126.6, 125.7, 123.0, 120.3, 114.6, 114.1, 111.4, 74.3, 59.9, 37.0, 20.0, 18.8. HRMS (ESI-TOF) *m/z*: [M + H^+] Calcd for $C_{24}H_{23}N_2O$ 355.1805, Found. 355.1808.

2,5-Dimethyl-12a-phenyl-5, 12a-dihydroindolo[1,2-*c*]quinazolin-12(*6H*)-one (±27an):

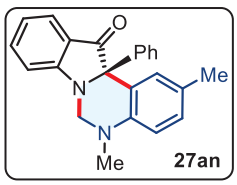

Purification with petroleum ether: acetone (8/2) as eluent); yellow solid (157 mg, 92% yield, mp = 202-204 ºC). ^{1}H NMR (400 MHz, $CDCl_3$) δ 7.72 (d, *J* = 7.7 Hz, 1H), 7.56 (t, *J* = 7.3 Hz, 1H), 7.48 (s, 1H), 7.35 – 7.29 (m, 3H), 7.27 – 7.18 (m, 2H), 7.14 (d, *J* = 8.3 Hz, 1H), 7.04 – 6.98 (m, 1H), 6.95 (t, *J* = 7.4 Hz, 1H), 6.63 (d, *J* = 8.4 Hz, 1H), 4.65 (d, *J* = 11.9 Hz, 1H), 4.21 (d, *J* = 11.9 Hz, 1H), 2.89 (s, 3H), 2.25 (s, 3H). $^{13}C\{^{1}H\}$ NMR (100 MHz, $CDCl_3$) δ 200.3, 160.7, 143.6, 142.3, 136.8, 130.1, 129.4, 128.7 (2C), 128.4 (2C), 128.0, 127.7, 125.7, 123.0, 120.4, 117.2, 112.7, 111.4, 74.4, 59.9, 37.0, 20.5. HRMS (ESI-TOF) *m/z*: [M + H^+] Calcd for $C_{23}H_{21}N_2O$ 341.1648, Found. 341.1650.

2-Ethyl-5-methyl-12a-phenyl-5, 12a-dihydroindolo[1,2-*c*]quinazolin-12(6*H*)-one (±27ao):

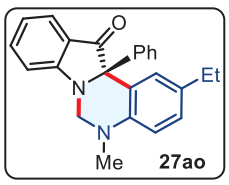

Purification with petroleum ether: acetone (8/2) as eluent); yellow solid (156 mg, 88% yield, mp = 192-195 ºC). ^{1}H NMR (400 MHz, $CDCl_3$) δ 7.72 (d, *J* = 7.6 Hz, 1H), 7.59 – 7.53 (m, 1H), 7.51 (d, *J* = 1.9 Hz, 1H), 7.31 (dd, *J* = 5.2, 1.8 Hz, 3H), 7.22 – 7.18 (m, 2H), 7.13 (d, *J* = 8.3 Hz, 1H), 7.04 (dd, *J* = 8.4, 2.0 Hz, 1H), 6.94 (t, *J* = 7.3 Hz, 1H), 6.66 (d, *J* = 8.4 Hz, 1H), 4.65 (d, *J* = 11.8 Hz, 1H),

4.21 (d, *J* = 11.9 Hz, 1H), 2.90 (s, 3H), 2.55 (q, *J* = 7.5 Hz, 2H), 1.18 (t, *J* = 7.6 Hz, 3H). $^{13}C\{^{1}H\}$ NMR (100 MHz, $CDCl_3$) δ 200.2, 160.7, 143.8, 142.3, 136.7, 134.2, 129.2, 128.6 (2C), 128.4 (2C), 128.1, 127.9, 125.7, 123.0, 120.3, 117.2, 112.7, 111.3, 74.5, 59.9, 37.0, 28.0, 15.8. HRMS (ESI-TOF) *m*/*z*: [M + H^+] Calcd for $C_{24}H_{23}N_2O$ 355.1805, Found. 355.1808.

2-Isopropyl-5-methyl-12a-phenyl-5, 12a-dihydroindolo[1,2-*c*]quinazolin-12(6*H*)-one (±27ap): 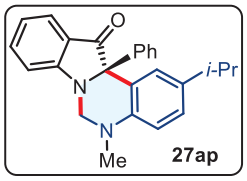

Purification with petroleum ether: acetone (8/2) as eluent); yellow solid (155 mg, 84% yield, mp = 122-124 °C). ^{1}H NMR (400 MHz, $CDCl_3$) δ 7.72 (d, *J* = 7.6 Hz, 1H), 7.59 – 7.54 (m, 2H), 7.31 (td, *J* = 5.0, 1.7 Hz, 3H), 7.22 – 7.18 (m, 2H), 7.14 (d, *J* = 8.3 Hz, 1H), 7.09 (dd, *J* = 8.5, 2.1 Hz, 1H), 6.95 (t, *J* = 7.4 Hz, 1H), 6.67 (d, *J* = 8.5 Hz, 1H), 4.66 (d, *J* = 11.8 Hz, 1H), 4.21 (d, *J* = 11.9 Hz, 1H), 2.90 (s, 3H), 2.83 (dt, *J* = 13.8, 6.9 Hz, 1H), 1.20 (dd, *J* = 6.9, 4.0 Hz, 6H). $^{13}C\{^{1}H\}$ NMR (100 MHz, $CDCl_3$) δ 200.1, 160.7, 143.9, 142.3, 138.8, 136.7, 128.6 (2C), 128.4 (2C), 128.1, 127.9, 126.4, 125.7, 123.0, 120.3, 117.0, 112.6, 111.3, 74.5, 59.9, 36.9, 33.2, 24.2, 23.9. HRMS (ESI-TOF) *m*/*z*: [M + H^+] Calcd for $C_{25}H_{25}N_2O$ 369.1961, Found. 369.1965.

2-Butyl-5-methyl-12a-phenyl-5, 12a-dihydroindolo[1,2-*c*]quinazolin-12(6*H*)-one (±27aq): 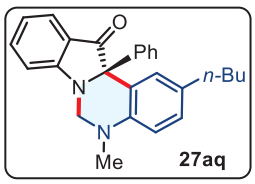

Purification with petroleum ether: acetone (8/2) as eluent); yellow solid (159 mg, 83% yield, mp = 172-174 °C). ^{1}H NMR (400 MHz, $CDCl_3$) δ 7.74 – 7.70 (m, 1H), 7.56 (m, 1H), 7.49 (d, *J* = 2.1 Hz, 1H), 7.31 (qd, *J* = 4.3, 1.6 Hz, 3H), 7.22 – 7.17 (m, 2H), 7.13 (d, *J* = 8.3 Hz, 1H), 7.02 (dd, *J* = 8.4, 2.1 Hz, 1H), 6.98 – 6.92 (m, 1H), 6.64 (d, *J* = 8.4 Hz, 1H), 4.65 (d, *J* = 11.8 Hz, 1H), 4.21 (d, *J* = 11.9 Hz, 1H), 2.89 (s, 3H), 2.54 – 2.48 (m, 2H), 1.58 – 1.48 (m, 2H), 1.32 (dq, *J* = 14.6, 7.3 Hz, 2H), 0.90 (t, *J* = 7.3 Hz, 3H). $^{13}C\{^{1}H\}$ NMR (100 MHz, $CDCl_3$) δ 200.2, 160.7, 143.8, 142.4, 136.7, 132.9, 129.7, 128.7, 128.6 (2C), 128.4 (2C), 127.9, 125.7, 123.1, 120.4, 117.1, 112.6, 111.3, 74.4, 59.9, 36.9, 34.7, 33.9, 22.3, 13.9. HRMS (ESI-TOF) *m*/*z*: [M + H^+] Calcd for $C_{26}H_{27}N_2O$ 383.2118, Found. 383.2120.

3-(Tert-butyl)-5-methyl-12a-phenyl-5, 12a-dihydroindolo[1,2-*c*]quinazolin-12(6*H*)-one (±27ar): 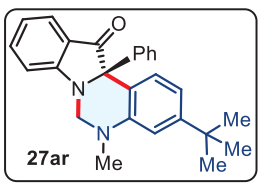

Purification with petroleum ether: acetone (8/2) as eluent); yellow solid (164 mg, 86% yield, mp = 122-123 °C). ^{1}H NMR (400 MHz, $CDCl_3$) δ 7.70 (d, *J* = 7.6 Hz, 1H), 7.59 (d, *J* = 8.3 Hz, 1H), 7.57 – 7.52 (m, 1H), 7.33 – 7.27 (m, 3H), 7.24 – 7.21 (m, 2H), 7.14 (d, *J* = 8.3 Hz, 1H), 6.92 (t, *J* = 7.4 Hz, 1H), 6.86 (dd, *J* = 8.3, 1.8 Hz, 1H), 6.70 (d, *J* = 1.7 Hz, 1H), 4.67 (d, *J* =

11.9 Hz, 1H), 4.24 (d, *J* = 11.9 Hz, 1H), 2.93 (s, 3H), 1.28 (s, 9H). $^{13}C\{^1H\}$ NMR (100 MHz, $CDCl_3$) δ 200.2, 160.7, 151.6, 145.3, 142.2, 136.7, 129.5, 128.6 (2C), 128.3 (2C), 127.9, 125.7, 123.1, 120.4, 116.0, 114.3, 111.4, 109.5, 74.3, 60.0, 36.9, 34.7, 31.2 (3C). HRMS (ESI-TOF) *m*/*z*: [M + H^+] Calcd for $C_{26}H_{27}N_2O$ 383.2118, Found. 383.2120.

2-(Tert-butyl)-5-methyl-12a-phenyl-5, 12a-dihydroindolo[1,2-*c*]quinazolin-12(6*H*)-one (±27as): Purification with petroleum ether: acetone (8/2) as eluent); yellow solid (166 mg, 87% yield, mp = 142-143 °C). ^1H NMR (400 MHz, $CDCl_3$) δ 7.76 (d, *J* = 2.3 Hz, 1H), 7.75 – 7.71 (m, 1H), 7.56 (m, 1H), 7.34 – 7.28 (m, 3H), 7.26 – 7.20 (m, 3H), 7.14 (d, *J* = 8.3 Hz, 1H), 6.97 – 6.92 (m, 1H), 6.67 (d, *J* = 8.7 Hz, 1H), 4.66 (d, *J* = 11.8 Hz, 1H), 4.21 (d, *J* = 11.9 Hz, 1H), 2.90 (s, 3H), 1.29 (s, 9H). $^{13}C\{^1H\}$ NMR (100 MHz, $CDCl_3$) δ 200.1, 160.7, 143.5, 142.3, 141.0, 136.7, 128.5 (2C), 128.3 (2C), 127.9, 127.0, 125.7, 125.5, 123.0, 120.3, 116.7, 112.2, 111.2, 74.5, 59.8, 36.8, 34.0, 31.4 (3C). HRMS (ESI-TOF) *m*/*z*: [M + H^+] Calcd for $C_{26}H_{27}N_2O$ 383.2118, Found. 383.2120.

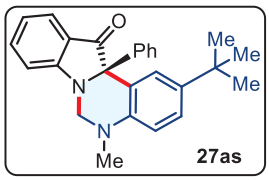

5-Methyl-2,12a-diphenyl-5, 12a-dihydroindolo[1,2-*c*]quinazolin-12(6*H*)-one (±27at): Purification with petroleum ether: acetone (8/2) as eluent); yellow solid (171 mg, 85% yield, mp = 166-168 °C). ^1H NMR (400 MHz, $CDCl_3$) δ 8.01 (d, *J* = 2.2 Hz, 1H), 7.77 – 7.74 (m, 1H), 7.62 – 7.56 (m, 3H), 7.49 (dd, *J* = 8.6, 2.3 Hz, 1H), 7.39 (tt, *J* = 8.3, 1.8 Hz, 2H), 7.36 – 7.32 (m, 3H), 7.27 (m, 3H), 7.17 (d, *J* = 8.3 Hz, 1H), 6.98 (m, 1H), 6.79 (d, *J* = 8.6 Hz, 1H), 4.72 (d, *J* = 11.9 Hz, 1H), 4.32 (d, *J* = 12.0 Hz, 1H), 2.98 (s, 3H). $^{13}C\{^1H\}$ NMR (100 MHz, $CDCl_3$) δ 200.0, 160.7, 145.1, 142.1, 140.5, 136.9, 130.9, 128.7 (4C), 128.5 (2C), 128.4, 128.1, 127.3, 126.5 (3C), 125.8, 123.0, 120.6, 117.4, 112.9, 111.3, 74.5, 59.7, 36.8. HRMS (ESI-TOF) *m*/*z*: [M + H^+] Calcd for $C_{28}H_{23}N_2O$ 403.1805, Found. 403.1806.

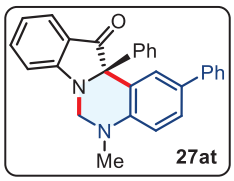

7-Methyl-14b-phenyl-6,7,9,14b-tetrahydro-15*H*-indeno[1,2-g]indolo[1,2-c]quinazolin-15-one (±27au): Purification with petroleum ether: acetone (8/2) as eluent); yellow solid (168 mg, 81% yield, mp = 205-207 °C). ^1H NMR (400 MHz, $CDCl_3$) δ 8.05 (s, 1H), 7.71 (d, *J* = 7.6 Hz, 1H), 7.66 (d, *J* = 7.6 Hz, 1H), 7.58 – 7.53 (m, 1H), 7.42 (d, *J* = 7.4 Hz, 1H), 7.30 (dp, *J* = 6.3, 3.0 Hz, 4H), 7.25 – 7.21 (m, 2H), 7.19 – 7.16 (m, 1H), 7.13 (d, *J* = 8.4 Hz, 1H), 6.93 (t, *J* = 7.4 Hz, 1H), 6.89 (s, 1H), 4.69 (d, *J* = 11.9 Hz, 1H), 4.29 (d, *J* = 11.9 Hz, 1H), 3.89 – 3.71 (m, 2H),

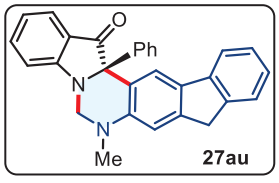

2.97 (s, 3H). $^{13}C\{^{1}H\}$ NMR (100 MHz, $CDCl_3$) δ 200.3, 160.6, 145.0, 144.4, 142.3, 142.1, 141.8, 136.8, 132.6, 128.8 (2C), 128.4 (2C), 128.0, 126.7, 125.8, 125.4, 124.6, 123.0, 121.3, 120.5, 119.4, 115.8, 111.3, 109.2, 74.7, 59.8, 37.2, 36.9. HRMS (ESI-TOF) *m/z*: [M + H^+] Calcd for $C_{29}H_{23}N_2O$ 415.1805, Found. 415.1807.

2-Methoxy-5-methyl-12a-phenyl-5, 12a-dihydroindolo[1,2-*c*]quinazolin-12(6*H*)-one

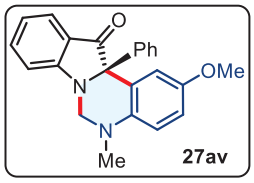

(±27av): Purification with petroleum ether: acetone (8/2) as eluent); yellow solid (159 mg, 89% yield, mp = 182-185 ºC). ^{1}H NMR (400 MHz, $CDCl_3$) δ 7.73 (d, *J* = 7.6 Hz, 1H), 7.60 – 7.54 (m, 1H), 7.31 (dd, *J* = 5.0, 1.7 Hz, 3H), 7.27 (d, *J* = 2.9 Hz, 1H), 7.21 (dd, *J* = 6.6, 3.0 Hz, 2H), 7.15 (d, *J* = 8.3 Hz, 1H), 6.95 (t, *J* = 7.4 Hz, 1H), 6.82 (dd, *J* = 9.0, 2.9 Hz, 1H), 6.69 (d, *J* = 9.0 Hz, 1H), 4.64 (d, *J* = 11.8 Hz, 1H), 4.17 (d, *J* = 11.9 Hz, 1H), 3.73 (s, 3H), 2.87 (s, 3H). $^{13}C\{^{1}H\}$ NMR (100 MHz, $CDCl_3$) δ 200.1, 160.8, 152.3, 142.3, 140.4, 136.9, 128.6 (2C), 128.4 (2C), 128.0, 125.6, 123.0, 120.4, 118.4, 115.9, 114.2, 114.0, 111.5, 74.5, 60.2, 55.7, 37.4. HRMS (ESI-TOF) *m/z*: [M + H^+] Calcd for $C_{23}H_{21}N_2O_2$ 357.1598, Found. 357.1599.

1,2,3-Trimethoxy-5-methyl-12a-phenyl-5, 12a-dihydroindolo[1,2-*c*]quinazolin-12(6*H*)-one

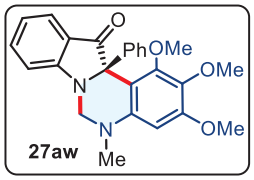

(±27aw): Purification with petroleum ether: acetone (8/2) as eluent); yellow solid (162 mg, 78% yield, mp = 170-171 ºC). ^{1}H NMR (400 MHz, $CDCl_3$) δ 7.72 (d, *J* = 7.4 Hz, 1H), 7.52 (m, 1H), 7.35 – 7.27 (m, 3H), 7.24 – 7.20 (m, 2H), 7.05 (d, *J* = 8.3 Hz, 1H), 6.95 (t, *J* = 7.4 Hz, 1H), 5.99 (s, 1H), 4.53 (d, *J* = 11.9 Hz, 1H), 4.13 (d, *J* = 12.0 Hz, 1H), 3.83 (s, 3H), 3.73 (s, 3H), 3.64 (s, 3H), 2.93 (s, 3H). $^{13}C\{^{1}H\}$ NMR (100 MHz, $CDCl_3$) δ 198.5, 159.0, 155.0, 154.0, 143.6, 142.3, 136.1, 135.0, 128.1 (2C), 128.0 (2C), 127.4, 125.4, 124.6, 120.6, 111.7, 104.2, 92.0, 75.3, 60.7, 60.6, 60.0, 55.7, 37.7. HRMS (ESI-TOF) *m/z*: [M + H^+] Calcd for $C_{25}H_{25}N_2O_4$ 417.1809, Found. 417.1811.

2,3-Dimethoxy-5-methyl-12a-phenyl-5, 12a-dihydroindolo[1,2-*c*]quinazolin-12(6*H*)-one

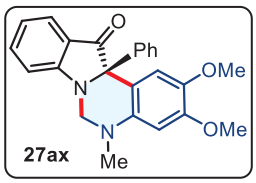

(±27ax): Purification with petroleum ether: acetone (8/2) as eluent); yellow solid (160 mg, 83% yield, mp = 156-158 ºC). ^{1}H NMR (400 MHz, $CDCl_3$) δ 7.74 – 7.71 (m, 1H), 7.57 (m, 1H), 7.31 (dt, *J* = 5.8, 2.6 Hz, 3H), 7.21 – 7.17 (m, 3H), 7.15 (d, *J* = 8.3 Hz, 1H), 6.99 – 6.93 (m, 1H), 6.30 (s, 1H), 4.64 (d, *J* = 11.9 Hz, 1H), 4.16 (d, *J* = 12.0 Hz, 1H), 3.85 (s, 3H), 3.79 (s, 3H), 2.91 (s, 3H). $^{13}C\{^{1}H\}$ NMR (100 MHz, $CDCl_3$) δ 200.4, 160.7, 149.6, 142.4, 142.1, 140.8, 136.8, 128.7 (2C), 128.4 (2C), 128.0,

125.7, 123.1, 120.5, 112.8, 111.4, 108.7, 97.7, 74.0, 60.1, 56.4, 55.8, 37.6. HRMS (ESI-TOF) *m*/*z*: [M + H$^+$] Calcd for $C_{24}H_{23}N_2O_3$ 387.1703, Found. 387.1705.

3-Ethynyl-5-methyl-12a-phenyl-5, 12a-dihydroindolo[1,2-*c*]quinazolin-12(6*H*)-one (±27ay):

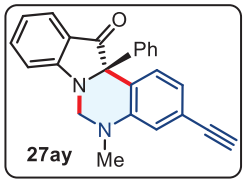

Purification with petroleum ether: acetone (8/2) as eluent); yellow solid (154 mg, 88% yield, mp = 98-101 °C). ^{1}H NMR (400 MHz, $CDCl_3$) δ 7.72 (d, *J* = 7.7 Hz, 1H), 7.62 (d, *J* = 8.1 Hz, 1H), 7.58 (t, *J* = 7.8 Hz, 1H), 7.34 – 7.29 (m, 3H), 7.21 – 7.11 (m, 3H), 7.00 – 6.93 (m, 2H), 6.81 (s, 1H), 4.68 (d, *J* = 12.0 Hz, 1H), 4.28 (d, *J* = 12.0 Hz, 1H), 3.03 (s, 1H), 2.92 (s, 3H). ^{13}C{^{1}H} NMR (100 MHz, $CDCl_3$) δ 199.6, 160.5, 145.4, 141.7, 137.0, 129.9, 128.6 (2C), 128.5 (2C), 128.2, 125.8, 122.9, 122.3, 121.8, 120.7, 118.0, 115.7, 111.3, 83.8, 77.0, 74.2, 59.5, 36.7. HRMS (ESI-TOF) *m*/*z*: [M + H$^+$] Calcd for $C_{24}H_{19}N_2O$ 351.1492, Found. 351.1495.

5-Methyl-2-(methylthio)-12a-phenyl-5, 12a-dihydroindolo[1,2-*c*]quinazolin-12(6*H*)-one

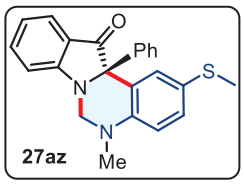

(±27az): Purification with petroleum ether: acetone (8/2) as eluent); yellow solid (147 mg, 79% yield, mp = 186-188 °C). ^{1}H NMR (400 MHz, $CDCl_3$) δ 7.74 – 7.70 (m, 1H), 7.67 (d, *J* = 2.3 Hz, 1H), 7.57 (m, 1H), 7.34 – 7.30 (m, 3H), 7.19 (m, 3H), 7.13 (d, *J* = 8.3 Hz, 1H), 6.99 – 6.93 (m, 1H), 6.64 (d, *J* = 8.7 Hz, 1H), 4.67 (d, *J* = 11.9 Hz, 1H), 4.24 (d, *J* = 12.0 Hz, 1H), 2.91 (s, 3H), 2.40 (s, 3H). ^{13}C{^{1}H} NMR (100 MHz, $CDCl_3$) δ 199.7, 160.5, 144.1, 141.9, 136.9, 130.1, 129.7, 128.6 (2C), 128.4 (2C), 128.1, 126.3, 125.8, 122.9, 120.5, 117.9, 113.2, 111.2, 74.2, 59.6, 36.8, 18.0. HRMS (ESI-TOF) *m*/*z*: [M + H$^+$] Calcd for $C_{23}H_{21}N_2OS$ 373.1369, Found. 373.1370.

2-(2-Hydroxyethyl)-5-methyl-12a-phenyl-5, 12a-dihydroindolo[1,2-*c*]quinazolin-12(6*H*)-one

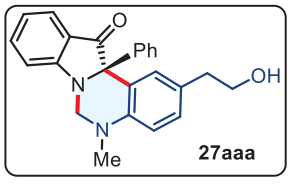

(±27aaa): Purification with petroleum ether: acetone (8/2) as eluent); yellow solid (143 mg, 77% yield, mp = 120-123 °C). ^{1}H NMR (400 MHz, $CDCl_3$) δ 7.74 – 7.70 (m, 1H), 7.57 (m, 1H), 7.53 (d, *J* = 2.0 Hz, 1H), 7.33 – 7.28 (m, 3H), 7.19 (dt, *J* = 5.5, 2.0 Hz, 2H), 7.14 (d, *J* = 8.3 Hz, 1H), 7.07 (dd, *J* = 8.4, 2.1 Hz, 1H), 6.98 – 6.93 (m, 1H), 6.66 (d, *J* = 8.4 Hz, 1H), 5.30 (s, 1H), 4.66 (d, *J* = 11.9 Hz, 1H), 4.23 (d, *J* = 11.9 Hz, 1H), 3.78 (t, *J* = 6.6 Hz, 2H), 2.91 (s, 3H), 2.77 (t, *J* = 6.6 Hz, 2H). ^{13}C{^{1}H} NMR (100 MHz, $CDCl_3$) δ 200.2, 160.7, 144.5, 142.2, 136.9, 130.2, 129.5, 128.6 (2C), 128.4 (2C), 128.1 (2C), 125.8, 123.0, 120.5, 117.5, 112.8, 111.4, 74.4, 63.9, 59.8, 38.3, 36.9. HRMS (ESI-TOF) *m*/*z*: [M + H$^+$] Calcd for $C_{24}H_{23}N_2O_2$ 371.1754, Found. 371.1755.

2-(2-Methoxyethyl)-5-methyl-12a-phenyl-5, 12a-dihydroindolo[1,2-*c*]quinazolin-12(6*H*)-one

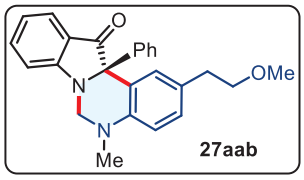

(±27aab): Purification with petroleum ether: acetone (8/2) as eluent); yellow solid (154 mg, 80% yield, mp = 133-136 ºC). ^{1}H NMR (400 MHz, $CDCl_3$) δ 7.72 (d, *J* = 7.6 Hz, 1H), 7.57 (t, *J* = 7.7 Hz, 1H), 7.53 (s, 1H), 7.35 – 7.29 (m, 3H), 7.20 (dd, *J* = 6.8, 2.3 Hz, 2H), 7.14 (d, *J* = 8.3 Hz, 1H), 7.10 – 7.05 (m, 1H), 6.95 (t, *J* = 7.4 Hz, 1H), 6.65 (d, *J* = 8.4 Hz, 1H), 4.66 (d, *J* = 11.9 Hz, 1H), 4.22 (d, *J* = 11.9 Hz, 1H), 3.54 (td, *J* = 7.3, 4.6 Hz, 2H), 3.34 (s, 3H), 2.90 (s, 3H), 2.79 (t, *J* = 7.1 Hz, 2H). ^{13}C{^{1}H} NMR (100 MHz, $CDCl_3$) δ 200.1, 160.7, 144.2, 142.2, 136.8, 130.0, 129.3, 128.6 (3C), 128.4 (2C), 128.0, 125.7, 123.0, 120.4, 117.1, 112.7, 111.3, 74.4, 73.7, 59.8, 58.5, 36.8, 35.1. HRMS (ESI-TOF) *m*/*z*: [M + H^{+}] Calcd for $C_{25}H_{25}N_2O_2$ 385.1911, Found. 385.1915.

2-(2-Chloroethyl)-5-methyl-12a-phenyl-5, 12a-dihydroindolo[1,2-*c*]quinazolin-12(6*H*)-one

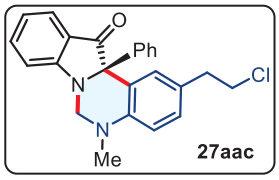

(±27aac): Purification with petroleum ether: acetone (8/2) as eluent); yellow solid (152 mg, 78% yield, mp = 153-155 ºC). ^{1}H NMR (400 MHz, $CDCl_3$) δ 7.74 – 7.70 (m, 1H), 7.57 (m, 1H), 7.52 (d, *J* = 2.1 Hz, 1H), 7.31 (dd, *J* = 5.0, 1.9 Hz, 3H), 7.20 – 7.16 (m, 2H), 7.14 (d, *J* = 8.3 Hz, 1H), 7.06 (dd, *J* = 8.4, 2.1 Hz, 1H), 6.98 – 6.94 (m, 1H), 6.66 (d, *J* = 8.4 Hz, 1H), 4.67 (d, *J* = 11.9 Hz, 1H), 4.24 (d, *J* = 11.9 Hz, 1H), 3.64 (qt, *J* = 10.6, 7.4 Hz, 2H), 2.96 (t, *J* = 7.5 Hz, 2H), 2.91 (s, 3H). ^{13}C{^{1}H} NMR (100 MHz, $CDCl_3$) δ 200.1, 160.7, 144.7, 142.1, 136.9, 130.1, 129.3, 128.6 (2C), 128.5 (2C), 128.1, 127.8, 125.8, 123.0, 120.5, 117.3, 112.7, 111.3, 74.3, 59.7, 45.4, 38.3, 36.8. HRMS (ESI-TOF) *m*/*z*: [M + H^{+}] Calcd for $C_{24}H_{22}ClN_2O$ 389.1415, Found. 389.1415.

2-((Allyloxy)methyl)-5-methyl-12a-phenyl-5, 12a-dihydroindolo[1,2-*c*]quinazolin-12(6*H*)-one (±27aad): Purification with petroleum ether: acetone (8/2) as eluent); yellow solid (165 mg, 83% yield, mp = 107-110 ºC). ^{1}H NMR (400 MHz, $CDCl_3$) δ 7.71 (d, *J* = 7.4 Hz, 1H), 7.61 (d, *J* = 1.9 Hz, 1H), 7.59 – 7.55 (m, 1H), 7.30 (dt, *J* = 5.6, 2.6 Hz, 3H), 7.24 (dd, *J* = 8.5, 2.0 Hz, 1H), 7.22 – 7.18 (m, 2H), 7.13 (d, *J* = 8.3 Hz, 1H), 6.95 (t, *J* = 7.4 Hz, 1H), 6.70 (d, *J* = 8.5 Hz, 1H), 5.99 – 5.88 (m, 1H), 5.27 (dq, *J* = 17.2, 1.5 Hz, 1H), 5.20 – 5.15 (m, 1H), 4.67 (d, *J* = 11.9 Hz, 1H), 4.45 – 4.37 (m, 2H), 4.26 (d, *J* = 12.0 Hz, 1H), 3.98 (d, *J* = 5.7 Hz, 2H), 2.92 (s, 3H). ^{13}C{^{1}H} NMR (100 MHz, $CDCl_3$) δ 200.0, 160.6, 145.3, 142.1, 136.8, 134.9, 129.8, 128.8, 128.7 (2C),

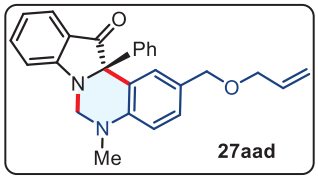

128.4 (2C), 128.0, 127.9, 125.8, 123.0, 120.5, 117.1, 116.7, 112.7, 111.3, 74.3, 71.8, 70.8, 59.7, 36.8. HRMS (ESI-TOF) *m/z*: [M + H^+] Calcd for $C_{26}H_{25}N_2O_2$ 397.1911, Found. 397.1915.

5-Ethyl-2-methyl-12a-phenyl-5, 12a-dihydroindolo[1,2-*c*]quinazolin-12(6*H*)-one (±27aae):

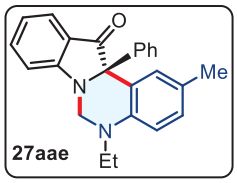

Purification with petroleum ether: acetone (8/2) as eluent); yellow solid (133 mg, 75% yield, mp = 165-167 °C). ^{1}H NMR (400 MHz, $CDCl_3$) δ 7.70 (d, *J* = 7.5 Hz, 1H), 7.55 (t, *J* = 7.5 Hz, 1H), 7.47 (s, 1H), 7.31 (s, 3H), 7.22 (d, *J* = 7.1 Hz, 2H), 7.09 (d, *J* = 8.2 Hz, 1H), 6.95 (dt, *J* = 15.1, 8.0 Hz, 2H), 6.62 (d, *J* = 8.4 Hz, 1H), 4.67 (d, *J* = 12.0 Hz, 1H), 4.31 (d, *J* = 12.1 Hz, 1H), 3.44 (dt, *J* = 14.2, 7.2 Hz, 1H), 3.32 (dq, *J* = 14.3, 6.9 Hz, 1H), 2.23 (s, 3H), 1.16 (t, *J* = 6.9 Hz, 3H).^{13}C{^{1}H} NMR (100 MHz, $CDCl_3$) δ 200.3, 160.7, 142.3, 141.8, 136.7, 130.4, 129.4, 128.8 (2C), 128.4 (2C), 127.9, 126.8, 125.7, 123.0, 120.3, 116.6, 112.3, 111.2, 74.5, 57.1, 43.5, 20.5, 11.5. HRMS (ESI-TOF) *m/z*: [M + H^+] Calcd for $C_{24}H_{23}N_2O$ 355.1805, Found. 355.1808.

2-(5-Methyl-12-oxo-12a-phenyl-5, 6, 12, 12a-tetrahydroindolo[1,2-*c*]quinazolin-2-yl)ethyl 2-(2-((2,6-dichlorophenyl)amino)phenyl)acetate (±27aaf):

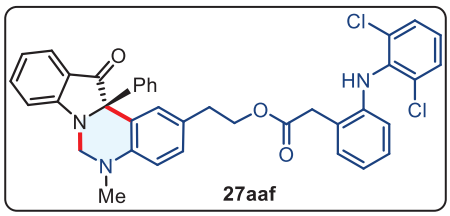

Purification with petroleum ether: acetone (8/2) as eluent); yellow solid (246 mg, 76% yield, mp = 208-210 °C). ^{1}H NMR (400 MHz, $CDCl_3$) δ 7.72 (d, *J* = 7.5 Hz, 1H), 7.60 – 7.53 (m, 2H), 7.34 – 7.29 (m, 4H), 7.20 (m, 3H), 7.16 – 7.09 (m, 2H), 6.97 (m, 5H), 6.59 (d, *J* = 8.5 Hz, 1H), 6.54 (d, *J* = 8.0 Hz, 1H), 4.66 (d, *J* = 11.9 Hz, 1H), 4.27 (m, 3H), 3.86 – 3.74 (m, 2H), 2.87 (d, *J* = 10.3 Hz, 5H). ^{13}C{^{1}H} NMR (100 MHz, $CDCl_3$) δ 200.0, 172.3, 160.7, 144.5, 142.7, 142.2, 137.8, 136.8, 130.9, 130.3, 129.5, 129.2, 128.8 (2C), 128.6 (3C), 128.4 (2C), 128.0, 127.8, 127.4, 125.7, 124.4, 123.9, 123.0, 121.9, 120.5, 118.1, 117.2, 112.7, 111.3, 74.3, 66.0, 59.7, 38.5, 36.8, 34.2. HRMS (ESI-TOF) *m/z*: [M + H^+] Calcd for $C_{38}H_{32}Cl_2N_3O_3$ 648.1815, Found. 648.1817.

5-Methyl-12-oxo-12a-phenyl-5, 6, 12, 12a-tetrahydroindolo[1, 2-*c*]quinazolin-2-yl)ethyl 2-(4-isobutylphenyl)propanoate (±27aag):

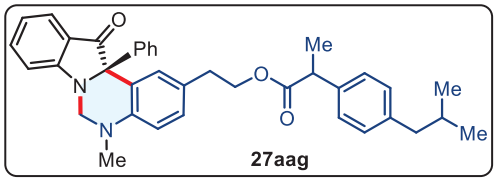

Purification with petroleum ether: acetone (8/2) as eluent); yellow solid (207 mg, 74% yield, mp = 130-133 °C). ^{1}H NMR (400 MHz, $CDCl_3$) δ 7.74 – 7.69 (m, 1H), 7.57 (m, 1H), 7.52 (d, *J* = 1.8 Hz, 1H), 7.33 – 7.28 (m, 3H), 7.20 – 7.12 (m, 5H), 7.06 (d, *J* = 7.4 Hz, 2H), 6.94 (m, 2H), 6.60 (dd, *J* = 8.5, 3.6 Hz, 1H), 4.67 (d, *J* = 11.9 Hz, 1H), 4.27 – 4.13 (m, 3H), 3.67

(p, *J* = 7.1 Hz, 1H), 2.90 (s, 3H), 2.79 (td, *J* = 6.8, 3.4 Hz, 2H), 2.43 (d, *J* = 7.0 Hz, 2H), 1.90 – 1.78 (m, 1H), 1.45 (dd, *J* = 8.8, 7.2 Hz, 3H), 0.90 (dd, *J* = 6.6, 1.0 Hz, 6H). $^{13}C\{^{1}H\}$ NMR (100 MHz, $CDCl_3$) δ 200.0, 174.7, 160.6, 144.4, 142.2, 140.3, 137.7, 136.8, 130.2, 129.2 (3C), 128.6 (2C), 128.4 (2C), 128.0, 127.6, 127.2 (2C), 125.7, 123.0, 120.4, 117.2, 112.7, 111.3, 74.3, 65.4, 59.7, 45.1, 45.0, 36.8, 34.2, 30.8, 22.4 (2C), 18.3. HRMS (ESI-TOF) *m*/*z*: [M + H^+] Calcd for $C_{37}H_{39}N_2O_3$ 559.2955, Found. 559.2932.

2-(5-Methyl-12-oxo-12a-phenyl-5, 6, 12, 12a-tetrahydroindolo[1, 2-*c*]quinazolin-2-yl)ethyl 2-acetoxybenzoate (±27aah): Purification with petroleum ether: acetone (8/2) as eluent); yellow solid (192 mg, 72% yield, mp = 153-155 ºC). ^{1}H NMR (400 MHz, $CDCl_3$) δ 7.98 (d, *J* = 7.5 Hz, 1H), 7.70 (d, *J* = 7.6 Hz, 1H), 7.55 (dd, *J* = 19.1, 8.7 Hz, 3H), 7.28 (d, *J* = 14.5 Hz, 3H), 7.21 – 7.05 (m, 6H), 6.95 (t, *J* = 7.4 Hz, 1H), 6.67 (d, *J* = 8.4 Hz, 1H), 4.66 (d, *J* = 11.9 Hz, 1H), 4.41 (q, *J* = 6.6 Hz, 2H), 4.23 (d, *J* = 11.9 Hz, 1H), 2.98 – 2.92 (m, 2H), 2.90 (s, 3H), 2.29 (s, 3H). $^{13}C\{^{1}H\}$ NMR (100 MHz, $CDCl_3$) δ 200.1, 169.8, 164.3, 160.7, 150.7, 144.5, 142.2, 136.9, 133.7, 131.9, 130.2, 129.3, 128.6 (2C), 128.4 (2C), 128.0, 127.4, 126.1, 125.8, 123.7, 123.2, 123.0, 120.5, 117.3, 112.9, 111.3, 74.4, 66.0, 59.7, 36.9, 34.3, 21.0. HRMS (ESI-TOF) *m*/*z*: [M + H^+] Calcd for $C_{33}H_{29}N_2O_5$ 533.2071, Found. 533.2072.

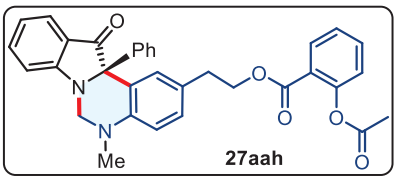

Control experiment

To a 10 mL dried undivided reaction cell equipped with a stirring bar were added **26a** (0.5 mmol, 1.0 equiv), **17a** (0.5 mmol, 1.0 equiv), *n*-Bu_4NBF_4 (82 mg, 0.25 mmol, 0.5 equiv.), and TEMPO (16 mg, 0.1 mmol, 20 mol%), AcOH (60 mg, 1.0 mmol, 2.0 equiv.), TEMPO (2.0 mmol) and BHT (2.0 mmol) dissolved in CH_3CN (10 mL). The carbon-plate anode and nickel-plate cathode were dipped into the reaction mixture and electrolyzed at a constant current condition (6 mA) under standard conditions. The desired product **27aa** formation was not observed on TLC.

Supportive experiment to the radical reaction

2-(4-(Dimethylamino)phenyl)-2-phenylindolin-3-one (±29): To a stirred solution of **26a** (0.5 mmol) in CH_3CN (3.0 mL) at room temperature was added **17a** (0.5 mmol) and AcOH (1.0 mmol). The mixture was stirred at room temperature for 16 h and quenched by a saturated solution of $NaHCO_3$ (10.0 mL). The aqueous layer was extracted with EtOAc (10.0 mL). The

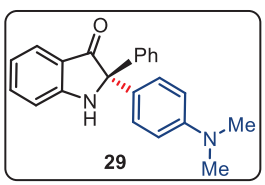

combined organic mixture was concentrated under reduced pressure. Purification by column chromatography using petroleum ether/acetone (8/2) as the eluent afforded **29** as a yellow solid (151 mg, 92% yield, mp = 180-183 ºC). ^{1}H NMR (400 MHz, $CDCl_3$) δ 7.67 – 7.62 (m, 1H), 7.46 (m, 3H), 7.34 – 7.27 (m, 3H), 7.25 – 7.20 (m, 2H), 6.89 (d, *J* = 8.2 Hz, 1H), 6.86 – 6.81 (m, 1H), 6.69 – 6.63 (m, 2H), 5.26 (s, 1H), 2.93 (s, 6H). ^{13}C{^{1}H} NMR (100 MHz, $CDCl_3$) δ 201.4, 160.0, 150.0, 141.3, 137.3, 128.6, 128.3 (2C), 128.1 (2C), 127.5, 127.4 (2C), 125.3, 119.9, 119.2, 112.4, 112.3 (2C), 74.6, 40.4 (2C). HRMS (ESI-TOF) *m*/*z*: [M + H^{+}] Calcd for $C_{22}H_{21}N_2O$ 329.1648, Found. 329.1650.

Gram-scale synthesis of 27aa. A 100 mL three-neck round bottom flask (as an undivided cell) was charged with **26a** (1.1 g, 5.3 mmol, 1.0 equiv), **17a** (0.642 g, 5.3 mmol, 1.0 equiv), *n*-Bu_4NBF_4 (873 g, 2.65 mmol, 0.5 equiv), and TEMPO (0.166 g, 1.06 mmol, 20 mol%) and AcOH (636 mg, 10.6 mmol, 2.0 equiv.) in CH_3CN (36 mL). The carbon-plate anode and nickel-plate cathode that were connected to a DC-regulated power supply dipped into the reaction mixture and electrolyzed at a constant current condition (6 mA) under an air atmosphere at room temperature. The reaction progress was monitored by TLC. The reaction solvent was evaporated under reduced pressure once the reaction was finished, after the usual workup and Purification by column chromatography furnished compound **27aa** (1.34 g) with 78% yield.

2, 5-Dimethyl-12a-phenyl-5, 6, 12, 12a-tetrahydroindolo[1, 2-*c*]quinazolin-12-ol (±28): To a stirred solution of **27aa** (0.3 mmol) in dry 1,4-Dioxane (4.0 mL) at 0 °C was added LiBr (1.2 mmol) and $NaBH_4$ (6.3 mmol) portion-wise over 5 min. The mixture was stirred at room temperature for 16 h and quenched slowly with aqueous NH_4Cl solution (10.0 mL). The aqueous layer was extracted with EtOAc (10.0 mL). The combined organic mixture was concentrated under reduced pressure. Purification by column chromatography using petroleum ether/acetone (8/2) as the eluent afforded **28** as a colourless liquid (83 mg, 81% yield)**.** ^{1}H NMR (400 MHz, $CDCl_3$) δ 7.54 – 7.50 (m, 2H), 7.34 – 7.27 (m, 4H), 7.26 – 7.20 (m, 2H), 7.02 (d, *J* = 8.3 Hz, 1H), 6.83 (t, *J* = 7.4 Hz, 1H), 6.73 (d, *J* = 7.9 Hz, 1H), 6.64 (d, *J* = 8.4 Hz, 1H), 5.80 (d, *J* = 11.6 Hz, 1H), 4.44 (d, *J* = 11.7 Hz, 1H), 4.04 (d, *J* = 11.7 Hz, 1H), 2.82 (s, 3H), 2.29 (s, 3H), 1.79 (d, *J* = 11.6 Hz, 1H). ^{13}C{^{1}H} NMR (100 MHz, $CDCl_3$) δ 148.5, 146.7, 146.0, 132.5, 131.2, 129.5, 129.0, 128.0 (4C), 127.2, 125.7, 124.8, 119.9, 119.0, 113.1, 109.5, 83.9, 76.6, 61.9, 37.2, 20.7. HRMS (ESI-TOF) *m*/*z*: [M + H^{+}] Calcd for $C_{23}H_{23}N_2O$ 343.1805, Found. 343.1807.

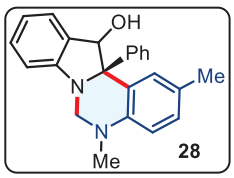

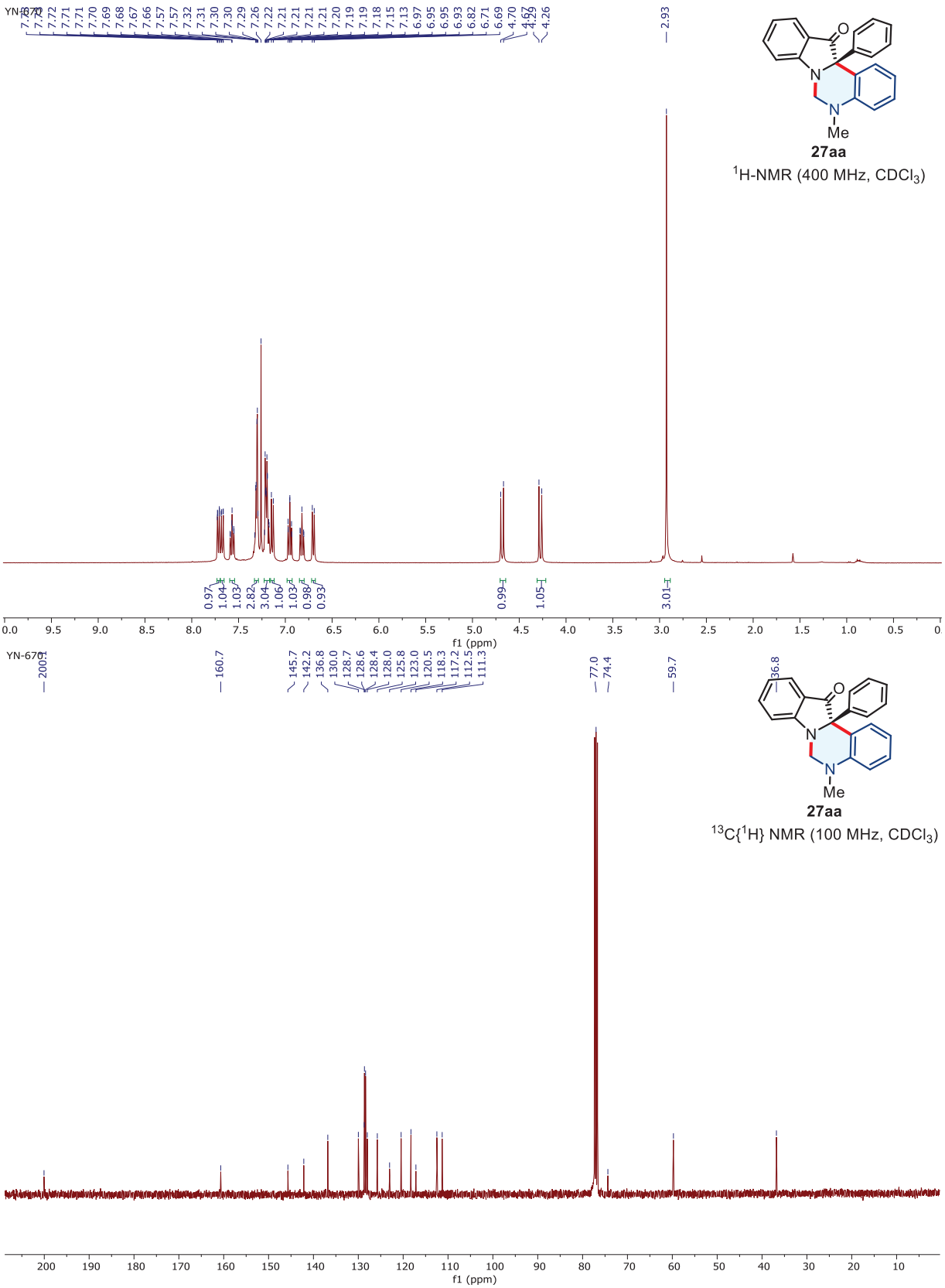

Figure 5.5: ^{1}H and ^{13}C NMR spectra of **27aa**

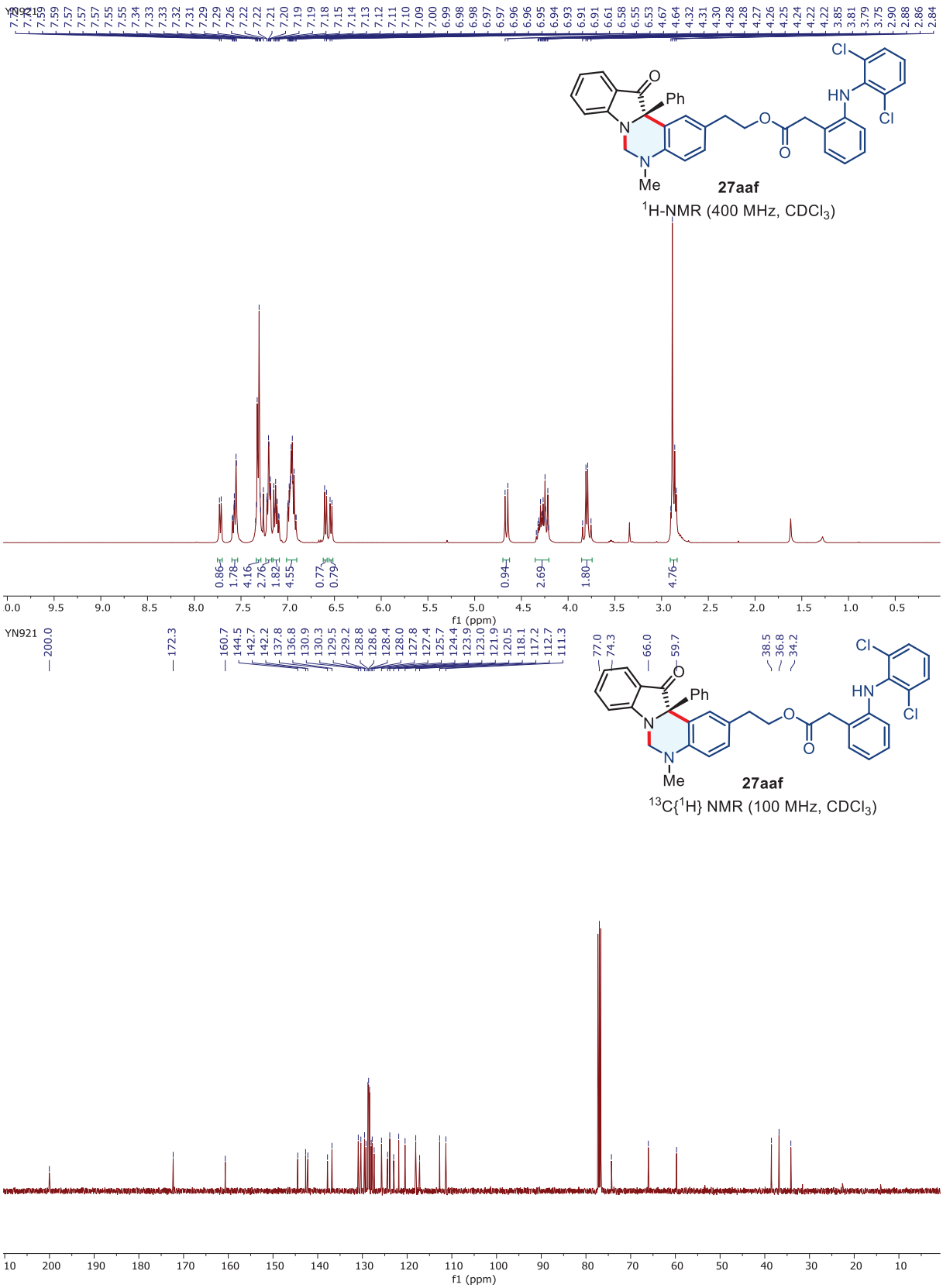

Figure 5.6: ^{1}H and ^{13}C NMR spectra of **27aaf**

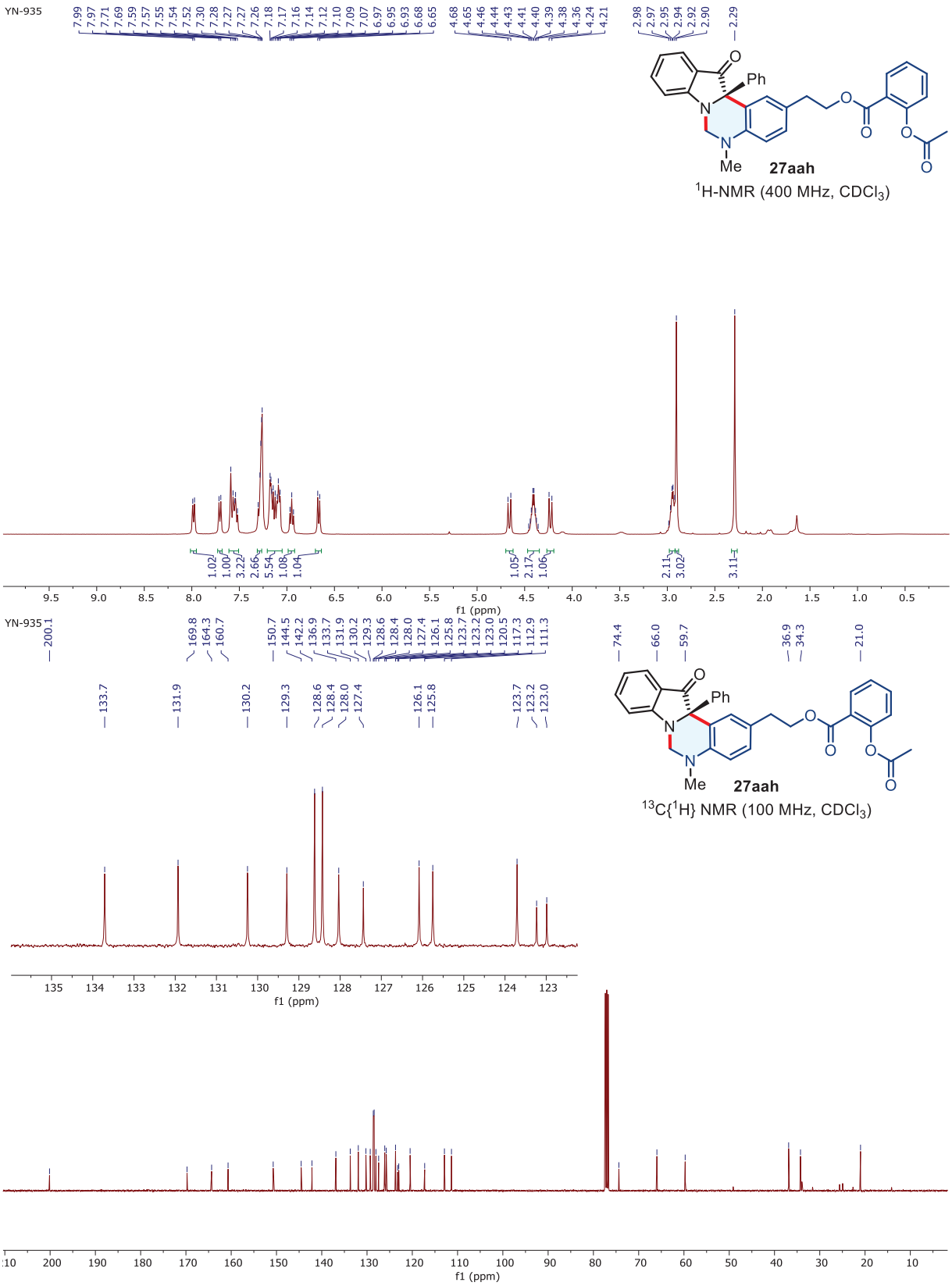

Figure 5.7: ^{1}H and ^{13}C NMR spectra of **27aah**

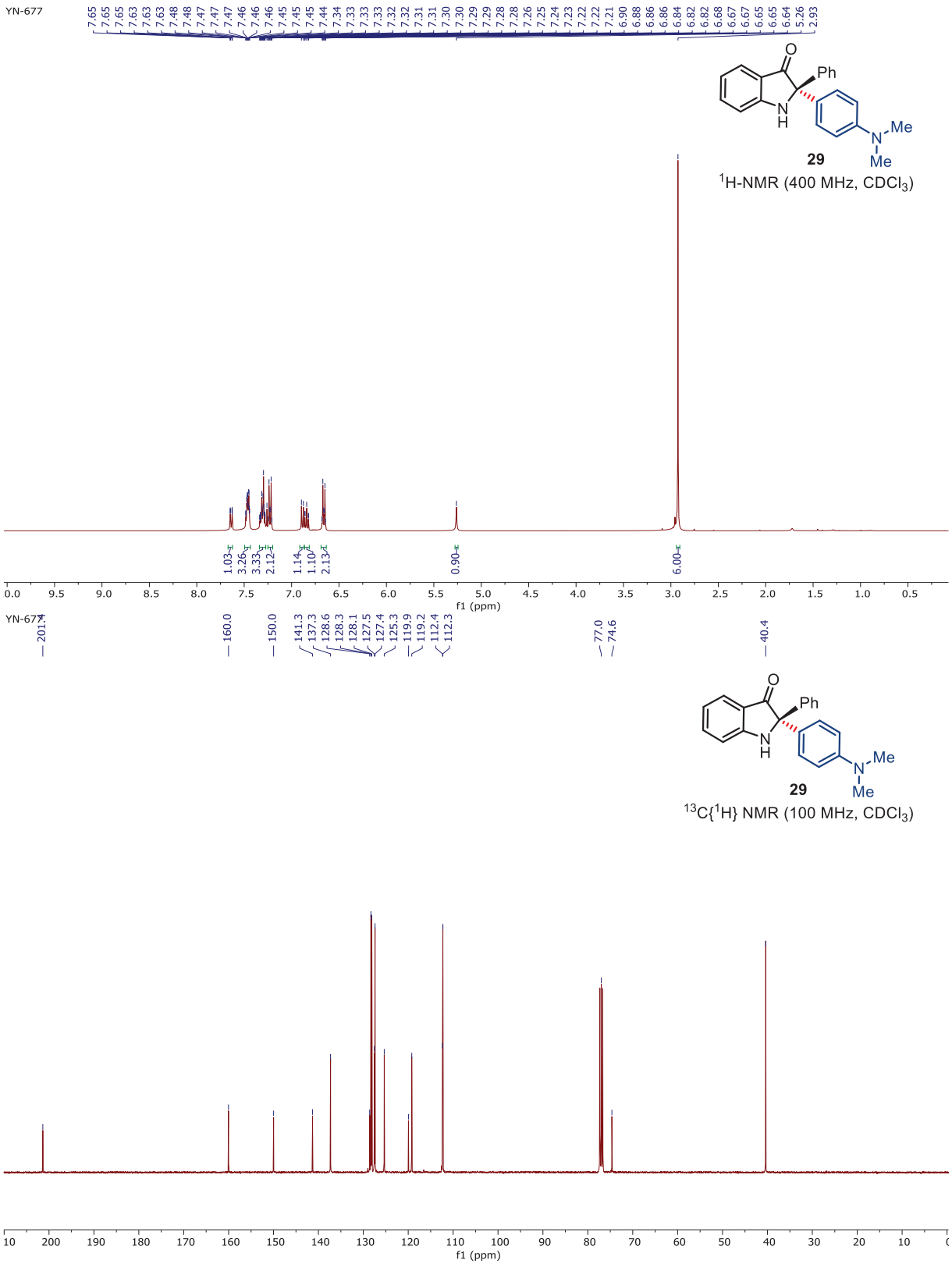

Figure 5.8: ^{1}H and ^{13}C NMR spectra of **29**

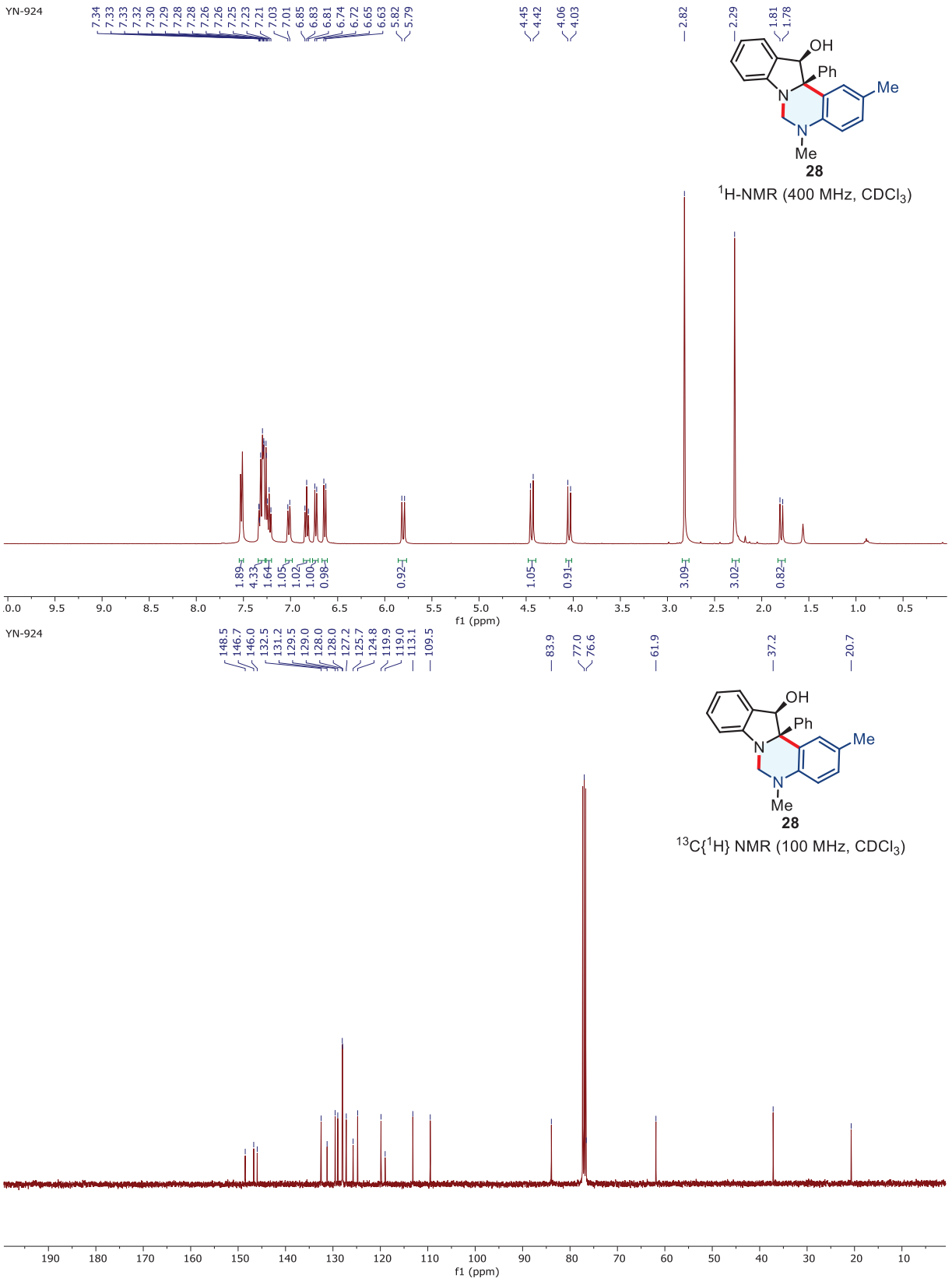

Figure 5.9: ^{1}H and ^{13}C NMR spectra of **28**

5.9 Single crystal X-ray diffraction experiment and analysis

5.9.1 Single crystal XRD experiments for (27ma)

The single crystal X-ray diffraction data has been collected using graphite-monochromatic MoKα radiation (λ = 0.71073 Å) equipped with a SuperNova diffractometer, a single source at offset/far, with a HyPix3000 detector using ω scans at 293K with diffraction angles ranging from 6.6° to 54.2°. The diffraction data were integrated and corrected for polarization and Lorentz effects, as well as an empirical absorption correction, was applied using SCALE3 ABSPACK in CrysAlisPro software (version 1.171.42.90a) [1]. The structure was solved via the intrinsic phasing method using SHELXT [2] structure solution program and the position of all the non-hydrogen atoms was refined anistropically via full-matrix least-squares approach on F^2 using SHELXL [3, 4] program. During the refinement process, all hydrogen atom positions were determined using difference Fourier maps, and these atoms were constrained to ride on their parent atoms during each refinement cycle. A total of 342 parameters were refined using 3956 unique reflections, which converged the final R-factor to 0.042, weighted R-factor (wR) to 0.112 and the goodness of fit (S) being 1.10 in the final refinement cycle. A precise crystallographic data was included in the Table 5.4.

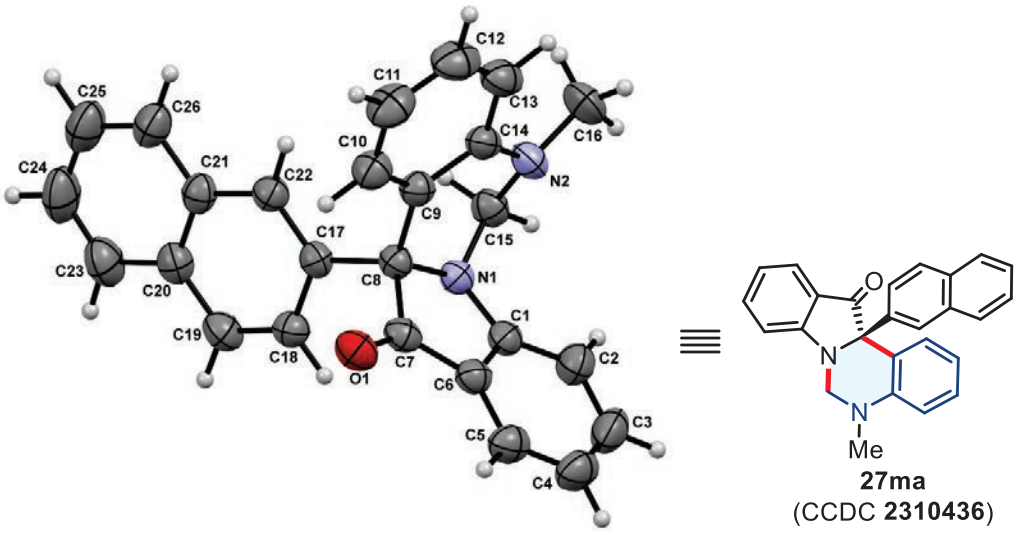

Figure 5.10 ORTEP diagram of compound **27ma** (CCDC **2310436**)

Table 5.4. A precise crystallographic data for **27ma**

Crystal data	
CCDC number	**2310436**
Chemical formula	$C_{26}H_{20}N_2O$
M_r	376.44

Crystal system, space group	Monoclinic, $P2_1/n$
Temperature (K)	293
a, b, c (Å)	8.8142 (3), 20.3997 (6), 11.2243 (3)
β (°)	102.970 (3)
V (Å^3)	1966.72 (11)
Z	4
F(000)	792
D_x (Mg m^{-3})	1.271
Radiation type	Mo $K\alpha$
No. of reflections for cell measurement	13716
θ range (°) for cell measurement	3.5–27.0
μ (mm^{-1})	0.08
Crystal shape	Block
Colour	Clear light colourless
Crystal size (mm)	0.02 × 0.02 × 0.02
Data collection	
Diffractometer	SuperNova, Single source at offset/far, HyPix3000
Radiation source	micro-focus sealed X-ray tube, SuperNova (Mo) X-ray Source
Monochromator	Mirror
Detector resolution (pixels mm^{-1})	10.0000
Scan method	ω scans
Absorption correction	Multi-scan CrysAlisPro 1.171.42.90a (Rigaku Oxford Diffraction, 2023) Empirical absorption correction using spherical harmonics, implemented in SCALE3 ABSPACK scaling algorithm.
T_{min}, T_{max}	0.462, 1.000
No. of measured, independent and observed [$I > 2\sigma(I)$] reflections	21653, 3956, 3059
R_{int}	0.041
θ values (°)	θ_{max} = 27.1, θ_{min} = 3.3
(sin θ/λ)$_{max}$ (Å^{-1})	0.642
Range of h, k, l	h = −10→10, k = −25→26, l = −13→14
Refinement	
Refinement on	F^2
$R[F^2 > 2\sigma(F^2)]$, $wR(F^2)$, S	0.042, 0.112, 1.10
No. of reflections	3956
No. of parameters	342
No. of restraints	0
H-atom treatment	All H-atom parameters refined
Weighting scheme	$w = 1/[\sigma^2(F_o^2) + (0.0507P)^2 + 0.2167P]$ where $P = (F_o^2 + 2F_c^2)/3$
$(\Delta/\sigma)_{max}$	< 0.001

$\Delta\rho_{max}$, $\Delta\rho_{min}$ (e Å^{-3})	0.14, −0.15

5.9.2 Single crystal XRD experiments for (27ab)

The single crystal X-ray diffraction data has been collected using graphite-monochromatic MoKα radiation (λ = 0.71073 Å) equipped with a SuperNova diffractometer, single source at offset/far, with a HyPix3000 detector using ω scans at 293K with diffraction angles ranging from 6.4° to 54.4°. The diffraction data were integrated and corrected for polarization and Lorentz effects, as well as an empirical absorption correction was applied using SCALE3 ABSPACK in CrysAlisPro software (version 1.171.42.90a) [1]. The structure was solved via intrinsic phasing method using SHELXT [2] structure solution program and the position of all the non-hydrogen atoms was refined anistropically via full-matrix least-squares approach on F^2 using SHELXL [3, 4] program. During the refinement process, all hydrogen atom positions were determined using difference Fourier maps and these atoms were constrained to ride on their parent atoms during each refinement cycle. A total of 303 parameters were refined using 3379 unique reflections, which converged the final R-factor to 0.045, weighted R-factor (wR) to 0.118 and the goodness of fit (S) being 1.04 in the final refinement cycle. A precise crystallographic data was included in the Table 5.5.

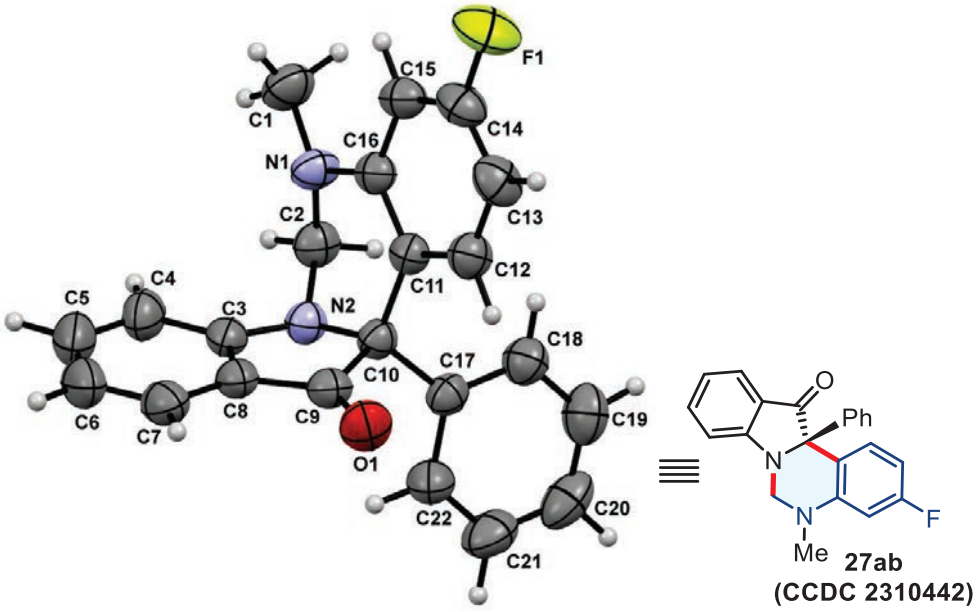

Figure 5.11 ORTEP diagram of compound **27ab** (CCDC **2310442**)

Table 5.5. A precise crystallographic data for **27ab**

Crystal data	

CCDC number	**2310442**
Chemical formula	$C_{22}H_{17}FN_2O$
M_r	344.37
Crystal system, space group	Monoclinic, $P2_1/n$
Temperature (K)	293
a, b, c (Å)	8.3503 (3), 11.6445 (5), 17.5649 (5)
β (°)	91.530 (3)
V (Å^3)	1707.32 (11)
Z	4
F(000)	720
D_x (Mg m^{-3})	1.340
Radiation type	Mo $K\alpha$
No. of reflections for cell measurement	7153
θ range (°) for cell measurement	3.5–26.2
μ (mm^{-1})	0.09
Crystal shape	Block
Colour	Clear light colourless
Crystal size (mm)	0.02 × 0.02 × 0.02
Data collection	
Diffractometer	SuperNova, Single source at offset/far, HyPix3000
Radiation source	micro-focus sealed X-ray tube, SuperNova (Mo) X-ray Source
Monochromator	Mirror
Detector resolution (pixels mm^{-1})	10.0000
Scan method	ω scans
Absorption correction	Multi-scan CrysAlisPro 1.171.42.90a (Rigaku Oxford Diffraction, 2023) Empirical absorption correction using spherical harmonics, implemented in SCALE3 ABSPACK scaling algorithm.
T_{min}, T_{max}	0.683, 1.000
No. of measured, independent and observed [$I > 2\sigma(I)$] reflections	16248, 3379, 2142
R_{int}	0.040
θ values (°)	θ_{max} = 27.2, θ_{min} = 3.2
(sin θ/λ)$_{max}$ (Å^{-1})	0.642
Range of h, k, l	h = −9→10, k = −14→14, l = −22→17
Refinement	
Refinement on	F^2
$R[F^2 > 2\sigma(F^2)]$, $wR(F^2)$, S	0.045, 0.118, 1.04
No. of reflections	3379
No. of parameters	303
No. of restraints	0
H-atom treatment	All H-atom parameters refined

Weighting scheme	$w = 1/[\sigma^2(F_o^2) + (0.0504P)^2 + 0.2106P]$ where $P = (F_o^2 + 2F_c^2)/3$
$(\Delta/\sigma)_{max}$	0.001
$\Delta\rho_{max}$, $\Delta\rho_{min}$ (e Å^{-3})	0.13, −0.19

5.9.3 Single crystal XRD experiments for (27aj)

The single crystal X-ray diffraction data has been collected using graphite-monochromatic MoKα radiation (λ = 0.71073 Å) equipped with a SuperNova diffractometer, single source at offset/far, with a HyPix3000 detector using ω scans at 293K with diffraction angles ranging from 6.8° to 54.2°. The diffraction data were integrated and corrected for polarization and Lorentz effects, as well as an empirical absorption correction was applied using SCALE3 ABSPACK in CrysAlisPro software (version 1.171.42.90a) [1]. The structure was solved via intrinsic phasing method using SHELXT [2] structure solution program and the position of all the non-hydrogen atoms was refined anistropically via full-matrix least-squares approach on F^2 using SHELXL [3, 4] program. During the refinement process, all hydrogen atom positions were determined using difference Fourier maps and these atoms were constrained to ride on their parent atoms during each refinement cycle. A total of 303 parameters were refined using 3425 unique reflections, which converged the final R-factor to 0.046, weighted R-factor (wR) to 0.090 and the goodness of fit (S) being 1.03 in the final refinement cycle. A precise crystallographic data was included in the Table 5.6.

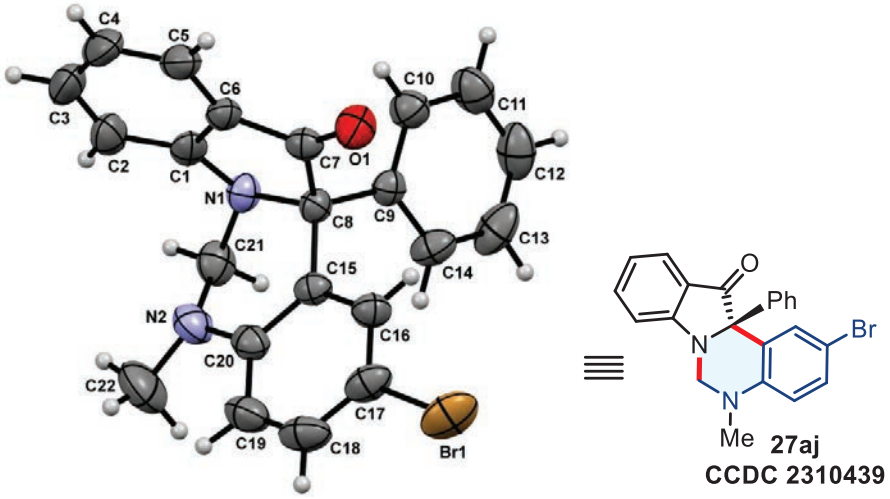

Figure 5.12 ORTEP diagram of compound **27aj** (CCDC **2310439**)

Table 5.6. A precise crystallographic data for **27aj**

Crystal data	

CCDC number	**2310439**
Chemical formula	$C_{22}H_{17}BrN_2O$
M_r	405.28
Crystal system, space group	Monoclinic, $P2_1/c$
Temperature (K)	293
a, b, c (Å)	8.4190 (3), 25.9317 (9), 8.1104 (3)
β (°)	94.599 (3)
V (Å^3)	1764.95 (11)
Z	4
F(000)	824
D_x (Mg m^{-3})	1.525
Radiation type	Mo $K\alpha$
No. of reflections for cell measurement	6615
θ range (°) for cell measurement	3.4–24.9
μ (mm^{-1})	2.34
Crystal shape	Block
Colour	Clear light colourless
Crystal size (mm)	0.02 × 0.02 × 0.02
Data collection	
Diffractometer	SuperNova, Single source at offset/far, HyPix3000
Radiation source	micro-focus sealed X-ray tube, SuperNova (Mo) X-ray Source
Monochromator	Mirror
Detector resolution (pixels mm^{-1})	10.0000
Scan method	ω scans
Absorption correction	Multi-scan CrysAlisPro 1.171.42.90a (Rigaku Oxford Diffraction, 2023) Empirical absorption correction using spherical harmonics, implemented in SCALE3 ABSPACK scaling algorithm.
T_{min}, T_{max}	0.758, 1.000
No. of measured, independent and observed [$I > 2\sigma(I)$] reflections	15758, 3425, 2408
R_{int}	0.040
θ values (°)	θ_{max} = 27.1, θ_{min} = 3.4
(sin θ/λ)$_{max}$ (Å^{-1})	0.641
Range of h, k, l	h = −10→10, k = −32→31, l = −10→10
Refinement	
Refinement on	F^2
$R[F^2 > 2\sigma(F^2)]$, $wR(F^2)$, S	0.046, 0.090, 1.03
No. of reflections	3425
No. of parameters	303
No. of restraints	0

H-atom treatment	All H-atom parameters refined
Weighting scheme	$w = 1/[\sigma^2(F_o^2) + (0.0272P)^2 + 1.3639P]$ where $P = (F_o^2 + 2F_c^2)/3$
$(\Delta/\sigma)_{max}$	0.001
$\Delta\rho_{max}$, $\Delta\rho_{min}$ (e Å^{-3})	0.43, −0.42

5.9.2 Single crystal XRD experiments for (27ao)

The single crystal X-ray diffraction data has been collected using graphite-monochromatic MoKα radiation (λ = 0.71073 Å) equipped with a SuperNova diffractometer, single source at offset/far, with a HyPix3000 detector using ω scans at 293K with diffraction angles ranging from 7.2° to 61.0°. The diffraction data were integrated and corrected for polarization and Lorentz effects, as well as an empirical absorption correction was applied using SCALE3 ABSPACK in CrysAlisPro software (version 1.171.42.90a) [1]. The structure was solved via intrinsic phasing method using SHELXT [2] structure solution program and the position of all the non-hydrogen atoms was refined anistropically via full-matrix least-squares approach on F^2 using SHELXL [3, 4] program. During the refinement process, the H-atom positions were determined using difference Fourier maps, with an exception of those on C1 and C2 (which were fixed geometrically at the ideal locations), and these atoms were constrained to ride on their parent atoms during each refinement cycle. A total of 313 parameters were refined using 3528 unique reflections, which converged the final R-factor to 0.051, weighted R-factor (wR) to 0.140 and the goodness of fit (S) being 1.02 in the final refinement cycle. A precise crystallographic data was included in the Table 5.7.

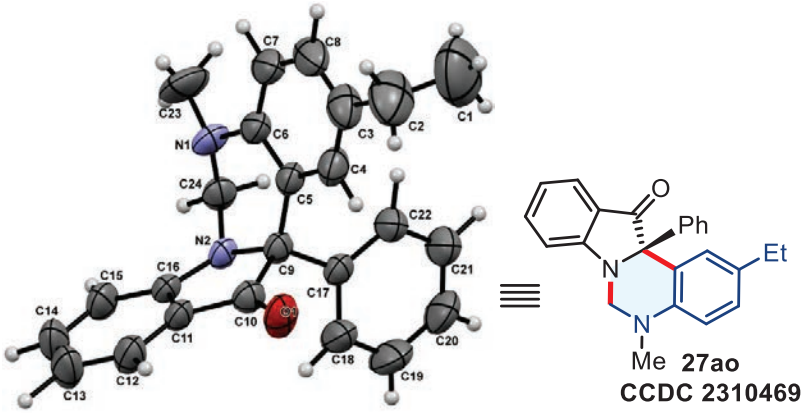

Figure 5.13 ORTEP diagram of compound **27ao** (CCDC **2310469**)

Table 5.7 A precise crystallographic data for **27ao**

Crystal data	

CCDC number	**2310469**
Chemical formula	$C_{24}H_{22}N_2O$
M_r	354.43
Crystal system, space group	Orthorhombic, $Pna2_1$
Temperature (K)	293
a, b, c (Å)	18.1966 (7), 11.0144 (4), 9.6570 (4)
V (Å^3)	1935.50 (13)
Z	4
F(000)	752
D_x (Mg m^{-3})	1.216
Radiation type	Mo $K\alpha$
No. of reflections for cell measurement	6527
θ range (°) for cell measurement	3.6–26.5
μ (mm^{-1})	0.08
Crystal shape	Block
Colour	Clear light colourless
Crystal size (mm)	0.02 × 0.02 × 0.02
Data collection	
Diffractometer	SuperNova, Single source at offset/far, HyPix3000
Radiation source	micro-focus sealed X-ray tube, SuperNova (Mo) X-ray Source
Monochromator	Mirror
Detector resolution (pixels mm^{-1})	10.0000
Scan method	ω scans
Absorption correction	Multi-scan CrysAlisPro 1.171.42.90a (Rigaku Oxford Diffraction, 2023) Empirical absorption correction using spherical harmonics, implemented in SCALE3 ABSPACK scaling algorithm.
T_{min}, T_{max}	0.515, 1.000
No. of measured, independent and observed [$I > 2\sigma(I)$] reflections	9826, 3528, 2794
R_{int}	0.026
θ values (°)	θ_{max} = 30.5, θ_{min} = 3.6
(sin θ/λ)$_{max}$ (Å^{-1})	0.714
Range of h, k, l	h = −22→20, k = −11→12, l = −13→13
Refinement	
Refinement on	F^2
$R[F^2 > 2\sigma(F^2)]$, $wR(F^2)$, S	0.051, 0.140, 1.02
No. of reflections	3528
No. of parameters	313
No. of restraints	1
H-atom treatment	H atoms treated by a mixture of independent and constrained refinement

Weighting scheme	$w = 1/[\sigma^2(F_o^2) + (0.0925P)^2]$ where $P = (F_o^2 + 2F_c^2)/3$
$(\Delta/\sigma)_{max}$	< 0.001
$\Delta\rho_{max}$, $\Delta\rho_{min}$ (e Å^{-3})	0.17, −0.23
Absolute structure	Flack x determined using 954 quotients [(I+)-(I-)]/[(I+)+(I-)] (Parsons, Flack and Wagner, Acta Cryst. B69 (2013) 249-259).
Absolute structure parameter	−0.3 (8)

5.10 References

1. Blackman, A. J.; Hambley, T. W.; Picker, K.; Taylor, W. C. *Tetrahedron Lett.* **1987**, *28*, 5561–5562.
2. Liu, Y.; McWhorter, W. W. *J. Am. Chem. Soc.* **2003**, *125*, 4240–4252.
3. Rohini, R.; Shanker, K.; Reddy, P. M.; Sekhar, V. C.; Ravinder, V. *Arch. Pharm.* **2009**, *342*, 533–540.
4. Rohini, R.; Reddy, P. M.; Shanker, K.; Hu, A.; Ravinder, V. *Eur. J. Med. Chem.* **2010**, *45*, 1200–1205.
5. Sharma, V.; Kumar, P.; Pathak, D. *J. Heterocycl. Chem.* **2010**, *47*, 491–502.
6. Guo, S. H.; Tao, L.; Zhang, W. W.; Zhang, X. Y.; Fan, X. S. *J. Org. Chem.* **2015**, *80*, 10955–10964.
7. Douki, K.; Ono, H.; Taniguchi, T.; Shimokawa, J.; Kitamura, M.; Fukuyama, T. *J. Am. Chem. Soc.* **2016**, *138*, 14578–14581.
8. Sravanthi, T. V.; Manju, S. L. *Eur. J. Pharm. Sci.* **2016**, *91*, 1–10.
9. Jeon, J.; Lee, S. E.; Cheon, C.-H. *Org. Lett.* **2021**, *23*, 2169–2173.
10. Puli, V. S.; Kilaru, S.; Bhongiri, Y.; Marri, S. R.; Tripathi, A.; Chetti, P.; Chatterjee, A.; Vukoti, K. K.; Pola, S. *J. Phys. Org. Chem.* **2021**, *34*, e4276.
11. Baidilov, D.; Elkin, P. K.; Athe, S.; Rawal, V. H. *J. Am. Chem. Soc.* **2023**, *145*, 14831–14838.
12. Yu, H.; Zhang, J.; Ma, D.; Li, X.; X, T. *J. Am. Chem. Soc.* **2023**, *145*, 22335–22340.
13. Zhu, J.; Xie, H.; Chen, Z.; Li, S.; Wu, Y. *Chem. Commun.* **2011**, *47*, 1512–1514.
14. Sang, P.; Xie, Y.; Zou, J.; Zhang, Y. *Org. Lett.* **2012**, *14*, 3894–3897.
15. Xu, M.; Xu, K.; Wang, S.; Yao, Z.-J. *Tetrahedron Lett.* **2013**, *54*, 4675–4678.
16. Guo, S.; Tao, L.; Zhang, W.; Zhang, X.; Fan, X. *J. Org. Chem.* **2015**, *80*, 10955–10964.
17. Guo, S.; Wang, F.; Tao, L.; Zhang, X.; Fan, X. *J. Org. Chem.* **2018**, *83*, 3889–3896.

18. Wang, X.; Zhang, J.; Chen, D.; Wang, B.; Yang, X.; Ma, Y.; Szostak, M. *Org. Lett.* **2019**, *21*, 7038–7043.
19. Chen, G.; Cai, X.; Zhang, X.; Fan, X. *J. Org. Chem.* **2022**, *87*, 9815–9828.
20. Ju, X.; Li, D.; Li, W.; Yu, W.; Bian, F. *Adv. Synth. Catal.* **2012**, *354*, 3561–3567.
21. Zhu, S.; Das, A.; Bui, L.; Zhou, H.; Curran, D. P.; Rueping, M. *J. Am. Chem. Soc.* **2013**, *135*, 1823–1829.
22. Tang, J.; Grampp, G.; Liu, Y.; Wang, B.-X.; Tao, F.-F.; Wang, L.-J.; Liang, X.-Z.; Xiao, H.-Q.; Shen, Y.-M. *J. Org. Chem.* **2015**, *80*, 2724–2732.
23. Liang, Z.; Xu, S.; Tian, W.; Zhang, R. Beilstein *J. Org. Chem.* **2015**, *11*, 425–430.
24. Nicholls, T. P.; Constable, G. E.; Robertson, J. C.; Gardiner, M. G.; Bissember, A. C. *ACS Catal.* **2016**, *6*, 451–457.
25. Wang, Z. J.; Ghasimi, S.; Landfester, K.; Zhang, K. A. I. *Adv. Synth. Catal.* **2016**, *358*, 2576–2582.
26. Xin, J.-R.; Guo, J.-T.; Vigliaturo, D.; He, Y.-H.; Guan, Z. *Tetrahedron.* **2017**, *73*, 4627–4633.
27. Yadav, A. K.; Yadav, L. D. S. *Tetrahedron Lett.* **2017**, *58*, 552–555.
28. Guo, J.-T.; Yang, D.-C.; Guan, Z.; He, Y.-H. *J. Org. Chem.* **2017**, *82*, 1888–1894.
29. Yang, X. L.; Guo, J. D.; Lei, T.; Chen, B.; Tung, C. H.; Wu, L. Z. *Org. Lett.* **2018**, *20*, 2916–2920.
30. Hsu, C. W.; Sunden, H. *Org. Lett.* **2018**, *20*, 2051–2054.
31. Yang, X.; Liang, T.; Sun, J.; Zaworotko, M. J.; Chen, Y.; Cheng, P.; Zhang, Z. *ACS Catal.* **2019**, *9*, 7486–7493.
32. Mandal, T.; Das, S.; De Sarkar, S. *Adv. Synth. Catal.* **2019**, *361*, 3200–3209.
33. Runemark, A.; Zacharias, S. C.; Sundén, H. *J. Org. Chem.* **2021**, *86*, 1901–1910.
34. Nikitas, N. F.; Theodoropoulou, M. A.; Kokotos, C. G. *Eur. J. Org. Chem.* **2021**, *2021*, 1168–1173.
35. Runemark, A.; Sundén, H. *J. Org. Chem.* **2022**, *87*, 1457–1469.
36. Huang, P.; Wang, P.; Wang, S.; Tang, S.; Lei, A. *Green Chem.* **2018**, *20*, 4870– 4874.
37. (a) E. Fischer, F. Jourdan, *Ber. Dtsch. Chem. Ges.,* **1883**, *16*, 2241-2245. (b) B. Robinson, *The Fischer Indole Synthesis.*, John Wiley & Sons Inc, New York, 1982. (c) Y. Wei, I. Deb

and N. Yoshikai, *J. Am. Chem. Soc.,* **2012**, *134*, 9098–9101. (d) Slätt, J.; Bergman, J. Oxygenation of 2,3-dihydroindoles, *Tetrahedron.,* **2002**, *58*, 9187–9191.

38. (a) J.-S. Li, Y.-J. Liu, G.-W. Zhang, J.-A. Ma, *Org., Lett*. **2017**, *19*, 6364–6367. (b) Lindsay, A. C.; Leung, I. K. H.; Sperry, J. *Org. Lett*., **2016**, *18*, 5404–5407. (c) Ling, K.-Q. *Synth. Commun*., **1995**, *25*, 3831–3838. (d) Liu, J.-X.; Zhou, Q.-Q.; Deng, J.-G.; Chen, Y.-C. *Org. Biomol. Chem*., **2013**, *11*, 8175–8178. (e) Najahi, E.; Valentin, A.; Fabre, P.-L.; Reybier, K.; Nepveu, F. Eur. *J. Med. Chem*., **2014**, *78*, 269–274. (f) Huang, J.-R.; Qin, L.; Zhu, Y.-Q.; Song, Q.; Dong, L. *Chem. Commun*., **2015**, *51*, 2844–2847.

39. (a) Kawade, R. K.; Huple, D. B.; Lin, R-J.; Liu, R-S. *Chem. Commun*., **2015**, *51*, 6625–6628. (b) Toyooka, G.; Tuji, A.; Fujita, K. *Synthesis*., **2018**, *50*, 4617–4626. (c) Jiang, X.; Wang, C.; Wei, Y.; Xue, D.; Liu, Z.; Xiao, J. *Chem. Eur. J*., **2014**, *20*, 58–62. (d) Wang, M-Y.; Wang, N.; Liu, X-F.; Qiao, C.; He, L-N. *Green Chem*., **2018**, *20*, 1564–1570. (e) Wang, C.; Qin, J.; Shen, X.; Riedel, R.; Harms, K.; Meggers, E. *Angew. Chem. Int. Ed*., **2016**, *55*, 685–688. (f) Kon, K.; Siddiki, H.; Onodera, W.; Shimizu, K. *Chem. Eur. J*., **2014**, *20*, 6264–6267. (g) Kwong, F. Y.; Klapars, A.; Buchwald, S. L. *Org. Lett*., **2002**, *4*, 581–584. (h) Tayama, E.; Yanaki, T.; Iwamoto, H.; Hasegawa, E. *Eur. J. Org. Chem*., **2010**, 6719–6721.

CHAPTER 6

Conclusions

6.1 General conclusions

The work discussed in this thesis entitled **"Electrochemical Carbon-Carbon and Carbon-Heteroatom Bond Formation to Access Bioactive Compounds"** provides a brief description of the development of the new method for the synthesis of *α*-aminated esters, C2-heteroquaternary indolin-3-ones, 2,3-diarylquinoxalines, and dihydroindolo[1,2-*c*]quinazolin-12(6*H*)-one by using electrochemical oxidative process. The developed strategy utilizes commercially available inexpensive starting materials.

6.2 Specific conclusions

The work mentioned in this thesis is divided into six chapters.

The First Chapter describes a brief historical overview, concepts, techniques, methodology, and the importance of electro-organic synthesis. This thesis work generally follows the electrochemical oxidative pathway; some of the selected electrochemical oxidative transformations are also discussed in this chapter **(Scheme 6.1)**.

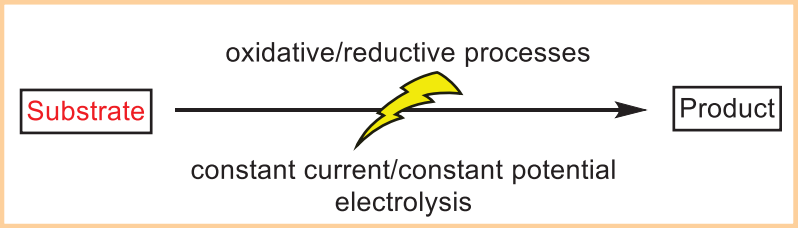

Scheme 6.1 General information of electro-organic synthesis and application

The Second Chapter described an efficient electrochemical protocol for intermolecular oxidative coupling between *α*-aryl acetates (C(sp^3)-H bond) and secondary amines (N-H bond). The mild electrocatalytic condition furnishes *α*-amino-esters by stitching together two electronically mismatched units through C-N bond formation, with a high yield (up to 92%). The reactions can be scaled up without impacting the process efficiency, and the resulting *α*-amino-esters can be functionalized to other similar biorelevant compounds **(Scheme 6.2)**.

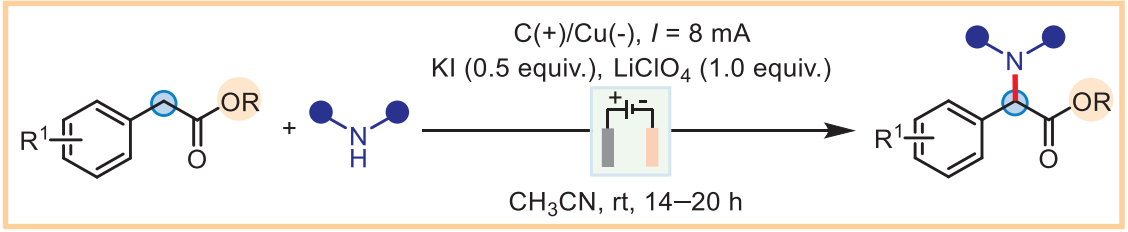

Scheme 6.2 Electrochemical oxidative *α*-amination of *α*-aryl acetates

The Third chapter revealed a highly competent electrochemical method for directly synthesizing C2-quaternary-centered indolin-3-ones from 2-arylindoles. Including self-dimerization of 2-arylindoles, several nucleophiles, such as indole, 1,3-dicarbonyls, pyrrole, allylsilane, and TMSCN, were added to *in situ* generated indole-3-ones through oxidative dearomatization of 2-arylindoles with good yields. The developed method has been applied for the product's gram scale preparation, metagenediindole-A synthesis, and other late-stage synthetic transformations. This method has overcome limited nucleophiles addition to 2-arylindoles under electrochemical conditions **(Scheme 6.3)**.

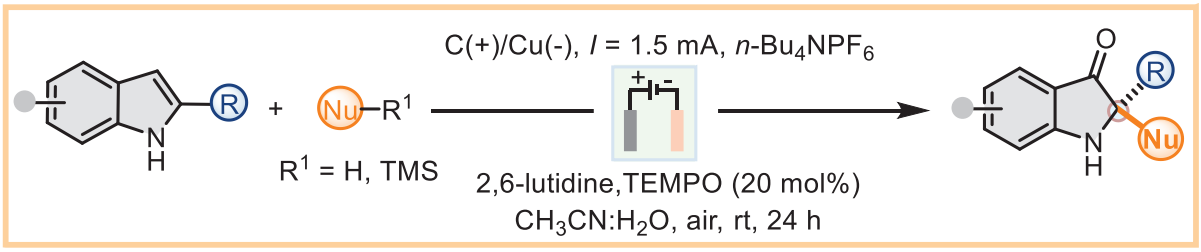

Scheme 6.3 Electrochemical oxidative C2-quaternary indolin-3-ones

The Fourth Chapter describes an efficient electrochemical protocol for directly synthesizing 2-aryl-3-(2-aminoaryl) quinoxalines from 2-aryl indoles. The reaction proceeds through in situ generations of 2-arylindole-3-ones under electrochemical oxidative dearomatization of 2-arylindoles, followed by a ring opening-cyclization sequence with 1,2-diamino arenes to construct substituted quinoxaline compounds with good yields. Apart from gram-scale synthesis, the prepared compounds were tested for late-stage functionalization **(Scheme 6.4)**.

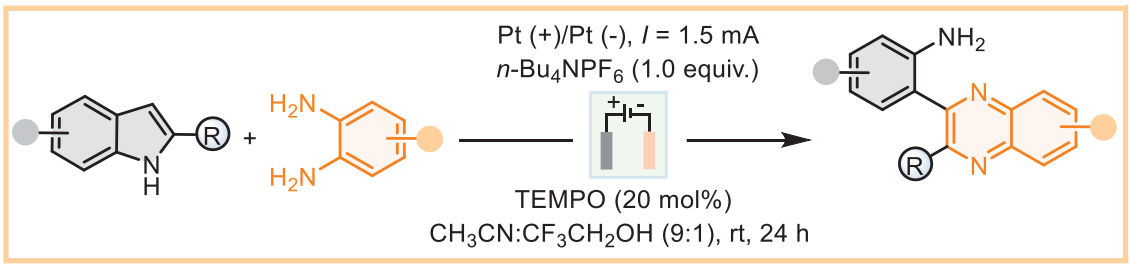

Scheme 6.4 Electrochemical synthesis of quinoxaline from 2-arylindoles

Chapter Fifth describes a novel method for the electrochemical oxidative intermolecular [4 + 2] annulation of tertiary aryl amines and cyclic ketimines to access functionalized dihydroindolo[1,2-*c*]quinazolin-12(6*H*)-one moiety. This developed protocol can occur under air and metal-free conditions at room temperature and a wide range of functional groups proved to

be compatible under our optimized conditions. The reaction conditions were consistent with some drug structure derivatives **(Scheme 6.5)**.

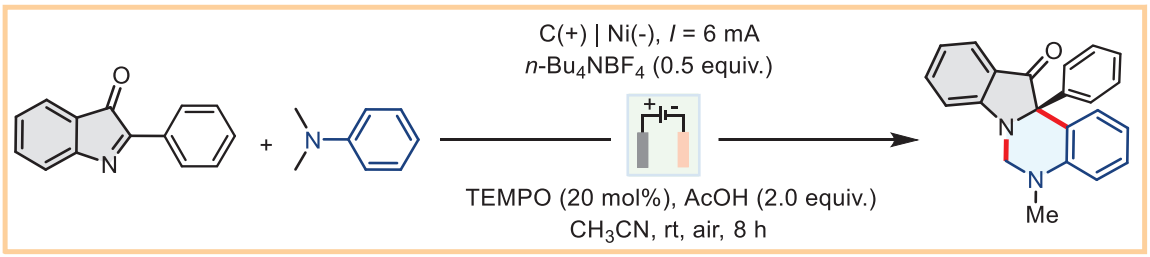

Scheme 6.5 Electrochemical oxidative [4 + 2] annulation between cyclic ketimine and tertiary anilines

6.3 Future scope of the research work

Electro-organic chemistry has received the attention of chemists due to its efficiency and ability to form organic molecules by adding or removing electrons. Organic electrosynthesis represents the synthetic chemist's desire to move towards a greener and more efficient methodology, as it utilizes the cheapest and most versatile redox agent available on the market: electricity. In addition, the flexibility of electrons as redox agents can reduce or even eliminate our reliance on standard, often toxic, and environmental harmful metal-derived oxidizing agents. Organic electrosynthesis and its applications in academia and industry are gaining popularity as we seek more efficient and effective synthetic transformations.

This thesis revolves around developing a new electrochemical methodology for organic reactions, mainly through mediators like iodide salt and TEMPO by electrochemical oxidative process. Having seen the potential of existing work, our group is committed to exploring the additional direction from this outcome. The following method may be developed using the electrochemical oxidative technique.

(i) The [4 + 2] annulation between acyclic/cyclic imines, alkene, alkyne, and tertiary anilines can be achieved through the electrochemical oxidative method **(Scheme 6.6)**.

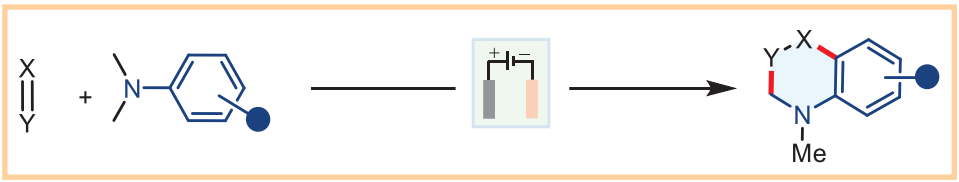

Scheme 6.6 Electrochemical oxidative [4 + 2] annulation

(ii) The direct constructions of carbon-carbon (C–C) bonds can be achieved through an electro-oxidative strategy. The reaction between the acyclic/cyclic imines and tertiary anilines to synthesize aminomethylated products **(Scheme 6.7)**.

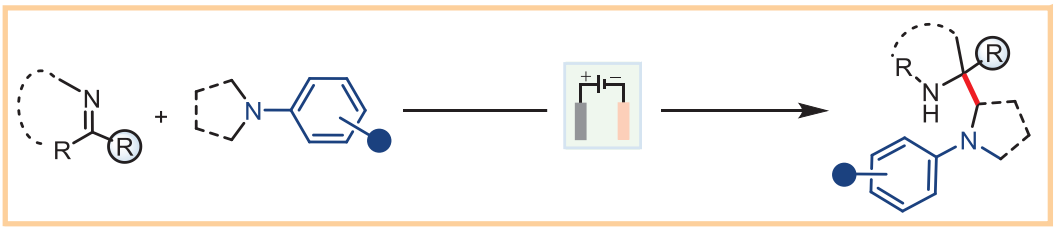

Scheme 6.7 Electrochemical C-H aminomethylation of acyclic/cyclic imines

(iii) The intermolecular electrochemical coupling between the benzylic C(sp^3)–H bond and secondary amines towards the synthesis of α-amino α-aryl acetates in an asymmetric fashion can be achieved by using a chiral auxiliary **(Scheme 6.8)**.

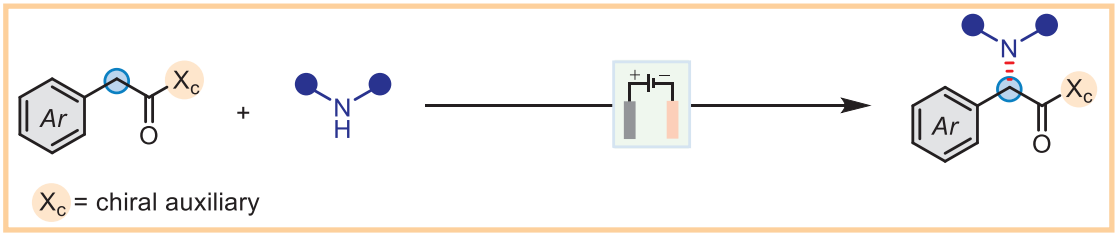

Scheme 6.8 Electrochemical oxidative asymmetric α-amination of α-aryl acetates

Appendices

List of Publication [A-1]

6. Electrochemical oxidative [4 + 2] Annulation between Cyclic Ketimines and Tertiary Anilines for the Synthesis of Dihydroindolo[1,2-*c*]quinazolin-12(6*H*)-one. **Yadav. K. Nagare**, I. Kumar* (manuscript under preparation).

5. Electrochemical Synthesis of 2-Aryl-3-(2-aminoaryl) quinoxalines via Oxidative Dearomatization/Ring-Opening/Cyclization Cascade Sequence of 2-Arylindoles with 1,2-Diaminoarenes. **Yadav. K. Nagare**, J. Yadav, A. J. Dolas, I. A. Shah, K. Rangan, R. Choudhary, E. Iype, I. Kumar. ***J. Org. Chem*., 2023**, *88*, 11111–11121.

4. Electrochemical Oxidative Addition of Nucleophiles on 2-Arylindoles: Synthesis of C2-Heteroquaternary Indolin-3-ones. **Yadav. K. Nagare**, I. A. Shah, J. Yadav, A. P. Pawar, K. Rangan, R. Choudhary, E. Iype, I. Kumar. ***J. Org. Chem*., 2022**, *23*, 15771-15782.

3. Enantioselective Direct Synthesis of C3-Hydroxyalkylated Pyrrole via an Amine-Catalyzed Aldol/Paal–Knorr Reaction Sequence. A. P. Pawar, J. Yadav, A. J. Dolas, **Yadav. K. Nagare**, E. Iype, K. Rangan, I. Kumar. ***Org. Lett*., 2021,** *24*, 7549–7554.

2. Electrochemical Oxidative Coupling between Benzylic C(sp^3)-H and N-H of Secondary Amines: Rapid Synthesis of α-Amino α-Aryl Esters. **Yadav. K. Nagare**, I. A. Shah, J. Yadav, A. P. Pawar, R. Choudhary, P. Chauhan, I. Kumar. ***J. Org. Chem*., 2021,** *86*, 9682-9691.

1. Direct Amine-Catalyzed Enantioselective Synthesis of Pentacyclic Dibenzo[*b*,*f*][1,4]oxazepine /Thiazepine-Fused Isoquinuclidines along with DFT Calculations. J. Yadav, A. P. Pawar, **Yadav. K. Nagare**, E. Iype, K. Rangan, J. Ohshita, D. Kumar, I. Kumar. ***J. Org. Chem*., 2020,** *85*, 14094-14108.

List of Presentations [A-2]

1. **Yadav Kacharu Nagare**, I. Kumar. "Electrochemical Oxidative Dearomatization of 2-Arylindole to access C2-Heteroquaternary indolin-3-ones and 2,3-Diarylquinoxalines." at 32nd CRSI National Symposium in Chemistry (**CRSI-NSC-32**) BITS PILANI, Rajasthan, India 1st- 4th February 2024 (Poster Presentation - Received **ACS-Best Poster Presentation Award**).
2. **Yadav Kacharu Nagare**, I. Kumar. "Synthesis of *α*-Amino *α*-Aryl Esters by Electrochemical Oxidative Coupling Between Benzylic C(sp^3)-H and N-H of Secondary Amines." at 17th J-NOST National Conference for Young Researchers (**J-NOST-2023**) IISER, Pune, India 10th-12th October 2023 (Oral Presentation).
3. **Yadav Kacharu Nagare**, I. Kumar. "Electrochemical Oxidative Addition of Nucleophiles on 2-Arylindoles: Synthesis of C2-Heteroquaternary Indolin-3-ones." at 27th FCASI International Conference (**FCASI-2023**) University of Rajasthan, Jaipur, India 20th-21st April 2023 (Poster Presentation).
4. **Yadav Kacharu Nagare**, I. Kumar. "Synthesis of *α*-Amino *α*-Aryl Esters by Electrochemical Oxidative Coupling Between Benzylic C(sp^3)-H and N-H of Secondary Amines." at 27th ISCB International Conference (**ISBC-2022**) Birla Institute of Technology, Mesra, Ranchi, India 16th-19th November 2022 (Poster Presentation).
5. **Yadav Kacharu Nagare**, I. Kumar "Synthesis of *α*-Amino *α*-Aryl Esters by Electrochemical Oxidative Coupling Between Benzylic C(sp^3)-H and N-H of Secondary Amines." **One-day MINI-SYMPOSIUM**, Department of Chemistry, **BITS Pilani**, Pilani (Rajasthan), India 28th February 2022. (Poster Presentation).
6. **Yadav Kacharu Nagare,** I. Kumar, "Electrochemical Oxidative Coupling Between Benzylic C(sp3)–H and N–H of Secondary Amines: Rapid Synthesis of α-Amino α-Aryl Esters" #**RSC Poster-2022**, Twitter Web, Online Mode, 1st March 2022. (Poster presentation).

Brief Biography of the Candidate [A-3]

Nagare Yadav Kacharu was born in August 1992 in the small village Mahajanpur of Nashik district in Maharashtra, India. He obtained his B.Sc. (Chemistry) and M.Sc. (Organic Chemistry) from Pune University, Maharashtra, India. After his M.Sc. studies, Yadav gained experience in the industry as a synthetic organic chemist (2015-2019) before undertaking a Ph.D. in the development of electrochemical approaches to C-C and C-O bond formation to enable the electrosynthesis of bioactive compounds (BITS, India). In Nov 2019, he joined the Department of Chemistry, BITS Pilani, for a Ph.D. under Prof. Indresh Kumar's guidance. In Sep 2020, he was awarded a Prime Minister Research Fellowship (PMRF) in chemical sciences by SERB-FICCI New Delhi, Govt. of India. He has published five research articles in international journals; some are at the communication stage, and a few others are being prepared for the manuscript. In addition, he has filed one patent to protect commercially viable aspects of his work. He presented his papers at many national/international conferences/symposiums; he received the ACS-Best Poster Presentation Award at the 32nd CRSI National Symposium in Chemistry (CRSI-NSC-32) conference. His research mainly focuses on the application of electro-organic chemistry in the preparation of bioactive heterocycles via carbon-carbon and carbon-heteroatom bond formation.

Brief Biography of the Supervisor [A-4]

Prof. Indresh Kumar is a Professor of Chemistry at the Birla Institute of Technology and Science Pilani, Pilani campus (Rajasthan). Dr Kumar did his B.Sc. (Chemistry) and M.Sc. (Organic Chemistry) from Ch. Charan Singh University, Meerut (U.P), India. He completed his PhD in Organic Chemistry from the National Chemical Laboratory (CSIR), Pune, with Dr C. V. Rode (Scientist-F) from 2007-08. He did his Post-doctoral research work with Prof. Yujiro Hayashi at the Tokyo University of Sciences, Tokyo. He joined Shri Mata Vaishno Devi University, Katra (J&K), India, as an Assistant Professor in Chemistry in 2009 and continued till January 2012.

Prof. Kumar is the recipient of "Professor D.K. Banerjee Memorial Lecture Award-2016" from the Department of Organic Chemistry, IISc., Bangalore., and the award of "Outstanding Potential for Excellence in Research and Academics (OPERA)" from 2014-15 from BITS Pilani, ISCB Young Scientist award in Chemical Sciences from Indian Society of Chemists and Biologists, Lucknow for 2016. He has 14 years of research experience and 12 years of teaching experience. He has authored 52 research papers in peer-reviewed journals, and his work has been widely recognized and cited by the scientific community. He has participated in several national and international symposia/conferences and delivered more than 45 invited lectures. Four (04) students (as sole supervisor) and two (02) students (as co-supervisor) have already obtained PhD degrees; seven (07) students are currently pursuing research for their PhD research under his guidance. Dr Kumar has completed five research projects as Principal Investigator sponsored by UGC, DST-SERB New Delhi, and BITS Pilani. Currently, he has one major project from DST-SERB New Delhi and another continued industry project sponsored by Praveen Labs Pvt. Ltd. (Surat). He has also served as a reviewer for several journals. He is a lifetime member of the Indian Society of Chemists and Biologists, Lucknow and the Chemical Research Society of India, Bangalore. Prof. Kumar has authored a book entitled "Dienamine Catalysis for Organic Synthesis", published by RSC-London. His main research interests are asymmetric organocatalysis, the development of new synthetic methodology, and the total synthesis of biologically active compounds.

Brief Biography of the Co-supervisor [A-5]

Dr. Rahul Chaudhari is a Manager at Praveen Laboratories Pvt. Ltd. Surat. Dr Chaudhary did his B.Sc. (Chemistry) and M.Sc. (Organic Chemistry) from V.N.S.G University (Gujarat), India. He completed his Ph.D. in Organic Chemistry including medicinal chemistry, from the V.N.S.G University (Gujarat), India, in 2005.

Dr. Chaudhari has 19 years of industry experience in the R&D department. His current job role at Praveen lab is the development of patent non-fringing processes, designing organic synthesis of API and intermediates with cost evaluation, checking lab validation, and finally, being transferred to the plant for regular production, product development and transfer to pilot scale and plant scale, etc.

PUBLICATIONS

JOC The Journal of Organic Chemistry

pubs.acs.org/joc Article

Direct Amine-Catalyzed Enantioselective Synthesis of Pentacyclic Dibenzo[*b*,*f*][1,4]oxazepine/Thiazepine-Fused Isoquinuclidines along with DFT Calculations

Jyothi Yadav, Amol Prakash Pawar, Yadav Kacharu Nagare, Eldhose Iype, Krishnan Rangan, Joji Ohshita, Dalip Kumar, and Indresh Kumar*

Cite This: *J. Org. Chem.* 2020, 85, 14094−14108 Read Online

ACCESS | Metrics & More | Article Recommendations | Supporting Information

ABSTRACT: A direct protocol for the asymmetric synthesis of dibenzoxazepine/thiazepine-fused [2.2.2] isoquinuclidines is developed. The reaction proceeds through a proline-catalyzed direct Mannich reaction followed by an intramolecular aza-Michael cascade sequence between 2-cyclohexene-1-one and various tricyclic imines, like dibenzoxazepines/thiazepines, as an overall [4 + 2] aza-Diels−Alder reaction. A series of pentacyclic isoquinuclidines have been prepared, with complete endo-selectivity, in good to high yields and excellent enantioselectivity (>99:1). Density functional theory (DFT) calculations further support the observed high stereochemical outcome of the reaction.

JOC The Journal of Organic Chemistry

pubs.acs.org/joc Article

Electrochemical Oxidative Coupling Between Benzylic C(sp^3)−H and N−H of Secondary Amines: Rapid Synthesis of α-Amino α-Aryl Esters

Yadav Kacharu Nagare, Imtiyaz Ahmad Shah, Jyothi Yadav, Amol Prakash Pawar, Rahul Choudhary, Pankaj Chauhan, and Indresh Kumar*

Cite This: *J. Org. Chem.* 2021, 86, 9682−9691 Read Online

ACCESS | Metrics & More | Article Recommendations | Supporting Information

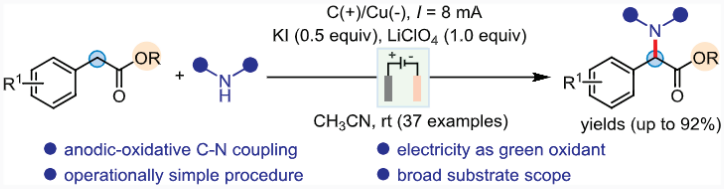

ABSTRACT: An intermolecular electrochemical coupling between the benzylic C(sp^3)−H bond and various secondary amines is reported. The electronic behavior of two electronically rich units viz the α-position of α-aryl acetates and amines was engineered electrochemically, thus facilitating their reactivity for the direct access of α-amino esters. A series of acyclic/cyclic secondary amines and α-aryl acetates were tested to furnish the corresponding α-amino esters with high yields (up to 92%) under mild conditions.

PUBLICATIONS

JOC The Journal of Organic Chemistry

pubs.acs.org/joc Article

Electrochemical Oxidative Addition of Nucleophiles on 2-Arylindoles: Synthesis of C2-Heteroquaternary Indolin-3-ones

Yadav Kacharu Nagare, Imtiyaz Ahmad Shah, Jyothi Yadav, Amol Prakash Pawar, Krishnan Rangan, Rahul Choudhary, Eldhose Iype, and Indresh Kumar*

Cite This: J. Org. Chem. 2022, 87, 15771–15782 Read Online

ACCESS | Metrics & More | Article Recommendations | Supporting Information

ABSTRACT: An electrochemical method has been developed to synthesize 2,2-disubstituted indolin-3-ones under mild conditions. A series of nucleophiles have been added to the 2-arylindole-3-ones, generated in situ under metal-free electrochemical oxidative dearomatization of 2-arylindoles, to afford 2,2-disubstituted 3-carbonyl indoles with heteroquaternary centers in 57−79% yields.

OL Organic Letters

pubs.acs.org/OrgLett Letter

Enantioselective Direct Synthesis of C3-Hydroxyalkylated Pyrrole via an Amine-Catalyzed Aldol/Paal−Knorr Reaction Sequence

Amol Prakash Pawar, Jyothi Yadav, Atul Jankiram Dolas, Yadav Kacharu Nagare, Eldhose Iype, Krishnan Rangan, and Indresh Kumar*

Cite This: Org. Lett. 2022, 24, 7549–7554 Read Online

ACCESS | Metrics & More | Article Recommendations | Supporting Information

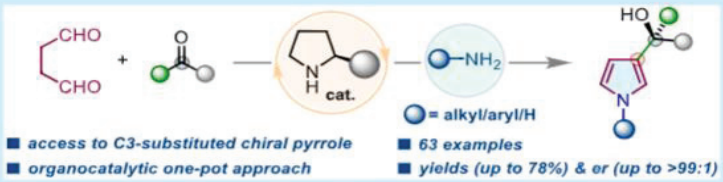

ABSTRACT: Creating functionality with chirality at position C3 of pyrrole is challenging. An operationally simple organocatalytic method has been developed to generate functionality with a chiral tertiary/quaternary stereocenter at position C3 of pyrrole. The process proceeds through an amine-catalyzed direct aldol reaction of succinaldehyde with various acceptor carbonyls, followed by a Paal−Knorr reaction with a primary amine in the same pot. A series of chiral C3-hydroxyalkylated *N*-alkyl/Ar/H-pyrroles have been synthesized for the first time with good to high yields and excellent enantioselectivity.

PUBLICATIONS

JOC The Journal of Organic Chemistry

pubs.acs.org/joc Article

Electrochemical Synthesis of 2-Aryl-3-(2-aminoaryl)quinoxalines via Oxidative Dearomatization/Ring-Opening/Cyclization Cascade Sequence of 2-Arylindoles with 1,2-Diaminoarenes

Yadav Kacharu Nagare, Jyothi Yadav, Atul Jankiram Dolas, Imtiyaz Ahmad Shah, Krishnan Rangan, Rahul Choudhary, Eldhose Iype, and Indresh Kumar*

Cite This: J. Org. Chem. 2023, 88, 11111−11121 Read Online

ACCESS | Metrics & More | Article Recommendations | Supporting Information

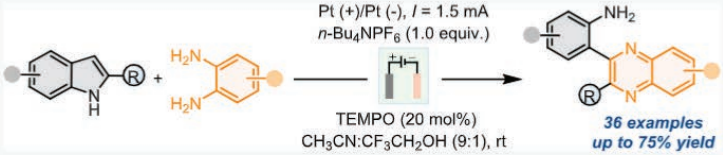

ABSTRACT: A straightforward method has been developed to synthesize 2-aryl-3-(2-aminoaryl) quinoxalines from 2-arylindoles and 1,2-diaminoarenes under mild electrochemical conditions. The reaction proceeds through in situ generations of 2-arylindole-3-ones under electrochemical oxidative dearomatization of 2-arylindoles, followed by a ring opening-cyclization sequence with 1,2-diaminoarenes. A series of 2-aryl-3-(2-aminoaryl) quinoxalines have been prepared with moderate to good yields (up to 75%).